Isolation, structure elucidation and cytotoxic activity of cucurbitacins from *Elaeocarpus petiolatus*

THESIS SUBMITTED IN FULFILMENT OF THE

REQUIRMENTS FOR THE DEGREE OF

MASTER OF PHILOSOPHY

SCHOOL OF BIOSCIENCES

UNIVERSITY OF NOTTINGHAM MALAYSIA CAMPUS

2018

BY

CHO EUN SEON

ACKNOWLEDGEMENTS

First and foremost, I would like to convey my deepest thanks to my supervisors Dr. Lim Kuan Hon and Prof. Sandy Loh Hwei San for their utmost patience, support and guidance throughout the course of this research and the time of writing this thesis.

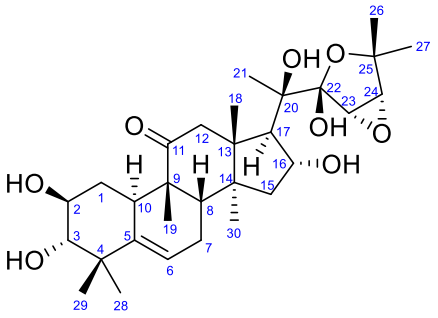
This research would have been impossible without the aid and continual support from my senior colleagues, Mr. Premanand Krishnan, Dr. Ibrahim Babangida Abubakar, and the rest of my fellow friends and colleagues in the natural products research group, namely Margret Chinoso Ezeoko, Lee Fong Kai, Amjad Ayad Qatran Al-Khdhairawi and Chan Zi Yang. I would like to thank each one of them for their companionship, support and sharing laughter throughout this long journey. The assistance from the staff at the Faculty of Science, University of Nottingham Malaysia Campus is greatly appreciated as well.

I would also like to thank Prof. Festo Massawe, the head of School of Biosciences in University of Nottingham Malaysia Campus for his guidance and support. Furthermore, I would like to show my great appreciation to Dr. Low Yun Yee and Miss Dawn Sim from Department of Chemistry, University of Malaya for performing the required NMR and X-ray diffraction experiments and Dr. Mai Chun Wai from International Medical University, for carrying out the biological assay reported in this thesis.

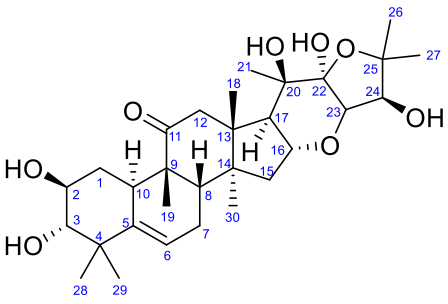
Last but not least, I would like to extend my deepest gratitude to my family and friends for their invaluable support and always being there for me whenever I needed them. Without them, I would have never been able to complete this journey.

ABSTRACT

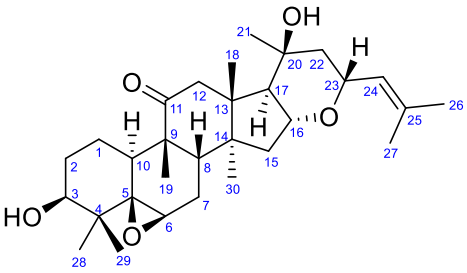
Four new cucurbitacins (**1-4**) along with six known compounds, namely, 16α,23α-epoxy-3β,20β-dihydroxy-10αH,23βH-cucurbit-5,24-dien-11-one (**5**), 16α,23α-epoxy-3β,20β-dihydroxy-10αH,23βH-cucurbit-5,24-dien-11-one 3-O-β-$_D$-glucopyranoside (**6**), elaeocarpucin F (**7**), hexanocucurbitacin F (**8**), β-sitosterol (**9**), and vomifoliol (**10**), were isolated from the leaves and bark of *Elaeocarpus petiolatus*. The structures of the new cucurbitacin compounds were elucidated based on detailed analyses of their 1D and 2D NMR, HRESIMS and MS data. The absolute configuration of compound **1** was established by X-ray diffraction analysis. Compound **1** represents a rare cucurbitacin incorporating an unusual furan-bearing side chain with ketal and epoxide functions, while compound **2** possesses a rare six-fused ring system incorporating a pyranofuranyl ring system. Compound **3** is a new C-5,C-6-epoxide containing cucurbitacin, while compound **4** represents a new acetate derivative of the known cucurbitacin glycoside **6**. Compounds **1**, **2** and **4** were assessed for their anticancer activity *in vitro* by using a panel of human cancer cell types, including breast, pancreatic, nasopharyngeal and colon cancer cells. The pure compound **1** showed good cytotoxic effects on breast cancer cell lines (MDA-MB-468, MDA-MB-231, MCF7 and SKBR3) and colorectal cancer cell line (SW48). On the other hand, compound **2** only showed appreciable potency against the MDA-MB-468 and MDA-MB-231 breast cancer cell lines, while compound **4** only showed appreciable potency against the MDA-MB-468 cell line. Further mechanistic investigations are still necessitated in order to determine the potential therapeutic application of these three pure compounds.



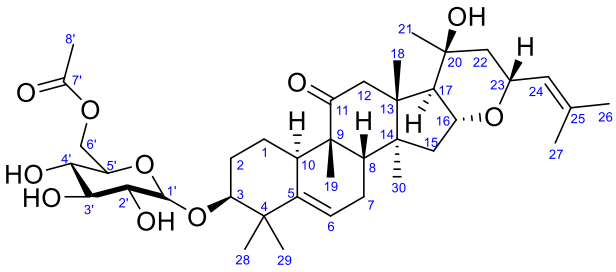
1



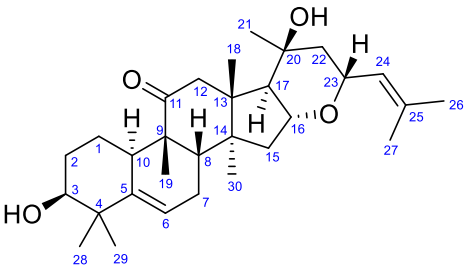
2



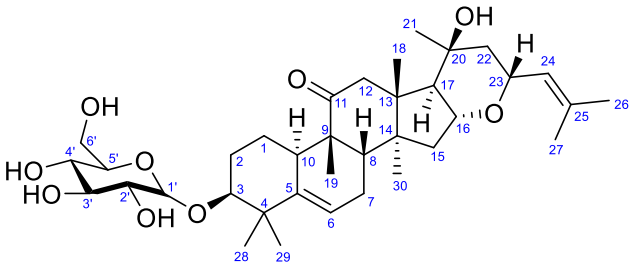
3



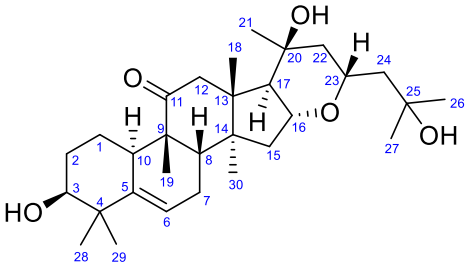
4



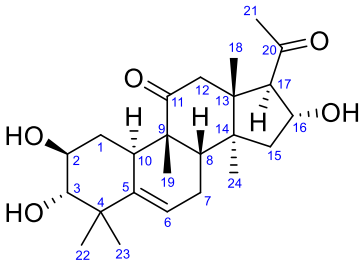
5



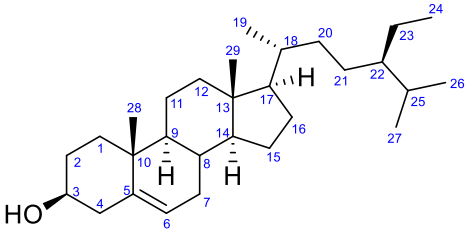
6



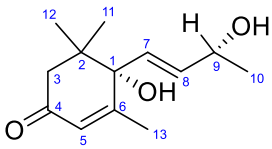
7



8



9



10

TABLE OF CONTENTS

ACKNOWLEDGEMENTS ii

ABSTRACT iii

LIST OF ABBREVIATION vii

LIST OF FIGURES viii

LIST OF TABLES x

LIST OF APPENDICES xi

Chapter One : Introduction 1

1.1 General 1

1.2 Terpenoids 2

1.2.1 Formation of isopentenyl pyrophosphate (IPP) and dimethylallyl diphosphate (DMAPP) via mevalonate and methylerythritol phosphate pathways 4

1.3 Steroids 7

1.4 Cucurbitacins 8

1.4.1 Biosynthesis of cucurbitacins 9

1.4.2 Classification of cucurbitacins 10

1.5 The Genus *Elaeocarpus* 37

1.5.1 *Elaeocarpus petiolatus* 38

1.5.2 Cucurbitacins from *Elaeocarpus* 39

1.6 Anti-cancer Application of Phytochemicals 40

1.6.1 Mechanism of action involved in cancer chemoprevention and treatment 41

1.6.2 Cytotoxicity or anti-proliferative property of cucurbitacins 43

1.7 Significance and Objectives of the Study 45

Chapter Two : Results and Discussion 46

2.1 Overview 46

2.2 Structure Elucidation 46

2.2.1 Compound **1** 46

2.2.2 Compound **2** 54

2.2.3 Compound **3** 61

2.2.4 Compound **4** 67

2.2.5 Compound **5** 72

2.2.6 Compound **6** 76
2.2.7 Compound **7** 82
2.2.8 Compound **8** 85
2.2.9 Compound **9** 85
2.2.10 Compound **10** 91
2.3 Biological Activity 93

Chapter Three : Experimental Section 95
3.1 General 95
3.2 Extraction of Plant Material 98
3.2.1 *Elaeocarpus petiolatus* leaves (EPL) 98
3.2.2 *Elaeocarpus petiolatus* bark (EPB) 98
3.3 Isolation of Plant Material 99
3.3.1 Flash column chromatography (CC) 99
3.3.2 Thin layer chromatography (TLC) 101
3.3.3 Centrifugal thin layer chromatography (CTLC) 102
3.4 Analysis of Extracted Compounds 104
3.5 Compound Data 105
3.6 Cytotoxic Test 106
3.6.1 Cell lines and cell culture 106
3.6.2 Luminescent cell viability assay 106

References 107

LIST OF ABBREVIATION

DMAPP	dimethylallyl diphosphate
IPP	isopentenyl pyrophosphate
MVA	mevalonic acid
MEP	methylerythrithol phosphate
HMG-CoA	3-hydroxy-3-methylglutaryl-CoA
FPP	farnesyl pyrophosphate
COX	cyclooxygenase
STAT3	signal transducer and activator of transcription 3
HER2	human epidermal growth factor receptor
EA	ethyl acetate
MeOH	methanol
$CHCl_3$	chloroform
CC	column chromatography
TLC	thin layer chromatography
CTLC	centrifugal thin layer chromatography
NMR	nuclear magnetic resonance
EPL	*Elaeocarpus petiolatus* leaves
EPB	*Elaeocarpus petiolatus* bark
DMSO	dimethyl sulfoxide
HRESIMS	high resolution electrospray ionization
ppm	part per million
δ	chemical shift
HSQC	heteronuclear single quantum coherence
COSY	correlation spectroscopy
HMBC	heteronuclear multiple bond correlation
NOESY	nuclear overhauser effect spectroscopy
UV	ultraviolet
IR	infrared

LIST OF FIGURES

Figure 1.1 Structure of an isoprene unit 2

Figure 1.2 Biochemically active isoprene units: a) Dimethylallyl PP (DMAPP) and b) Isopentenyl PP (IPP) 3

Figure 1.3 Simple combinations of isoprene units in head-to-tail configuration 3

Figure 1.4 Simple combinations of isoprene units in tail-to-tail configuration 3

Figure 1.5 a) Mevalonic acid (MVA) and b) 2-C-methyl-D-erythritol 4-P (MEP) 4

Figure 1.6 a) Acetyl-CoA, b) Acetoacetyl-CoA and c) 3-hydroxy-3-methylglutaryl-CoA (HMG-CoA)-13 4

Figure 1.7 a) Pyruvic acid, c) D-glyceraldehyde 3-P, c) 1-deoxy-D-xylulose 5-P, d) 4-(CDP)-2-C-methyl-D-erythirtol and e) 2-C-methyl-D-erythritol-2,4-cyclophosphate 5

Figure 1.8 Farnesyl pyrophosphate (FPP) 5

Figure 1.9 MV and MEP pathways 6

Figure 1.10 a) Steroid backbone and b) Numbering system of steroid backbone carbon backbone 7

Figure 1.11 Biosynthetic pathway of cucurbitacin E 9

Figure 1.12 Bark and leaves of *Elaeocarpus petiolatus,* collected in Kajang, Selangor, Malaysia 38

Figure 1.13 Extrinsic and intrinsic apoptotic pathway 41

Figure 2.1 ^{13}C NMR spectrum of compound **1** (150 MHz, $CDCl_3$) 48

Figure 2.2 ^{1}H NMR spectrum of compound **1** (600 MHz, $CDCl_3$) 49

Figure 2.3 Partial structures revealed by COSY and HSQC of compound **1** 50

Figure 2.4 Selected HMBC correlations of compound **1** 51

Figure 2.5 Selected NOESY correlations of compound **1** 52

Figure 2.6 X-ray crystal structure of compound **1** 52

Figure 2.7 Proposed biosynthetic pathway of compound **1** 53

Figure 2.8 ^{13}C NMR spectrum of compound **2** (150 MHz, $CDCl_3$) 56

Figure 2.9 ^{1}H NMR spectrum of compound **2** (600 MHz, $CDCl_3$) 57

Figure 2.10 Partial structures revealed by COSY and HSQC of compound **2** 58

Figure 2.11 Selected HMBC correlations of compound **2** 59

Figure 2.12 Selected NOESY correlations of compound **2** 59

Figure 2.13 Proposed biosynthetic pathway of compound **2** 60

Figure 2.14 ^{13}C NMR spectrum of compound **3** (150 MHz, $CDCl_3$) 63

Figure 2.15 ^{1}H NMR spectrum of compound **3** (600 MHz, $CDCl_3$) 64

Figure 2.16 Partial structures revealed by COSY and HSQC of compound **3** 65

Figure 2.17 Selected HMBC correlations of compound **3** 65

Figure 2.18 Selected NOESY correlations of compound **3**.....66

Figure 2.19 ^{13}C NMR spectrum of compound **4** (150 MHz, $CDCl_3$) 69

Figure 2.20 ^{1}H NMR spectrum of compound **4** (600 MHz, $CDCl_3$) 70

Figure 2.21 Partial structures revealed by COSY and HSQC of compound **4**.....71

Figure 2.22 Selected HMBC correlations of compound **4** 71

Figure 2.23 Selected NOESY correlations of compound **4** 71

Figure 2.24 ^{1}H NMR spectrum of compound **5** (600 MHz, $CDCl_3$).....74

Figure 2.25 X-ray crystal structure of compound **5** 75

Figure 2.26 ^{1}H NMR spectrum of compound **6** (600 MHz, $CDCl_3$) 78

Figure 2.27 ^{13}C NMR spectrum of compound **6** (150 MHz, $CDCl_3$) 79

Figure 2.28 Partial structures revealed by COSY and HSQC of compound **6** 80

Figure 2.29 Selected HMBC correlations of compound **6** 80

Figure 2.30 ^{1}H NMR spectrum of compound **7** (600 MHz, $CDCl_3$) 84

Figure 2.31 ^{1}H NMR spectrum of compound **8** (600 MHz, pyridine-d_5).....87

Figure 2.32 ^{1}H NMR spectrum of compound **9** (600 MHz, $CDCl_3$) 90

Figure 2.33 ^{1}H NMR spectrum of compound **10** (600 MHz, $CDCl_3$) 92

Figure 3.1 Isolation of cucurbitacins from the leaves of *E. petiolatus* 96

Figure 3.2 Isolation of cucurbitacins form the bark of *E. petiolatus*.....97

Figure 3.3 Column chromatography set up. a) Slurry packed in the column, b) Sample loading and c) Separating fractions by collecting the bands 100

Figure 3.4 TLC Plate showing cucurbitacin compounds a) under UV and b) heating the plate after spraying with vanillin reagent 102

Figure 3.5 Centrifugal thin layer chromatography. a) Solvent system, b) UV detector, c) Chromatotron and d) Collected fraction 103

LIST OF TABLES

Table 1.1 Cucurbitacins A – T and their derivatives: Source and structure 10

Table 1.2 Norcucurbitacins and other cucurbitacins: Source and structure 23

Table 1.3 Cucurbitacins from *Elaeocarpus* 39

Table 1.4 Cucurbitacins isolated from different plant species and their cytotoxic activities on human cancer cells 44

Table 2.1 ^{1}H and ^{13}C NMR data of compound **1**[a] 47

Table 2.2 ^{1}H and ^{13}C NMR data of compound **2**[a] 55

Table 2.3 ^{1}H and ^{13}C NMR data of compound **3** [a] 62

Table 2.4 ^{1}H and ^{13}C NMR data of compound **4**[a] 68

Table 2.5 ^{1}H NMR data of compound **5** and known cucurbitacin from literature 73

Table 2.6 ^{1}H and ^{13}C NMR data of compound **6**[a] 77

Table 2.7 ^{1}H NMR data of compound **7** and elaeocarpucin F from literature 83

Table 2.8 ^{1}H NMR data of compound **8** and hexanocucurbitacin F from literature[a] 86

Table 2.9 ^{13}C NMR data of compound **9** and β-sitosterol from literature 89

Table 2.10 ^{1}H NMR data of compound **10** and vomifoliol from literature 91

Table 2.11 Cytotoxic effects of compounds **1**, **2** and **4** 94

Table 3.1 Combined fractions of leaves of *Elaeocarpus petiolatus* from column chromatography 100

Table 3.2 Combined fractions of bark of *Elaeocarpus petiolatus* from column chromatography 101

Table 3.3 Recipe to make vanillin reagent 101

Table 3.4 Recipe table for plate preparation 102

LIST OF APPENDICES

Appendix 1: COSY spectrum of compound **1**

Appendix 2: HSQC spectrum of compound **1**

Appendix 3: HMBC spectrum of compound **1**

Appendix 4: NOESY spectrum of compound **1**

Appendix 5: COSY spectrum of compound **2**

Appendix 6: HSQC spectrum of compound **2**

Appendix 7: HMBC spectrum of compound **2**

Appendix 8: NOESY spectrum of compound **2**

Appendix 9: COSY spectrum of compound **3**

Appendix 10: HSQC spectrum of compound **3**

Appendix 11: HMBC spectrum of compound **3**

Appendix 12: NOESY spectrum of compound **3**

Appendix 13: COSY spectrum of compound **4**

Appendix 14: HSQC spectrum of compound **4**

Appendix 15: HMBC spectrum of compound **4**

Appendix 16: NOESY spectrum of compound **4**

Appendix 17: COSY spectrum of compound **6**

Appendix 18: HSQC spectrum of compound **6**

Appendix 19: HMBC spectrum of compound **6**

Appendix 20: NOESY spectrum of compound **6**

Appendix 21: MS spectrum of compound **1**

Appendix 22: MS spectrum of compound **2**

Appendix 23: MS spectrum of compound **3**

Appendix 24: MS spectrum of compound **4**

Appendix 25: MS spectrum of compound **5**

Appendix 26: MS spectrum of compound **6**

Appendix 27: MS spectrum of compound **7**

Appendix 28: MS spectrum of compound **8**

Appendix 29: MS spectrum of compound **9**

Appendix 30: MS spectrum of compound **10**

Appendix 31: IR spectrum of compound **1**

Appendix 32: IR spectrum of compound **2**

Appendix 33: IR spectrum of compound **3**

Chapter One

Introduction

1.1 General

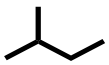
For thousands of years human beings have been living together and relied on nature for their basic needs in life such as clothing, food and shelter. Historical records have shown that our ancestors relived pain by chewing herbs, treated wound by using leaves and cured injuries and illness by using various plant products.[1] Today, especially in developing countries, people are still relying on traditional medicines for their basic health care.[2] Due to the diversity of plant-derived compounds, numerous natural products have served as leads for drug development and many have been developed into useful drugs. It is noteworthy that almost half of the bestselling pharmaceuticals are either natural products or natural product-related.[3] For instance, for the past 30 years, more than 50% of drugs used in cancer chemotherapy were natural products.[2] There are four classes of plant-derived anticancer agents in the pharmaceutical market today, namely, *Vinca* alkaloids, epipodophyllotoxins, camptothecin derivatives and taxanes.[4] As an example of a taxane agent, paclitaxel was isolated from the bark of *Taxus brevifolia* and it is widely used to treat breast and ovarian carcinomas.[5] Plants still have enormous potential to provide newer drugs as out of 250,000 to 500,000 plants on earth, only about 5-10% of plants have been investigated for their biological potential. The plant kingdom therefore remains a main source of new compounds with therapeutic potentials.[6]

Secondary metabolites are regarded as an important subset of natural products and they were postulated to play roles in plant defense, competition and signaling. However, secondary metabolites play little or no role in plant growth.[7] Secondary metabolites can be broadly categorized into three main groups, namely, alkaloids, phenolics and terpenoids. Since secondary metabolites are produced by living organisms, they are arguably considered more biologically friendly compared to synthetic compounds.[8] Among the number of plant-derived compounds, terpenes (including terpenoids) can be found in all classes of living organism and account for about 60% of all secondary metabolites. Triterpenoids, constructed from six isoprene units, possess rich chemistry and biological property.[9–11] With regard to the structures of known isoprenoids, the estimated number of terpenes is 30,500 and has pharmaceutical market of $12 billion in

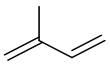
2002.[3] In the last ten years, the cucurbitacin group of triterpenoids was shown to inhibit proliferation and induce apoptosis by utilizing a long array of *in vitro* and *in vivo* cancer cell models.[12–14] Hence, the purpose of this study was to isolate and investigate triterpenoids, specifically cucurbitacins, that are present in *Elaeocarpus* species for structure determination and antiproliferative activity towards human cancer cells.

1.2 Terpenoids

Terpenoid or terpene was named from turpentine or terpentin in German, where it was first isolated from.[15] Terpenoids are derived from the condensation of several C_5 isoprene units (Figure 1.1). The various terpenoids formed are classified according to the number of isoprene units present, namely, (C_5) hemiterpenoids, (C_{10}) monoterpenoids, (C_{15}) sesquiterpenoids, (C_{20}) diterpenoids, (C_{25}) sesterterpenoids, (C_{30}) triterpenoids, (C_{40}) tetraterpenoids and (C_5)n poly-terpenoids.[16]



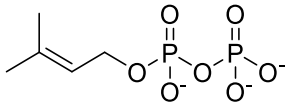
C_5 isoprene unit



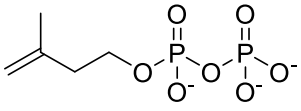
Isoprene (hemiterpene)

Figure 1.1 Structure of an isoprene unit

Terpenes are made up of two or more isoprene units, while hemiterpene (Figure 1.1) is a single isoprene. However, naturally produced isoprene cannot be used to form terpenoid compounds. Instead, nature uses biochemically active isoprene units known as dimethylallyl diphosphate (DMAPP) (Figure 1.2a) and isopentenyl pyrophosphate/diphosphate (IPP) as building blocks (Figure 1.2b). These diphosphate esters are formed in the plant chloroplast and are readily coupled to form terpenes.[17,18]



a



b

Figure 1.2 Biochemically active isoprene units: a) Dimethylallyl PP (DMAPP) and b) Isopentenyl PP (IPP)

The simple combinations of isoprene units to form terpenoids are usually formed in a head-to-tail configuration such as that shown in geraniol (C_{10}), farnesol (C_{15}), and gernaylgeraniol (C_{20}) (Figure 1.3). Squalene (C_{30}) and phytoene (C_{40}) are rare examples of terpenoids which display a tail-to-tail linkage in the middle of the molecules (Figure 1.4).[19]

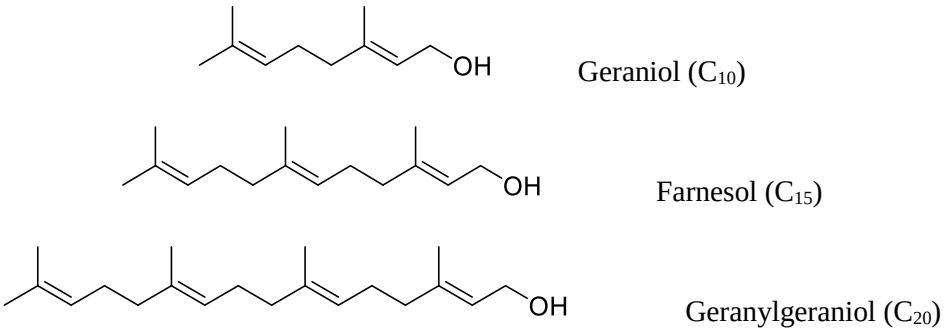


Figure 1.3 Simple combinations of isoprene units in a head-to-tail configuration

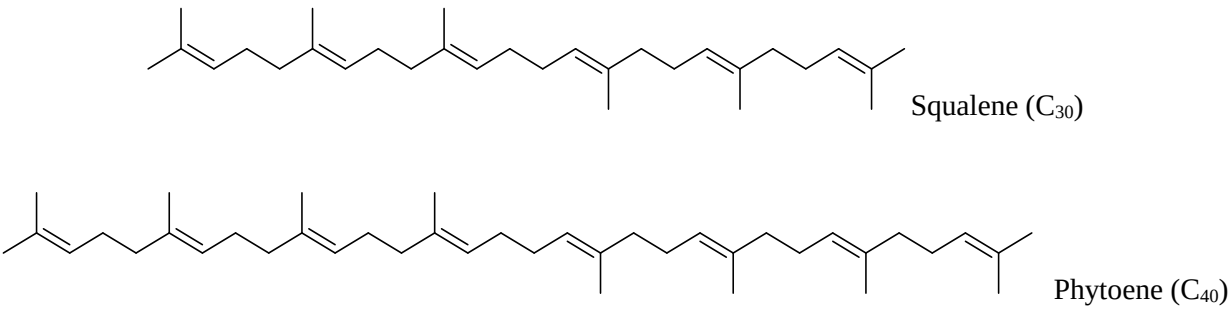


Figure 1.4 Simple combinations of isoprene units in a tail-to-tail configuration

1.2.1 Formation of isopentenyl pyrophosphate (IPP) and dimethylallyl diphosphate (DMAPP) via mevalonate (MV) and methylerythritol phosphate (MEP) pathways

The biochemically active isoprene units, IPP and DMAPP (Figure 1.2), may be formed by two pathways with two different intermediates known as mevalonic acid (MVA) or methylerythrithol phosphate (MEP) (Figure 1.5).



a b

Figure 1.5 a) Mevalonic acid (MVA) and b) 2-C-methyl-D-erythritol 4-P (MEP)

The mevalonate (MV) pathway (Figure 1.9) begins with three molecules of acetyl-coenzyme A (Figure 1.6a). First two molecules of acetyl-CoA combine to form acetoacetyl-CoA (Figure 1.6b) and the third joins to form 3-hydroxy-3-methylglutaryl-CoA (HMG-CoA) (Figure 1.6c). HMG-CoA then goes through two-step reduction to produce MVA with the help of the enzyme HMG-CoA reductase. The six-carbon containing MVA is then finally converted into the five-carbon phosphorylated isoprene units, IPP and DMAPP. Statins target the MV pathway to reduce cholesterol levels via inhibiting HMG-CoA reductase.[19]



a b c

Figure 1.6 a) Acetyl-CoA, b) Acetoacetyl-CoA and c) 3-hydroxy-3-methylglutaryl-CoA (HMG-CoA)

The MEP pathway (Figure 1.9) begins with pyruvic acid (Figure 1.7a) and glyceraldehyde 3-phosphate (Figure 1.7b) that generate 1-deoxy-D-xylulose 5-phosphate (Figure 1.7c), which then produces MEP. MEP then reacts with cytidine triphosphate to form cytidine diphospho derivative (Figure 1.7d), which undergoes phosphorylation via ATP. The 2-phosphate of the resultant intermediate then loses

cytidine monophosphate to generate a cyclic phosphoanhydride (Figure 1.7e). The consequent steps then finally produce IPP and DMAPP. The drug to target microbial diseases like malaria or tuberculosis is used to disrupt MEP pathway.[19]

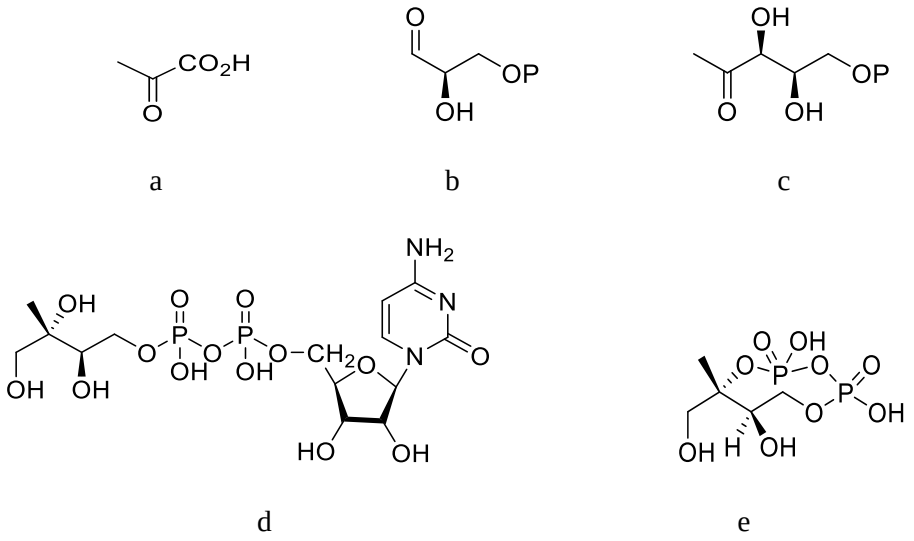


Figure 1.7 a) Pyruvic acid, b) D-glyceraldehyde 3-P, c) 1-deoxy-D-xylulose 5-P, d) 4-(CDP)-2-C-methyl-D-erythirtol and e) 2-C-methyl-D-erythritol-2,4-cyclophosphate

The MEP pathway is an essential cellular metabolic pathway found in eukaryotes and most bacteria. However, the MEP pathway lacks in animals and fungi and thus the MV pathway is applied to compensate for this. In plants, both the MEP and MV pathways are found in the cytosol and chloroplasts. DMAPP reacts with 2 units of IPP to form farnesyl pyrophosphate (FPP) (Figure 1.8), which is the precursor to various sesquiterpenoid and triterpenoid compounds. Mostly, triterpenoids are built by the MV pathway, whilst C_{10}, C_{20}, and C_{30}-terpenoids are produced by the MEP pathway in the chloroplasts.[19]

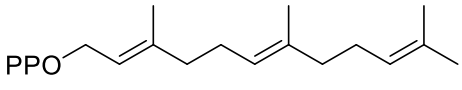


Figure 1.8 Farnesyl pyrophosphate (FPP)

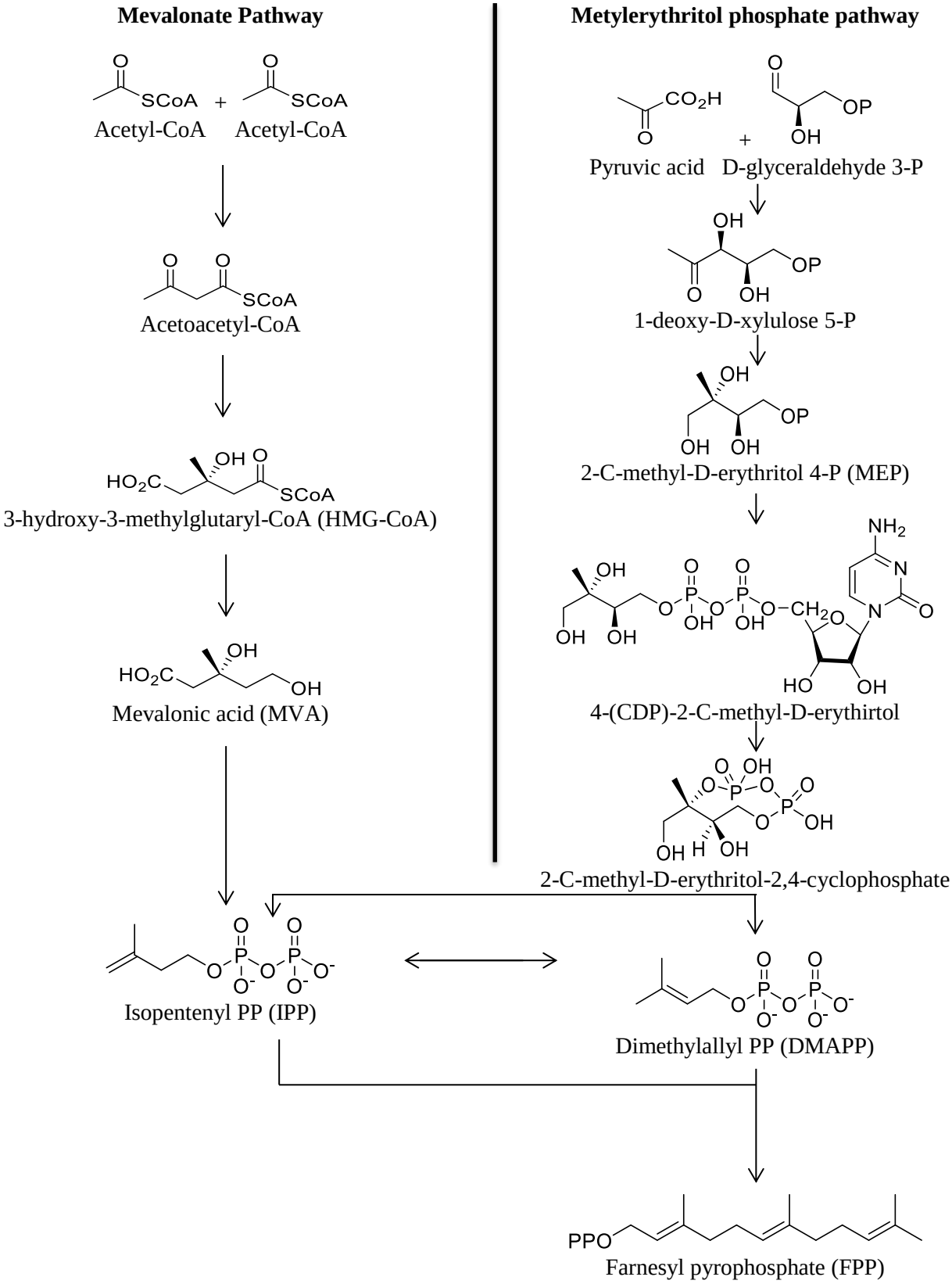
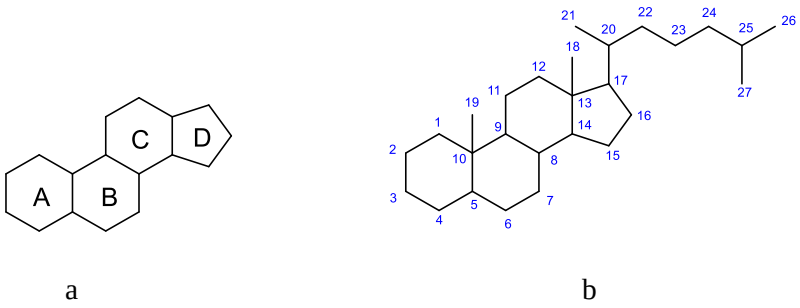


Figure 1.9 MV and MEP pathways

1.3 Steroids

Steroids are modified triterpenoids and they are the most described subgroup of triterpenes. All triterpenoids including the entire family of steroids are derived from squalene (Figure 1.4), which works as a biological precursor.[15] Steroids can be easily identified by its four fused, nonplanar hydrocarbon rings.[20] Six-membered ring A is on the left and is attached by another cyclohexane ring B followed by ring C and the cyclopentane ring D (Figure 1.10a). Carbon number is counted from ring A, continues at B, C, and D. Two methyl groups attached to C-10 and C-13 are numbered as 19 and 18, respectively (Figure 1.10b). The numbering then continues in the side chain.[21] Modifications at the side chain help to create many biologically essential natural products, such as mammalian sex hormones, bile acids, sterols, corticosteroids and steroidal saponins.[19] Steroids have also been shown to possess anti-herbivore functions via its bitter tasting property in the plant and these bitter steroids are known to be cucurbitacin compounds.



a b

Figure 1.10 a) Steroid backbone and b) Numbering system of the steroid carbon backbone

1.4 Cucurbitacins

Over the decades, many cucurbitacins and its derivatives have been isolated from various plant species. The cucurbitacins were originally isolated from family Cucurbitacea (cucumber, melon or marrow family) in 1831 and trivial name for the first cucurbitacin was α-elaterin. Determination of the chemical structure of elaterin was started from the beginning of the 20th century, but its structure was only confirmed in 1960's. The defined chemical structure of cucurbitacin helped to identify other cucurbitacins found in various plant families including *Elaeocarpaceae*.[22]

Cucurbitacins contain diverse oxygenated tetracyclic triterpenes with a cucurbitacin skeleton. They can be differentiated from other tetracyclic triterpenes by the numerous hydroxyl, acetoxy and keto groups they contain.[16]

Cucurbitacins were isolated either as monoglycosylated or aglycone compounds. The sugar moiety present can be D-glucose or L-rhamnose, which usually linked to C-2 of the cucurbitacin skeletons (e.g., 2-O-β-glucoside). It is still unknown whether the aglycones of cucurbitacins are the original form present in plants or whether they are the product of hydrolysis by active β-glycosidase, which may be destroyed during preparation for the chemical analysis.[23]

Generally, all cucurbitacins are in crystalline form and are soluble in chloroform. They are famous for its bitterness and toxicity that act to protect the plant from parasitic and protozoal infections and are used for their cytostatic effect.[16] Most cucurbitacins have shown promising biological activities, such as anti-diabetic, anti-tumor, anti-inflammatory, anti-microbial, hepatoprotective, cardiovascular, anthelmintic and anti-cancer properties. [12]

1.4.1 Biosynthesis of cucurbitacins

Two molecules of FPP are joined in a tail-to-tail configuration to form the immediate precursor, squalene, which was first isolated from the liver oil of shark.[19] Squalene then undergoes cyclization via the intermediate of 2,3-oxidosqualene (Figure 1.11) that was catalyzed by squalene epoxidase. When the cyclization takes place, the tertiary protosteryl cation (Figure 1.11) is formed. The formation of double bond at C-5 and C-6 will terminate the Wagner-Meerwein rearrangements of the protosteryl cation and generates cucurbitadienol (Figure 1.11). The cucurbitadienol then undergoes various oxidative modifications to form cucurbitacin E (Figure 1.11).[19]

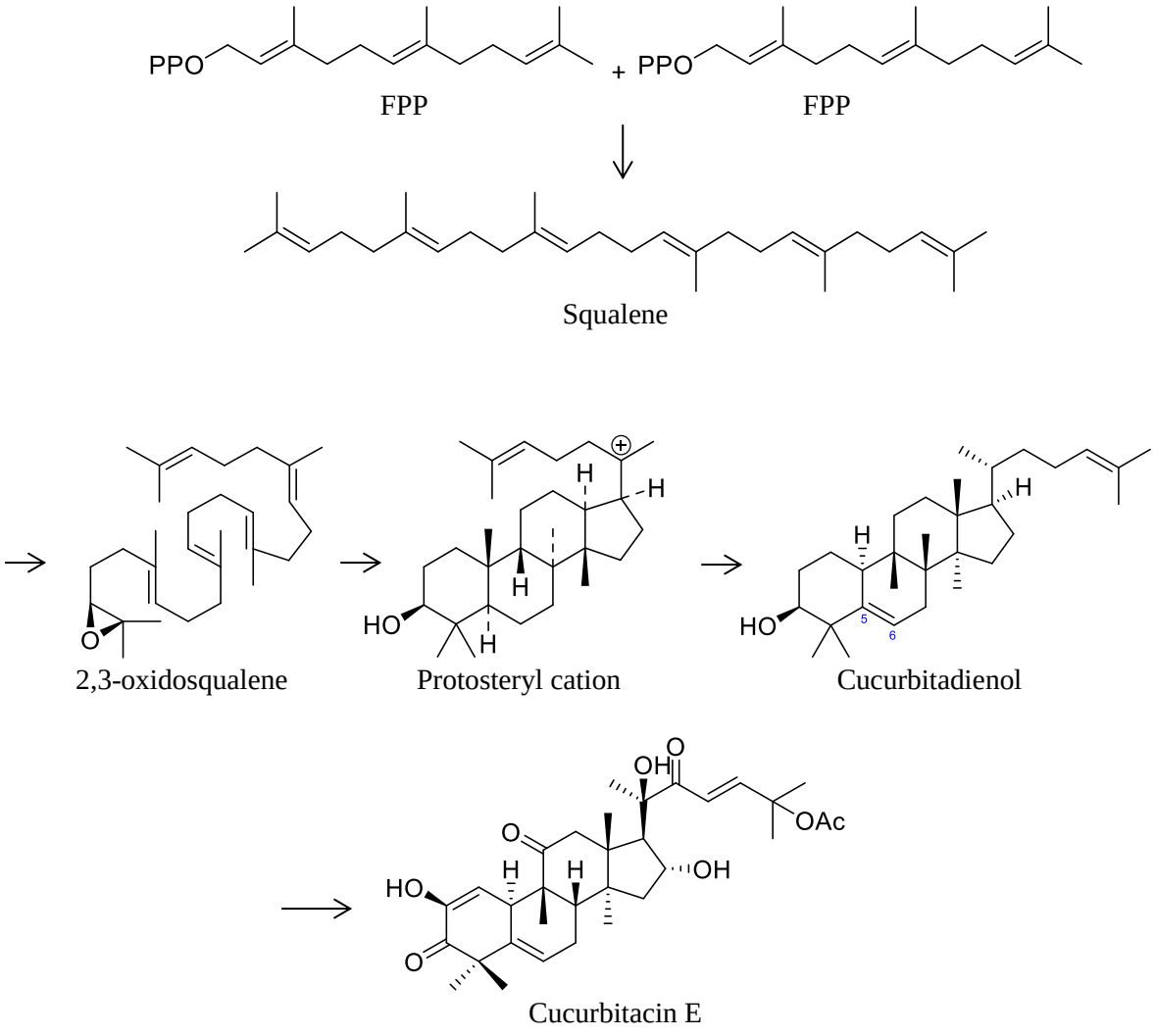


Figure 1.11 Biosynthetic pathway of cucurbitacin E

1.4.2 Classification of cucurbitacins

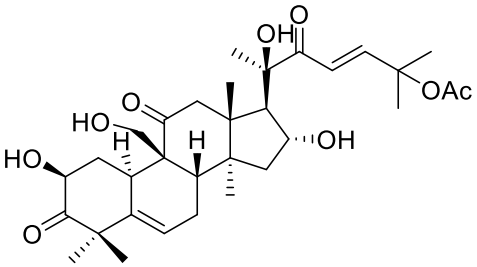
Cucurbitacins can be classified by the letters A – T. Elaterin, the first cucurbitacin to be isolated, however it was structurally described much later, and hence it was known as cucurbitacin E. Cucurbitacins D and I are also known to be elaterins A and B, respectively.[22] A large number of studies were carried out later and Table 1.1 lists the source and structure of cucurbitacins A – T and their derivatives, while Table 1.2 lists norcucurbitacins and other cucurbitacin compounds. Norcucurbitacin (C_{28} or C_{29}) refers to a cucurbitacin that has one or two carbons removed from the typical cucurbitacin carbon skeleton (C_{30}).

Table 1.1 Cucurbitacins A – T and their derivatives: Source and structure

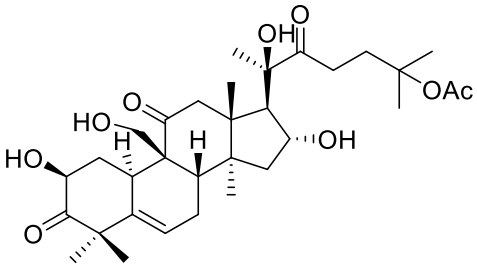
Compound	Plant isolated	Structure	Reference
Cucurbitacin A			
Cucurbitacin A	*Cucumis hookeri*	11	[24]
Dihydrocucurbitacin A	*Cucumis leptodermis*	12	[24]
Deacetoxydihydrocucurbitacin A	*Cucumis myriocarpus*	13	[24]
Cucurbitacin B			
Cucurbitacin B	Fruit of *Leucopaxillus gentianeus*	14	[25,26]
Cucurbitacin B glucoside	Rhizomes of *Begonia heracleifolia*	15	[23]
23,24-dihydrocucurbitacin B 2-O-glucoside	Roots of *Picrorhiza kurrooa*	16	[23]
Deacetoxycucurbitacin B 2-O-glucoside	Roots of *Picrorhiza kurrooa*	17	[23]
Isocucurbitacin B	Juice of *Echinocystis fabacea*	18	[23,26]
Dihydroisocucurbitacin B 3-glucoside	*Wilbrandia ebracteata*	19	[23]
23,24-dihydro-3-*epi*-isocucurbitacin B	*Bryonia verrucosa*	20	[23]
23,24-dihydro-3-*epi*-isocucurbitacin B	*Bryonia verrucosa*	21	[23]
23,24-dihydro-3-*epi*-isocucurbitacin B	*Bryonia verrucosa*	22	[23]
Cucurbitacin C			
Cucurbitacin C	*Cucumis sativus*	23	[23,27]
Cucurbitacin D and R			
Cucurbitacin D (Elatericin A)	Fruit of *Leucopaxillus gentianeus*	24	[25,28]
23,24-dihydrocucurbitacin D (Cucurbitacin R)	Roots of *Trichosanthes kirilowii*	25	[23]
3-*epi*-isocucurbitacin D	Seed of *Physocarpus*	26	[23,28]
Cucurbitacin D 2-O-glucoside	Seed of *Physocarpus*	27	[23]
Datiscoside 1	*Datisca glomerata*	28	[23]
Datiscoside 2	*Datisca glomerata*	29	[23]
Datiscoside F	*Datisca glomerata*	30	[23]

Datiscoside G	*Datisca glomerata*	31	[23]
23,24-dihydro-*epi*-isocucurbitacin D	*Acanthosicyos horridus*	32	[23]
22-deoxocucurbitacin D	*Wilbrandia ebracteata*	33	[23]
Anhydro-22-deoxo-3-*epi*-isocucurbitacin D	*Ecballium elaterium*	34	[23]
2-Deoxycucurbitacin D	*Sloanea zuliaensis*	35	[29]
25-O-acetyl-2-deoxycucurbitacin (amarinin)	*Luffa amara*	36	[23]
Compound 25	*Wilbrandia ebracteata*	37	[23]
(23S,24Z)-16,23-epoxycucurbitacin D	Juice of *Ecballium elaterium*	38	[23]
Cucurbitacin E			
Cucurbitacin E (Elaterin)	Roots of *Wilbrandia ebracteata*	39	[23,30]
Dihydrocucurbitacin E	Roots of *Wilbrandia ebracteata*	40	[23,30]
Dihydrocucurbitacin E 2-glucoside	Roots of *Wilbrandia ebracteata*	41	[23,30]
Isocucurbitacin E	*Cucumis phrophetarum*	42	[23]
23,24-dihydroisocucurbitacin E	*Cucumis phrophetarum*	43	[23]
16,23-Epoxycucurbitacin E 2-O-glucoside	*Gymnopetalum integrifolium*	44	[23]
Cucurbitacin F			
Cucurbitacin F	*Physocarpus capitatus*	45	[31]
Cucurbitacin F 25-acetate	*Sloanea zuliaensis*	46	[29]
23,24-dihydrocucurbitacin F	*Elaeocarpus dolichostylus*	47	[9]
25-acetoxy-23,24-dihydrocucurbitacin F (hemslecin A)	*Hemsleya amabilis*	48	[23]
Hemslecin D	*Hemsleya lijiangensis*	49	[23]
Hemslecin E	*Hemsleya lijiangensis*	50	[23]
Hemslecin F	*Hemsleya lijiangensis*	51	[23]
Dihydrocucurbitacin F glucoside	*Hemsleya amabilis*	52	[23]
Cucurbitacin II Glucoside	*Hemsleya amabilis*	53	[23]
Hemslecin G	*Hemsleya gigantha*	54	[23]
Hexanorcucurbitacin F	*Elaeocarpus dolichostylus*	55	[9]
Perseapicroside A	*Persea Mexicana*	56	[23]
Scandenoside R9	*Hemsleya panacis-sandens*	57	[23]
15-oxo-cucurbitacin F	*Cowania mexicana*	58	[23]
15-oxo-23,24-dihydrocucurbitacin F	*Cowania mexicana*	59	[23]
Aglycone of datiscosides B	*Datisca glomerata*	60	[23]
Aglycone of datiscosides D	*Datisca glomerata*	61	[23]
Aglycone of datiscosides H	*Datisca glomerata*	62	[23]
Hemslecin C	*Datisca glomerata*	63	[23]
Cucurbitacins G and H			
Cucurbitacins G	Roots of *Wilbrandia ebracteata*	64	[23]
Cucurbitacins H	Roots of *Wilbrandia ebracteata*	65	[23]
3-*epi*-isocucurbitacin G	Roots of *Wilbrandia ebracteata*	66	[23]
Cucurbitacins I			

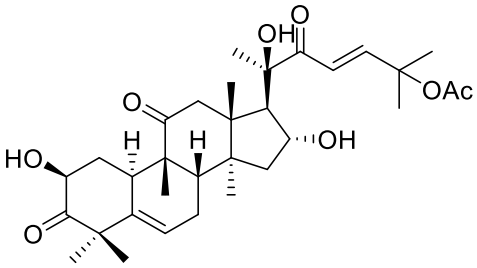
Cucurbitacin I (Elatericin B)	*Ecballium elaterium*	67	[32]
Hexanorcucurbitacin I	*Ecballium elaterium*	68	[23]
Khekadaengosides D	Fruits of *Trichosanthes*	69	[23]
Khekadaengosides K	Fruits of *Trichosanthes*	70	[23]
11-deoxocucurbitacin I	*Desfontainia spinosa*	71	[23]
23,24-dihydro-11-deoxocucurbitacin I	*Desfontainia spinosa*	72	[23]
Spinosides A	*Desfontainia spinose*	73	[23]
Spinosides B	*Desfontainia spinose*	74	[23]
Cucurbitacin L			
Cucurbitacin L	*Citrullus colocynthis*	75	[23]
Brydioside A	*Bryonia dioica*	76	[23]
Bryoamaride	*Bryonia dioica*	77	[23]
25-O-acetylbryoamaride	*Trichosanthes tricuspidata*	78	[23]
Khekadaengosides A	*Trichosanthes tricuspidata*	79	[23]
Khekadaengosides B	*Trichosanthes tricuspidata*	80	[23]
Cucurbitacins J and K			
Cucurbitacin J	*Iberis amara*	81	[23]
Cucurbitacin K	*Iberis amara*	82	[23]
Cucurbitacin J 2-O-β-Glycopyranoside	*Trichosanthes tricuspidata*	83	[23]
Cucurbitacin K 2-O-β-Glycopyranoside	*Trichosanthes tricuspidata*	84	[23]
Cucurbitacins O, P and Q			
Cucurbitacin O	*Brandegea bigelovii*	85	[23]
Cucurbitacin P	*Brandegea bigelovii*	86	[23]
Cucurbitacin Q	*Brandegea bigelovii*	87	[23]
Cucurbitacin Q 2-O-glucoside	*Picrorhiza kurrooa*	88	[23]
16-deoxy-Δ^{16}-hexanorcucurbitacin O	*Ecballium elaterium*	89	[23]
Deacetylpicracin	*Picrorhiza scrophulariaeflora*	90	[33]
Picracin	*Picrorhiza scrophulariaeflora*	91	[33]
Deacetylpicracin 2-O-glucoside	*Picrorhiza kurrooa*	92	[23]
Picracin 2-O-glucoside	*Picrorhiza kurrooa*	93	[23]
23,24-dihydro-deacetylpicracin 2-O-glucoside	*Picrorhiza kurrooa*	94	[23]
22-deoxocucurbitacin O	*Wilbrandia ebracteata*	95	[23]
Cucurbitacins S and T			
Cucurbitacin S	*Bryonia dioica*	96	[23]
Cucurbitacin S hemiacetal	*Bryonia dioica*	97	[23]
Cucurbitacin T	Fruits of *Colocynthis vulgaris*	98	[23]



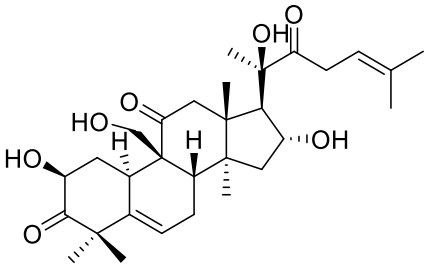
11



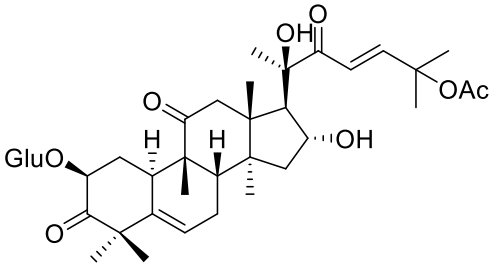
12



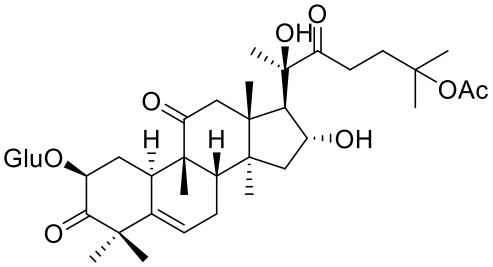
13



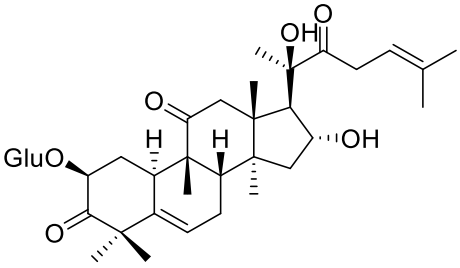
14



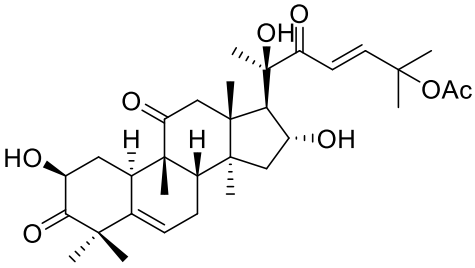
15



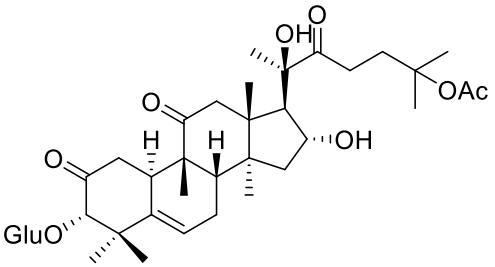
16



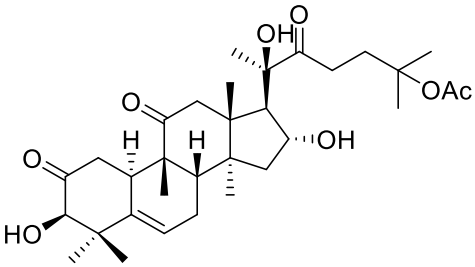
17



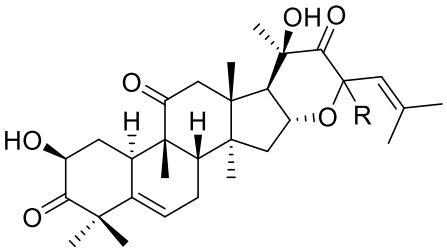
18



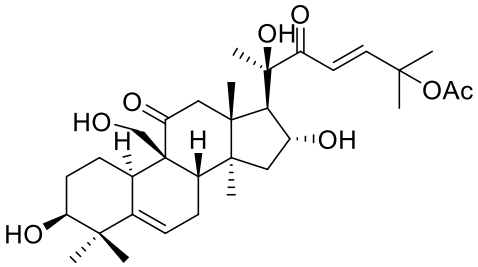
19



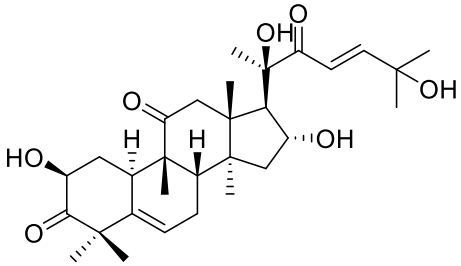
20



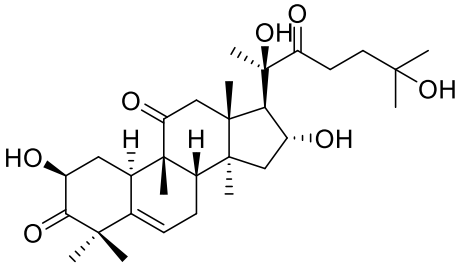
21/22



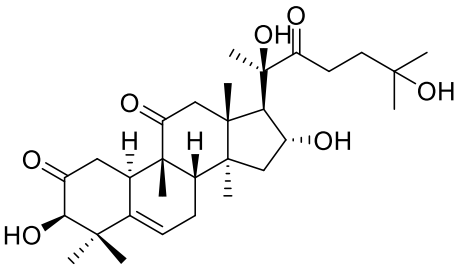
23



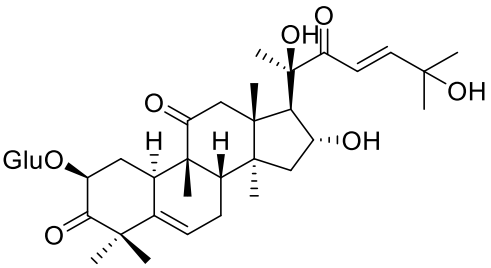
24



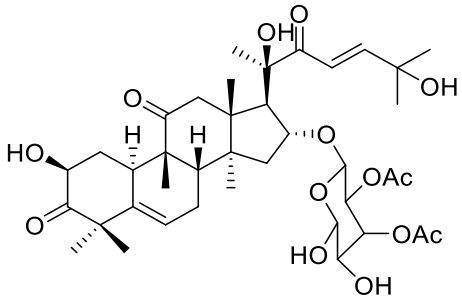
25



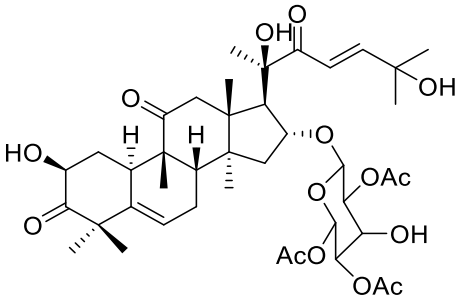
26



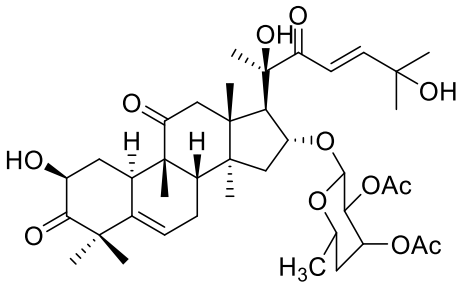
27



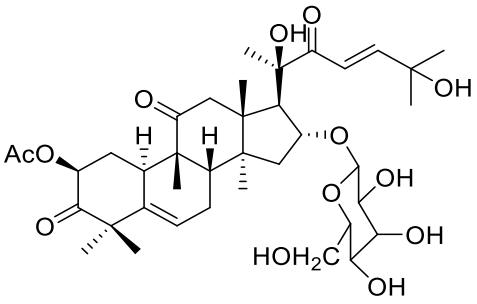
28



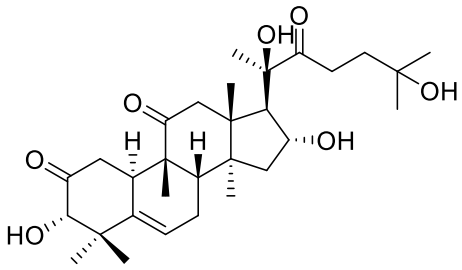
29



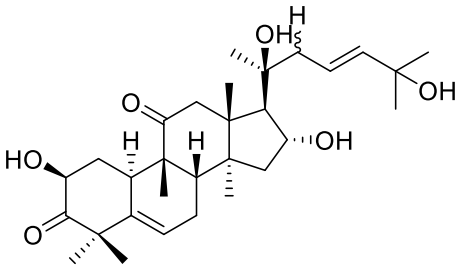
30



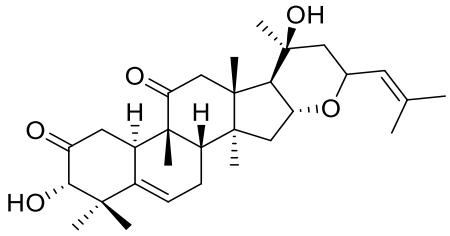
31



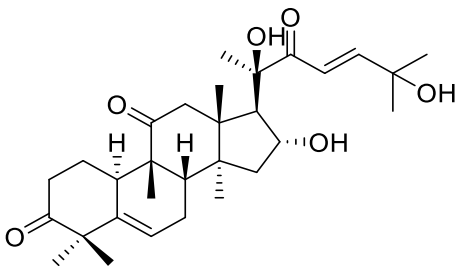
32



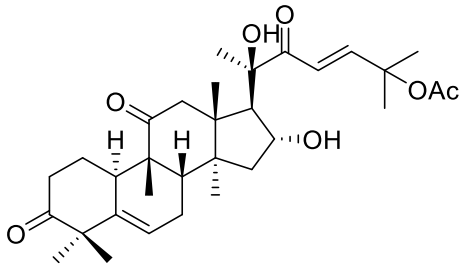
33



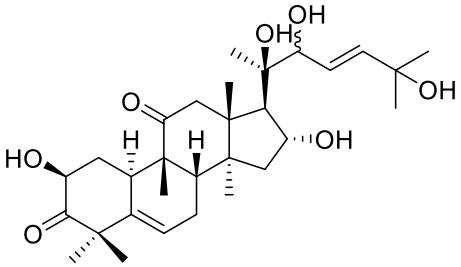
34



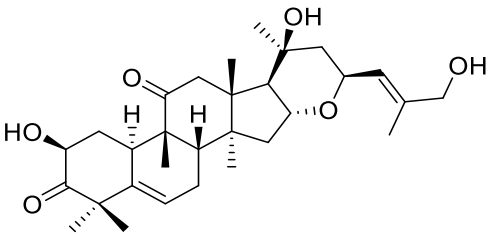
35



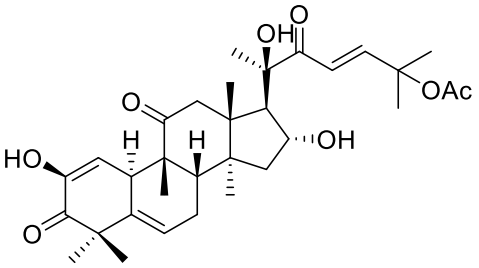
36



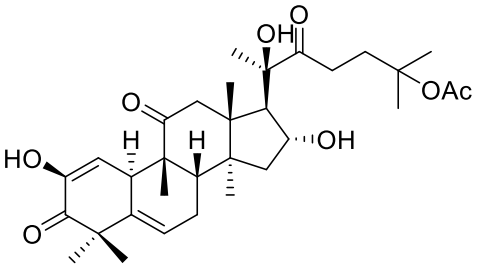
37



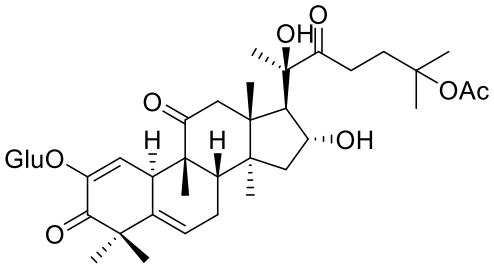
38



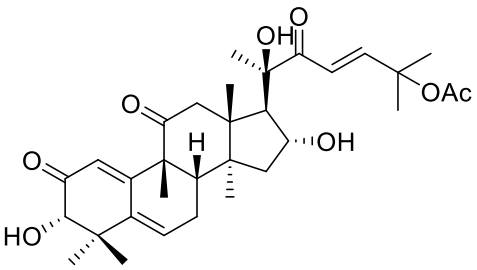
39



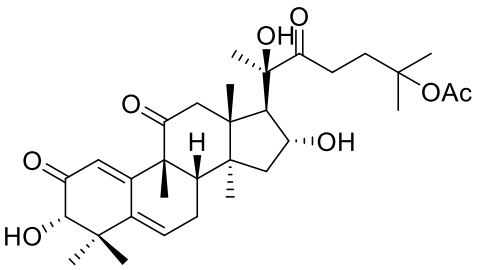
40



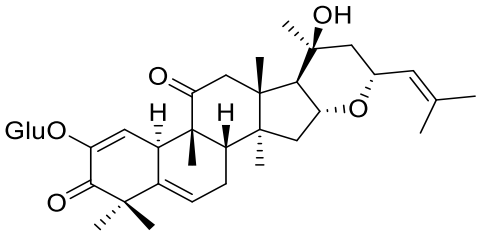
41



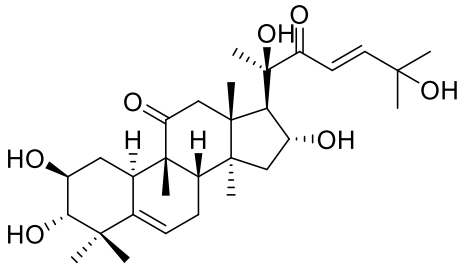
42



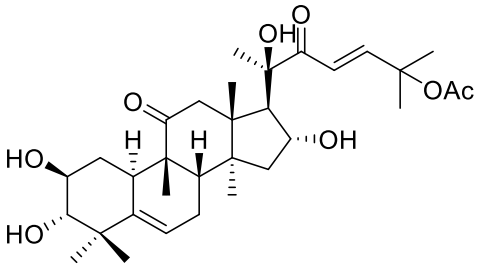
43



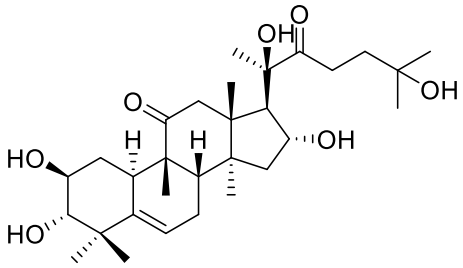
44



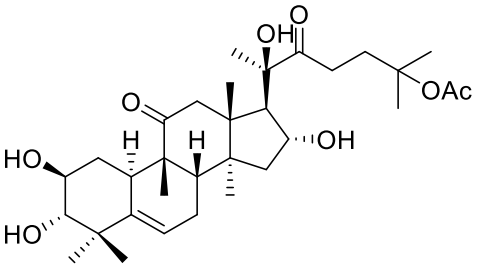
45



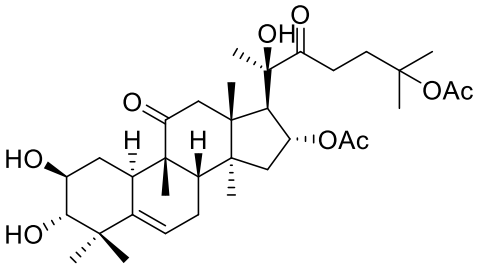
46



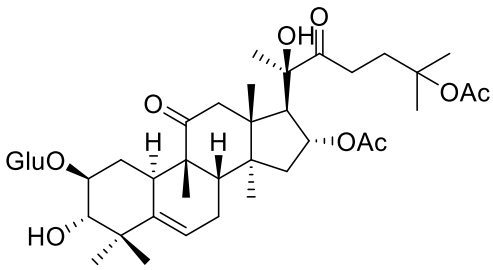
47



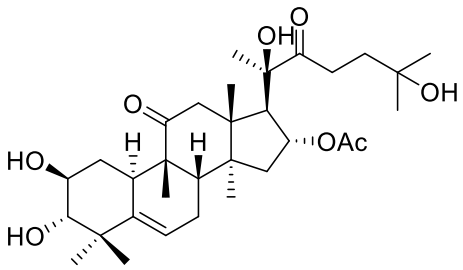
48



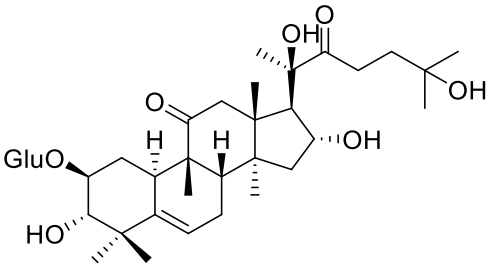
49



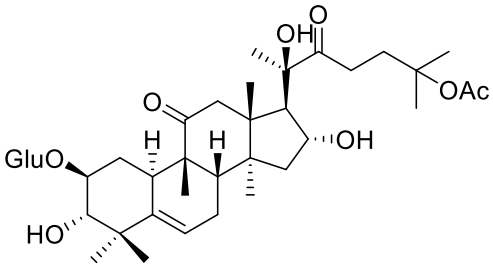
50



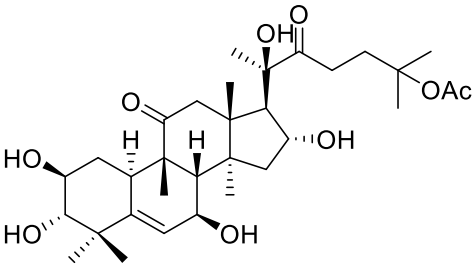
51



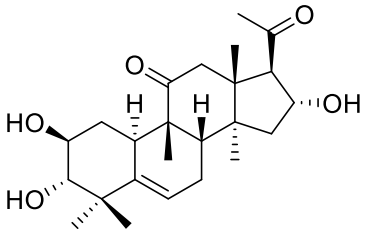
52



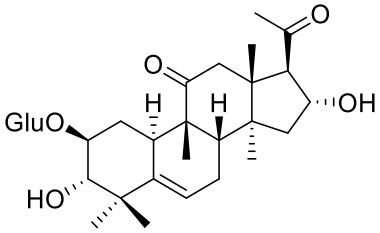
53



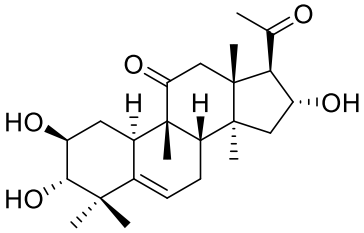
54



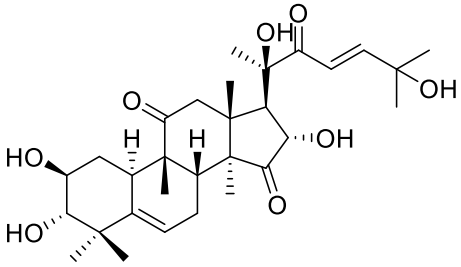
55



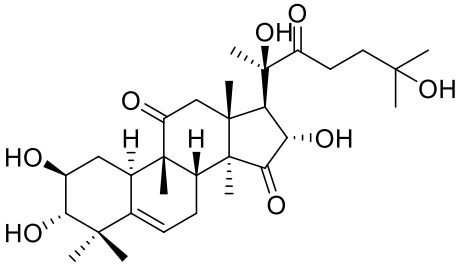
56



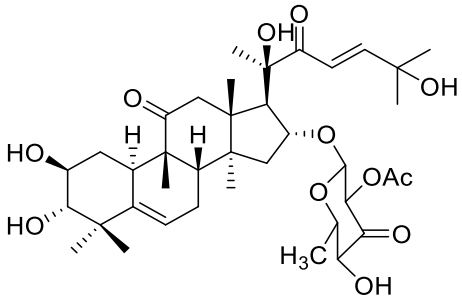
57



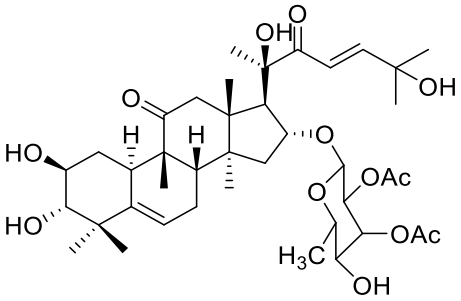
58



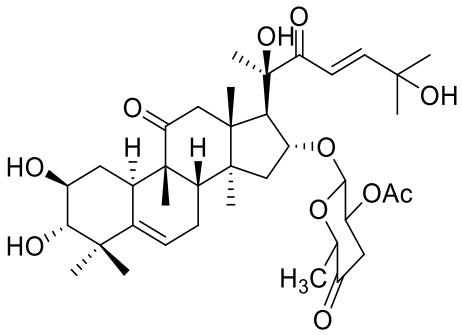
59



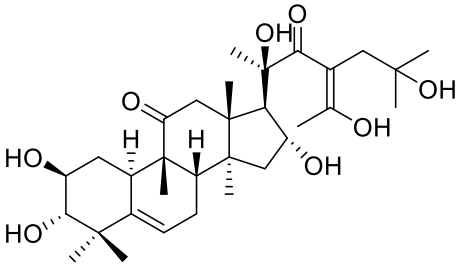
60



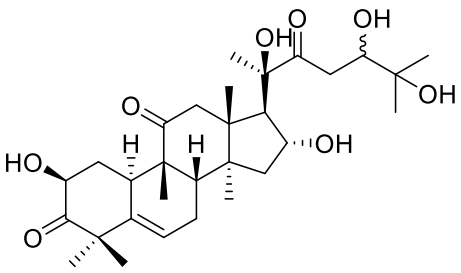
61



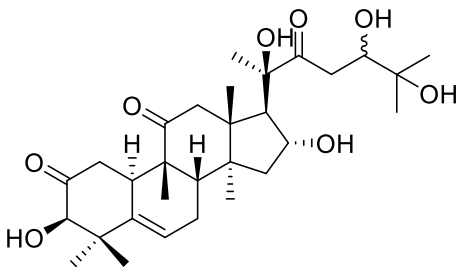
62



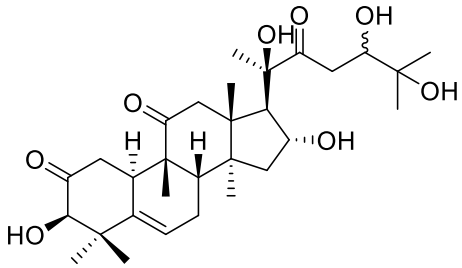
63



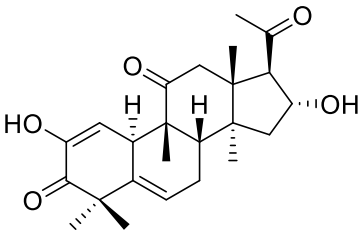
64/65



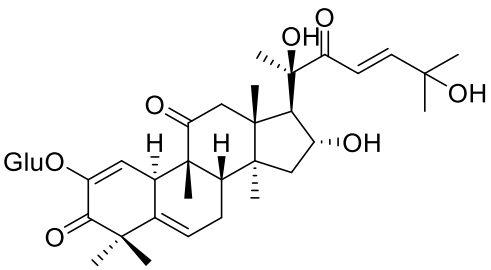
66



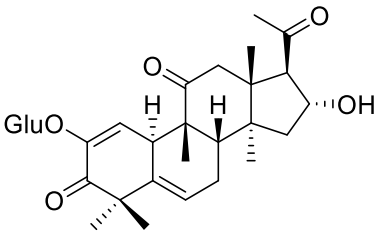
67



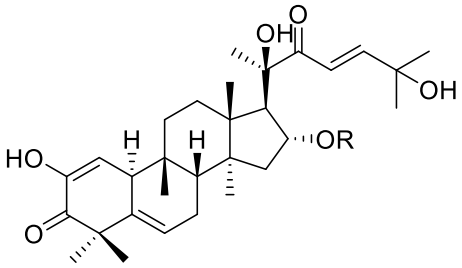
68

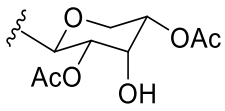


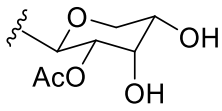
69

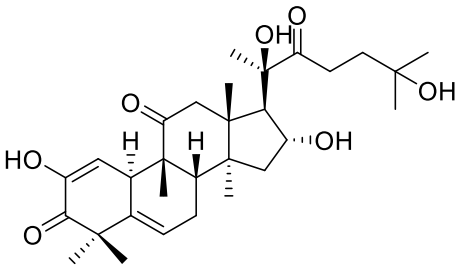


70

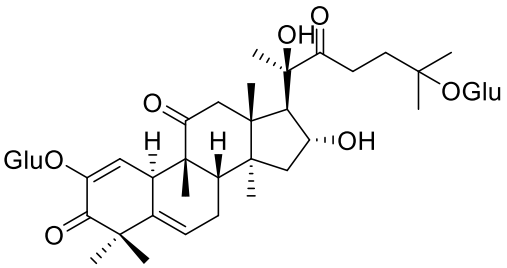


71 R=H, **72** R=H; 23,24-dihydro, **73** R = 

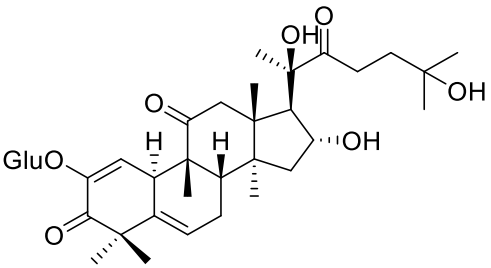
, **74** R = 



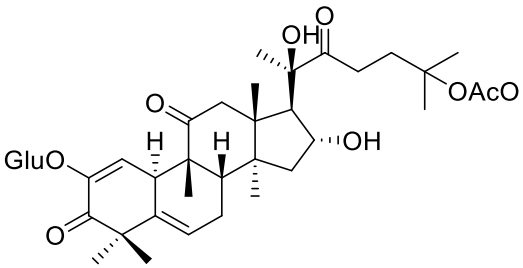
75



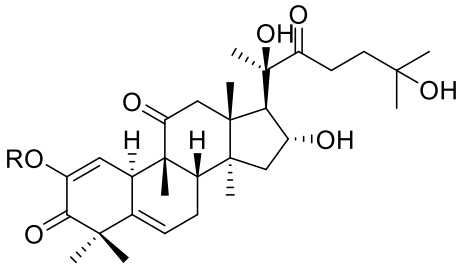
76



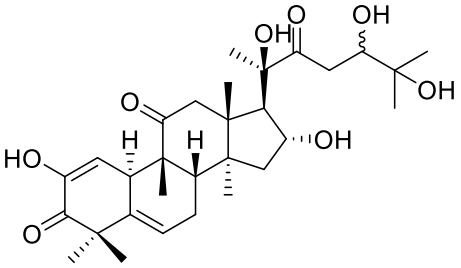
77



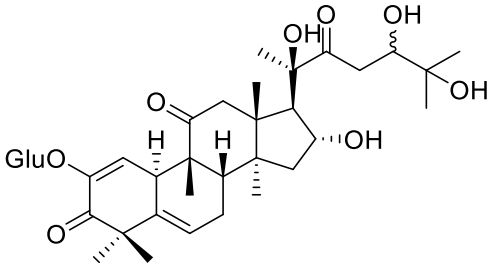
78



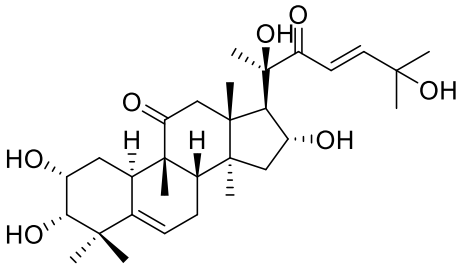
79 R=α-rhamnopyranosyl(1-2)Glu, **80** R=α-glucopyranosyl(1-4)Glu



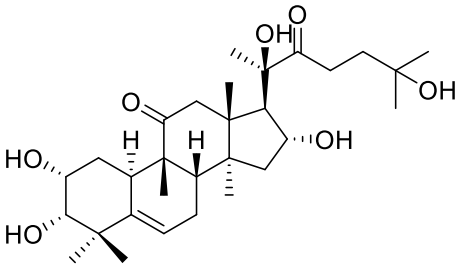
81/82



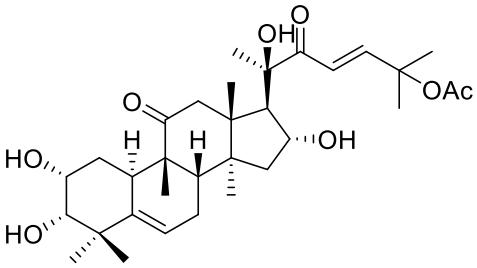
83/84



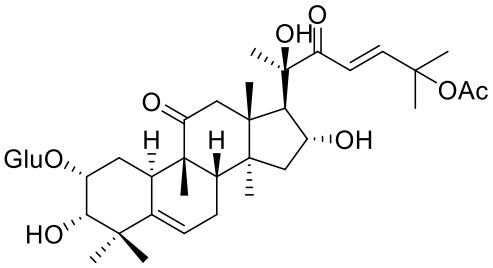
85



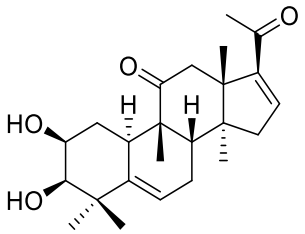
86



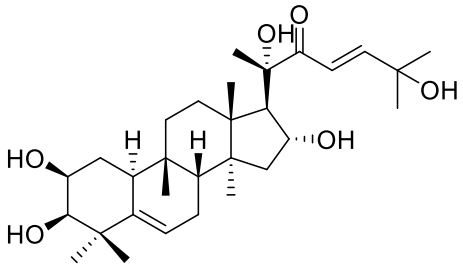
87



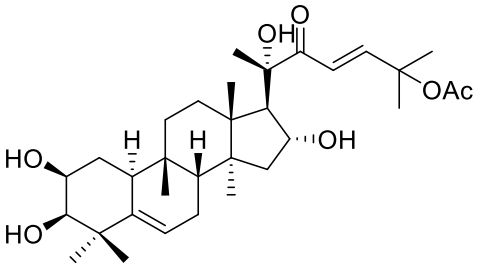
88



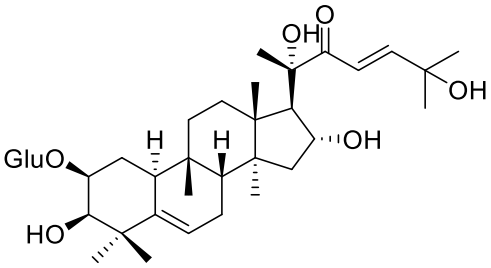
89



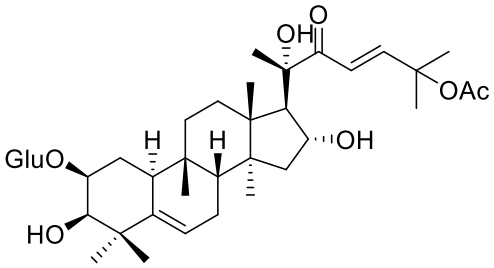
90



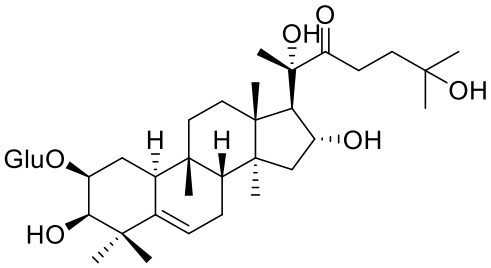
91



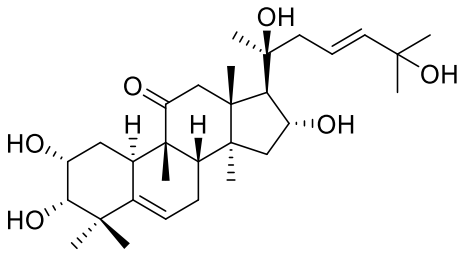
92



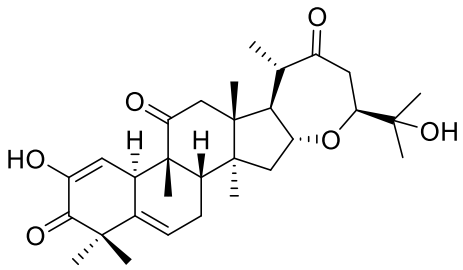
93



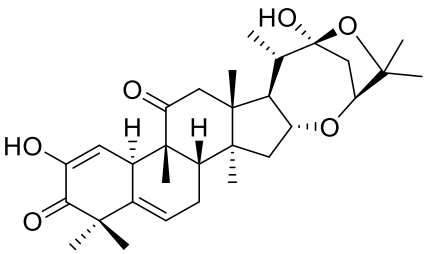
94



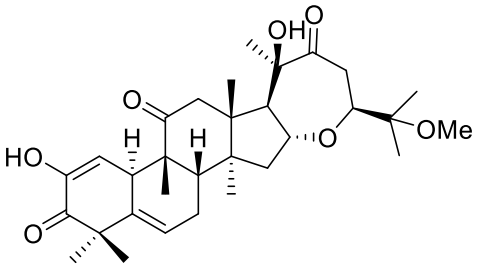
95



96



97



98

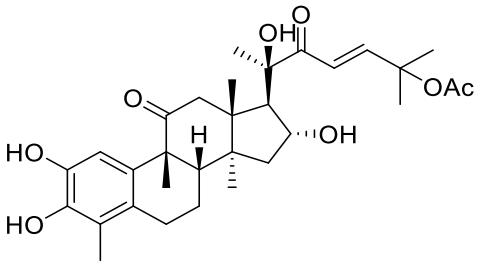
Table 1.2 Norcucurbitacins and other cucurbitacins: Source and structure

Compound	Plant isolated	Structure	Reference
28/ 29 – Norcucurbitacins			
Fevicordin A	*Fevillea cordifolia*	**99**	[23]
Fevicordin A 2-O-glucoside	*Fevillea cordifolia*	**100**	[23]
Fevicordin A 2-O-gentiobioside	*Fevillea cordifolia*	**101**	[23]
Fevicordin B	*Fevillea cordifolia*	**102**	[23]
Fevicordin B 2-O-glucoside	*Fevillea cordifolia*	**103**	[23]
Fevicordin B 2-O-gentiobioside	*Fevillea cordifolia*	**104**	[23]
Fevicordin C 2-O-glucoside	*Fevillea cordifolia*	**105**	[23]
Fevicordin C 2-O-gentiobioside	*Fevillea cordifolia*	**106**	[23]
Fevicordin D 2-O-glucoside (Cayaponoside C)	*Fevillea cordifolia*	**107**	[23]
Fevicordin D 2-O-gentiobioside	*Fevillea cordifolia*	**108**	[23]
Fevicordin E 2-O-glucoside	*Fevillea cordifolia*	**109**	[23]
Fevicordin E 2-O-gentiobioside	*Fevillea cordifolia*	**110**	[23]
Fevicordin F 2-O-gentiobioside	*Fevillea cordifolia*	**111**	[23]
Andirobicin A 2-O-glucoside	*Fevillea trilobata*	**112**	[23]
Andirobicin A 2-O-gentiobioside	*Fevillea trilobata*	**113**	[23]
Andirobicin B 2-O-glucoside (Cayaponoside C_2)	*Fevillea trilobata*	**114**	[23]
Andirobicin C 2-O-gentiobioside	*Fevillea trilobata*	**115**	[23]
Cayaponoside A_3	*Cayaponia tayuya*	**116**	[23]
Cayaponoside A_4	*Cayaponia tayuya*	**117**	[23]
Cayaponoside A_5	*Cayaponia tayuya*	**118**	[23]
Cayaponoside A_6	*Cayaponia tayuya*	**119**	[23]
Cayaponoside B	*Cayaponia tayuya*	**120**	[23]
Cayaponoside B_2	*Cayaponia tayuya*	**121**	[23]
Cayaponoside B_3	*Cayaponia tayuya*	**122**	[23]
Cayaponoside B_5	*Cayaponia tayuya*	**123**	[23]
Cayaponoside C_4	*Cayaponia tayuya*	**124**	[23]

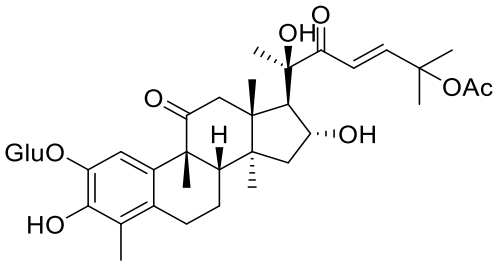
Cayaponoside C_{5b}	*Cayaponia tayuya*	**125**	[23]
Cayaponoside D	*Cayaponia tayuya*	**126**	[23]
Cayaponoside D_1	*Cayaponia tayuya*	**127**	[23]
Cayaponoside D_2	*Cayaponia tayuya*	**128**	[23]
Cayaponoside A_1	*Cayaponia tayuya*	**129**	[23]
Cayaponoside B_{6a}	*Cayaponia tayuya*	**130**	[23]
Cayaponoside B_{6b}	*Cayaponia tayuya*	**131**	[23]
Cayaponoside C_3	*Cayaponia tayuya*	**132**	[23]
Cayaponoside D_{3a}	*Cayaponia tayuya*	**133**	[23]
Cayaponoside D_{3b}	*Cayaponia tayuya*	**134**	[23]
Cabenosides A	Roots of *Caput nigri*	**135**	[23]
Cabenosides B	Roots of *Caput nigri*	**136**	[23]
Siraitic acids A	*Siraitia grosvenori*	**137**	[23]
Siraitic acids B	*Siraitia grosvenori*	**138**	[23]
Siraitic acids C	*Siraitia grosvenori*	**139**	[23]
Siraitic acids D	*Siraitia grosvenori*	**140**	[23]
Siraitic acids E	*Siraitia grosvenori*	**141**	[23]
Other cucurbitacins			
Momordicosides F_1	*Momordica charantia*	**142**	[23]
Momordicosides F_2	*Momordica charantia*	**143**	[23]
Momordicosides G	*Momordica charantia*	**144**	[23]
Momordicosides I	*Momordica charantia*	**145**	[23]
Momordicosides K	*Momordica charantia*	**146**	[23]
Momordicosides L	*Momordica charantia*	**147**	[23]
Momordicines I	*Momordica charantia*	**148**	[23]
Momordicines II	*Momordica charantia*	**149**	[23]
Momordiciens III	*Momordica charantia*	**150**	[23]
Goyaglycosides A	*Momordica charantia*	**151**	[23]
Goyaglycosides B	*Momordica charantia*	**152**	[23]
Goyaglycosides C	*Momordica charantia*	**153**	[23]
Goyaglycosides D	*Momordica charantia*	**154**	[23]
Goyaglycosides E	*Momordica charantia*	**155**	[23]
Goyaglycosides F	*Momordica charantia*	**156**	[23]
Goyaglycosides G	*Momordica charantia*	**157**	[23]
Goyaglycosides H	*Momordica charantia*	**158**	[23]
Picfeltarraegenins I	*Picria feltarrae*	**159**	[23]
Picfeltarraegenins II	*Picria feltarrae*	**160**	[23]
Picfeltarraegenins III	*Picria feltarrae*	**161**	[23]
Picfeltarraegenins IV	*Picria feltarrae*	**162**	[23]
Picfeltarraegenins V	*Picria feltarrae*	**163**	[23]
Picfeltarraegenins VI	*Picria feltarrae*	**164**	[23]
Picfeltarraenone	*Picria feltarrae*	**165**	[23]
Carnosiflosides I	*Hemsleya carnosiflora*	**166**	[23]

Carnosiflosides II	*Hemsleya carnosiflora*	**167**	[23]
Carnosiflosides III	*Hemsleya carnosiflora*	**168**	[23]
Carnosiflosides IV	*Hemsleya carnosiflora*	**169**	[23]
Carnosiflosides V	*Hemsleya carnosiflora*	**170**	[23]
Carnosiflosides VI	*Hemsleya carnosiflora*	**171**	[23]
Scandenosides R1	*Hemsleya panacis-scandens*	**172**	[23]
Scandenosides R2	*Hemsleya panacis-scandens*	**173**	[23]
Scandenosides R3	*Hemsleya panacis-scandens*	**174**	[23]
Scandenosides R4	*Hemsleya panacis-scandens*	**175**	[23]
Scandenosides R5	*Hemsleya panacis-scandens*	**176**	[23]
Scandenosides R6	*Hemsleya panacis-scandens*	**177**	[23]
Scandenosides R7	*Hemsleya panacis-scandens*	**178**	[23]
Scandenosides R8	*Hemsleya panacis-scandens*	**179**	[23]
Scandenosides R10	*Hemsleya panacis-scandens*	**180**	[23]
Scandenosides R11	*Hemsleya panacis-scandens*	**181**	[23]
Siamenoside I	*Siraitia siamensis*	**182**	[23]
5α,6α-Epoxymogroside IE_1	*Momordica grosvenori*	**183**	[23]
Foetidissimosides E	Roots of *Cucurbita foetidissima*	**184**	[23]
Foetidissimosides F	Roots of *Cucurbita foetidissima*	**185**	[23]
Hydroxyhebevinogenin	*Hebeloma vinosophyllum*	**186**	[23]
Methoxyhebevinogenin	*Hebeloma vinosophyllum*	**187**	[23]
Kinoins A	*Ibervillea sonorae*	**188**	[23]
Kinoins B	*Ibervillea sonorae*	**189**	[23]
Kinoins C	*Ibervillea sonorae*	**190**	[23]
Rosacea acids A	*Russula rosacea*	**191**	[23]
Rosacea acids B	*Russula rosacea*	**192**	[23]
Lepida acid A	*Russula lepida*	**193**	[23]
Cordifolin A	*Fevillea cordifolia*	**194**	[23]
Cordifolin A glycoside	*Fevillea cordifolia*	**195**	[23]
Cordifolin B	*Fevillea cordifolia*	**196**	[23]
Cordifolin C	*Fevillea cordifolia*	**197**	[23]
Cabenosides D	*Caput nigri*	**198**	[23]
Cabenosides E	*Caput nigri*	**199**	[23]
Cabenosides F	*Caput nigri*	**200**	[23]
Cabenosides G	*Caput nigri*	**201**	[23]
Cabenosides H	*Caput nigri*	**202**	[23]
Cabenosides I	*Caput nigri*	**203**	[23]
Cabenosides J	*Caput nigri*	**204**	[23]
Cabenosides K	*Caput nigri*	**205**	[23]
Cabenosides L	*Caput nigri*	**206**	[23]
Bryoniosides A	*Bryonia dioica*	**207**	[23]
Bryoniosides B	*Bryonia dioica*	**208**	[23]
Bryoniosides C	*Bryonia dioica*	**209**	[23]

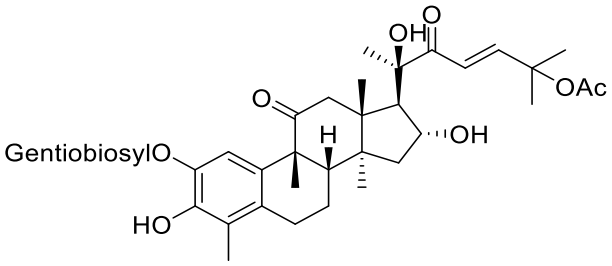
Bryoniosides D	*Bryonia dioica*	**210**	[23]
Bryoniosides E	*Bryonia dioica*	**211**	[23]
Bryoniosides F	*Bryonia dioica*	**212**	[23]
Bryoniosides G	*Bryonia dioica*	**213**	[23]
Lovenone	*Adalaria loveni*	**214**	[23]
Neocucurbitacin A	*Luffa operculata*	**215**	[23]
Neocucurbitacin B	*Luffa operculata*	**216**	[23]
Cucurbitacin U gentiobioside	Seeds of *Fevillea cordifolia*	**217**	[23]
Cucurbitacin V gentiobioside	Seeds of *Fevillea cordifolia*	**218**	[23]
Khekadaengoside L -aglycone	Fruits of *Trichosanthes tircuspidata*	**219**	[23]
Elaeocarpucin A	*Elaeocarpucin chinensis*	**220**	[34]
Elaeocarpucin B	*Elaeocarpucin chinensis*	**221**	[34]
Elaeocarpucin C	*Elaeocarpucin chinensis*	**222**	[34]
Elaeocarpucin D	*Elaeocarpucin chinensis*	**223**	[34]
Elaeocarpucin E	*Elaeocarpucin chinensis*	**224**	[34]
Elaeocarpucin F	*Elaeocarpucin chinensis*	**225**	[34]
Elaeocarpucin G	*Elaeocarpucin chinensis*	**226**	[34]
Elaeocarpucin H	*Elaeocarpucin chinensis*	**227**	[34]
Mogroside I E-1	*Elaeocarpus glabripetalus*	**228**	[35]
5R,6R-Epoxyinogroside I E-1	*Elaeocarpus glabripetalus*	**229**	[35]
19-norlanosta-5,24-diene-11-one	*Elaeocarpus hainanensis*	**230**	[36]
16α,23α-epoxy-3β,20β-dihydroxy-10αH,23βH-cucurbit-5,24-dien-11-one	*Elaeocarpus hainanensis*	**231**	[36]
16α,23α-epoxy-3β,20β-dihydroxy-10αH,23βH-cucurbit-5,24-dien-11-one 3-O-β-$_D$-glucopyranoside	*Elaeocarpus hainanensis*	**232**	[36]



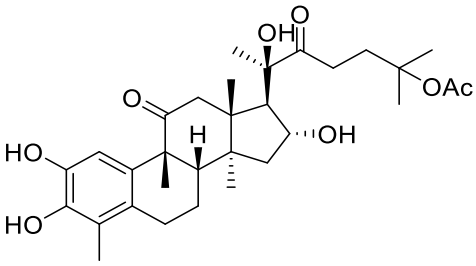
99



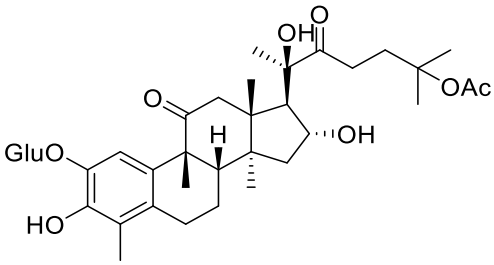
100



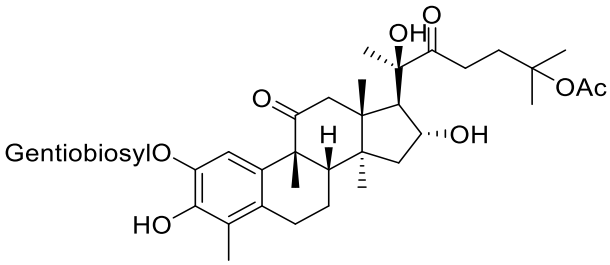
101



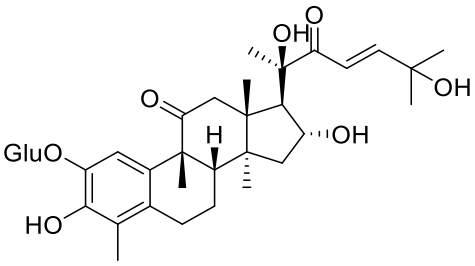
102



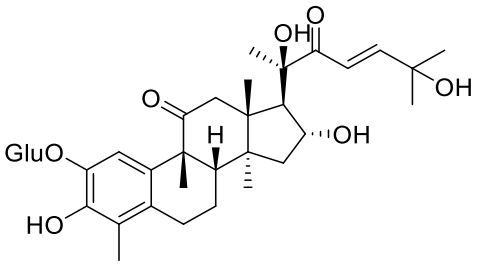
103



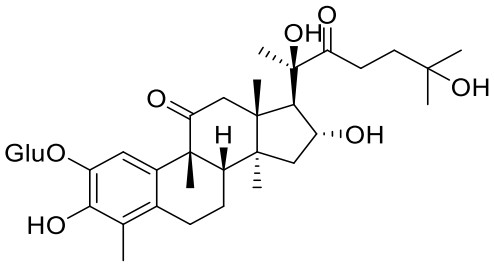
104



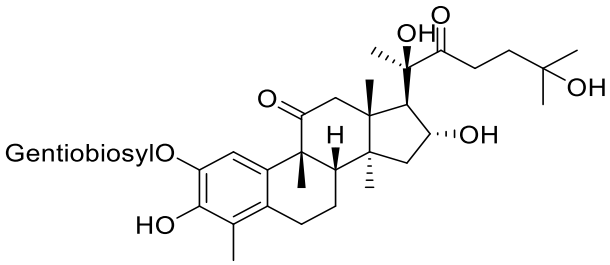
105



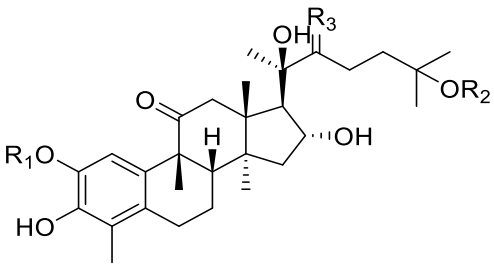
106



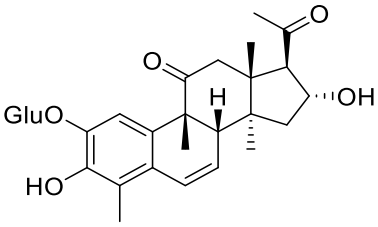
107



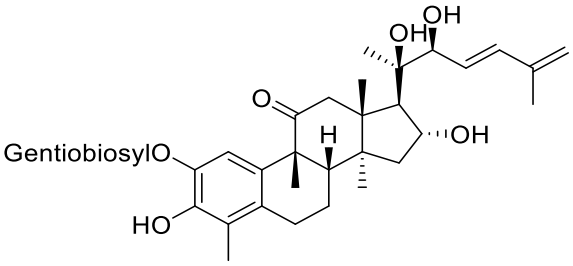
108



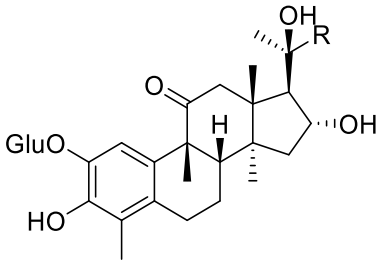
109 R_1=Glu, R_2=H, R_3=H,H
110 R_1=Gentiobiosyl, R_2=H, R_3=H,H
111 R_1=Gentiobiosyl, R_2=H, R_3=bOH,H
112 R_1=Glu, R_2=Me, R_3=OH,H
113 R_1=Gentiobiosyl, R_2=Me, R_3=bOH,H

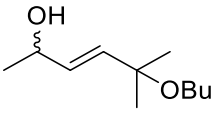


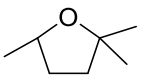
114

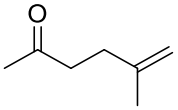


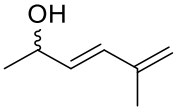
115

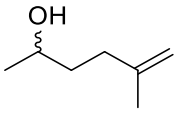


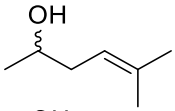
116


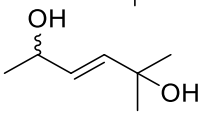
117


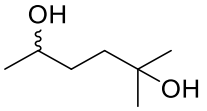
119


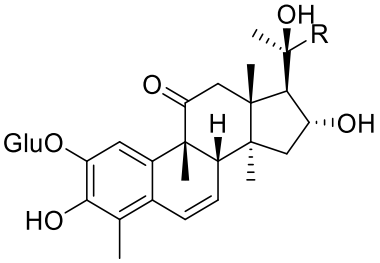
120


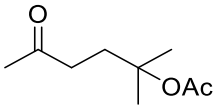
121


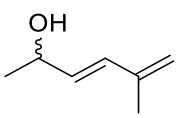
122


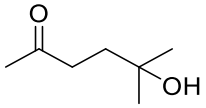
126


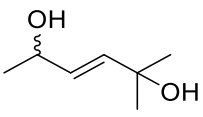
127


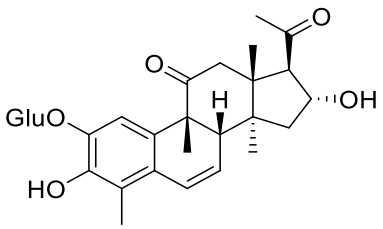


118


123


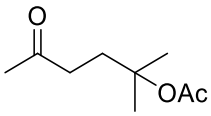
125


128


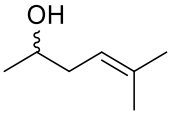


124

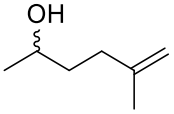
129



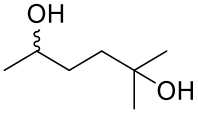
130



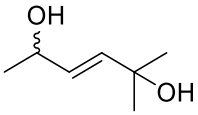
131



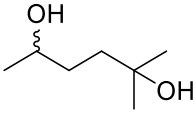
132

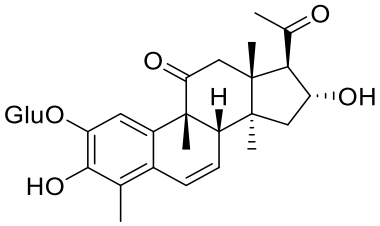


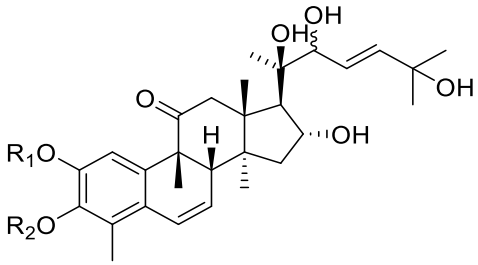
133



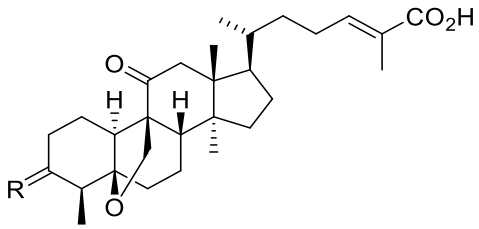
134



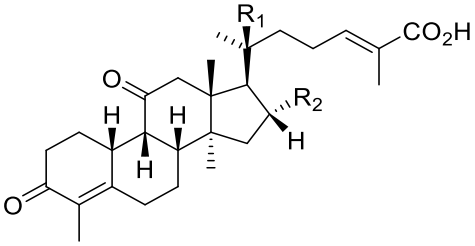




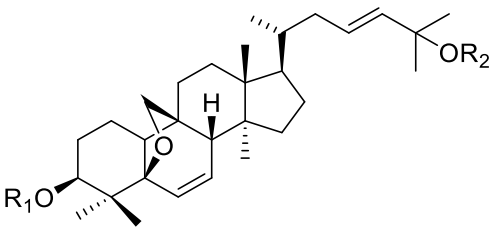
135 R_1=Glu, R_2=Glu
136 R_1=Glu(1-2)Glu, R_2=H



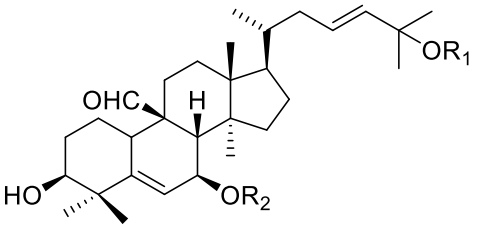
137 R=bOH, H
138 R=O



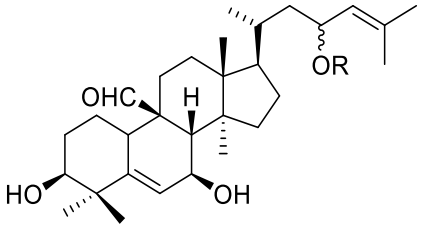
139 R_1=H, R_2=H
140 R_1=OH, R_2=H
141 R_1=H, R_2=OH



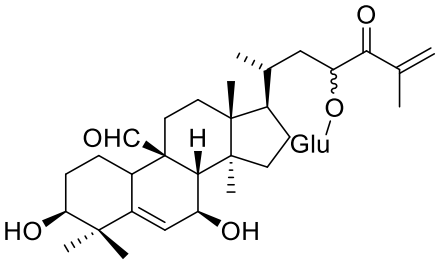
142 R_1=Glu, R_2=CH_3
143 R_1=b-D-allopyranosyl, R_2=H
144 R_1=b-D-allopyranosyl, R_2=CH_3
145 R_1=Glu, R_2=H



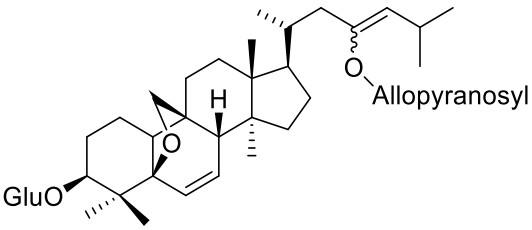
146 R_1=CH_3, R_2=Glu
147 R_1=H, R_2=Glu



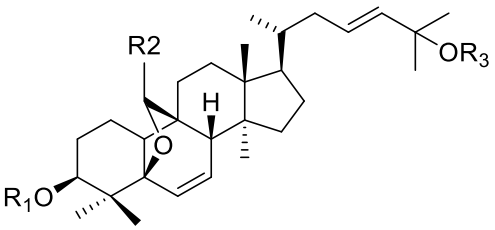
148 R=H
149 R=Glu



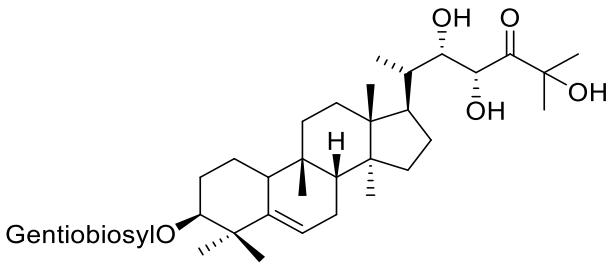
150



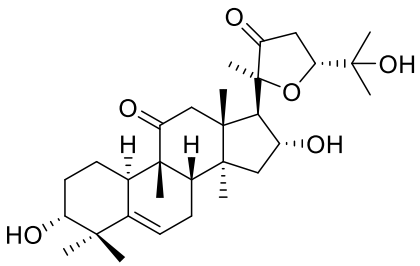
156



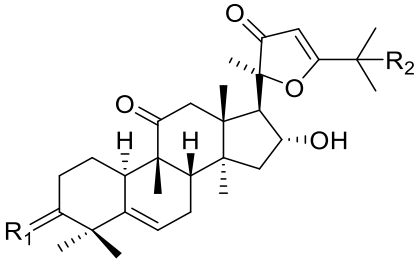
151 R_1=Glu, R_2=OMe, R_3=H
152 R_1=b-D-Allopyranosyl, R_2=OMe, R_3=H
153 R_1=Glu, R_2=OMe, R_3=Me
154 R_1=b-D-Allopyranosyl, R_2=OMe, R_3=Me
155 R_1=b-D-Allopyranosyl, R_2=H, R_3=Glu
157 R_1=b-D-Allopyranosyl, R_2=OMe, R_3=Glu



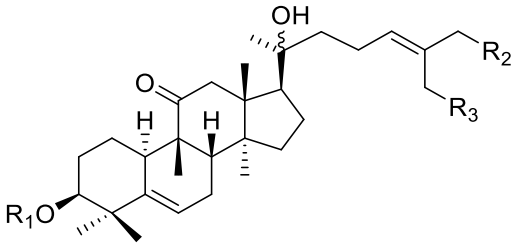
158



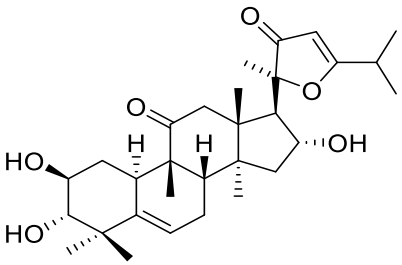
160



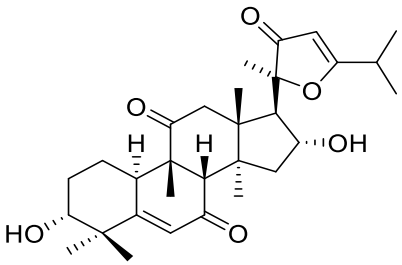
159 R_1=H,aOH, R_2=H
161 R_1=H,aOH, R_2=OH
164 R_1=H,aOAc, R_2=H
165 R_1=O, R_2=H



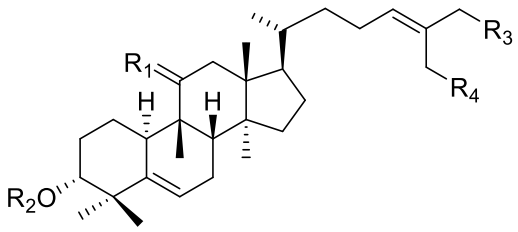
172 R_1=Glu, R_2=OH, R_3=H
173 R_1=Glu, R_2=H, R_3=OH
174 R_1=Glu, R_2=O-Glu, R_3=H
175 R_1=Glu, R_2=H, R_3=O-Glu



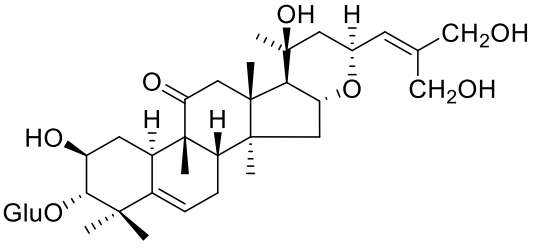
162



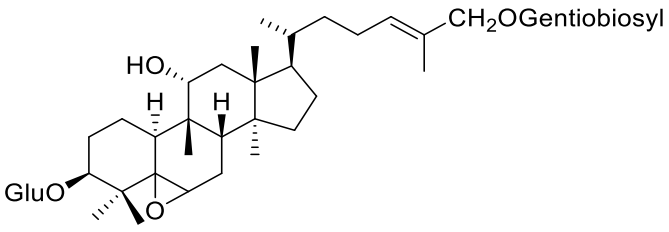
163



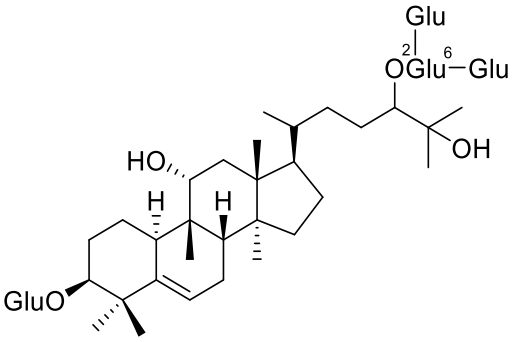
166 R_1=O, R_2=H, R_3=O-Gentiobiosyl, R_4=H
167 R_1=O, R_2=Glu, R_3=O-Sophorosyl, R_4=H
168 R_1=O, R_2=Glu, R_3=O-Gentiobiosyl, R_4=H
169 R_1=O, R_2=Glu, R_3=H, R_4=O-Gentiobiosyl
170 R_1=aOH,H, R_2=Glu, R_3=O-Sophorosyl, R_4=H
171 R_1=aOH,H, R_2=Glu, R_3=O-Gentiobiosyl, R_4=H
176 R_1=O, R_2=Glu, R_3=H, R_4=O-Sophorosyl
177 R_1=aOH,H, R_2=Glu, R_3=H, R_4=O-Sophorosyl
178 R_1=bOH,H, R_2=Glu, R_3=O-Gentiobiosyl, R_4=H
179 R_1=O, R_2=Glu, R_3=O-Glu, R_4=H



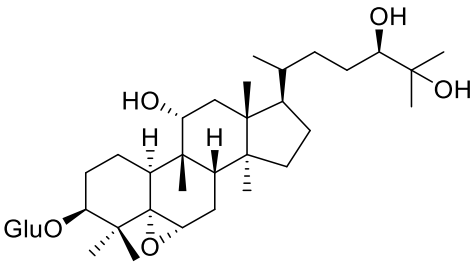
180



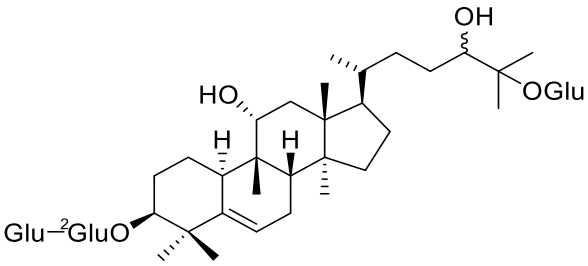
181



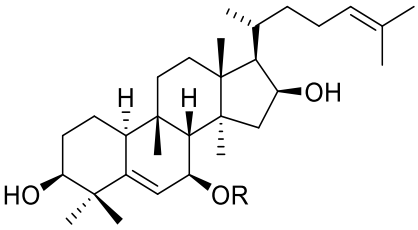
182



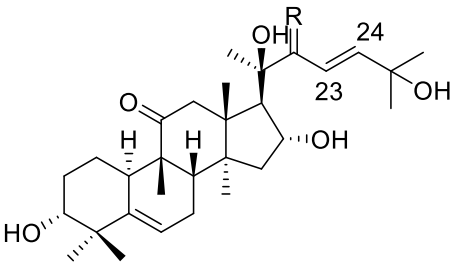
183



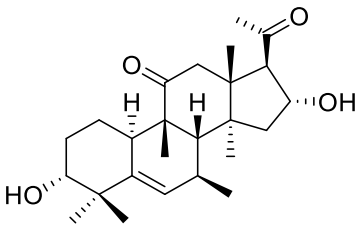
184/185



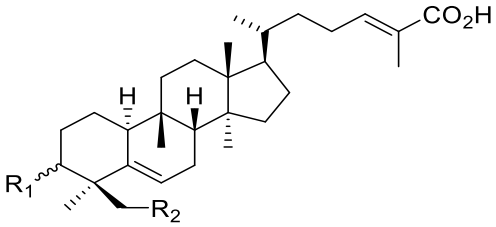
186 R=H, **187** R=Me



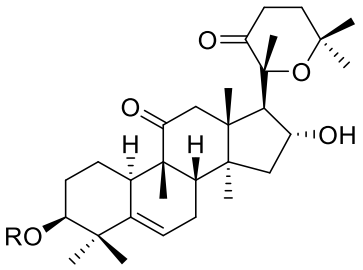
188 R=bOH, H
189 R=O, 23,24-dihydro



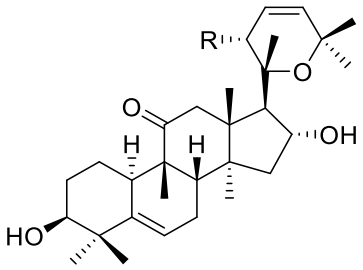
190



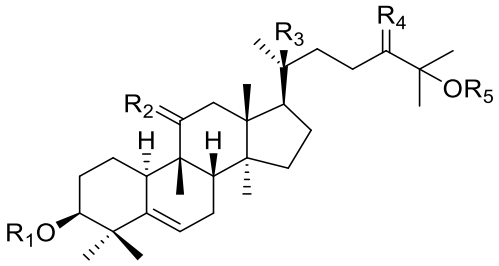
191 R_1=aOH, R_2=OH
192 R_1=aOH, R_2=H
193 R_1=bOH, R_2=H



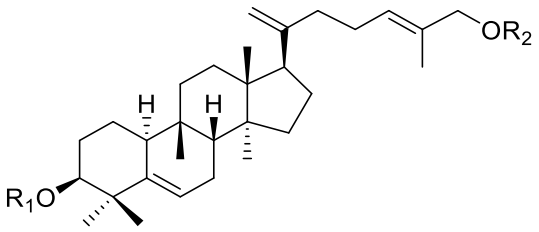
194 R=H, **195** R=Gentiobiosyl



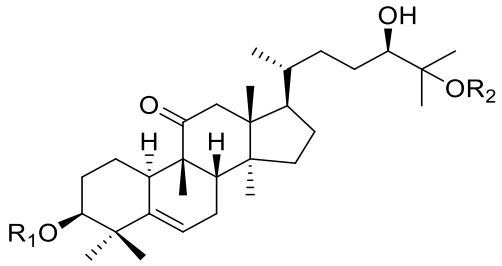
196 R=OH, **197** R=H



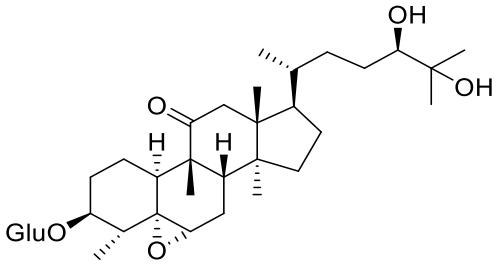
198 R_1=Glu, R_2=O, R_3=H, R_4=OH, H, R_5=H
199 R_1=Glu, R_2=aOH, H, R_3=H, R_4=O, R_5=Glu
200 R_1=Sophorosul, R_2=aOH, H, R_3=H, R_4=O, R_5=Glu
201 R_1=Gentiobiosyl, R_2=aOH, H, R_3=H, R_4=O, R_5=Glu
202 R_1=Gentiobiosyl, R_2=O, R_3=H, R_4=O, R_5=Glu
203 R_1=Glu, R_2=aOH, H, R_3=OH, H R_4=Glu
204 R_1=Sophorosyl, R_2=aOH, H, R_3=OH, R_4=OH, H, R_5=Glu



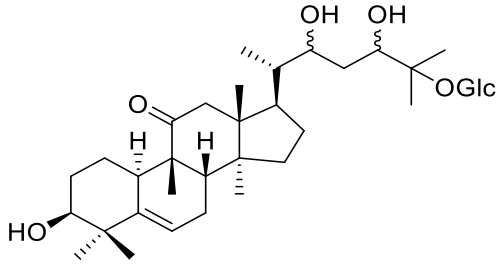
205 R_1=Gentiobiosyl R_2=Glu
206 R_1=Gentiobiosyl R_2=Gentiobiosyl



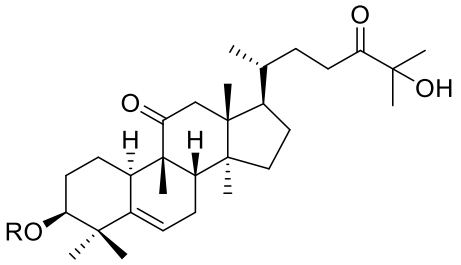
207 R_1=H R_2=Glu
208 R_1=a-L-rhamnopyranosyl(1-2)Glu R_2=H
209 R_1=a-L-rhamnopyranosyl(4-Ac)(1-2)Glu R_2=H



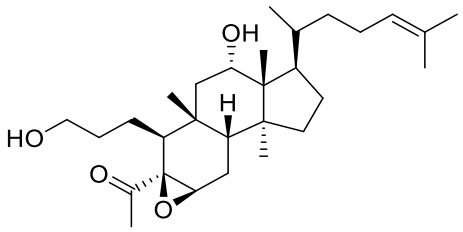
210



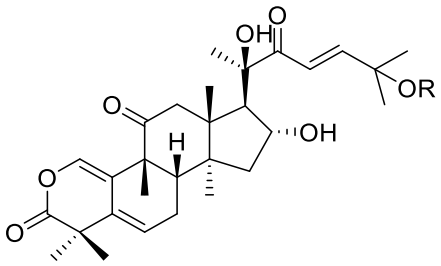
211



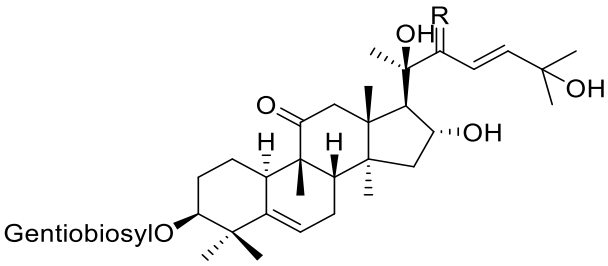
212 R=Glu
213 R=a-L-rhamnopyranosyl (1-2)Glu



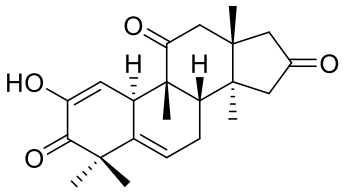
214



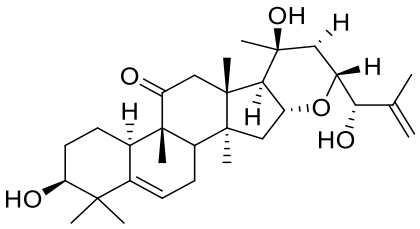
215 R=Ac, **216** R=H



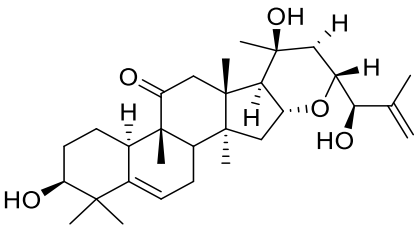
217 R=O, **218** R=H;23,24-dihydro



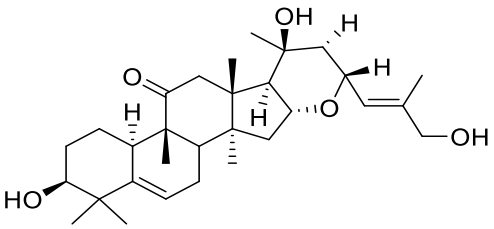
219



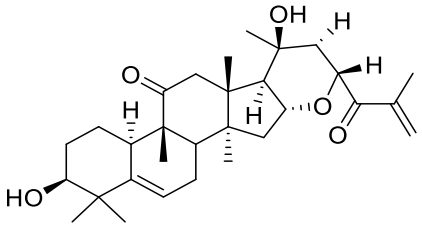
220



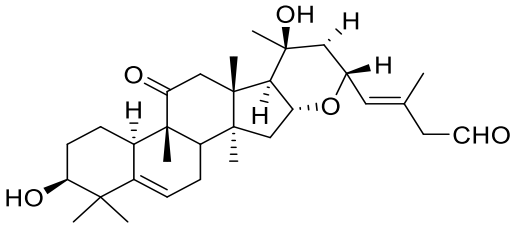
221



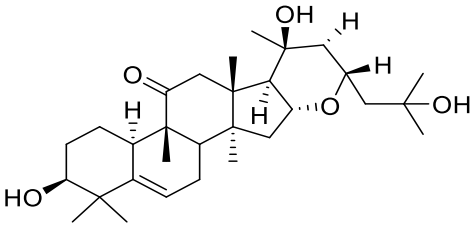
222



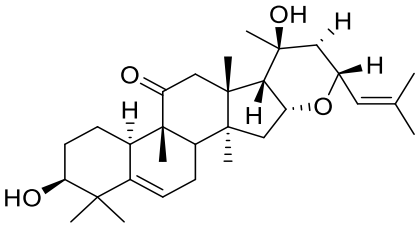
223



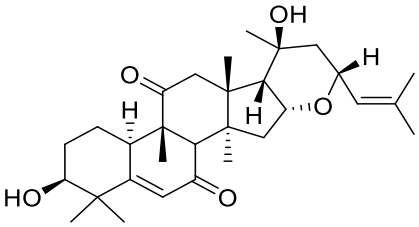
224



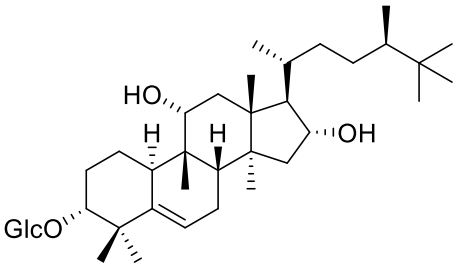
225



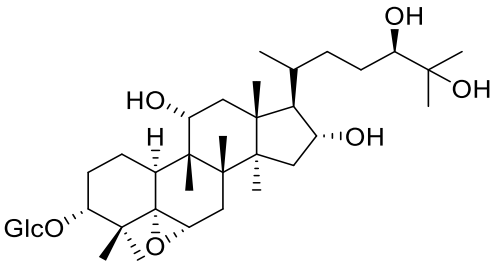
226



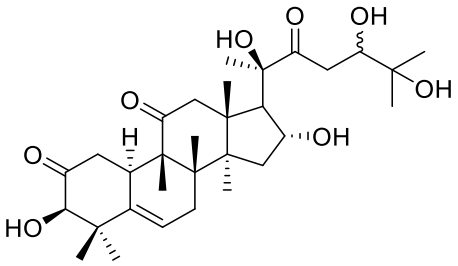
227



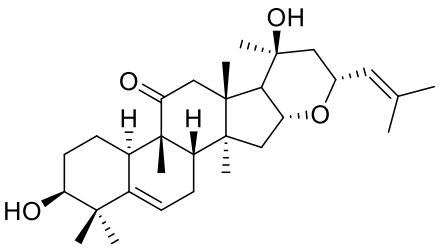
228



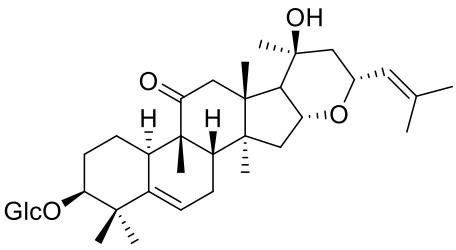
229



230



231



232

1.5 The Genus *Elaeocarpus*

The name *Elaeocarpus* was derived from two Greek words, which means as an olive-shaped fruit, i.e., *elaeo* meaning olive and *carpus* meaning fruit. The *Elaeocarpacea* family has about 12 genera and 550 species. Among the flowering plants of *Elaeocarpacea* family, *Elaeocarpus* is the largest genus of the 12 genera. The genus *Elaeocarpus* are typically distributed in tropical and subtropical areas excluding Africa, and their origin is believed to be developed from Malaysia. Local Malay name for *Elaeocarpus* is sengkurat but it is usually known as medang, which is not specific for this genus.[37]

A woody plant of the *Elaeocarpus* is medium-sized tree being about 20 to 100 feet tall with diameter not more than 60 m. They grow on fertile and well-drained soil with sufficient water under the full sun. The leaves have rough edges with about 5 to 6 inches long and about 2 inches thick and are oval in shape. The bark can be cracked with the interior colour of yellow-brown and exterior colour of pink, grey and brown. The flowers with high fragrance are about half inch in diameter, white in colour and bisexual with dense spikes or fringed petals. The high fragrance and attractiveness of flowers attract insects and undergo pollination. The flowers then bear small olive-like fruits with blue in colour. The colour of the fruit attracts birds to help dispersing the seeds of the plant.[38]

Although the genus *Elaeocarpus* comprises of about 360 species, the number of species used for medicinal purposes is limited. There are many types of secondary metabolites found in *Elaeocarpus* including alkaloids, flavonoids and triterpenoids.[39]

1.5.1 *Elaeocarpus petiolatus*

Elaeocarpus petiolatus is the plant species investigated in the present study. It is a tropical and subtropical medium-sized evergreen tree growing up to 12 m tall. It has bole with short buttresses, granular yellow inner bark, apical buds coated with resin, and broad leaves with 5 to 9 veins on each side. It is widely spread in tropical forests in the Malay Peninsula, southern China, India, New Zealand, Fiji, and Hawaii in the east at elevations up to 1,300 meters.[40,41]

It is said that juice from the leaves was used to treat fever that was caused by malaria and sunstroke. Extracts from the roots were also used to treat fever.[41] In 2012, Kwon *et al.* reported that the ethanol extract of *Elaeocarpus petiolatus* showed anti-inflammatory activity via inhibition of inflammatory mediators such as prostaglandin, tumor necrosis factor-α, and interleukins in Raw264.7 cells stimulated with lipopolysaccharide.[40] In this study, the leaves and bark of *Elaeocarpus petiolatus* (Figure 1.12) were investigated separately as the amount and types of cucurbitacins may vary between plant parts.



Figure 1.12 Bark and leaves of *Elaeocarpus petiolatus*, collected in Kajang, Selangor, Malaysia

1.5.2 Cucurbitacins from *Elaeocarpus*

To date, about 150 compounds have been isolated from the genus *Elaeocarpus* and some of the compounds showed cytotoxic activities. Most of the cytotoxic activities shown were attributed to cucurbitacins. However, only five out of 550 species of *Elaeocarpus* have been studied and found to produce cucurbitacins. The list of isolated cucurbitacins is shown in Table 1.3.

Table 1.3 Cucurbitacins from *Elaeocarpus*

Plant isolated	Compound	Structure	Reference
Elaeocarpus dolichostylus	Cucurbitacin F	41	[9]
	Hexanorcucurbitacin F	51	
	23,24-dihydrocucurbitacin F	43	
Elaeocarpus chinensis	Elaeocarpucin A	216	[34]
	Elaeocarpucin B	217	
	Elaeocarpucin C	218	
	Elaeocarpucin D	219	
	Elaeocarpucin E	220	
	Elaeocarpucin F	221	
	Elaeocarpucin G	222	
	Elaeocarpucin H	223	
	Cucurbitacin D	20	
	3-*epi*-isocucurbitacin D	22	
	25-O-acetylcucurbitacin F	42	
	Cucurbitacin I	63	
	16α,23α-epoxy-3β,20β-dihydroxy-10αH,23βH-cucurbit-5,24-dien-11-one	1	
Elaeocarpus glabripetalus	Cucurbitacin D	20	[35]
	Mogroside I E-1	224	
	5R,6R-Epoxyinogroside I E-1	225	
Elaeocarpus hainanensis	16α,23α-epoxy-3β,20β-dihydroxy-10αH,23βH-cucurbit-5,24-dien-11-one	1	[36]
	16α,23α-epoxy-3β,20β-dihydroxy-10αH,23βH-cucurbit-5,24-dien-11-one 3-O-β-$_D$-glucopyranoside	2	
	16α,23α-epoxy-3β,20β-dihydroxy-10αH,23βH-cucurbit-5-ene-11-one 3-O-β-$_D$-glucopyranoside	226	
	19-norlanosta-5,24-diene-11-one	227	
	Cucurbitacin D	20	
	Cucurbitacin F	41	
	Cucurbitacin O	81	
	Cucurbitacin G	60	

	3-*epi*-isocucurbitacin G	62	
	Cucurbitacin I	63	
Elaeocarpus mastersii	Cucurbitacin D	20	[42]
	Cucurbitacin F	41	

1.6 Anti-cancer Application of Phytochemicals

Cancer is the second leading cause of death after cardiovascular disease and causes one in eight deaths worldwide. In, 2015 the number of cancer deaths were 8.7 million globally and in between 2005 and 2015, incident cancer cases increased by 33%. The number of cancer deaths globally is expected to increase from 7.1 million in 2002 to 11.5 million in 2030.[4,43]

Chemotherapy is used for cancer treatment. However, it has several limitations such as side-effects, drug resistance and toxicity towards normal cells. Lacking specificity towards cancer cells is also one of the limitations of chemotherapy drugs. Due to this, some people have resorted to the use of herbs or medicinal plants as therapeutic alternatives.[8] For instance, in the United States, approximately 50-60% of cancer patients utilize bioactive components derived from different plant parts in addition to the traditional therapeutic regimen such as chemotherapy and radiation therapy. Just to name a few phytochemicals used as cancer chemopreventive and treatment agents, they are: apigenin from parsley, curcumin from turmeric, cyanidins and resveratrol from grapes, epigallocatechin gallate and tea polyphenols from green tea, fisetin from strawberries and apples, genistein from soybean, gingerol from gingers, lycopene from tomato, rosmarinic acid from rosemary, vitamin D from mushroom, vitamin E from plant oil, and triterpenoids from wax-like coatings of fruits and medicinal herbs.[44]

1.6.1 Mechanism of action involved in cancer chemoprevention and treatment

1. Apoptotic mechanisms initiated by phytochemicals

The characteristics of the apoptotic cell include nuclear fragmentation, blebbing, and cell shrinkage. Apoptotic pathways can be divided into receptor-mediated (extrinsic) pathway and mitochondria-mediated (intrinsic) pathway. The extrinsic pathway involves cross-linking of death receptors with their ligands (e.g. CD95L, TRAIL and TNF-α) resulting sequential activation of caspase-8 and caspase-3, which links target proteins to result apoptosis. The intrinsic pathway stimuli, such as ROS, DNA-damaging reagents, or Ca^{2+} mobilizing stimuli directly or indirectly activate mitochondrial pathway to induce formation of apoptosome composed of cytochrome c, Apaf-1 and caspase-9, which activates caspase-3 and in turn results apop tosis.[45]

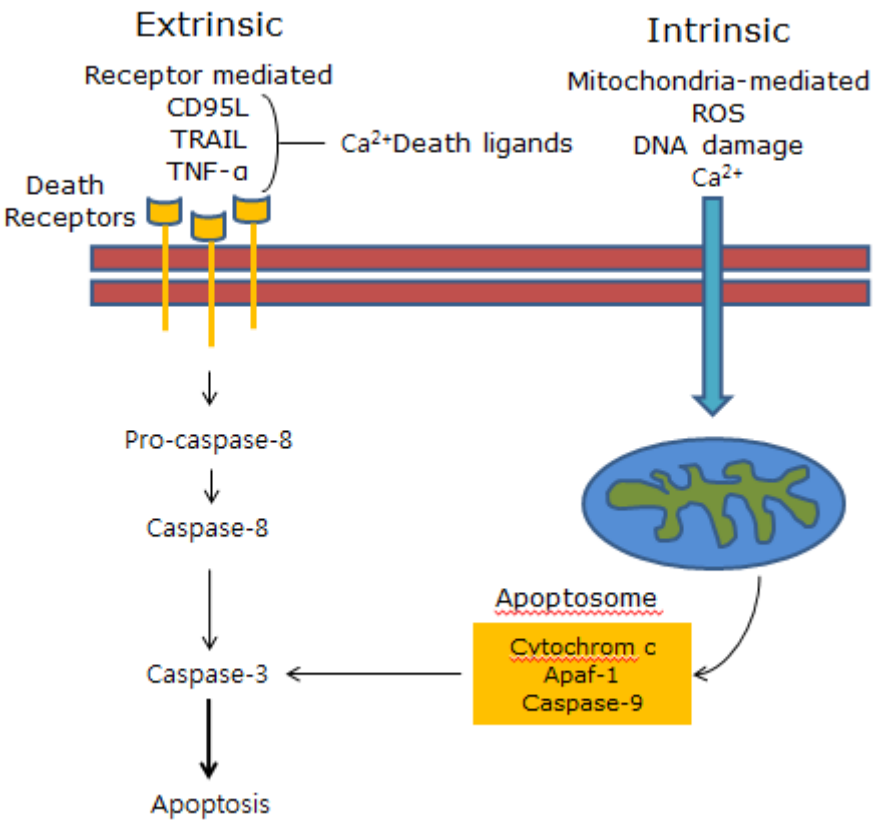


Figure 1.13 Extrinsic and intrinsic apoptotic pathway

Many phytochemicals were previously used as anti-inflammatory or anti-viral agents until the understanding of cancer mechanism gets deepened to reveal for their anti-tumor activity targeting on

apoptotic pathways in cancer. [46] In many types of cancer, apoptosis is a common phenomenon and is a critical step in preventing tumorigenesis and therapy resistance. Hence, apoptotic pathways are relevant targets for cancer therapies. Many bioactive compounds have been identified and most of them are plant secondary metabolites such as cucurbitacins, alkaloids and flavonoids. Some of them kill tumor cells by apoptosis induction and in 2013, Li-Weber reviewed apoptotic pathways in cancer triggered by traditional Chinese medicine.[44,45]

2. Cyclooxygenases-2

Cyclooxygenase (COX) is an enzyme that catalyzes conversion of arachidonic acid into PGH_2. Both COX-1 and COX-2 are isoenzymes while COX-1is constitutive and constantly being transcribed at a basal rate to release low amount of prostaglandin in different parts of tissue, COX-2 is inducible and normally low in most cells but when there are inflammatory signal, such as interleukins and cytokines, COX-2 is highly regulated and massive prostaglandin is released. COX-2 is elevated in 80-90% of colorectal and other cancers with larger tumor size and poor survival and therefore, it is proposed to be a nutritional target for colon cancer prevention. Cucurbitacin E isolated from *Citrullus lannatus var. citroides* inhibited both COX enzymes with more selectivity toward COX-2. [47]

3. Signal transducer and activator of transcription 3

Signal transducer and activator of transcription 3 (STAT3) is a cytoplasmic transcription factor that mediates the responsiveness of cell stimuli and plays a key role in many cellular processes such as apoptosis and cell growth. In response to cytokines and growth factors, it is activated through phosphorylation of tyrosine 705 and serine 727 and form homo or heterodimers that translocate to the cell nucleus. In cancer cells, constitutive activation of STAT3 is affiliated with poor diagnosis and has anti-apoptotic and proliferative effects. Cucurbitacins inhibits STAT3 in solid tumors.[48]

4. Other mechanisms

Besides the mechanisms mentioned above, there are many others that have not been mentioned. For example, mevalonate pathway may alter Ras signaling that can be inactivated by lycopene, the human epidermal growth factor receptor (HER2) in breast cancer prevention may be targeted by extra-virgin olive oil; hypoxia-induced factor-1α and matrix metalloproteinase-9 expression in colon cancer cells may be reduced by resveratrol, and many more.[44]

1.6.2 Cytotoxicity or anti-proliferative property of cucurbitacins

Cucurbitacins, work as chemical pheromones to protect plants from external invasion, first attracted attention in biological activity in 1960s.[49] They have shown promising anticancer activities, such as anti-proliferation, apoptosis and cell cycle arrest (Table 1.4). Among the apoptotic effects of cucurbitacins, the most significant mechanisms are their modification of mitochondrial transmembrane potential and transcriptional activities by nuclear genes or factors to activate/inhibit the pro/anti-apoptotic proteins.[12] Among the mechanisms tested on cucurbitacins, Janus kinase/signal transducer and activator of transcription 3 signaling pathway showed the most promising inhibition.[12] Cucurbitacin was a hot topic in drug discovery community and medicinal chemistry for its cytotoxic behavior. However, under strict medical control, non-specific and indirect cytotoxicity of cucurbitacin was substantially hindered and hence more studies are essential in order to unleash its anticancer application.[34,50–52]

Table 1.4 Cucurbitacins isolated from different plant species and their cytotoxic activities on human cancer cells

Cucurbitacin	Effectiveness on cancer cell lines	Mechanisms of action	Structure	Reference
Cucurbitacin A ***Trichosanthes cucumerina***	Lung: A549		7	[53]
Cucurbitacin B ***Trichosanthes cucumerina***	Breast: MCF7, SKBR2, T47D and MDA-MB435 Lung: A549, SK LU1 and NCI-H460 Colon: HCT-116 and COCA-2 Brain: SF-268	↓COX-2	10	[53–55]
Cucurbitacin E (Elaterin) Roots of ***Wilbrandia ebracteata*** Cucurbitacin E – glucoside ***Citrullus colocynthis***	Breast: MCF7 Lung: NCI-H460 Colon: HCT-116 Brain: SF-268 Prostate: PC-3 Liver: HepG2	↓COX-2	35	[12,53]
Cucurbitacin D (Elatericin A) Roots of ***Trichosanthes kirilowii***	Breast: MCF7 Lung: NCI-H460 Colon: HCT-116 Brain: SF-268	↓COX-2	20	[12,29,53]
Dihydrocucurbitacin B ***Wilbrandia ebracteata***	Breast: MCF7, SW620, SMMC-7721 and K562 Colon: HCT-116 and Hke3	↓COX-2	15	[12]
Cucurbitacin I (Elatericin B) ***Ecballium elaterium*** Cucurbitacin I - glucoside ***Ecballium elaterium***	Breast: MCF7, MDA-MB-231 and MDA-MB-468 Lung: NCI-H460 Colon: HCT-116 Brain: SF-268	↑Apoptosis ↓phospho-STAT3 ↓COX-2	63	[12,53,56]
Cucurbitacin Q ***Brandegea bigelovii***	Lung: A549 Breast: MDA-MB435 and MDA-MB453		83	[12,57]
Cucurbitacin R ***Cayaponia tayuya***	Colon: HCT-116 and Hke3		21	[12]

1.7 Significance and Objectives of the Study

There are approximately 27 species of *Elaeocarpus* that are native to the Malay Peninsula. However, to date there is no report on the cucurbitacin composition of any of the Malaysian *Elaeocarpus* species. This has led to the search for cucurbitacin-containing *Elaeocarpus* species occurring in Malaysia. The primary aim of this project was therefore to investigate the cucurbitacin composition of the leaves and bark of *Elaeocarpus petiolatus* as well as to probe the cytotoxic property of the selected cucurbitacins obtained. The specific objectives of the present project are:

1) To sequentially extract the ground leaf and bark materials with *n*-hexane and ethyl acetate.
2) To fractionate and purify triterpenoids from the ethyl acetate crude extract using chromatographic methods.
3) To characterize and elucidate the structures of the isolated compounds via spectroscopic techniques.
4) To assess the cytotoxic activity of the isolated cucurbitacins on a panel of human cancer cell lines.

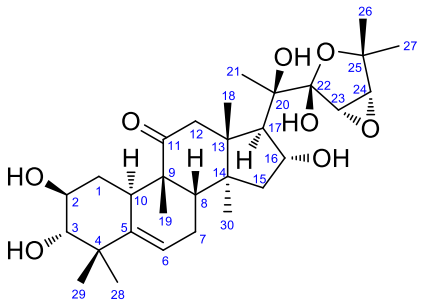
Chapter Two
Results and Discussion

2.1 Overview

From the dried-ground leaves and bark of *Elaeocarpus petiolatus*, eight cucurbitacins, i.e., **1-8**, along with β-sitosterol (**9**) and vomifoliol (**10**), were isolated. Compounds **4-7**, **9** and **10** were obtained from the leaves, while compounds **1-3** and **5-8** were obtained from the bark of *E. petiolatus*. Compounds **1-4** represent new cucurbitacins, while compounds **5-10** are known compounds. The structures of compounds **5-10** were determined primarily by comparing their spectroscopic data with published literature values. They were determined to be 16α,23α-epoxy-3β,20β-dihydroxy-10αH,23βH-cucurbit-5,24-dien-11-one (**5**),[36] 16α,23α-epoxy-3β,20β-dihydroxy-10αH,23βH-cucurbit-5,24-dien-11-one 3-O-β-$_D$-glucopyranoside (**6**),[36] elaeocarpucin F (**7**),[34] hexanocucurbitacin F (**8**),[58] β-sitosterol (**9**),[59] and vomifoliol (**10**).[60]

2.2 Structure Eucidation

2.2.1 Compound **1**



1

Compound **1** was initially obtained as a colorless oil and subsequently crystallized from $CHCl_3$/MeOH as light yellowish block crystals: mp 180-182 °C, with $[\alpha]^{23.5}_D$ +28 (*c* 0.9, $CHCl_3$). The UV spectrum showed no UV absorption, while the IR spectrum indicated the presence of OH (3408 cm^{-1}) and

carbonyl (1689 cm^{-1}) functions. The molecular formula of compound **1** was determined to be $C_{30}H_{46}O_8$, on the basis of HRESIMS measurements (*m/z* 535.32516, MH^+).

Table 2.1 ^1H and ^{13}C NMR data of compound **1**[a]

Position	δ_H (*J* in Hz)	δ_C
1	1.08, m	33.3
	1.87, m	
2	3.57, ddd (11.2, 9.7, 4.1)	71.0
3	2.97, d (9.2)	80.9
4		41.9
5		140.6
6	5.73, d (5.8)	119.2
7α	1.97, dd (18.3, 6.1)	23.8
7β	2.38, m	
8	1.92, m	42.5
9		48.2
10	2.33, m	33.9
11		213.7
12α	3.11, d (14.6)	49.2
12β	2.65, d (14.6)	
13		47.6
14		51.8
15α	1.53, d (13.4)	44.3
15β	1.87, m	
16	4.60, dd (8.4, 6.7)	71.2
17	2.42, d (6.4)	56.6
18	0.94, s	19.3
19	1.08, s	20.2
20		77.4
21	1.50, s	24.6
22		106.3
23	3.84, d (2.8)	59.6
24	3.47, d (2.8)	59.7
25		81.2
26	1.34, s	25.3
27	1.39, s	23
28	0.94, s	21.6
29	1.19, s	24.7
30	1.27, s	18.8

[a]$CDCl_3$, 600 MHz (^1H), 150 MHz (^{13}C)

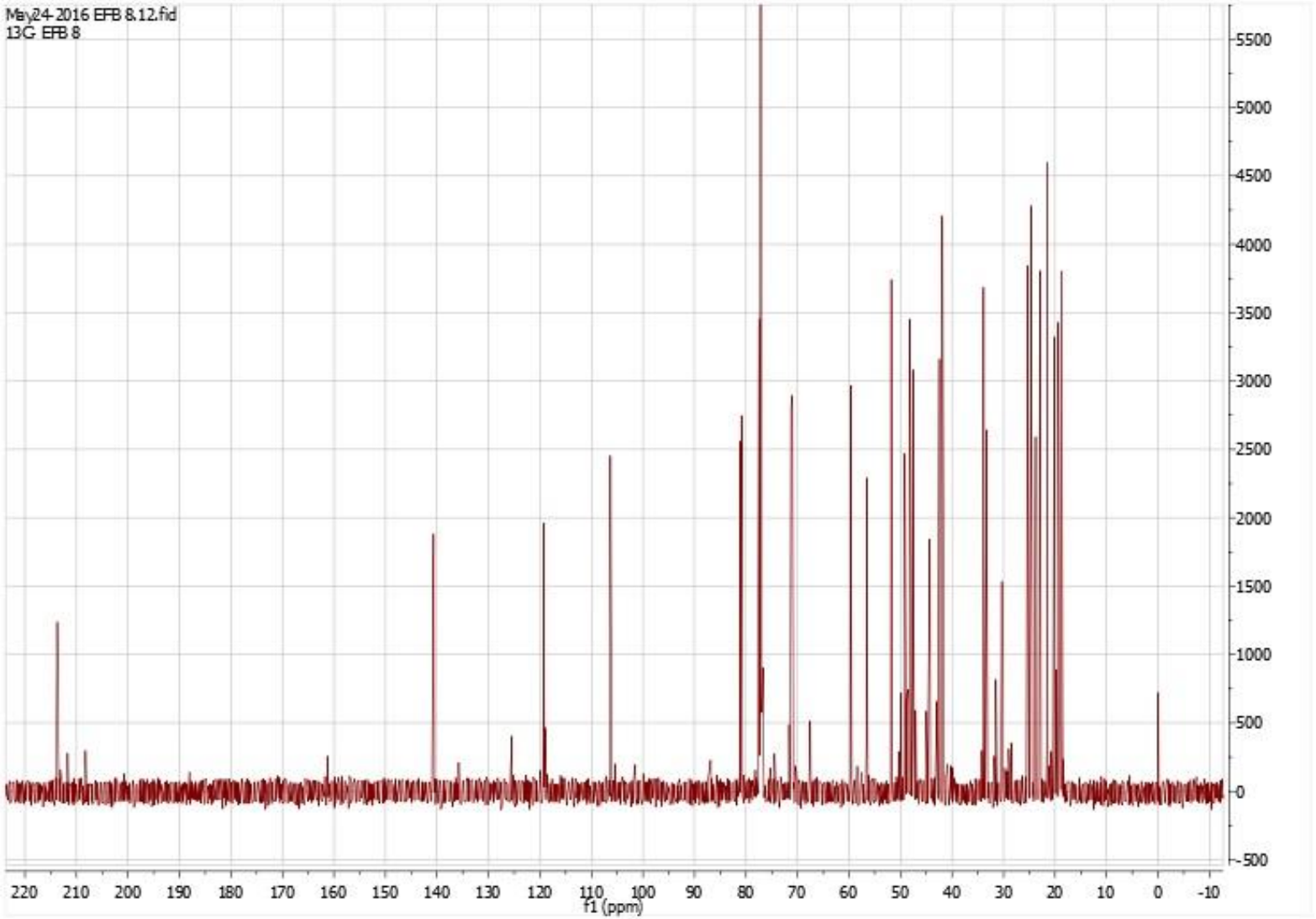


Figure 2.1 ^{13}C NMR spectrum of compound **1** (150 MHz, $CDCl_3$)

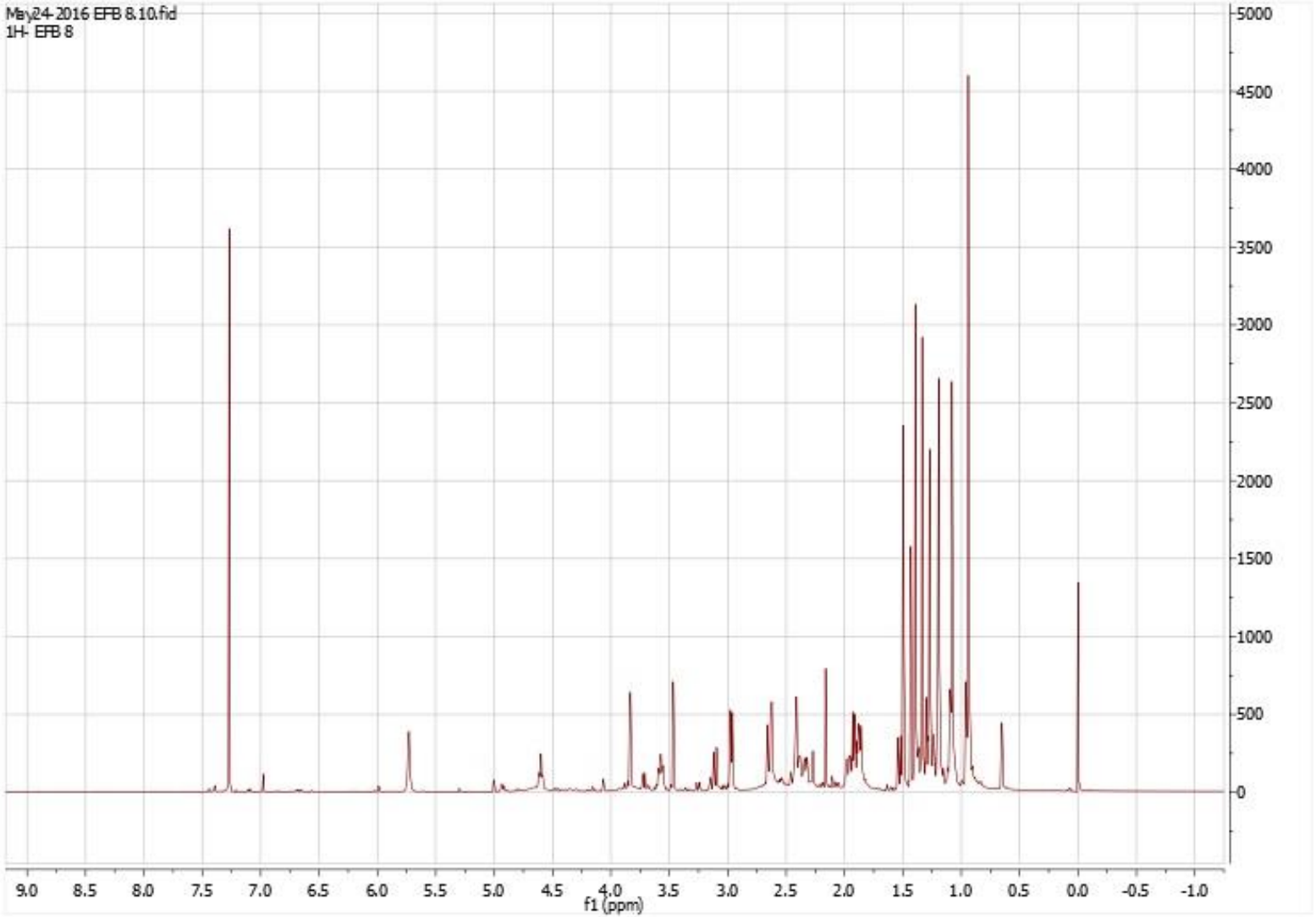


Figure 2.2 ^{1}H NMR spectrum of compound **1** (600 MHz, $CDCl_3$)

The ^{13}C NMR spectrum of compound **1** (Table 2.1 and Figure 2.1) showed a total of 30 resonances, comprising eight methyls, four methylenes, nine methines, and nine carbon atoms with no hydrogen attached. The observed carbon resonance at δ_C 213.7 was consistent with the presence of a ketone, while the resonances at δ_C 119.2 and 140.6 were due to trisubstituted double bond carbons. Additionally, the resonances at δ_C 59.6, 59.7, 71.0, 71.2 and 80.9 were due to five oxymethines, while the resonances at δ_C 77.4, 81.2 and 106.3 were due to two oxygenated tertiary carbons and a hemiketal carbon, respectively. The ^{1}H NMR spectrum of compound **1** (Table 2.1 and Figure 2.2) revealed the presence of eight methyl singlets at δ_H 0.94, 1.08, 1.50, 1.34, 1.39, 0.94, 1.19 and 1.27, a doublet due to an olefinic signal at δ_H 5.73, a pair of AB doublets due to a ketomethylene group at δ_H 2.65 and 3.11, and five oxymethine resonances at δ_H 2.97, 3.47, 3.57, 3.84 and 4.60. The ^{1}H and ^{13}C NMR spectra were somewhat similar to those of cucurbitacin F-type compounds,[23] with the presence of the characteristically deshielded methine triplet of doublets signal at δ_H 4.60 and olefinic doublet signal at δ_H 5.73, due to H-16 and H-6, respectively. There were however several distinct features in the NMR data of compound **1**. The presence of carbon resonances at δ_C 59.6 and 59.7, together with the corresponding hydrogen resonances at δ_H 3.84 and 3.47, indicated the presence of an epoxide group at C-23 and C-24 in place of the double bond usually found at these carbons.[61]

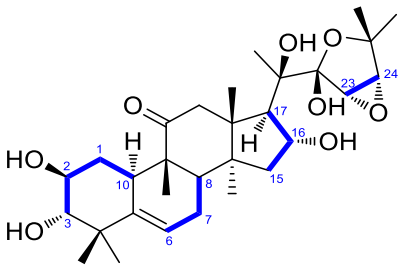


Figure 2.3 Partial structures revealed by COSY and HSQC of compound **1**

In order to obtain detailed structure of compound **1**, 2D NMR data were collected. The COSY (Appendix 1) and HSQC (Appendix 2) data revealed the presence of the $CHCHCH_2CH$, $CHCH_2CH$, CH_2CHCH and CHCH partial structures corresponding to the C-3–C-2–C-1–C-10, C-6–C-7–C-8, C-15–C-16–C-17 and C-23–C-24 fragments in the structure of compound **1** (Figure 2.3).

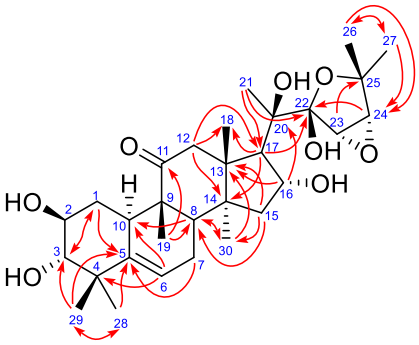


Figure 2.4 Selected HMBC correlations of compound **1**

The HMBC (Appendix 3) data, which correlate hydrogen to carbon that are two or three bonds away, provided firm confirmation for the structure of compound **1** (Figure 2.4). The partial structure of C-10–C-1–C-2–C-3, as revealed by the COSY data, was determined to be linked to C-4 from C-3 based on the correlations from H-29 to C-3, C-5; and from H-28 to C-5. The linkages to C-9 and C-5 from C-10 were based on the correlations from H-1 to C-5; and from H-6 and H-8 to C-10. The partial structure of C-6–C-7–C-8 was determined to be linked to C-5 from C-6 by the correlations from H-6 to C-4 and C-10. On the other hand, the linkages to C-9 and C-14 from C-8 were based on the correlations from H-8 to C-10 and C-30; and from H-15, H-19 and H-30 to C-8. The partial structure of C-15–C-16–C-17 was determined to be linked to C-14 from C-15 by the correlations from H-15 to C-8, C-13 and C-30. The linkages to C-13 and C-20 from C-17 were determined by the correlations from H-17 to C-14, C-18 and C-22; and from H-12 and H-21 to C-17. The presence of the furan partial structure (C-22–C-23–C-24–C-25) was supported by the correlations from H-23 to C-25; from H-17, H-21 and H-24 to C-22; and from H-26 and H-27 to C-24. The methyl C-18 was determined to be attached to C-13 by the correlations from H-12 and H-17 to C-18; attachment of methyl C-19 to C-9 by the correlations from H-19 to C-8 and C-11; attachment of methyl C-21 to C-20 by the correlations from H-21 to C-17 and C-22; attachment of methyls C-26 and C-27 to C-25 by the correlations from H-26 and H-27 to C-24; attachment of methyls C-28 and C-29 to C-4 by the correlations from H-28 and H-29 to C-3 and C-5; and attachment of methyl C-30 at C-14 by the correlations from H-30 to C-8 and C-13, and from H-8 and H-15 to C-30.

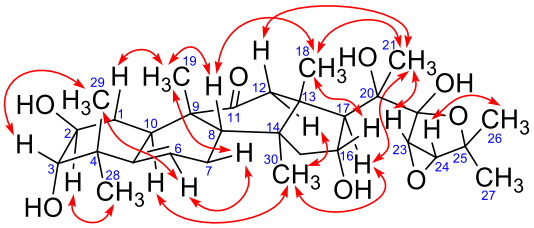


Figure 2.5 Selected NOESY correlations of compound **1**

Furthermore, spatial correlations provided by the NOESY (Appendix 4) data helped to address the stereochemical aspect of the structure of compound **1** (Figure 2.5). The NOEs observed for H-8/CH_3-18, H-8/CH_3-19 and H-16/H-18 revealed that H-8, H-16, CH_3-18 and CH_3-19 are all oriented on the β-face of the structure, thus requiring 16-OH to be α-oriented. On the other hand, NOEs observed for H-10/H-30 and H-17/CH_3-30 revealed H-10, H-17 and CH_3-30 to be oriented on the α-face of the structure, thus requiring the C-17–C-20 bond to be β-oriented. The NOEs observed for H-2/CH_3-28 and H-3/CH_3-29 indicated the 2β-OH and 3α-OH configurations. However, due to free rotation about the C-17–C-20 bond, the stereochemistry of the furan ring (including C-20) relative to the fused tetracyclic core structure could not be established by the NOESY data alone.

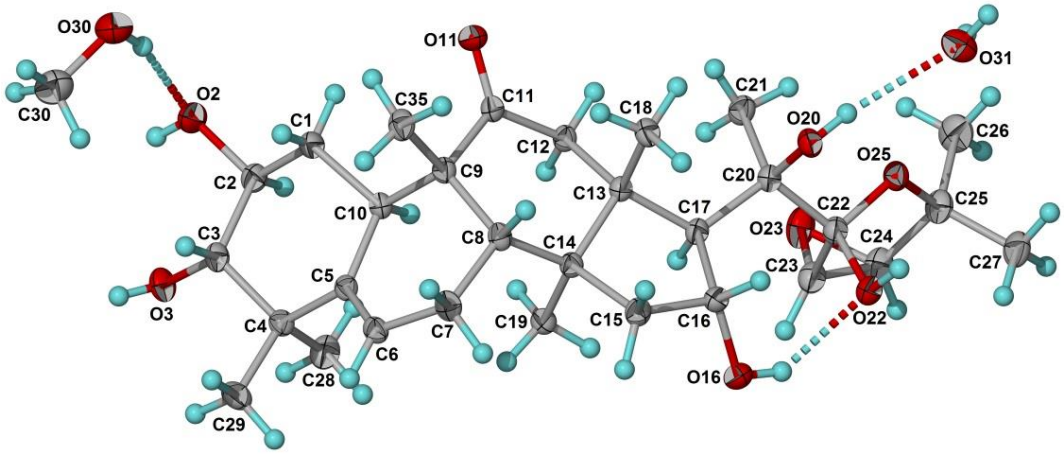


Figure 2.6 X-ray crystal structure of compound **1**

As suitable crystals were obtained for compound **1**, X-ray diffraction analysis using Cu Kα radiation was carried out to determine its absolute configuration (Figure 2.6). Compound **1** formed light yellowish block crystals, with a = 30.0782(5) Å, b = 8.53996(13) Å, c = 11.86480(17) Å, β = 102.2829 (13)°, V = 2977.91(8) Å^3. The X-ray data revealed that the structure proposed for compound **1** based on

analysis of the NMR data is confirmed. The absolute configurations at all stereogenic centres within the fused tetracyclic structure of compound **1** are identical to those in cucurbitacin F and hexanocucurbitacin F (which was also isolated in the present study). Additionally, the absolute configurations of the side chain furan moiety were established as 20*R*, 22*R*, 23*S* and 24*R*.

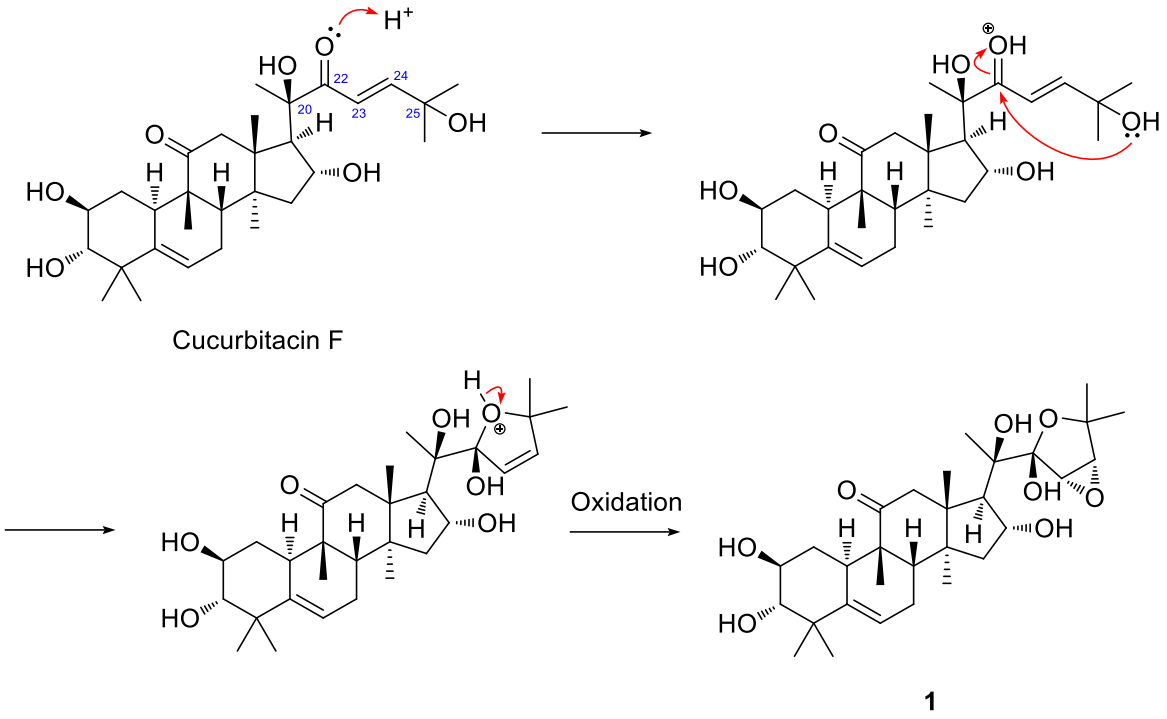
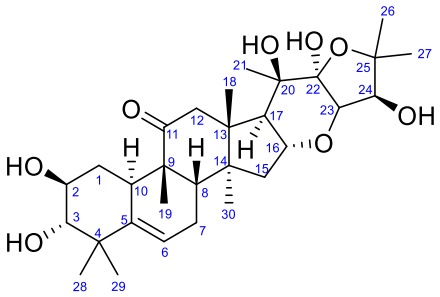


Figure 2.7 Proposed biosynthetic pathway of compound **1**

As mentioned above, the structure of compound **1** is identical to that of cucurbitacin F (Figure 2.7), except for the side chain moiety at C-17. This suggested that both compounds may be biogenetically related with cucurbitacin F being the precursor of compound **1**. A plausible biosynthetic pathway from cucurbitacin F to compound **1** is presented in Figure 3.7. Firstly, a nucleophilic addition of 25-OH onto the ketone group at C-22 constructed the furan moiety with C-22 being *R*-configured (22-OH is β). A subsequent epoxidation step of the C-23,C-24-double bond, which presumably takes place at the α-face since the β-face is more hindered, furnishes compound **1**.

2.2.2 Compound **2**



2

Compound **2** was obtained as a light yellowish oil with $[\alpha]^{23.5}_{D}$ +48 (*c* 0.4, $CHCl_3$). The UV spectrum showed no UV absorption, while the IR spectrum showed bands due to OH (3406 cm^{-1}) and carbonyl (1688 cm^{-1}) functions. The HRESIMS of compound **2** showed a significant pseudo-molecular ion peak at *m/z* 499.30541, which analyzed for $C_{30}H_{42}O_6 + H^+$ and corresponded to ($MH^+ - 2H_2O$). Therefore the molecular formula of compound **2** is $C_{30}H_{46}O_8$.

The ^{13}C NMR spectrum of compound **2** (Table 2.2 and Figure 2.8) showed a total of 30 resonances, comprising eight methyls, four methylenes, nine methines, and nine carbon atoms with no hydrogen attached. The observed quaternary carbon resonance at δ_C 213.7 was consistent with the presence of a ketone, while the resonances at δ_C 119.0 and 140.9 were due to a trisubstituted double bond carbons. Additionally, the resonances at δ_C 70.8, 75.4, 80.4, 80.7 and 86.9 were due to five oxymethines, while the resonances at δ_C 74.3, 87.0 and 105.2 were due to two oxygenated tertiary carbons and a hemiketal carbon, respectively. The ^1H NMR spectrum of compound **2** (Table 2.2 and Figure 2.9) revealed the presence of eight methyl singlets at δ_H 0.927, 0.934, 1.09, 1.18, 1.19, 1.26, 1.36 and 1.38, a doublet due to an olefinic signal at δ_H 5.71, a pair of AB doublets due to a ketomethylene group at δ_H 2.44 and 3.02, and five oxymethine resonances at δ_H 2.93, 3.54, 3.82, 4.04 and 4.47.

Table 2.2 ^{1}H and ^{13}C NMR data of compound **2**[a]

Position	δ_H (*J* in Hz)	δ_C
1	1.08, m	33.1
	1.86, m	
2	3.54, m	70.8
3	2.93, d (9.1)	80.7
4		41.9
5		140.9
6	5.71, d (5.9)	119
7α	1.92, dd (18.8, 6.1)	23.8
7β	2.39, m	
8	1.96, m	42.6
9		48.8
10	2.28, m	33.7
11		213.7
12α	3.02 d (14.8)	48
12β	2.44 d (14.8)	
13		48.9
14		47.7
15α	1.40, m	40.3
15β	1.82, m	
16	4.47, td (9.8, 2.3)	75.4
17	2.42, d (8.9)	50.4
18	0.927, s	19.8
19	1.09, s	20.7
20		74.3
21	1.26, s	20.3
22		105.2
23	4.04, s	86.9
24	3.82, s	80.4
25		87
26	1.36, s	25
27	1.38, s	28.6
28	0.934, s	21.5
29	1.18, s	24.6
30	1.19, s	20.3

[a]$CDCl_3$, 600 MHz (^{1}H), 150 MHz (^{13}C)

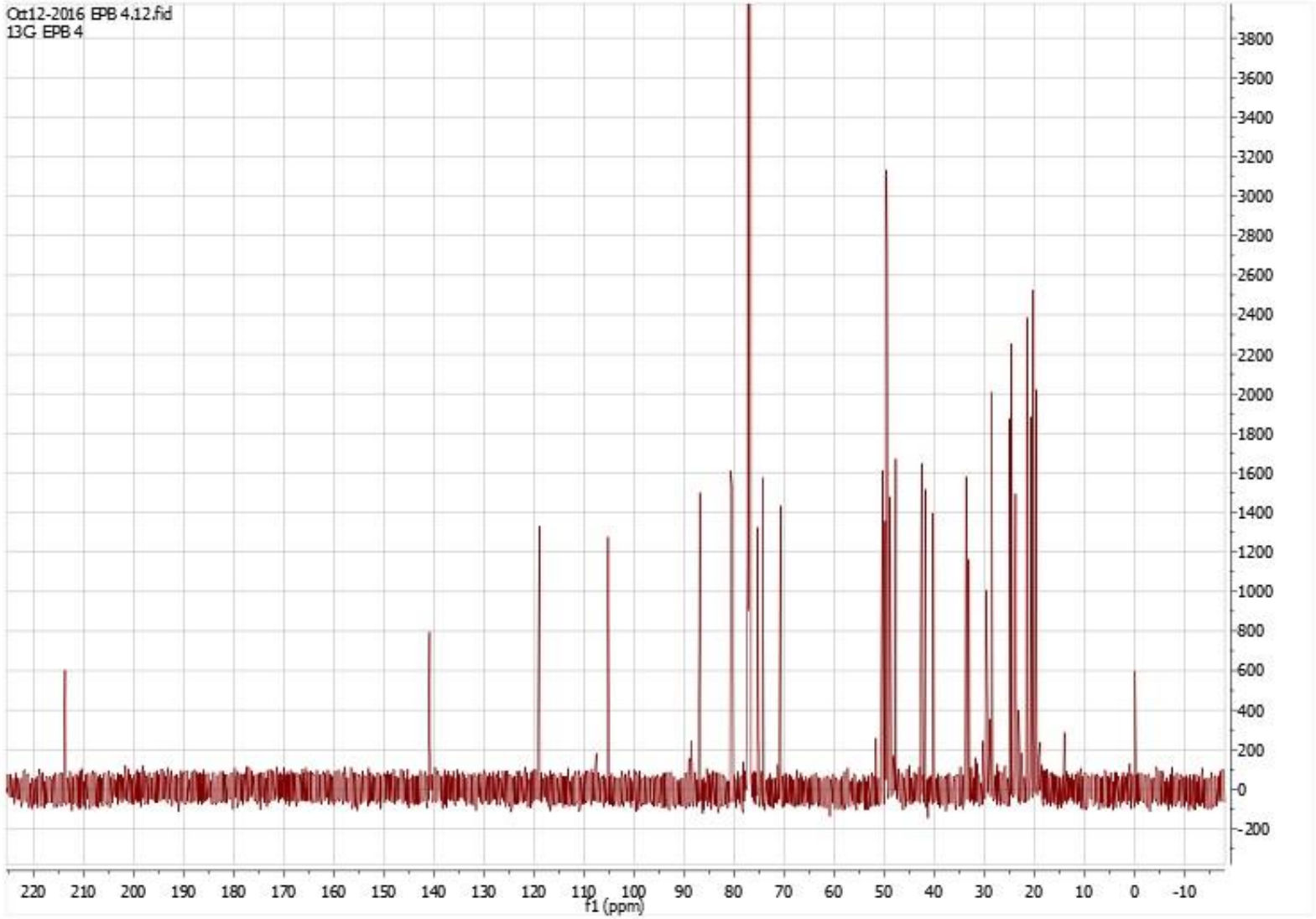


Figure 2.8 ^{13}C NMR spectrum of compound **2** (150 MHz, $CDCl_3$)

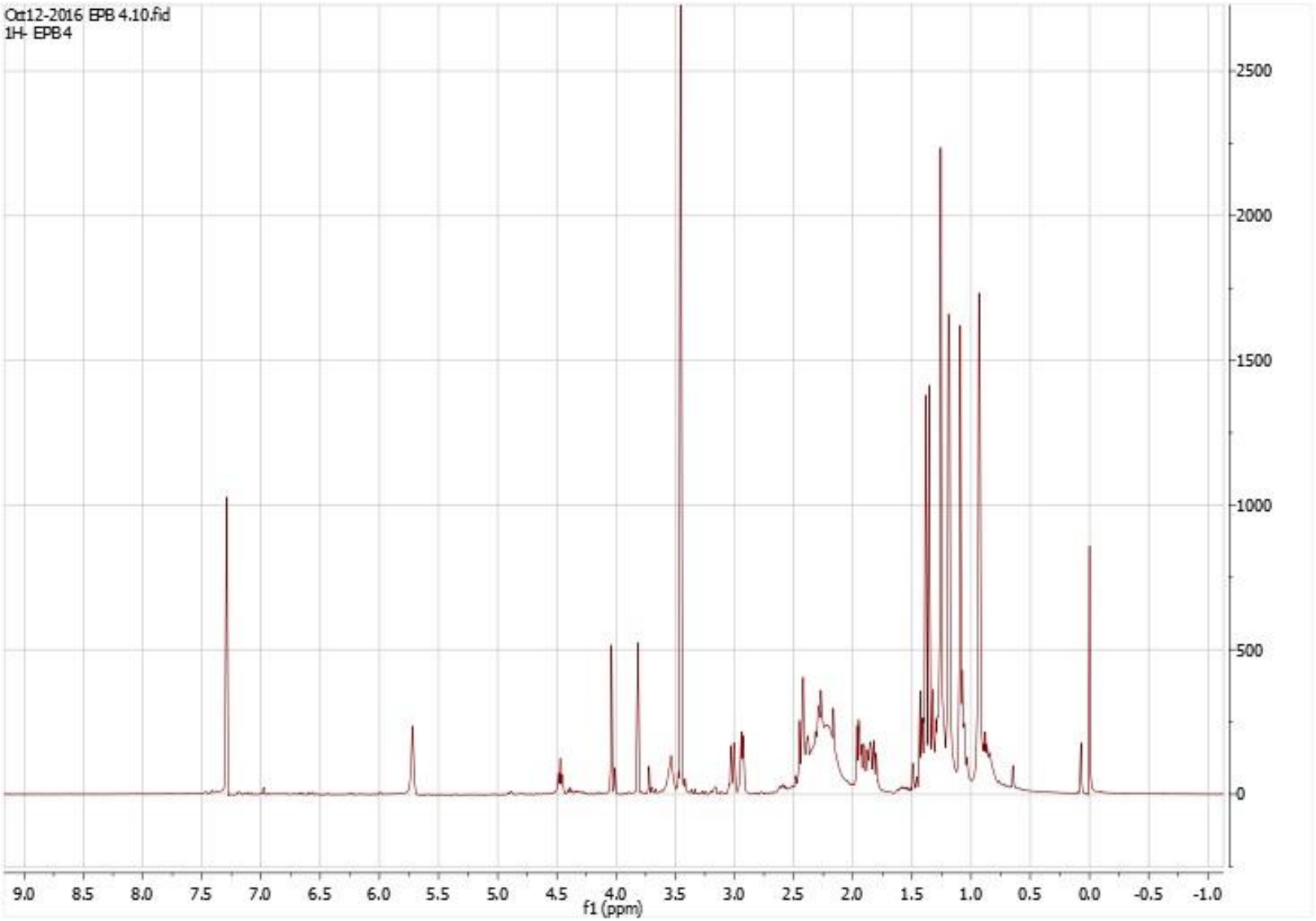


Figure 2.9 ^{1}H NMR spectrum of compound **2** (600 MHz, $CDCl_3$)

The ^{1}H and ^{13}C NMR spectra were somewhat similar to those of compound **1**, with the presence of the characteristically deshielded methine triplet of doublets signal at δ_H 4.47 and olefinic doublet signal at δ_H 5.71, due to H-16 and H-6, respectively. There were however several notable differences in the NMR data of compound **2** when compared with those of compound **1**. The H-16 oxymethine signal at δ_H 4.60 in compound **1** was shifted upfield to δ_H 4.47 in compound **2**, while the H-23 and H-24 oxymethine signals at δ_H 3.84 and 3.47 in compound **1** were shifted downfield to δ_H 4.04 and 3.82, respectively, in compound **2**. Additionally, the CH_3-21 singlet at δ_H 1.50 in compound **1** was shifted upfield to δ_H 1.26 in compound **2**, while the chemical shifts of the other seven methyls were essentially unchanged. The ^{13}C NMR data of the two compounds were also largely similar except for the absence of the epoxide carbon signals at δ_H 59.6 and 59.7 (due to C-23 and C-24 of compound **1**), which in the spectrum of compound **2**, have been replaced by signals at δ_H 86.9 and 80.4, respectively. Other notable differences in the chemical shifts between compounds **1** and **2** ($\Delta\delta_C$ > 3 ppm) involved C-16, C-17, C-20, C-21, C-25 and C-27. These observations indicated that a major change has occurred in the side chain and the hydroxyl group at C-16 of the cucurbitacin molecule in compound **1**.

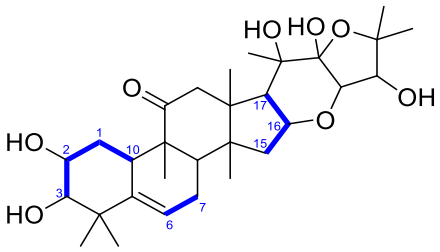


Figure 2.10 Partial structures revealed by COSY and HSQC of compound **2**

The COSY (Appendix 5) and HSQC (Appendix 6) data of compound **2** (Figure 2.10) revealed partial structures that corresponded to the A, B, C and D rings of the fused tetracyclic cucurbitane core also present in compound **1**. The fused tetracyclic core in compound **2** was further supported by the HMBC data (Figure 2.11), while the stereochemistry of the fused tetracyclic core was also determined to be identical to that in compound **1** by the NOESY data (Figure 2.12).

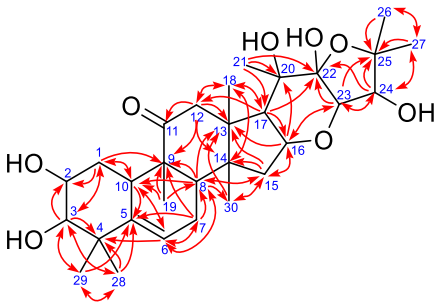


Figure 2.11 Selected HMBC correlations of compound **2**

The HMBC (Appendix 7) correlations from H-16 to C-23 and from H-23 to C-16 suggested that a fifth fused ring (pyran ring E) is present in compound **2**, constructed by linking C-16 and C-23 via an ether bond. This suggestion is consistent with the observation that the epoxide carbons in compound **1** (C-23 and C-24; δ_H 59.6 and 59.7) were replaced with oxymethine carbons that resonated at δ_H 86.9 and 80.4 in compound **2**. The presence of the pyran moiety in compound **2** is also in agreement with other HMBC correlations, i.e., from H-16 to C-20; from H-17 to C-22; from H-21 to C-17, C-20 and C-22; and from H-23 to C-22. Consequently, the side chain furan moiety present in compound **1** is now inferred to be the sixth fused ring (furan ring F) in compound **2**, which is supported by the HMBC correlations observed from H-23 to C-22 and C-24; from H-24 to C-22, C-23, and C-27; and from H-27 to C-24 and C-26.

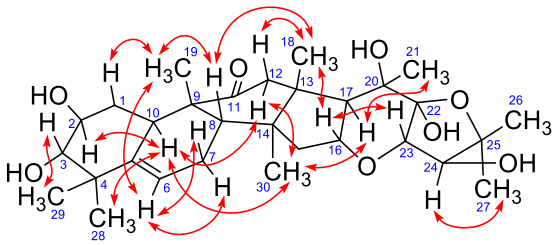


Figure 2.12 Selected NOESY correlations of compound **2**

The NOESY data (Appendix 8 and Figure 2.12) revealed some of the stereochemical aspects associated with the fused pyran and furan rings. The NOEs observed for H-16/H-18 and H-16/H-23 required H-23 to be β-oriented, while the NOEs observed for H-17/CH_3-30 and H-17/CH_3-21 required CH_3-21 to be α-oriented (20-OH is β-oriented). The absence of NOE interaction between H-23 and H-24 inferred that

H-24 is α-oriented (24-OH is β-oriented). The configuration at C-22 could not be determined with certainty. However, based on the proposed origin of compound **2**, 22-OH is speculated to be α-oriented (vide infra).

As with compound **1**, cucurbitacin F is also proposed to be the precursor of compound **2** (Figure 2.13). However, unlike compound **1**, nucleophilic addition of 25-OH onto the C-22 ketone is presumed to give rise to a furan ring with C-22 being *S*-configured in compound **2** (22-OH is α). This is consistent with the presence of the 23,24-β-epoxide group in compound **2** as epoxidation of C-23 and C-24 would occur at the less hindered β-face with 22-OH being α-oriented. Subsequently, a ring closure involving nucleophilic attack of 16-OH onto C-23 furnishes compound **2**.

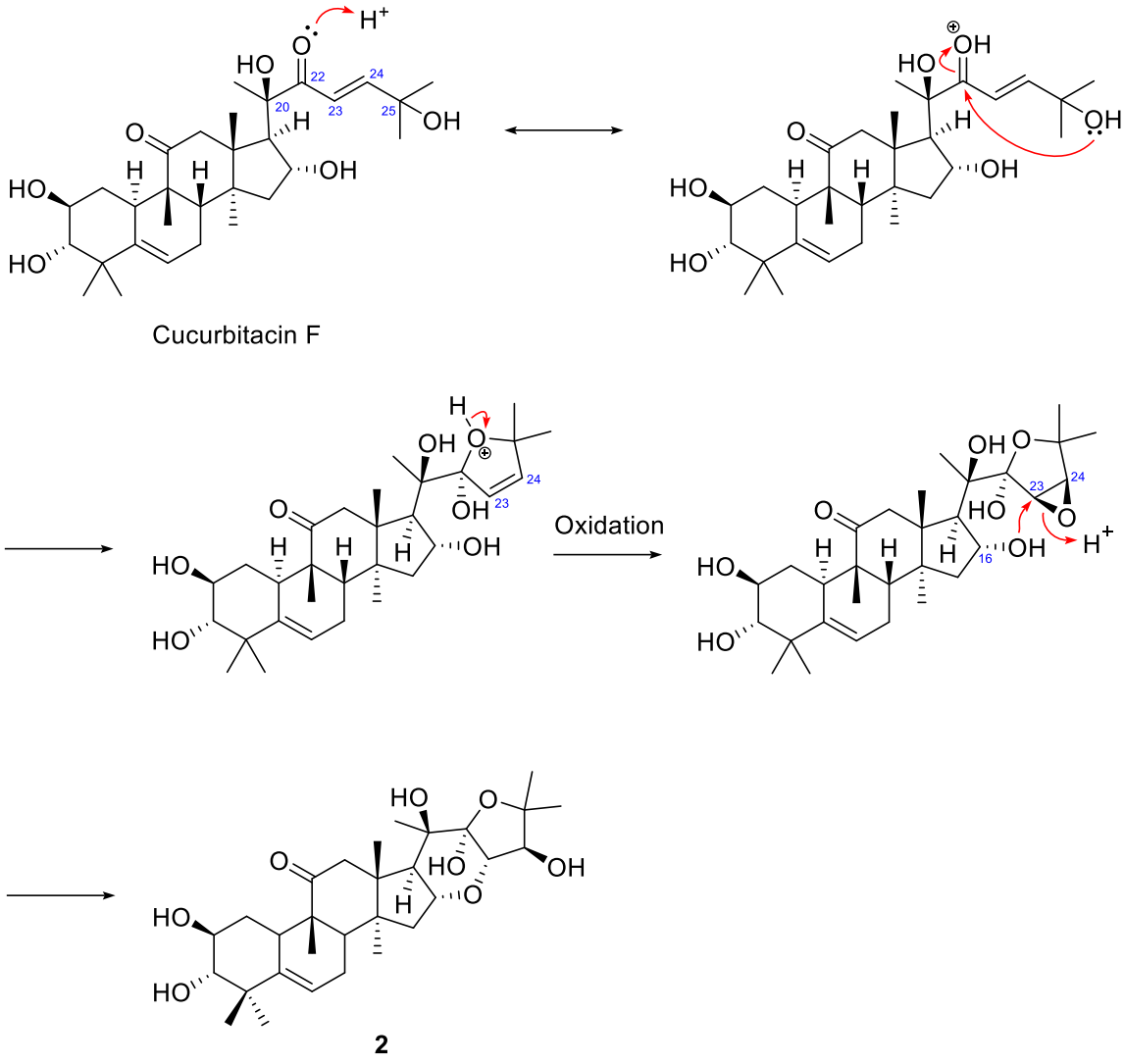
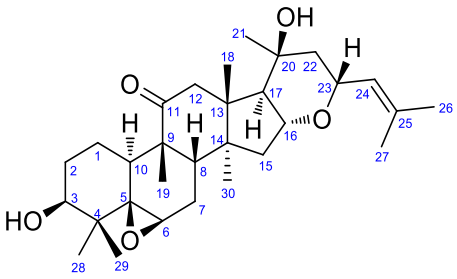


Figure 2.13 Proposed biosynthetic pathway of compound **2**

2.2.3 Compound **3**



3

Compound **3** was obtained as colorless oil with $[\alpha]^{23.5}_{D}$ +57 (*c* 0.3, $CHCl_3$). The UV spectrum showed no UV absorption, while the IR spectrum showed bands due to OH (3447 cm^{-1}) and carbonyl (1688 cm^{-1}) functions. On the basis of HRESIMS measurements (*m/z* 469.33265, $MH^+ - H_2O$), the molecular formula of compound **3** was determined to be $C_{30}H_{46}O_5$.

The ^{13}C NMR spectrum of compound **3** (Table 2.3 and Figure 2.14) showed a total of 30 resonances, comprising eight methyls, six methylenes, eight methines, and eight carbon atoms with no hydrogen attached. The observed quaternary carbon resonance at δ_C 212.8 was consistent with the presence of a ketone group, while the resonances at δ_C 125.0 and 136.4 were due to a trisubstituted double bond carbons. Additionally, the resonances at δ_C 52.2, 72.9, 75.9 and 77.8 were due to four oxymethines, while the resonance at δ_C 72.2 was due to one oxygenated tertiary carbon. The ^1H NMR spectrum of compound **3** (Table 2.3 and Figure 2.15) revealed the presence of eight methyl singlets at δ_H 0.89, 0.91, 1.10, 1.17, 1.27, 1.31, 1.69 and 1.72, a doublet due to an epoxide hydrogen signal at δ_H 3.26, a pair of AB doublets due to a ketomethylene group at δ_H 2.44 and 2.99, and three oxymethine resonances at δ_H 3.47, 4.37 and 4.54 (excluding the epoxide hydrogen).

Table 2.3 ^{1}H and ^{13}C NMR data of compound **3** [a]

Position	δ_H (*J* in Hz)	δ_C
1	0.92, m	19.6
	1.52, m	
2	1.78, m	29.6
3	3.47, br s	77.8
4		39.7
5		65.4
6	3.26, d (5.6)	52.2
7α	1.82, m	22.5
7β	2.25, dd (16.4, 8.9)	
8	1.86, d (8.7)	41.6
9		48.0
10	2.16, m	32.7
11		212.8
12α	2.99, d (14.7)	48.3
12β	2.44, d (14.7)	
13		49.0
14		47.0
15α	1.52, m	40.8
15β	1.82, m	
16	4.37, td (10.2, 3.6)	75.9
17	1.91, d (10)	55.5
18	0.89, s	18.9
19	1.17, s	19.2
20		72.2
21	1.31, s	29.2
22α	1.45, m	49.0
22β	1.36, m	
23	4.54, ddd (11.2, 8.3, 2.7)	72.9
24	5.15, d (8.2)	125
25		136.4
26	1.69, s	18.4
27	1.72, s	25.8
28	1.10, s	24.7
29	0.91, s	20.4
30	1.27, s	22.9

[a]$CDCl_3$, 600 MHz (^{1}H), 150 MHz (^{13}C)

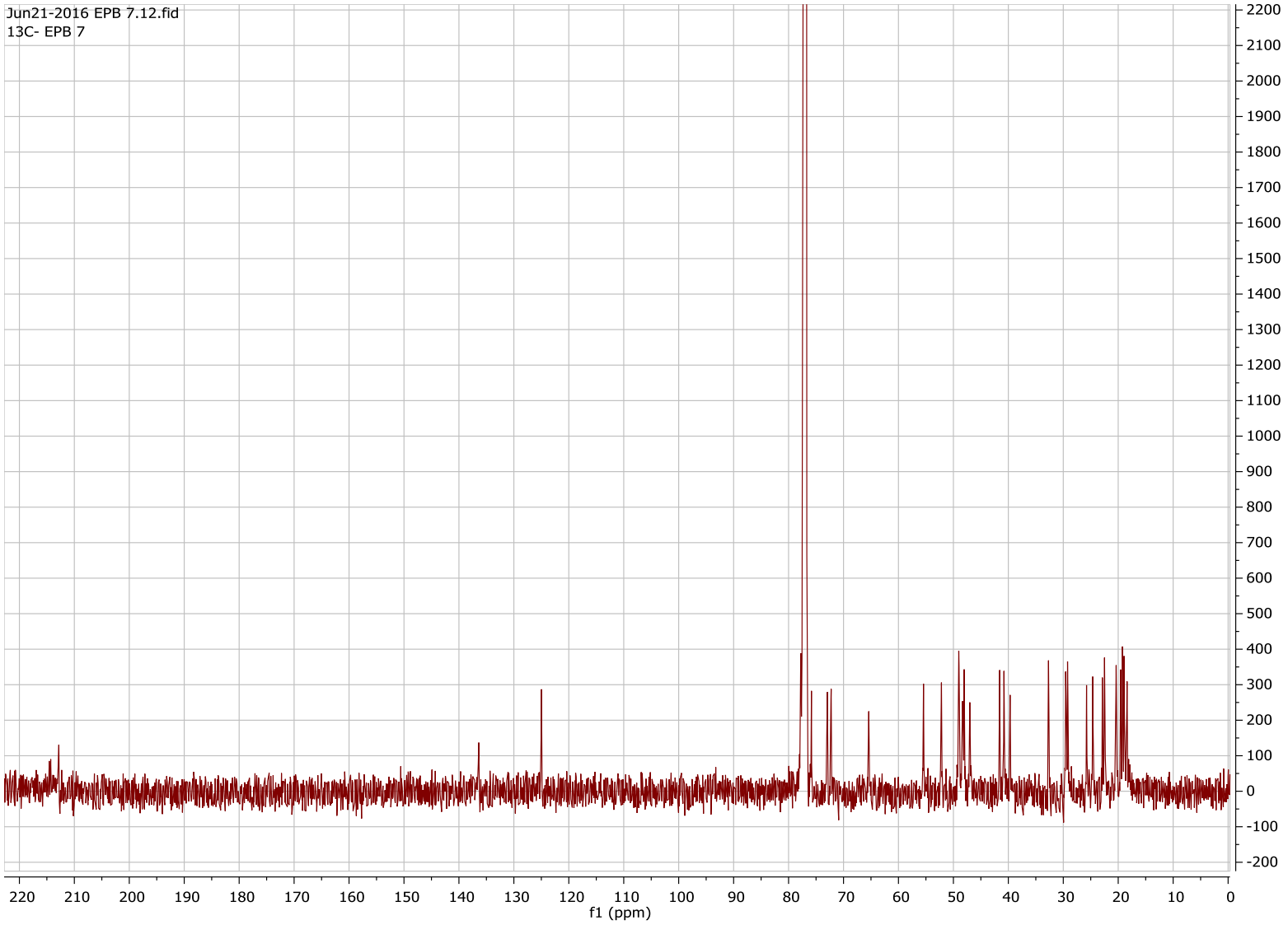


Figure 2.14 ^{13}C NMR spectrum of compound **3** (150 MHz, $CDCl_3$)

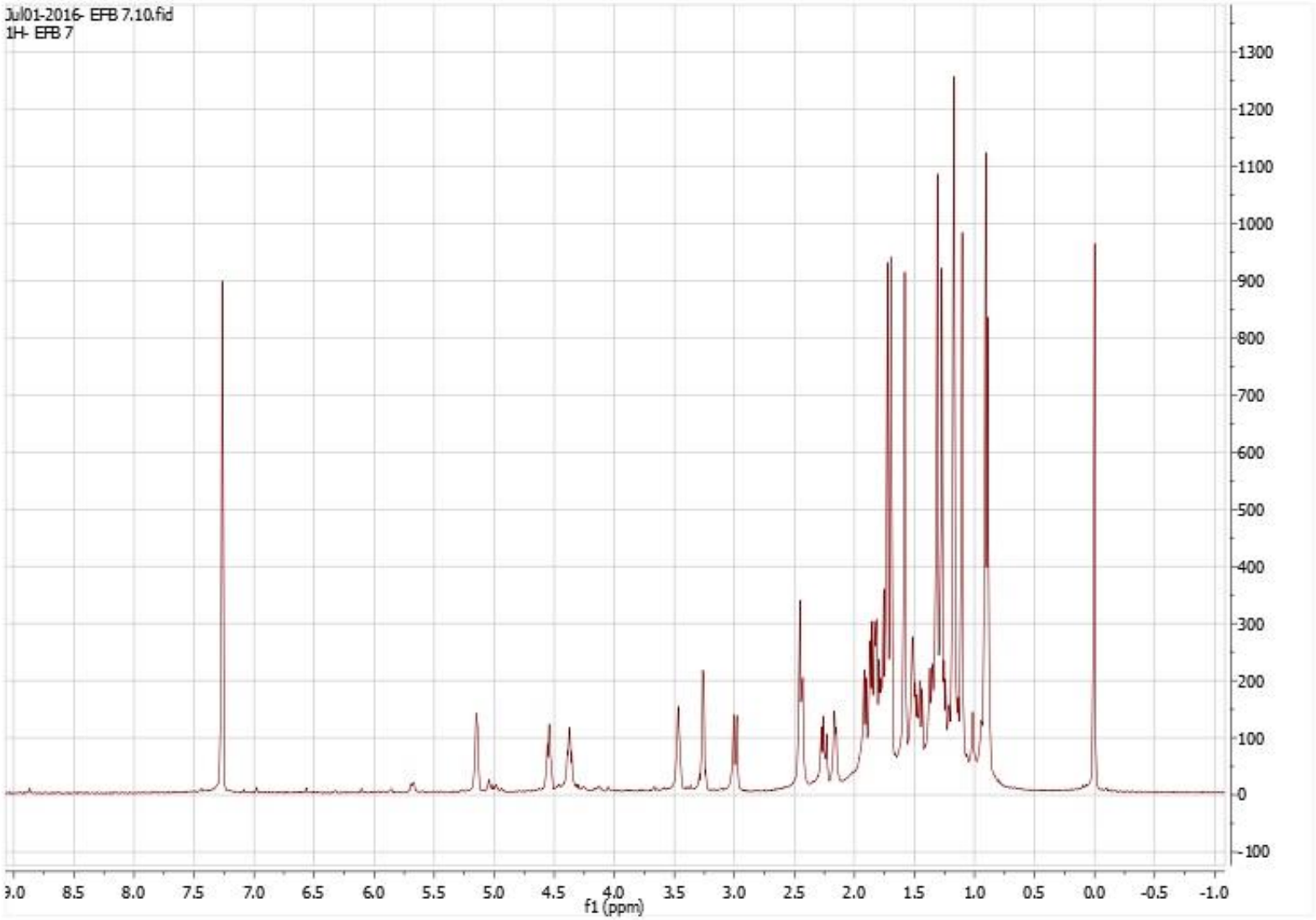


Figure 2.15 ^{1}H NMR spectrum of compound **3** (600 MHz, $CDCl_3$)

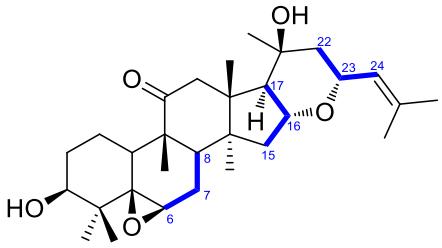


Figure 2.16 Partial structures revealed by COSY and HSQC of compound **3**

The ^{1}H and ^{13}C NMR spectra were somewhat similar to those of elaeocarpucin H (**227**),[34] with the presence of the characteristically deshielded methine triplet of doublets signal at δ_H 4.37, deshielded methine doublet of doublet of doublets at δ_H 4.54 and olefinic doublet signal at δ_H 5.15, due to H-16, H-23 and H-24, respectively.[34] There were however several distinct differences in the NMR data of compound **3** when compared with those of elaeocarpucin H.[34] The presence of carbon resonances at δ_C 65.4 and 52.2 in place of the olefinic carbon resonances at δ_C 167.0 and 125.6 due to C-5 and C-6 in elaeocarpucin H, coupled with the presence of the hydrogen resonance at δ_H 3.26, suggested that the trisubstituted double bond at C-5 and C-6 in elaeocarpucin H has been replaced with an epoxide function in compound **3**. This change was also reflected in the carbon shifts of CH_3-28 and CH_3-29 for both **3** and elaeocarpucin H, which were detected to differ quite significantly, i.e., δ_C 24.7 and 20.4 in compound **3** vs δ_C 27.8 and 24.8 in elaeocarpucin H, respectively. Additionally, the C-7 ketone function in elaeocarpucin H was also absent, being replaced with a methylene group in compound **3** (δ_H 1.82, 2.25; δ_C 22.5). The 2D structure of compound **3** is entirely consistent with the COSY (Appendix 9), HSQC (Appendix 10) and HMBC (Appendix 11) data (Figures 2.16 and 2.17).

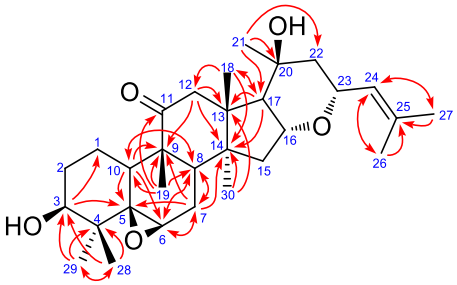


Figure 2.17 Selected HMBC correlations of compound **3**

The configurations at all stereocentres in compound **3**, except for the epoxide-containing C-5 and C-6, were found to be identical to those of elaeocarpucin H based on the NOESY data (Appendix 12 and Figure 2.18). As for the epoxy group, the NOEs observed for H-6/CH_3-29, H-6/H-7α, H-7β/CH_3-19, H-10/CH_3-28 and H-10/CH_3-30 revealed its orientation as β. The H-6/CH_3-29 and H-6/H-7α NOEs would not be possible if the epoxy group was α-oriented. This conclusion was further substantiated by a previous report,[62] which suggested that for cucurbitacin structures such as that of compound **3**, the presence of a sharp doublet due to the epoxidic H-6 at δ_H 3.23 – 3.39 with an unusually large coupling constant (J = 5.5 Hz), is indicative of 5β,6β-epoxides (for H-6 of compound **3**: δ_H 3.26, d, J = 5.6 Hz). Therefore, compound **3** is established as 7-deoxo-5β,6β-epoxyelaeocarpucin H.

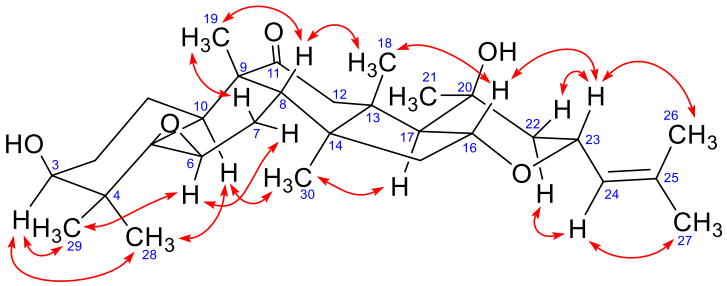
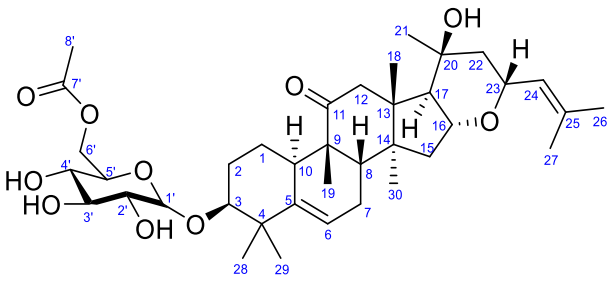


Figure 2.18 Selected NOESY correlations of compound **3**

2.2.4 Compound **4**



4

Compound **4** was obtained as a white amorphous powder with $[\alpha]^{23.5}_{D}$ +79 (*c* 1.0, $CHCl_3$). The UV spectrum showed no UV absorption, while the IR spectrum indicated the presence of OH (3414 cm^{-1}) and carbonyl (1683 cm^{-1}) functions. The molecular formula of compound **4** was determined to be $C_{38}H_{59}O_{10}$, on the basis of HRESIMS measurements (*m/z* 675.4074, MH^+).

The ^{13}C NMR spectrum of compound **4** (Table 2.4 and Figure 2.19), showed a total of 38 carbon resonances, comprising nine methyls, seven methylenes, thirteen methines, and nine carbon atoms with no hydrogen attached. The observed quaternary carbon resonance at δ_C 213.8 was consistent with the presence of a ketone group, while the resonances at δ_C 118.6, 125.1, 136.2, and 140.3 were due to two trisubstituted double bond carbons. Additionally, the resonances at δ_C 63.5, 86.7, 76.2, 76.1, 74.0, 73.6, 72.9, and 70.3 were due to one oxymethylene and seven oxymethines, while the resonance at δ_C 72.3, 104.2, and 171.6 were due to an oxygenated tertiary carbon, a hemiketal carbon and an acetyl carbonyl, respectively. The ^1H NMR data of compound **3** (Table 2.4 and Figure 2.20), revealed the presence of nine isolated methyl singlets at δ_H 0.93, 1.00, 1.10, 1.18, 1.21, 1.30, 1.69, 1.71, and 2.09 (acetyl), two doublets due to two olefinic signals at δ_H 5.57 and 5.14, a pair of AB doublets due to a ketomethylene group at δ_H 2.42 and 3.01, two oxymethylene resonances at δ_H 4.24 and 4.30, and seven oxymethine reseonances at δ_H 3.35, 3.35, 3.40, 3.40, 3.50, 4.36, and 4.53. The ^1H and ^{13}C NMR spectra are largely identical to those of 16α,23α-epoxy-3β,20β-dihydroxy-10αH,23βH-cucurbit-5,24-dien-11-one 3-O-β-$_D$-glucopyranoside (**232**), except for the presence of additional carbon resonances at δ_C 171.6 and 20.9 due to C-7' and C-8'(acetate group in the sugar moiety) in compound **4**.[36,63]

Table 2.4 ^{1}H and ^{13}C NMR data of compound **4**[a]

Position	δ_H (*J* in Hz)	δ_C
1	1.35, m	21.1
	1.53, m	
2	1.66, m	27.7
	1.91, m	
3	3.35, m	86.7
4		41.4
5		140.3
6	5.57, d (5.6)	118.6
7α	1.85, m	23.8
7β	2.38, m	
8	1.93, m	42.7
9		49.4
10	2.22, m	35.3
11		213.8
12α	3.01, d (14.6)	48.3
12β	2.42, d (14.6)	
13		48.0
14		48.3
15α	1.47, m	40.7
15β	1.83, m	
16	4.36, td (10.2, 3.2)	76.2
17	1.94, m	55.0
18	0.93, s	19.8
19	1.10, s	20.2
20		72.3
21	1.30, s	29.2
22α	1.44, m	49.0
22β	1.37, m	
23	4.53, ddd (11.2, 8.7, 2.6)	72.9
24	5.14, d (8.4)	125.1
25		136.2
26	1.69, s	18.4
27	1.71, s	25.8
28	1.00, s	27.5
29	1.18, s	25.5
30	1.21, s	21.0
1'	4.24, d (7.8)	104.2
2'	3.40, m	74.0
3'	3.50, m	76.1
4'	3.35, m	70.3
5'	3.40, m	73.6
6'	4.30, m	63.5
7'		171.6
8'	2.09, s	20.9

[a]$CDCl_3$, 600 MHz (^{1}H), 150 MHz (^{13}C)

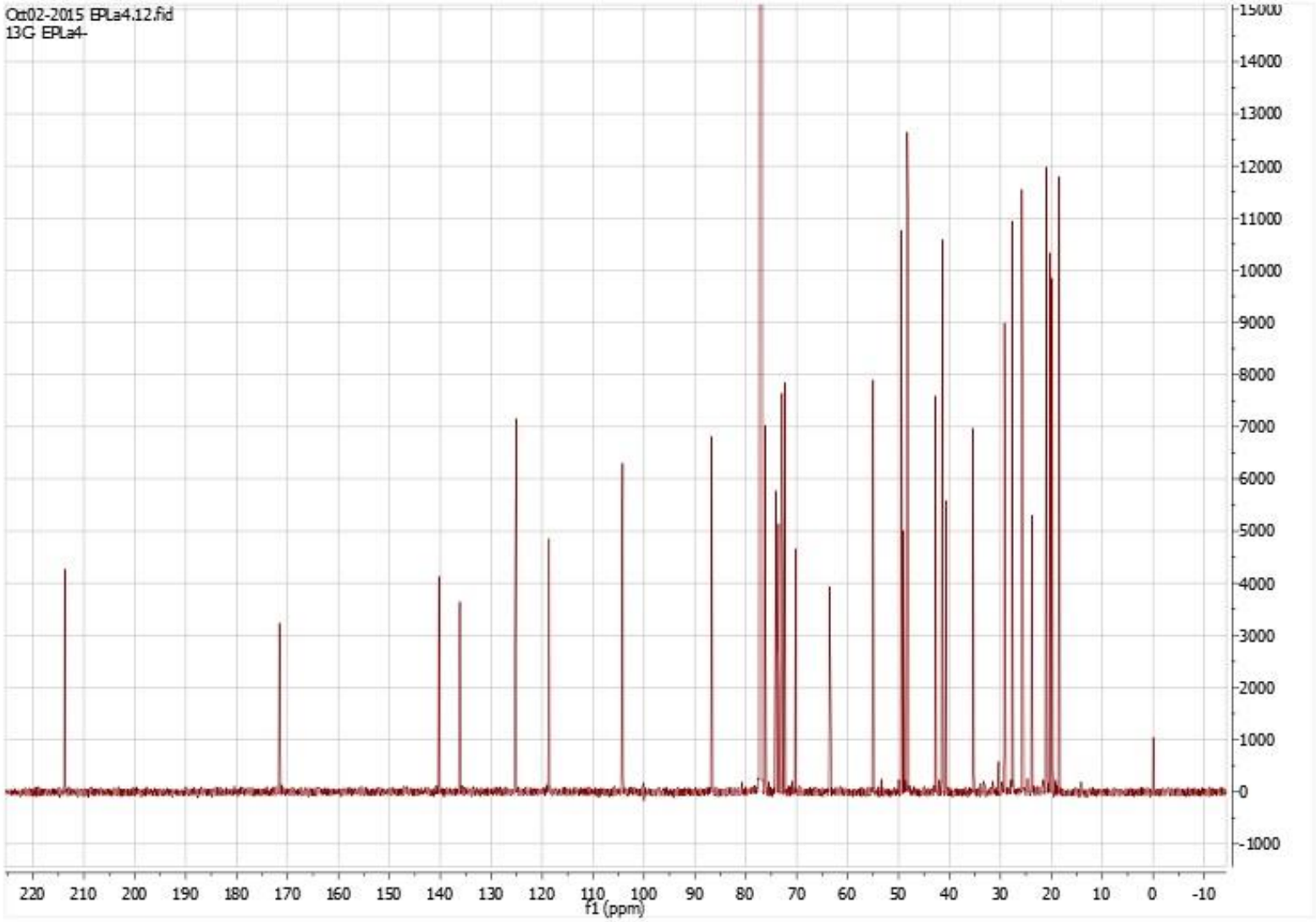


Figure 2.19 ^{13}C NMR spectrum of compound **4** (150 MHz, $CDCl_3$)

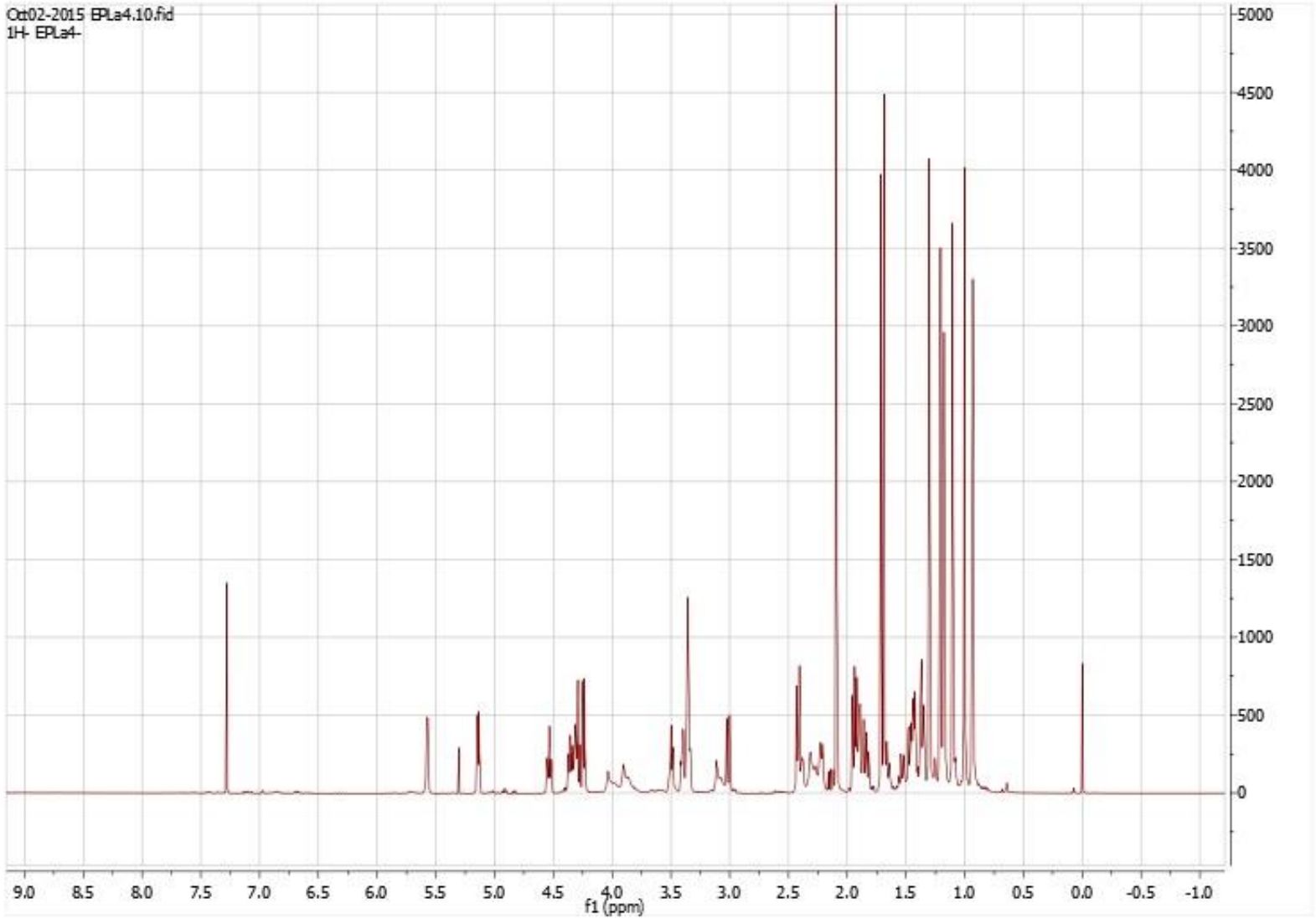


Figure 2.20 ^{1}H NMR spectrum of compound **4** (600 MHz, $CDCl_3$)

The 2D structure of compound **4** is entirely consistent with the COSY (Appendix 13), HSQC (Appendix 14) and HMBC (Appendix 15) data (Figures 2.21 and 2.22). The HMBC correlations from H-6' to C-7' supports the presence of an acetate group at C-6'. The structure proposed for compound **4** is also consistent with he NOESY (Appendix 16) data (Figure 2.23)**.**

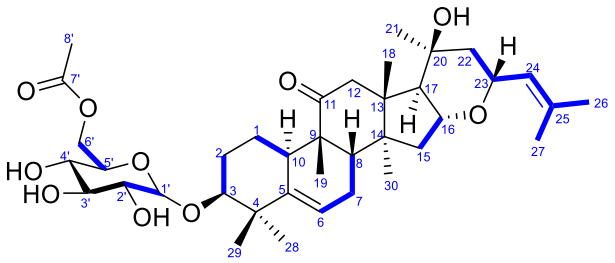


Figure 2.21 Partial structures revealed by COSY and HSQC of compound **4**

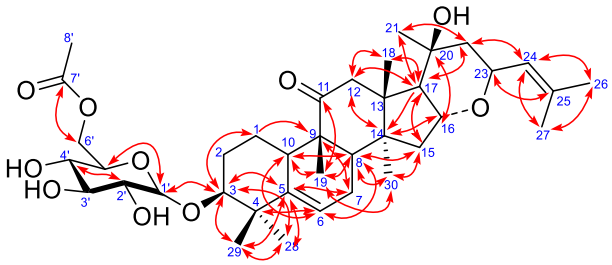


Figure 2.22 Selected HMBC correlations of compound **4**

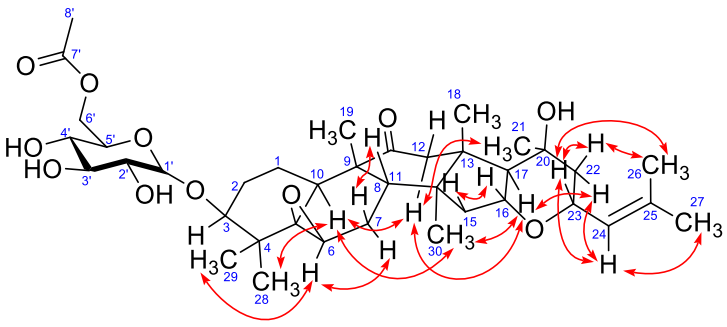
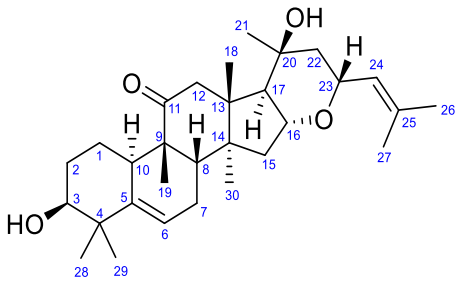


Figure 2.23 Selected NOESY correlations of compound **4**

2.2.5 Compound **5**



5

Compound **5** was obtained as colourless crystals. The melting point was determined to be 257 – 258 °C. The UV spectrum showed no absorption peak, while the IR spectrum showed absorption bands at 3459 and 1678 cm^{-1}, indicating the presence of OH and ketone groups respectively. The pseudo-molecular ion peak [MH^+] was measured at *m/z* 471.34766 by HRESIMS. The molecular formula of compound **5** was therefore determined to be $C_{30}H_{46}O_4$.

The ^1H NMR spectrum of the compound **5** showed 46 hydrogen resonances (Table 2.5, Figure 2.24). The eight 3H singlets (δ_H 0.94, H-18; δ_H 1.13, H-19; δ_H 1.21, H-21; δ_H 1.69, H-26; δ_H 1.71, H-27; δ_H 1.01, H-28; δ_H 1.19, H-29; δ_H 1.20, H-30) correspond to eight isolated methyl groups present in compound **1**. Among the five most deshielded hydrogen signals, three (i.e., δ_H 3.47, H-3; δ_H 4.35, H-16; δ_H 4.53, H-23) were due to oxymethine groups, while the other two (i.e., δ_H 5.67 and δ_H 5.14) were due to two olefinic methine hydrogens H-6 and H-24, respectively.

The ^1H data of compound **5** were closely comparable to those of compound **3**, except for the presence of signals due to the C-5–C-6 double bond in compound **5** in place of those of the C-5–C-6 epoxide function in compound **3**.[36] In the ^1H NMR spectrum of compound **5**, the resonance due to the olefinic H-6 was found at δ_H 5.64, while the corresponding signal appeared at δ_H 3.26 in the ^1H NMR spectrum of compound **3**.

Table 2.5 ^{1}H NMR Data of compound **5** and known cucurbitacin from literature

Position	**5**	Literature values
	δ_H (*J* in Hz)	δ_H (*J* in Hz)
1	1.32, m 1.52, m	1.42, m
2	1.64, m 1.71, m	1.71, m 1.62, m
3	3.47, m	3.42, br s
4	-	-
5	-	-
6	5.67, m	5.64, d (6.2)
7	1.88, m 2.38, m	1.86, m 2.37, m
8	1.93, m	1.90, m
9	-	-
10	2.24, m	2.22, m
11	-	-
12	2.45, m 3.02, d (14.7)	2.40, d (14.6) 2.98, d (14.6)
13	-	-
14	-	-
15	1.47, m 1.69, m	1.48, m 1.70, m
16	4.35, m	4.34, m
17	1.96, m	1.95, d (10.2)
18	0.94, s	0.92, s
19	1.13, s	1.10, s
20	-	-
21	1.21, s	1.28, s
22	1.36, m	1.37, m
23	4.53, m	4.48, m
24	5.14, d (8.5)	5.12, d (8.4)
25	-	-
26	1.69, s	1.68, s
27	1.71, s	1.69, s
28	1.01, s	0.99, s
29	1.19, s	1.15, s
30	1.20, s	1.18, s

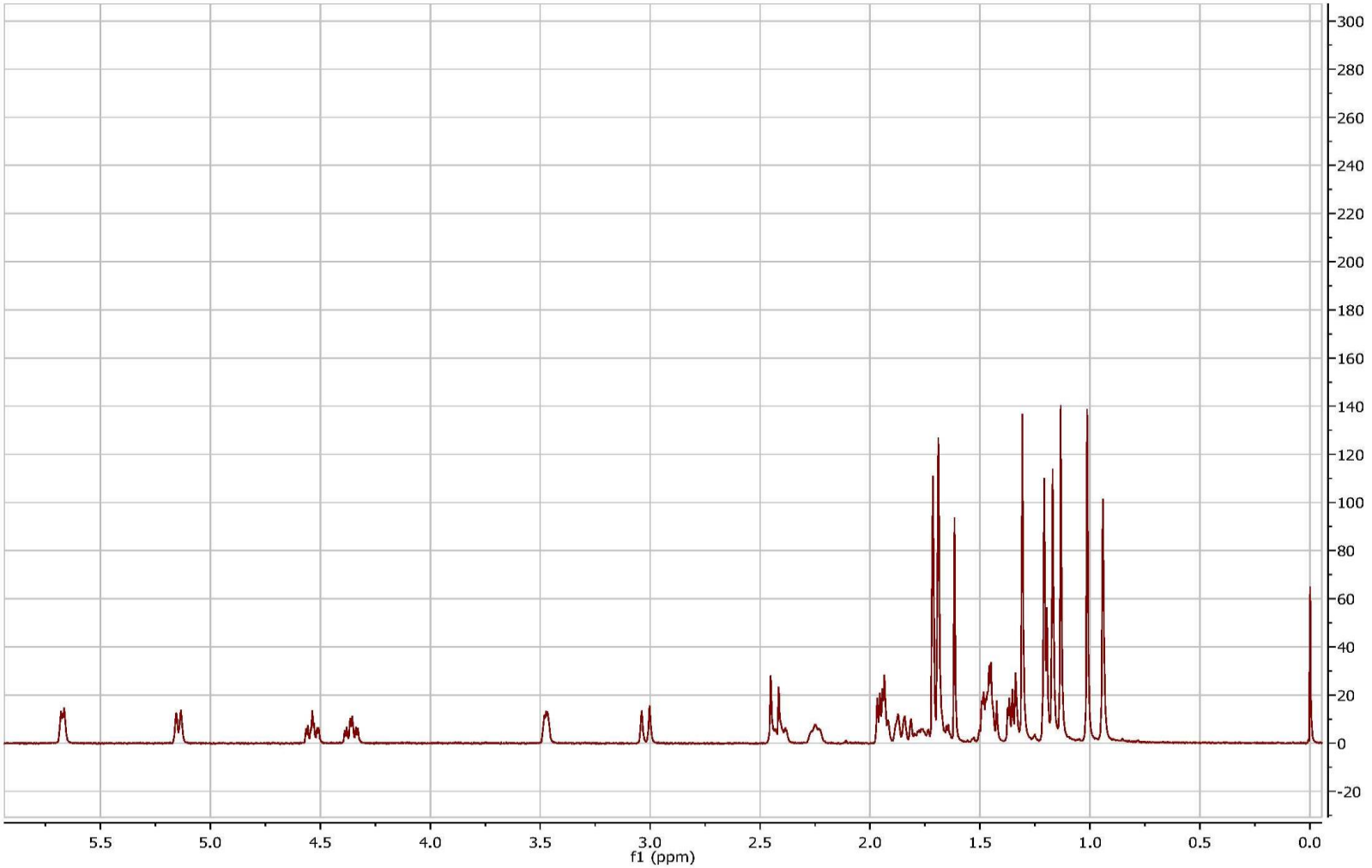


Figure 2.24 ^{1}H NMR spectrum of compound **5** (600 MHz, $CDCl_3$)

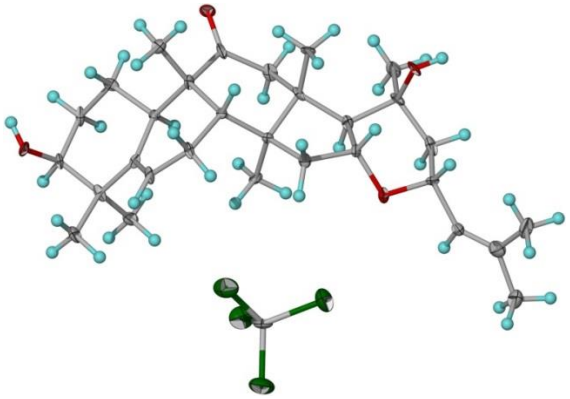
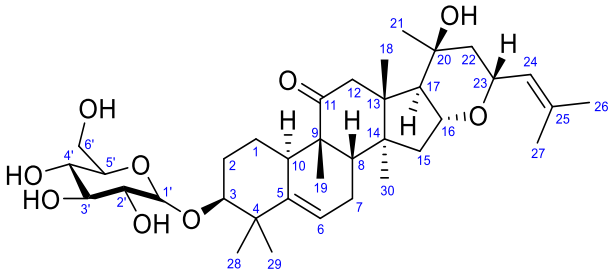


Figure 2.25 X-ray crystal structure of compound **5**

Since suitable crystals were obtained for compound **5**, X-ray diffraction analysis was carried out, which provided confirmation for the structure of compound **5** (Figure 2.25) as 16α,23α-epoxy-3β,20β-dihydroxy-10αH,23βH-cucurbit-5,24-dien-11-one (**231**), a known cucurbitacin previously isolated from *Elaeocarpus hainanensis* in 2008.[36]

2.2.6 Compound **6**



6

Compound **6** was obtained as a white amorphous solid. The UV spectrum of the compound **6** showed no absorption peak, while the IR spectrum showed absorption bands at 3410 and 1682 cm^{-1}, indicating the presence of OH and ketone groups respectively. The molecular formula of compound **6** was established as $C_{36}H_{56}O_9$ based on HRESIMS measurements (*m/z* 650.4251 [M + NH_4^+]).

The ^{13}C NMR spectrum presented in total 36 carbon resonances (Table 2.6 and Figure 2.27). Thirty of these are associated to the cucurbitacin fused-pentacyclic skeleton, while the remaining six are due a sugar moiety attached to C-3. Among the six carbon resonances due to the sugar moiety, five carbons (from C-1' to 5') corresponded to five oxygen bearing methines (δ_c 104.5, C-1'; δ_c 74.0, C-2'; δ_c 75.4, C-3'; δ_c 70.0, C-4'; δ_c 76.3, C-5'), while the other one corresponded to an oxygen bearing methylene (δ_c 61.9, C-6'). The most downfield signal was assigned to be C-1' as it is a central carbon of an acetal function group (-O-C-O-).

The ^1H NMR spectrum of compound **6** (Table 2.6 and Figure 2.26) showed a stark resemblance to that of compound **4**, showing that both compounds share the same cucurbitacin backbone. Six proton resonances, namely, H-1' to 6', were similar as ^{13}C NMR result by showing the most deshieled signal of C-1' as δ_H 4.29 (Table 2.4 and Table 2.6), except for the absence of acetate group attached at C-6' in sugar moiety.[36,64,65]

Table 2.6 ^{1}H and ^{13}C NMR data of compound **6**[a]

Position	δ_C	δ_H (*J* in Hz)
1	21.2	1.32, m 1.52, m
2	27.9	1.66, m 1.84, m
3	86.5	3.38, m
4	41.5	-
5	140.4	-
6	118.8	5.59, s
7	23.9	1.87, m 2.40, m
8	42.7	1.92, m
9	49	-
10	35.3	2.22, d (7.3)
11	213.9	-
12	48.1	2.41, m 3.02, d (9.6)
13	48.3	-
14	48.3	-
15	40.7	1.47, m 1.84, m
16	76.3	5.80, m
17	54.9	1.95, m
18	19.9	0.93, s
19	20.3	1.10, s
20	72.4	-
21	29.2	1.13, s
22	49.5	1.36, m 1.44, m
23	72.9	4.54, m
24	125.1	5.14, d (5.2)
25	136.1	-
26	18.4	1.69, s
27	25.8	1.71, s
28	27.8	1.00, s
29	25.5	1.19, s
30	21	1.21, s
1’	104.5	4.29, d (4.8)
2’	74	3.33, m
3’	75.4	3.25, d (5.6)
4’	70	3.52, m
5’	76.3	3.48, m
6’	61.9	3.79, m 3.79, m

[a]$CDCl_3$, 600 MHz (^{1}H), 150 MHz (^{13}C)

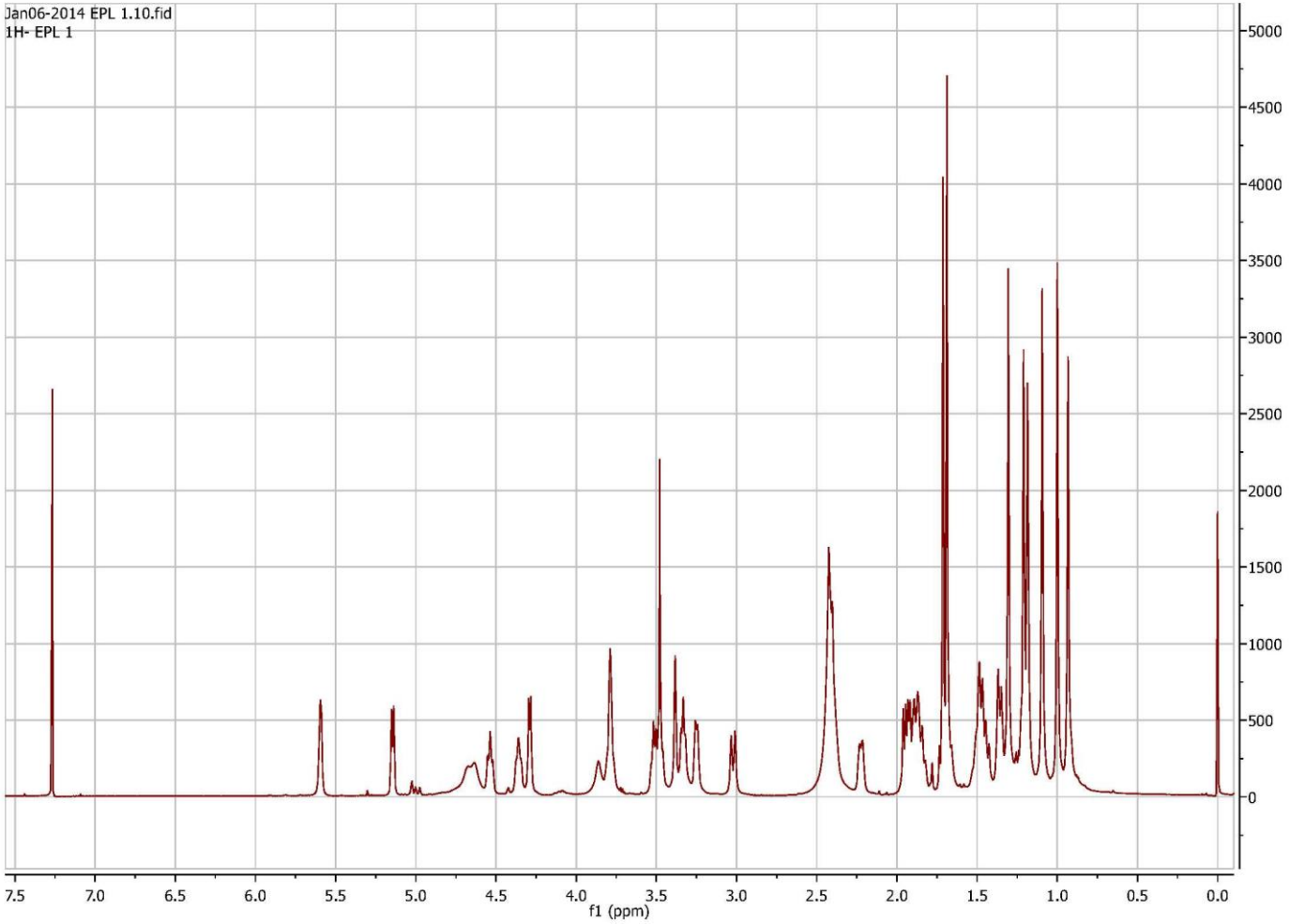


Figure 2.26 ^{1}H NMR spectrum of compound **6** (600 MHz, $CDCl_3$)

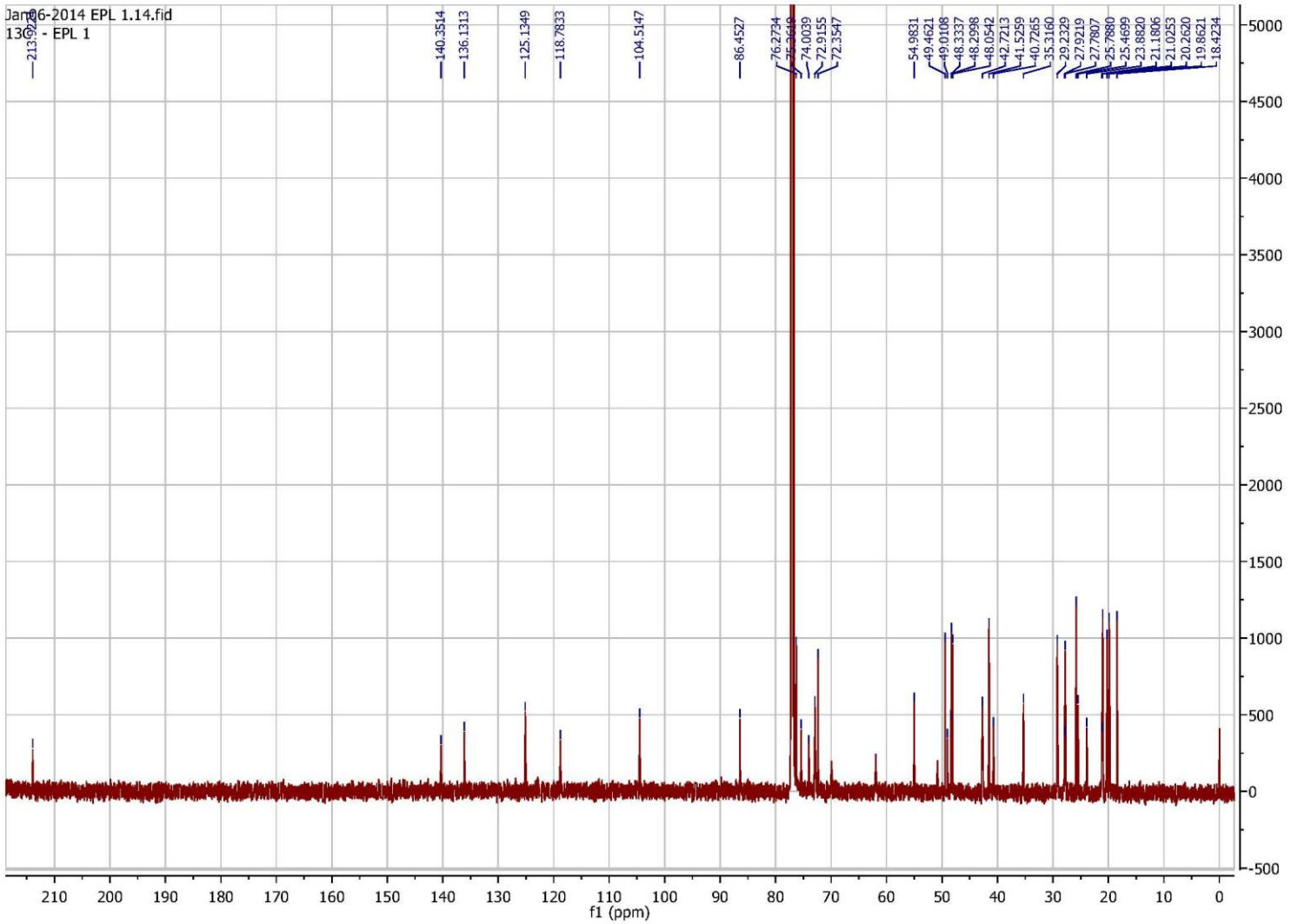


Figure 2.27 ^{13}C NMR spectrum of compound **6** (150 MHz, $CDCl_3$)

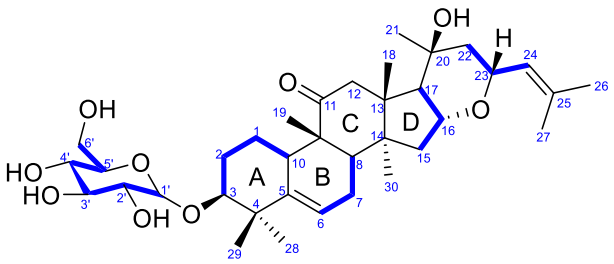


Figure 2.28 Partial structures revealed by COSY and HSQC of compound **6**

The COSY (Appendix 17) and HSQC (Appendix 18) data of compound **6** (Figure 2.28) revealed partial structures that corresponded to the fused pentacyclic cucurbitane core also present in compound **5**, namely, $CHCH_2CH_2CH$, $CHCH_2CH$, CH_2CHCH, and CH_2CHCH corresponding to the C-3–C-2–C-1–C-10, C-6–C-7–C-8, C-15–C-16–C-17, and C-22–C-23–C-24 fragments respectively. The $CHCHCHCHCHCH_2$ partial structure associated with the sugar moiety corresponded to the C-1'–C-2'–C-3'–C-4'–C-5'–C-6' fragment in compound **6**. The presence of the fused pentacyclic core and sugar moiety in compound **6** were further supported by the HMBC data (Appendix 19 and Figure 2.29).[66]

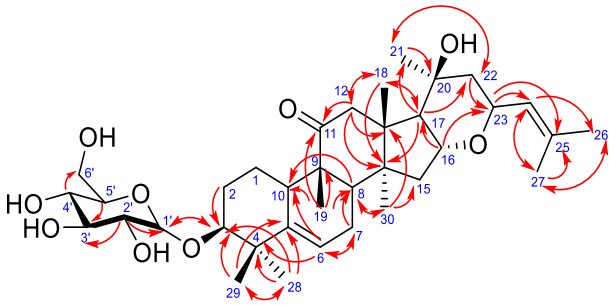
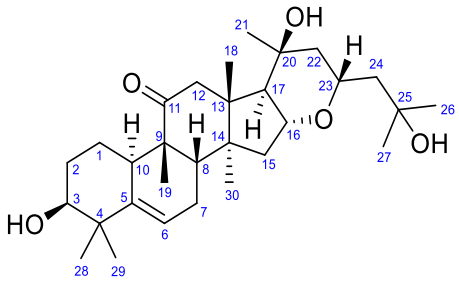


Figure 2.29 Selected HMBC correlations of compound **6**

Three-bond HMBC correlation from H-16 to C-23 confirmed the presence of the 16,23-ether group in the tetrahydropyran ring E (Figure 2.29). Two- and three-bond correlations, from H-23 to C-24 and C-25; H-24 to C-26 and C-27; H-26 to C-27; H-27 to C- 25 and C- 26, confirmed the presence of the isobutene side chain (C-24, C-25, C-26, C-27) attached to C-23. The CH_3-18 was determined to be linked to C-13 by the correlations from H-18 to C-12, C-14 and C-17; CH_3-19 was linked to C-9 by the correlations from H-19 to C-9, C-10, C-8 and C-11; CH_3-21 was linked to C-20 by the correlations from H-21 to C-20 and C-22 and H-17 to C-21; CH_3-28 and CH_3-29 were both linked to C-4 by the correlations from H-28 and H-29

to C-3, C-4, and C-5; and CH_3-30 was linked to C-14 by the correlations from H-30 to C-8, C-13 and C-15. Finally, the sugar moiety was then determined to be linked to C-3 via an ether bond at C-1' by the correlations from H-1' to C-3; and H-3 to C-1'. The complete structure of compound **6** was thus confirmed to be 16α,23α-epoxy-3β,20β-dihydroxy-10αH,23βH-cucurbit-5,24-dien-11-one 3-O-β-$_D$-glucopyranoside (**232**), representing the glycoside of compound **5**. Compound **6** was originally isolated from a species from the *Rosacea* family and subsequently isolated from *Elaeocarpus hainanensis*.[36]

2.2.7 Compound **7**



7

Compound **7** was obtained as colourless oil. The UV spectrum showed no absorption peak as with cucurbitacins **1** - **6**. The IR spectrum showed absorption bands at 3449 and 1686 cm^{-1}, indicating the presence of OH and ketone groups, respectively. The pseudo-molecular ion peak [MH^+] was detected at *m/z* 489.35550 by HRESIMS, which determined the molecular formula to be $C_{30}H_{48}O_5$.

The ^{1}H NMR data of compound **7** reminiscent those of compound **5**, except that the resonance due to the olefinic H-24 (part of a trisubstituted double bond) present in compound **5** has been replaced with the resonance due to the methylene group (CH_2-24), connected to a dimethylcarbinol group, in compound **7**. Compound **7** was identified as elaeocarpucin F since the ^{1}H NMR data of compound **7** (Table 2.7, Figure 2.30) largely resembles those reported in the literature in 2012 for elaeocarpucin F (**225**), which was recently isolated from *Elaeocarpus chinensis*.[34]

Table 2.7 ^{1}H NMR data of compound **7** and elaeocarpucin F from literature

Position	**7**	Literature values
	δ_H (*J* in Hz)	δ_H (*J* in Hz)
1	1.45, m	1.49, m
2	1.66, m 1.77, m	1.65, m 1.74, m
3	3.48, br s	3.48, br s
4	-	-
5	-	-
6	5.65, m	5.67, d (5.8)
7	1.88, m	1.90, m
8	2.44, m	2.44, m
9	-	-
10	2.27, m	2.24, m
11	-	-
12	2.41, m 3.02, d (14.7)	2.42, d (14.4) 3.01, d (14.4)
13	-	-
14	-	-
15	1.47, m 1.82, m	1.42, m 1.82, m
16	4.26, m	4.37, m
17	1.95, m	1.95, d (10.4)
18	0.92, s	0.93, s
19	1.13, s	1.13, s
20	-	-
21	1.29, s	1.31, s
22	1.34, m 1.44, m	1.31, m 1.45, m
23	4.22, m	4.22, m
24	1.88, m	1.87, m
25	-	-
26	1.21, s	1.20, s
27	1.28, s	1.27, s
28	1.01, s	1.01, s
29	1.17, s	1.17, s
30	1.20, s	1.20, s

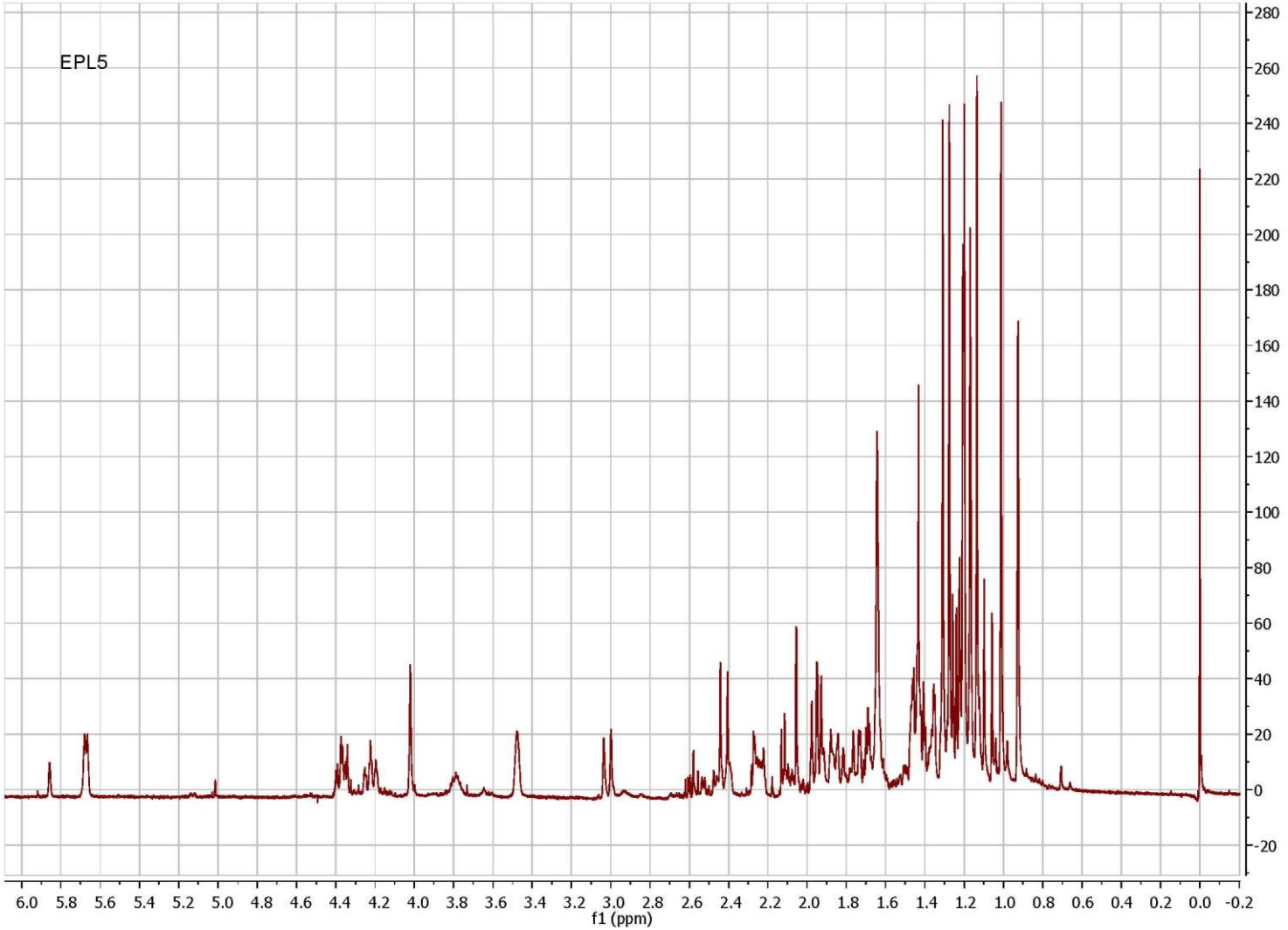
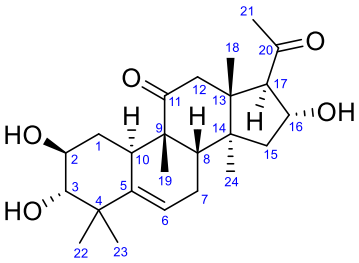


Figure 2.30 ^{1}H NMR spectrum of compound **7** (600 MHz, $CDCl_3$)

2.2.8 Compound **8**



8

Compound **8** was obtained as colourless oil. The UV spectrum showed no absorption peak as with cucurbitacins **1** - **7**. The pseudo-molecular ion peak [MH^+] was detected at *m/z* 405.27179 by HRESIMS, which determined the molecular formula to be $C_{24}H_{36}O_5$. Comparative study between the ^1H NMR data of compound **8** and previously published literature values of the similar compound has confirmed the compound to be hexanocucurbitacin F (**55**) (Table 2.8 and Figure 2.31).[58]

Table 2.8 ^{1}H NMR data for compound **8** and hexanocucurbitacin F from literature [a]

Position	**8**	Literature values
	δ_H (*J* in Hz)	δ_H (*J* in Hz)
1	2.40 dt (12.4, 4.0)	2.40 dt (12.4, 4.0)
	1.52 m	1.53 m
2	4.08 ddd (11.4, 9.1, 4.1)	4.09 m
3	3.41 d (9.1)	3.41 dd (9.1, 4.2)
4	-	-
5	-	-
6	5.72 d (5.8)	5.72 d (5.7)
7	2.33 m	2.24 dd (19.1, 7.6)
	1.97 m	1.97 m
8	1.88 d (7.7)	1.88 d (7.6)
9	-	-
10	2.74 d (11.7)	2.74 d (11.5)
11	-	-
12	3.34 d (14.3)	3.34 d (14.2)
	2.58 d (14.3)	2.58 d (14.2)
13	-	-
14	-	-
15	1.82 m	1.80 d (13)
16	5.33 t (7.1)	5.34 m
17	3.47 d (6.5)	3.48 d (6.5)
18	0.79 s	0.79 s
19	1.30 s	1.31 s
20		
21	2.14 s	2.14 s
22	1.21 s	1.22 s
23	1.47 s	1.47 s
24	1.54 s	1.54 s

[a]pyridin-d_5

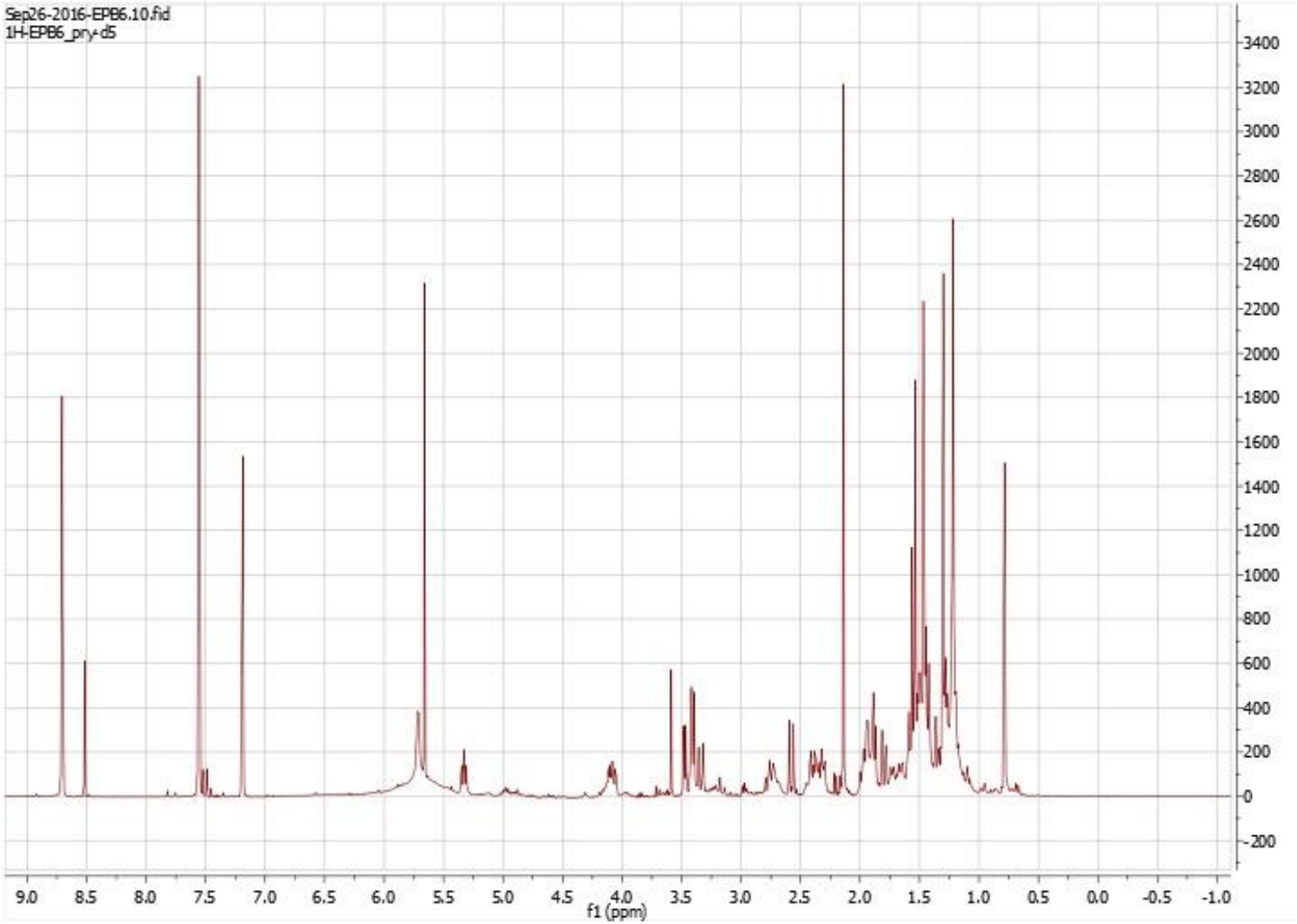
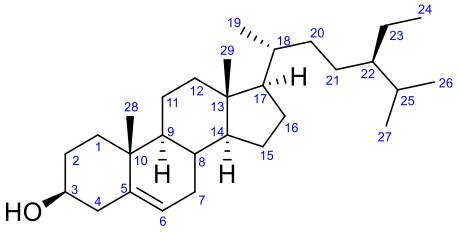


Figure 2.31 ^{1}H NMR spectrum of compound **8** (600 MHz, pyridine-d_5)

2.2.9 Compound **9**



9

The ^{1}H NMR spectrum of compound **9** revealed it to be a triterpenoid that has a lesser degree of oxygenation compared to compounds **1** – **8**, resulting in the extensive overlapped of hydrogen signals in the upfield region. As such, the identity of compound **9** could not be readily determined by comparison with literature data. Additionally, majority of the hydrogen signals could not be assigned due to the overlapped signals. Nonetheless, comparative study of the ^{13}C NMR data between compound **9** and literature values of β-sitosterol determined compound **9** to be β-sitosterol (Table 2.9 and Figure 2.32).[67] β-Sitosterol is a widely distributed phytosterol found in plants, and is characterized by anti-carcinogenic and anti-atherogenic properties.[68]

Table 2.9 ^{13}C NMR data of compound **9** and β-sitosterol from literature

Position	**9**	Literature values
	δ_C	δ_C
1	37.3	37.5
2	31.7	31.9
3	71.9	72.0
4	42.4	42.5
5	140.8	140.9
6	121.8	121.9
7	32.0	32.1
8	32.0	32.1
9	50.2	50.3
10	36.7	36.7
11	21.2	21.3
12	39.9	39.9
13	42.4	42.6
14	56.9	56.9
15	26.1	26.3
16	28.3	28.5
17	56.1	56.3
18	36.2	36.3
19	19.1	19.2
20	34.0	34.2
21	24.4	26.3
22	45.9	46.1
23	23.1	23.3
24	12.1	12.2
25	29.2	29.4
26	19.9	20.1
27	19.5	19.6
28	18.9	19.0
29	11.9	12.0

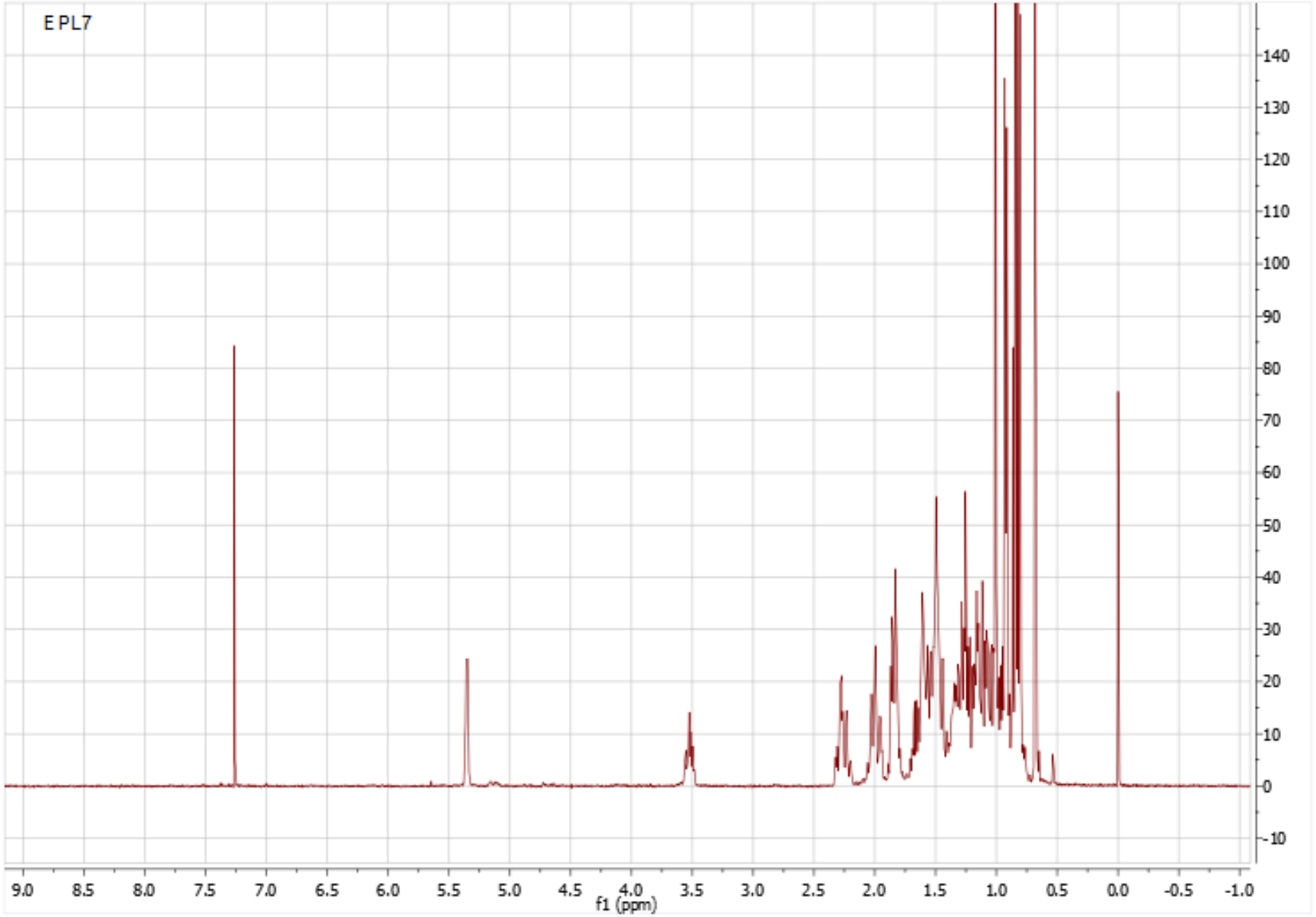
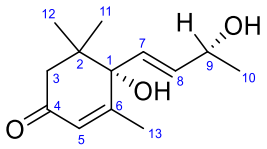


Figure 2.32 ^{1}H NMR spectrum of compound **9** (600 MHz, $CDCl_3$)

2.2.10 Compound **10**



10

Comparative study of ^{1}H NMR data between compound **10** and literature values of the similar compound has confirmed the compound **10** as a vomifoliol (Table 2.10 and Figure 2.33).[60] Vomifoliol was first isolated from leaves of *Rauwolfia vomitoria* in 1969 and is known to effect on plant stomatal aperture.[69,70]

Table 2.10 ^{1}H NMR data of compound **10** and vomifoliol from literature

Position	**10**	Literature values
	δ_H (*J* in Hz)	δ_H (*J* in Hz)
3	2.24 d (17.1) 2.45 d (17.3)	2.25 d (16.9) 2.45 d (16.9)
5	5.9 m	5.9 m
7	5.81 m	5.81 m
8	5.84 m	5.84 m
9	4.41 m	4.41 m
10	1.30 d (6.4)	1.29 d (6.4)
11	1.02 s	1.01 s
12	1.08 s	1.08s
13	1.90 s	1.89 s

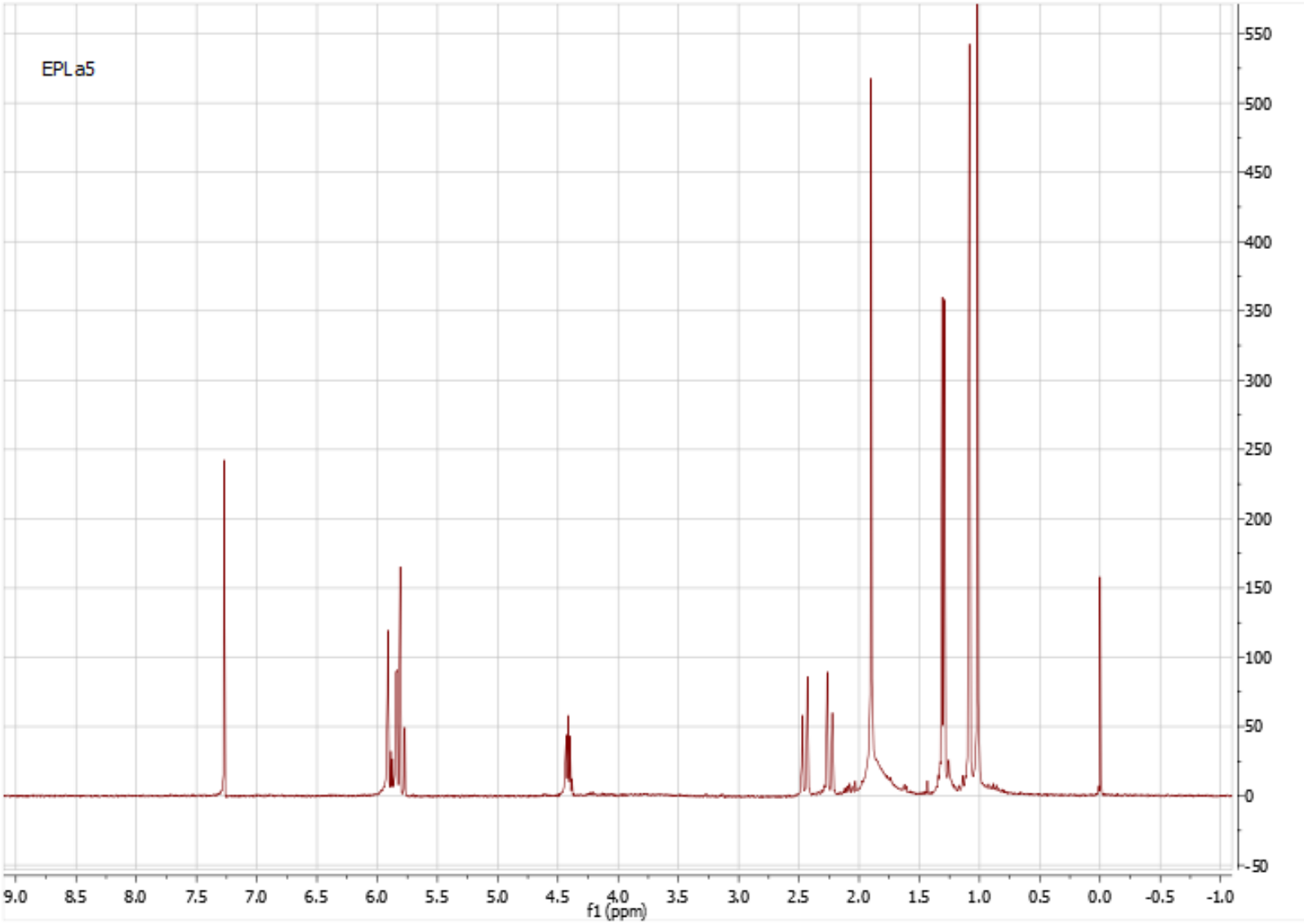


Figure 2.33 ^{1}H NMR spectrum of compound **10** (600 MHz, $CDCl_3$)

2.3 Biological Activity

Compounds **1**, **2** and **4** were evaluated for its cytotoxic activity (Table 2.11) against a panel of human cell lines, including a non-tumorigenic human breast epithelial cell line (MCF10A), five human breast cancer cell lines, three human pancreatic cancer, three nasopharyngeal cancer and four human colorectal cancer cells. Due to scarcity of compound **3**, it could not be tested along with compounds **1**, **2** and **4**. Compounds **1**, **2**, and **4** in general showed less cytotoxic towards nasopharyngeal and pancreatic cancer cell lines. On the other hand, compounds **1**, **2**, and **4** showed a selective cytotoxic effect against human breast cancer cell lines especially MDA-MB-468 which is a triple negative (estrogen receptor, ER^-; progesterone receptor, PR^-; epidermal growth factor receptor 2, $HER2^-$) breast cancer type that characterized by not expressing ER, PR and HER2 genes. This triple-negative breast cancer represents a significant clinical challenge because it does not respond to some targeted agents, particularly the endocrine therapy. Also, its metastatic potential is high and associated with a shorter median time to relapse and death.[71] Hence, compound **1** possessed the best potency against MDA-MB-468 cells suggesting a therapeutic potential in the future. Besides, compound **1** also displayed the most pronounced growth inhibitory activity against the colorectal cancer, SW48 cell line. Previous studies have hypothesized that the cytotoxic activities of cucurbitacin were due to arrangement of functional group at the side chain of the cucurbitacin.[72–74] It appears to suggest that the presence of the C-16/C-23 ether bridge that forms ring E is detrimental for cytotoxic activity. Accordingly, unlike compounds **2** and **4**, the absence of the ether bridge that links C-16 and C-23 in compound **1**, seems to support this hypothesis whereby **1** showed a pronounced cytotoxicity against SW48 cell line.

Hence, further investigations on the mechanism of action of compound **1** in breast and colorectal cancers might be interesting to discern its therapeutic application.

Table 2.11 Cytotoxic effects of compounds **1**, **2** and **4** in various cancer cells.

Compound / Cell lines	IC_{50} ± SD (μM)		
	1	**2**	**4**
Normal Breast			
MCF10A	49.74 ± 2.66	34.98 ± 1.24	41.93 ± 8.38
Breast Cancer			
MDA-MB-468	**7.42 ± 1.51**	**10.51 ± 1.70**	**10.72 ± 1.57**
MDA-MB-231	**9.17 ± 1.00**	**10.74 ± 1.43**	15.27 ± 0.45
MCF7	**9.29 ± 1.84**	18.99 ± 4.28	22.21 ± 2.88
SKBR3	**10.61 ± 3.20**	23.58 ± 2.53	33.91 ± 3.94
T47D	21.28 ± 3.00	20.02 ± 2.18	16.58 ± 8.15
Pancreas Cancer			
AsPC1	17.57 ± 1.30	11.62 ± 0.45	43.08 ± 5.17
SW1990	28.58 ± 3.66	33.58 ± 2.66	42.14 ± 1.25
BxPC3	23.77 ± 3.61	23.03 ± 1.81	>100
Nasopharyngeal Cancer			
HK1	78.53 ± 4.59	71.24 ± 1.53	72.18 ± 2.74
CNE1	83.24 ± 2.75	83.9 ± 1.30	88.45 ± 1.94
SUNE1	>100	24.78 ± 0.79	24.31 ± 1.67
Colorectal Cancer			
HT29	> 100	-	-
HCT116	92.79 ± 6.94	-	-
Caco2	61.82 ± 4.22	-	-
SW48	**4.62 ± 0.50**	-	-

IC_{50} = concentration of test compound where 50% of cells are killed; SD = standard deviation; *n* = number of triplicate

Data represents mean IC_{50} values ± SD, *n* = 3. Bold values indicate compound with good – moderate potency.

Chapter Three

Experimental Section

3.1 General

The leaves (619 g) and bark (1.42 kg) of *Elaeocarpus petiolatus* were collected from Kajang, Selangor, Malaysia, and the plant identity was determined by Dr. Yong Kien Thai (Institute of Biological Sciences, University of Malaya, Malaysia). The voucher specimen was kept at the Herbarium, University of Malaya.

Elaeocarpus petiolatus leaves and barks were collected and subjected to sequential extraction with *n*-hexane and ethyl acetate (EA). The EA crude extracts were dried and dissolved in MeOH: H_2O (4:1) and partitioned with hexane (1 L) and subsequently dissolved in MeOH: H_2O (1:4) and partitioned with $CHCl_3$ (1 L). The hexane layer was discarded. The concentrated $CHCl_3$ extracts were then fractionated by column chromatography (CC) to several main fractions. Promising compounds were identified by thin layer chromatography (TLC) and were further isolated to obtain pure compounds using centrifugal thin layer chromatography (CTLC). The cucurbitacin compounds were identified with the presence of blue or purple spots after spraying with vanillin reagent followed by heating of the plate. Separations of compounds were repeated by CTLC until pure cucurbitacins were obtained. Isolated pure cucurbitacin compounds were then sent to University of Malaya (UM) to collect data in characterizing the structure by using nuclear magnetic resonance (NMR). Collected NMR data were analysed and structure of the compounds were revealed. The elucidated structures of new compounds were evaluated for their cytotoxic activity against a panel of cancer cell lines. In this study, the normal human mammary epithelial cells (MCF10A), human breast cancer cells (MCF7, MDA-MB-231, and MDA-MB-468), and human colorectal cancer cells (HT29, HCT116, Caco2, and SW48) were attempted.

Based on TLC results, fractions were combined to afford eight combined fractions for *Elaeocarpus petiolatus* (EPL) (Table 3.1) and eleven for *Elaeocarpus petiolatus* bark (EPB) (Table 3.2). The combined fractions were then subjected to further purification by flash column chromatography

or centrifugal thin layer chromatography until pure compounds were obtained. Flow diagrams for both EPL and EPB are shown in Figure 3.4 and Figure 3.5.

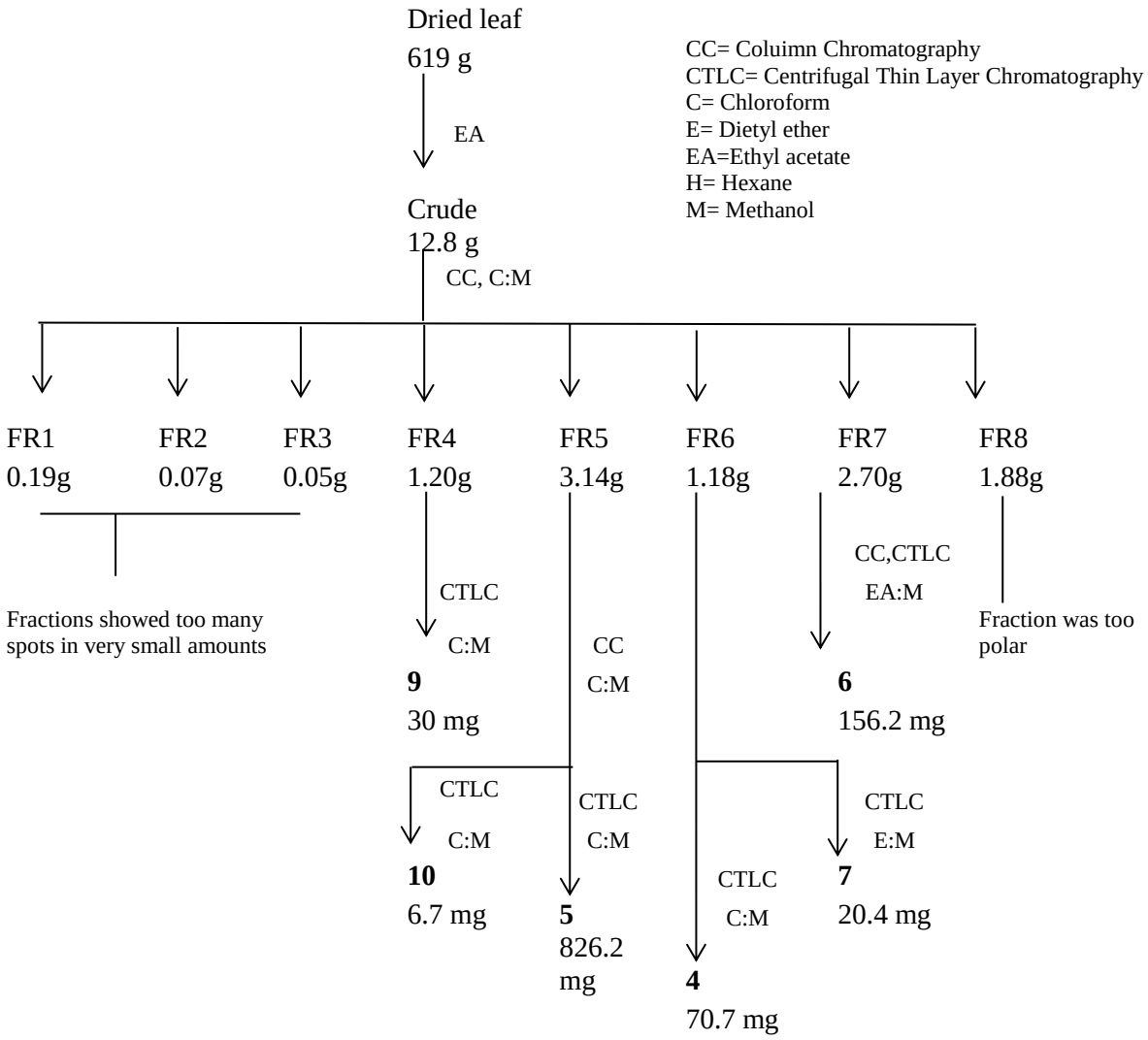


Figure 3.4 Isolation of cucurbitacins from the leaves of *E. petiolatus*

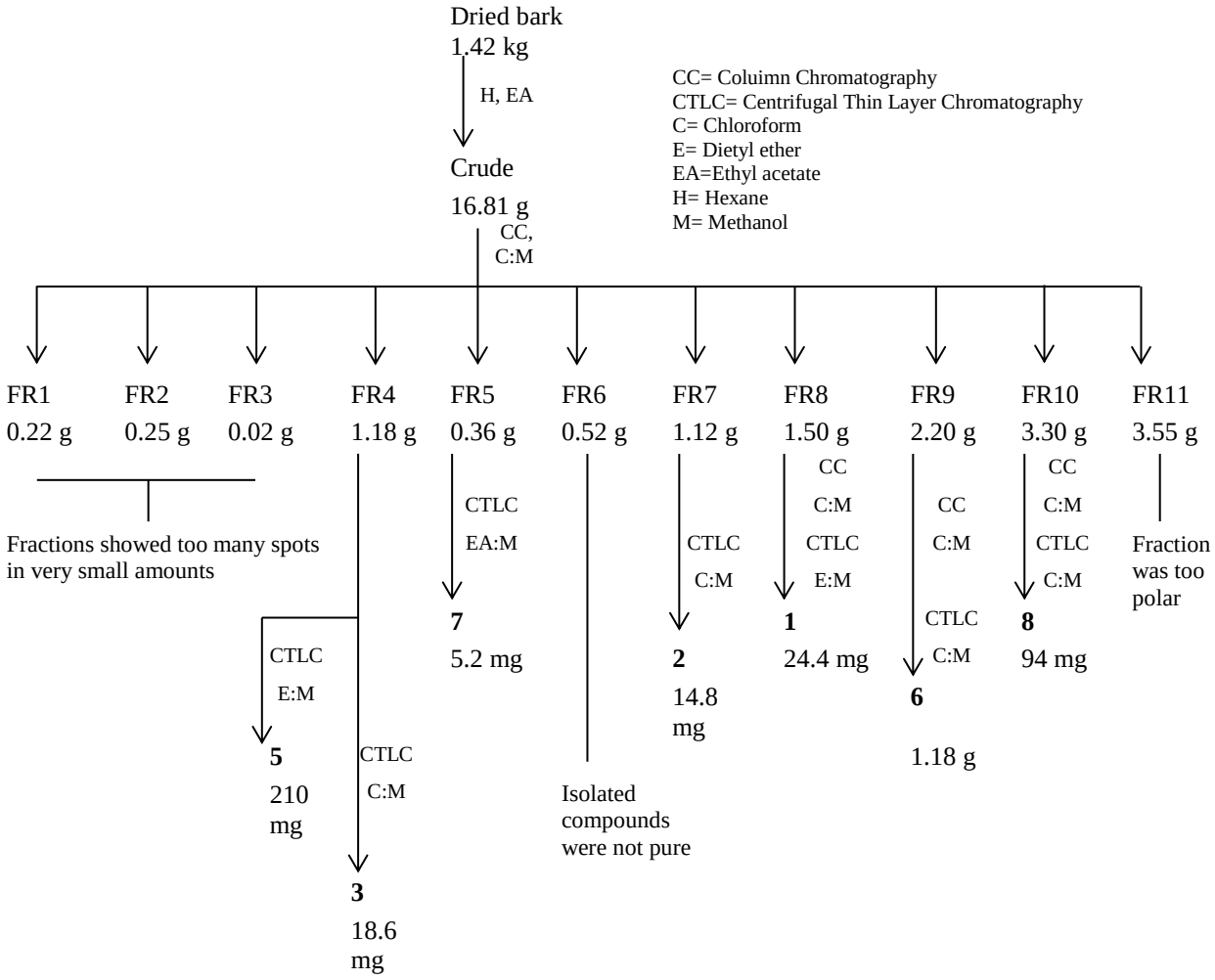


Figure 3.5 Isolation of cucurbitacins form the bark of *E. petiolatus*

3.2 Extraction of Plant Material

3.2.1 *Elaeocarpus petiolatus* leaves (EPL)

The leaves *of Elaeocarpus petiolatus* were dried and ground. The ground EPL (619 g) was then soaked in 3 L of EA for 3 days at room temperature. The EA extracts were filtered and collected. Further re-extractions were repeated for another two times in the same manner. The collected extracts were then combined and concentrated using rotary evaporator. In total, 43 g of gummy-like EA crude extract was obtained. Out of this crude extract, 12.84 g was then subjected to chromatographic separation to isolate pure compounds.

3.2.2 *Elaeocarpus petiolatus* bark (EPB)

Air dried EPB was grounded (1.42 kg) and soaked in 4 L *n*-hexane at 50 °C (water bath) for 2 h. The hexane extracts were filtered and collected. The extraction was repeated for three times. After extracted with *n*-hexane, the EPB materials were dried inside a fume hood (to completely remove hexane residual). EA (4 L) was then added to the EPB material and the same extraction procedure was repeated for another nine times. The combined filtrates for both the *n*-hexane and EA extracts were then concentrated using rotary evaporator to obtain the respective crude extracts.

The obtained dried EA crude extract was then dissolved in 1 L of MeOH-H_2O (4:1) and partitioned with 1 L *n*-hexane. The hexane layer was collected and concentrated using rotary evaporator and another 1 L *n*-hexane was added to partition again with MeOH-H_2O (4:1). This was repeated for another three times and the MeOH-H_2O (4:1) layer was concentrated using rotary evaporator and was reconstituted in MeOH-H_2O (1:4) and partitioned with 1 L $CHCl_3$. The solvent-solvent partitioning extraction was repeated five times by using new batch of 1L $CHCl_3$. The $CHCl_3$ extracts were combined and concentrated to dryness using rotary evaporator.

3.3 Isolation of Plant Material

The $CHCl_3$ extracts of both EPL and EPB underwent further fractionation by using flash column chromatography (CC) and centrifugal thin layer chromatography (CTLC). The initial starting solvent to fractionate the crude extracts were chosen based on the TLC profiles of the crude extracts.

3.3.1 Flash column chromatography (CC)

The EA extract of EPL (12.8 g) and $CHCl_3$ extract of EPB (16.81 g) were initially fractionated by column chromatography (Table 3.1 and Table 3.2). About 5 inches of silica in a 8 x 12 cm glass column was measured and was dissolved in starting solvent to make a slurry. The slurry was then poured into the column and packed until the silica has settled down (Figure 3.1a). Dissolved sample was then gently loaded (Figure 3.1b). The salt layer was added on top of the silica bed adsorbed with sample. Elution was collected into 2 L filtration flask (Figure 3.1c). The polarity of the solvent was increased by increasing the proportions of MeOH used in the eluent. The vacuum pump was used to increase the speed of the separation. Individually collected fractions were transferred into round bottomed flasks to concentrate the fractions. The fractions were then analyzed using TLC and collected into numbered specimen tubes. Based on the TLC results, fractions were combined to afford eight and eleven combined fractions for EPL (Table 3.1) and EPB (Table 3.2), respectively.

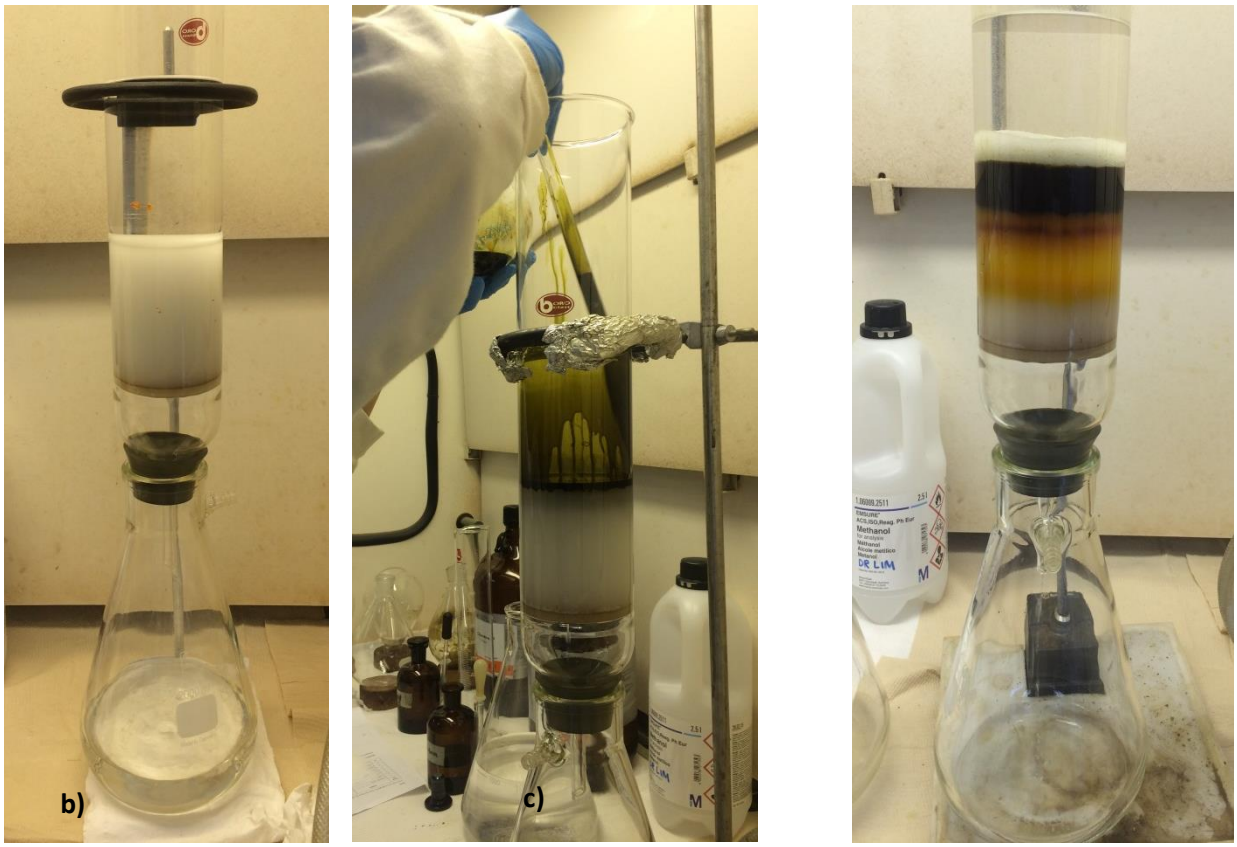


Figure 3.1 Column chromatography set up: a) Slurry packed in the column, b) Sample loading, and c) Separating fractions by collecting the bands.

Table 3.1 Combined fractions of leaves of *Elaeocarpus petiolatus* from column chromatography

Combined fraction number	Fractions	Mass of flask (g)	Mass of flask with sample (g)	Mass of sample (g)
1	2-4	52.67	52.86	0.19
2	5-7	53.18	53.25	0.07
3	8-11	51.49	51.54	0.05
4	12-40	52.72	53.92	1.20
5	41-43	49.27	52.41	3.14
6	44-48	54.23	55.41	1.18
7	49-54	53.58	56.28	2.70
8	55-60	56.05	57.93	1.88
Total mass of sample collected				**10.41**

Table 3.2 Combined fractions of bark of *Elaeocarpus petiolatus* from column chromatography

Combined fraction number	Fractions	Mass of flask (g)	Mass of flask with sample (g)	Mass of sample (g)
1	1	17.42	17.64	0.22
2	2-9	17.40	17.65	0.25
3	10-15	17.46	17.48	0.02
4	16-20	17.57	18.75	1.18
5	21-25	17.41	17.77	0.36
6	26-28	17.49	18.01	0.52
7	29	17.36	18.48	1.12
8	30	17.45	18.95	1.50
9	31	17.25	19.45	2.20
10	32-33	17.59	20.89	3.30
11	34-35	17.25	20.8	3.55
Total mass of sample collected				**14.22**

3.3.2 Thin layer chromatography (TLC)

The crude and collected fractionated cucurbitacin compounds were spotted onto a marked baseline of the 5 x 10 cm of TLC plates, which were pre-coated with 0.25 mm thick silica gel 60 F254 (Merck), using a fine glass spotter. After spotting, the plate was placed in a glass jar containing 10 ml of solvent system. The plate was allowed to develop until the solvent front reached approximately 1 cm from the top edge of the plate. The TLC plate was removed from the jar and solvent front was marked and air dried. The TLC plate was then observed under UV light and compound spots that were visible under UV light were marked accordingly. The TLC plate was then sprayed using vanillin reagent, which was used to identify cucurbitacin compounds in the *Elaeocarpus* plant extracts (Table 3.3). The dried TLC plate was gently heated using hotplate. The appearance of blue and purple spots indicated the presence of cucurbitacin compounds (Figure 3.3).

Table 3.3 Recipe to make vanillin reagent

Solution 1	Solution 2
20 mL of Sulphuric acid + 80 mL of distilled water	1.6 g of Vanillin + 50 mL of 95% Ethanol

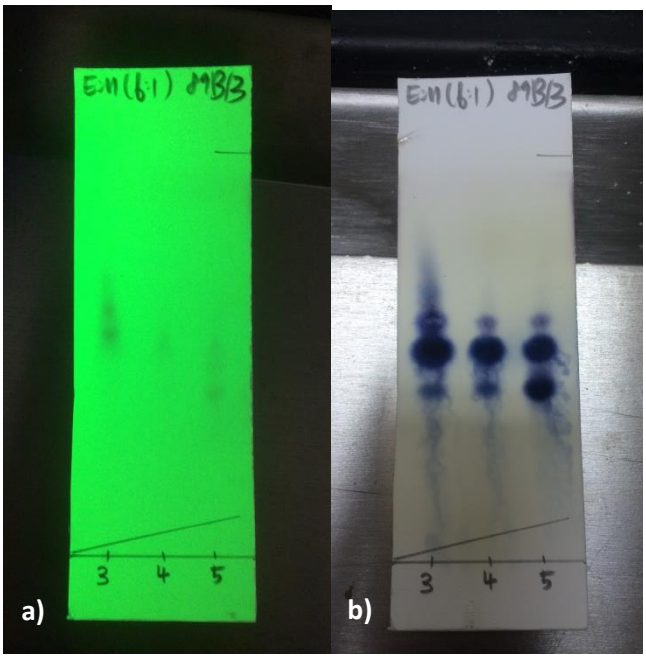


Figure 3.3 TLC Plate showing cucurbitacin compounds: a) under UV and b) heating the plate after spraying with vanillin reagent

3.3.3 Centrifugal thin layer chromatography (CTLC)

The thickness the CTLC plates used (i.e., 1 mm, 2 mm, or 4 mm) was determined by the weight of the sample (Table 3.4).

Table 3.4 Recipe table for plate preparation

Sample weight	< 400 mg	400 - 800 mg	800 mg - 1.6 g
Plate thickness	1 mm	2 mm	4 mm
Weight of Silica powder needed	40 g	60 g	110 g
Volume of cold distilled water	100 mL	120 mL	220 mL

The side of a clean glass plate was cellophane taped to prevent the slurry from leaking out. Weight of the silica was measured in a conical flask and 0 - 5 °C of cold distilled water was added to make a slurry. The mixture was vigorously shaken for 1 min and gently poured into the plate secured with cellophane tape. The plate was left to dry under room temperature for 30 min. The cellophane tape was then removed and the dried plate was baked in the oven for at least 5 hours at 50 °C. The plate was reactivated at 100 °C for

an hour before running CTLC. The baked silica plate was shaved using metal blades corresponding to the thickness of the silica plate.

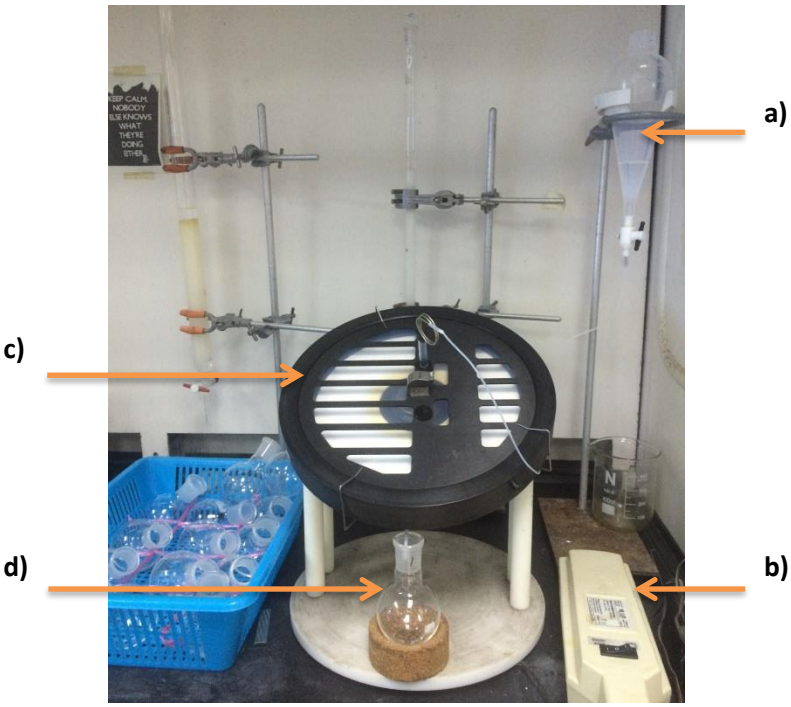


Figure 3.2 Centrifugal thin layer chromatography: a) Solvent system, b) UV detector, c) Chromatotron and d) Collected fraction

Before placing the plate, the chromatotron was cleaned using chloroform (Figure 3.2c). The plate was then placed on the chromatotron and was tightened properly. The chromatotron was switched on and the sample which was dissolved in minimum amount of chloroform was carefully loaded onto the center of the plate. Starting solvent (Figure 3.2a) was prepared based on the TLC result. Individual band, which might or not be visible under UV light (Figure 3.2b), was collected using a round bottomed flask. The sample was separated by collecting the bands (Figure 3.2d). Fractionated bands were concentrated using rotary evaporator and TLC was carried out to check for the presence of pure compounds.

3.4 Analysis of Extracted Compounds

Melting points were recorded on Stuart SMP-10 melting point apparatus and were uncorrected. Optical rotations were measured with a JASCO P-1020 digital polarimeter. UV spectra were measured with a GE Ultrospec 8000 spectrophotometer. IR spectra were obtained on a PerkinElmer Spectrum RX1 FT-IR Spectrophotometer. ^{1}H and ^{13}C NMR spectra were obtained in $CDCl_3$ using TMS as internal standard on a Bruker 600 MHz spectrometer operating at 600 MHz (^{1}H) and 150 MHz (^{13}C). HRESIMS were obtained on a JEOL Accu TOF-DART mass spectrometer.

X-ray diffraction analysis was carried out on a Rigaku Oxford (formerly Agilent Technologies) SuperNova Dual diffractometer with Cu Kα (λ = 1.54184 Å) radiation at 155 K. The structures were solved by direct methods (SHELXS-2014) and refined with full-matrix least-squares on F^2 (SHELXL-2014). All non-hydrogen atoms were refined anisotropically, and all hydrogen atoms were placed in idealized positions and refined as riding atoms with the relative isotropic parameters.

3.5 Compound Data

Compound (**1**): colourless crystals; mp 180-182 °C (dec); $[\alpha]_D$ +28 (c 0.9, $CHCl_3$); UV (EtOH); IR (dry film) ν_{max} 3408, 1689 cm^{-1}; ^1H NMR and ^{13}C NMR data, see Table 2.1; HREIMS m/z 535.32516 (calcd for $C_{30}H_{46}O_8$, 535.32516).

Compound (**2**): light yellowish oil;$[\alpha]_D$ +48 (c 0.4, $CHCl_3$); UV (EtOH); IR (dry film) ν_{max} 3406, 1688cm^{-1}; ^1H NMR and ^{13}C NMR data, see Table 2.2; HREIMS m/z 499.30541 (calcd for $C_{30}H_{46}O_8$, 499.30541).

Compound (**3**): colourless oil; $[\alpha]_D$ +57 (c 0.3, $CHCl_3$); UV (EtOH); IR (dry film) ν_{max} 3447, 1688 cm^{-1}; ^1H NMR and ^{13}C NMR data, see Table 2.3; HREIMS m/z 469.33265 (calcd for $C_{30}H_{46}O_4$, 469.33265).

Compound (**4**): white powder; $[\alpha]_D$ +79 (c 1.0, $CHCl_3$); UV (EtOH); IR (dry film) ν_{max} 3414, 1683 cm^{-1}; ^1H NMR and ^{13}C NMR data, see Table 2.4; HREIMS m/z 675.4074 (calcd for $C_{38}H_{59}O_{10}$, 675.4074).

Compound (**5**): colourless crystal; mp 257-258 °C (dec); UV (EtOH); IR (dry film) ν_{max} 3459, 1687 cm^{-1}; ^1H NMR data, see Table 2.5; HREIMS m/z 471.34766 (calcd for $C_{30}H_{46}O_4$, 471.34766).

Compound (**6**): white amorphous solid; UV (EtOH); IR (dry film) ν_{max} 3410, 1682 cm^{-1}; ^1H NMR and ^{13}C NMR data, see Table 2.6; HREIMS m/z 632.3924 (calcd for $C_{36}H_{56}O_9$, 632.3924).

Compound (**7**): colourless oil; UV (EtOH); IR (dry film) ν_{max} 3449, 1686 cm^{-1}; ^1H NMR data, see Table 2.7; HREIMS m/z 489.3555 (calcd for $C_{30}H_{48}O_5$, 489.3555).

Compound (**8**): colourless oil; UV (EtOH); IR (dry film), ^1H NMR data, see Table 2.8; HREIMS m/z 405.2641 (calcd for $C_{24}H_{36}O_5$, 405.2641).

3.6 Cytotoxic Test

3.6.1 Cell lines and cell culture

A panel of human breast cancer (MCF7, MDA-MB-231, MDA-MB-468, SKBR3, T47D), colorectal cancer (Caco2, HCT116, HT29, SW48), nasopharyngeal cancer (CNE1, HK1, SUNE1), pancreatic cancer (AsPC1, BxPC3, SW1990) and human non-tumorigenic breast epithelial cells (MCF10A) were purchased from the American Type Culture Collection. All cancer cells including MRC5 cells were maintained in RPMI 1640 medium with 10% fetal bovine serum (FBS), 100 IU/mL penicillin, and 100 µg/mL streptomycin (Sigma-Aldrich, St. Louis, MO, USA), while MCF10A cells were cultured with 5% horse serum, 20 ng/mL epidermal growth factor, 0.5 µg/mL hydrocortisone, 10 µg/mL insulin, 100 IU/mL penicillin, and 100 µg/mL streptomycin. All cells were maintained in an incubator at 37°C and 5% carbon dioxide.

3.6.2 Luminescent cell viability assay

This part of the research was carried out in the Center for Cancer and Stem Cell Research at International Medical University, Malaysia. Cell viability was determined using the CellTitre-Glo® Luminescent Cell Viability Assay kit (Promega, USA). All compounds were prepared in 100 mM dimethyl sulfoxide (DMSO) as stock solution and diluted to various concentrations (1.5 to 100μM) using sterile phosphate buffer solution. All cell lines were seeded in 384-well opaque plates for 24 h at a density of 1000 cells/well followed by treatment for 72 hours. Cells treated with 0.1% DMSO served as a negative control. Luminescence reading was measured using SpectraMax M3 Multi-Mode Microplate Reader (Radnor, USA). The inhibitory concentration of 50% cell viability (IC_{50}) was determined based on the luminescent readings of treated cells and negative control.

References

1 H. F. Ji, X. J. Li and H. Y. Zhang, *EMBO Rep.*, 2009, **10**, 194–200.

2 V. J. Raja, K.-H. Lim, C.-O. Leong, T.-S. Kam and T. D. Bradshaw, *Invest New Drugs*, 2014, **32**, 838–850.

3 A. L. Demain and P. Vaishnav, *Microb. Biotechnol.*, 2011, **4**, 687–699.

4 A. G. Desai, G. N. Qazi, R. K. Ganju, M. El-Tamer, J. Singh, A. K. Saxena, Y. S. Bedi, S. C. Taneja and H. K. Bhat, *Curr. Drug Metab.*, 2008, **9**, 581–591.

5 F. Lam, T. D. Bradshaw, H. Mao, S. Roberts, Y. Pan and S. Wang, *Invest. New Drugs*, 2012, **30**, 1899–1907.

6 R. P. Borris, *J. Ethnopharmacol.*, 1996, **51**, 29–38.

7 D. O. Kennedy and E. L. Wightman, *Adv. Nutr.*, 2011, **2**, 32–50.

8 F. E. Koehn and G. T. Carter, *Nat. Rev. Drug Discov.*, 2005, **4**, 206–220.

9 X. Fang, C. H. Phoebe, J. M. Pezzuto, H. H. Fong, N. R. Farnsworth, B. Yellin and S. M. Hecht, *J. Nat. Prod.*, **47**, 988–993.

10 A. K. Hule, A. S. Shah, M. N. Gambhire and A. R. Juvekar, *Indian J. Pharmacol.*, 2011, **43**, 56–59.

11 J. Nain, K. Garg and S. Dhahiya, *Int. J. Pharm. Pharm. Sci.*, 2012, **4**, 379-381.

12 A. A. Alghasham, *Int. J. Health Sci. (Qassim).*, 2013, **7**, 77–89.

13 T. Tannin-Spitz, S. Grossman, S. Dovrat, H. E. Gottlieb and M. Bergman, *Biochem. Pharmacol.*, 2007, **73**, 56–67.

14 C. Delporte, O. Muñozb, J. Rojas, M. Ferrándiz, M. Payá, S. Erazo, R. Negrete, S. Maldonado, A. San Feliciano and N. Backhouse, *Zeitschrift für Naturforsch. C*, 2002, **57**, 100–108.

15 R. Veberič, *BIOACTIVE COMPOUNDS IN FRUIT PLANTS*, University of Ljubljana, 2010.

16 P. Dzubak, M. Hajduch, D. Vydra, A. Hustova, M. Kvasnica, D. Biedermann, L. Markova, M. Urban and J. Sarek, *Nat. Prod. Rep.*, 2006, **23**, 394.

17 D. Lednicer, *Steroid Chemistry at a Glance*, John Wiley & Sons, 2011.

18 J. Harder, ed. K. N. Timmis, Springer Berlin Heidelberg, Berlin, Heidelberg, 2010, pp. 127–131.

19 P. M. Dewick, *Medicinal Natural Products: A Biosynthetic Approach*, John Wiley & Sons, 2009.

20 V. Donald, W. P. Charlotte and G. V. Judith, *Principles of Biochemistry*, 2013.

21 H. L. J. Makin and D. B. Gower, Eds., *Steroid Analysis*, Springer Netherlands, Dordrecht, 2010.

22 G. Jorn, S. Inge and C. A. Hans, *Cucurbitacins in plant food*, Nordic Council of Ministers, Copenhagen, 2006.

23 J. C. Chen, M. H. Chiu, R. L. Nie, G. A. Cordell and S. X. Qiu, *Nat. Prod. Rep.*, 2005, **22**, 386–399.

24 P. R. Enslin, J. M. Hugo, K. B. Norton and D. E. A. Rivett, *J. Chem. Soc.*, 1960, 4779.

25 M. Clericuzio, S. Tabasso, M. A. Bianco, G. Pratesi, G. Beretta, S. Tinelli, F. Zunino and G. Vidari, *J. Nat. Prod.*, 2006, **69**, 1796–1799.

26 M. F. Bean, M. Antoun, D. Abramson, C.-J. Chang, J. L. Mclaughlin and J. M. Cassady, *J. Nat. Prod.*, **48**.

27 G. Balliano, O. Caputo, F. Viola, L. DelPrino and L. Cattel, *Phytochemistry*, 1983, **22**, 909–913.

28 J. A. Hall, S. Seedarala, N. Rice, L. Kopel, F. Halaweish and B. S. J. Blagg, .

29 N. Rodriguez, Y. Vasquez, A. A. Hussein, P. D. Coley, P. N. Solis and M. P. Gupta, *J. Nat. Prod.*, 2003, **66**, 1515–1516.

30 G. Maatooq, S. W. H El-sharkawy, M. Afifi and J. Rosa, *J. Nat. Prod.*, 1995, **58**, 165–171.

31 K. N. Maloney, M. Fujita, U. S. Eggert, F. C. Schroeder, C. M. Field, T. J. Mitchison and J. Clardy, *J. Nat. Prod.*, 2008, **71**, 1927–1929.

32 P.-L. Wu, F.-W. Lin, T.-S. Wu, C.-S. Kuoh, K.-H. Lee and S.-J. Lee, *Chem. Pharm. Bull. (Tokyo).*, 2004, **52**, 345–349.

33 H. F. Smit, A. J. J van den Berg, B. H. Kroes, C. J. Beukelman, H. C. Quarles van Ufford, H. van Dijk and R. P. Labadie, *J. Nat. Prod.*, 2000, **63**, 1300–1302.

34 L. Pan, Y. Yong, Y. Deng, D. D. Lantvit, T. N. Ninh, H. Chai, E. J. Carcache de Blanco, D. D. Soejarto, S. M. Swanson and A. D. Kinghorn, *J. Nat. Prod.*, 2012, **75**, 444–452.

35 S. ZHANG, Z.-M. TAO, Y. ZHANG, Z.-W. SHEN and G.-W. QIN, *Chin. J. Nat. Med.*, 2010, **8**, 21–24.

36 D. Meng, S. Qiang, L. Lou and W. Zhao, *Planta Med.*, 2008, **74**, 1741–1744.

37 T. Tuyama, *Phytogeographical Consideration on the Genus Elaeocarpus of the Volcano and Bonin Islands*, *Natural Science Report*, 1952. **3**, 68–70.

38 Y. Baba and D. Crayn, *Kew Bull.*, **67**, 743–750.

39 R. K. Singh, S. B. Acharya and S. K. Bhattacharya, *Phytother. Res.*, 2000, **14**, 36–39.

40 O.-K. Kwon, K.-S. Ahn, J.-W. Park, H.-Y. Jang, H. Joung, H.-K. Lee and S.-R. Oh, *Inflammation*, 2012, **35**, 535–544.

41 in *CRC World Dictionary of Medicinal and Poisonous Plants*, CRC Press, 2012, pp. 1507–1712.

42 A. Ito, H.-B. Chai, D. Lee, L. B. S. Kardono, S. Riswan, N. R. Farnsworth, G. A. Cordell, J. M. Pezzuto and A. D. Kinghorn, *Phytochemistry*, 2002, **61**, 171–174.

43 C. Fitzmaurice, C. Allen, R. M. Barber *et al*, *JAMA Oncol.*, 2017, **3**, 524.

44 H. Wang, T. O. Khor, L. Shu, Z.-Y. Su, F. Fuentes, J.-H. Lee and A.-N. T. Kong, *Anticancer. Agents Med. Chem.*, 2012, **12**, 1281–1305.

45 M. Li-Weber, *Cancer Lett.*, 2013, **332**, 304–312.

46 J. C. Reed, *Am. J. Pathol.*, 2000, **157**, 1415–1430.

47 C. Cerella, C. Sobolewski and M. Dicato, *Biochem. Pharmacol.*, 2010, **80**, 1801–1815.

48 L. Klampfer, *Curr. Cancer Drug Targets*, 2006, **6**, 107–121.

49 X. Chen, J. Bao, J. Guo, Q. Ding, J. Lu, M. Huang and Y. Wang, *Anticancer. Drugs*, 2012, **23**, 777–787.

50 J. A. Beutler, ed. E. F. Koehn, Springer New York, New York, NY, 2013, pp. 213–237.

51 I. N. F. Dantas, G. C. M. Gadelha, D. C. Chaves, F. J. Q. Monte, C. Pessoa, M. O. de Moraes and L. V. Costa-Lotufo, *Zeitschrift für Naturforschung. C, J. Biosci.*, **61**, 643–646.

52 K. L. Lang, I. T. Silva, L. A. Zimmermann, V. R. Machado, M. R. Teixeira, M. I. Lapuh, M. A. Galetti, J. A. Palermo, G. M. Cabrera, L. S. C. Bernardes, C. M. O. Simões, E. P. Schenkel, M. S. B. Caro and F. J. Durán, *Bioorg. Med. Chem.*, 2012, **20**, 3016–3030.

53 B. Jayaprakasam, N. P. Seeram and M. G. Nair, *Cancer Lett.*, 2003, **189**, 11–16.

54 N. Wakimoto, D. Yin, J. O'Kelly, T. Haritunians, B. Karlan, J. Said, H. Xing and H. P. Koeffler, *Cancer Sci.*, 2008, **99**, 1793–1797.

55 S. Kongtun, W. Jiratchariyakul, T. Kummalue, P. Tan-ariya, S. Kunnachak and A. Wilhelm Frahm, *Planta Med.*, 2009, **75**, 839–842.

56 M. A. Blaskovich, J. Sun, A. Cantor, J. Turkson, R. Jove and S. M. Sebti, *Cancer Res.*, 2003, **63**.

57 J. Sun, M. A. Blaskovich, R. Jove, S. K. Livingston, D. Coppola and S. M. Sebti, *Oncogene*, 2005, **24**, 3236–3245.

58 C. T. Che, X. D. Fang, C. H. Phoebe, A. D. Kinghorn, N. R. Farnsworth, B. Yellin and S. M. Hecht, *J. Nat. Prod.*, **48**, 429–434.

59 Jeh-Jian Hsiao and Hung-Cheh Chiang, *Phytochemistry*, 1995, **39**, 899–902.

60 S. Hammami, H. Ben Jannet, A. Bergaoui, L. Ciavatta, G. Cimino and Z. Mighri, 2004.

61 a Baramee, J. Clardy, P. Kongsaeree, S. Rajviroongit, C. Suteerachanon, C. Thebtaranonth and Y. Thebtaranonth, *Chem. Commun.*, 1996, 1511.

62 J. R. Bull, *J. Chem. Soc., Perkin Trans. 1*, 1972, **0**, 627–632.

63 C. Z. Gu, J. J. Lv, X. X. Zhang, Y. J. Qiao, H. Yan, Y. Li, D. Wang, H. T. Zhu, H. R. Luo, C. R. Yang, M. Xu and Y. J. Zhang, *J. Nat. Prod.*, 2015, **78**, 1829–1840.

64 V. Sai, P. Chaturvedula and I. Prakash, *Security*, 2011, **2**, 135–139.

65 V. Sai, P. Chaturvedula and I. Prakash, 2011, **01**, 104–108.

66 M. U. Roslund, P. Tähtinen, M. Niemitz and R. Sjöholm, *Carbohydr. Res.*, 2008, **343**, 101–112.

67 V. Sai, P. Chaturvedula and I. Prakash, *Int. Curr. Pharm. J.*, 2012, **1**, 239–242.

68 L. Maguire, M. Konoplyannikov, A. Ford, A. R. Maguire and N. M. O'Brien, *Br. J. Nutr.*, 2003, **90**, 767–775.

69 J. L. Pousset and J. Poisson, *Tetrahedron Lett.*, 1969, **15**, 1173–1174.

70 K. L. Stuart and L. B. Coke, *Planta*, 1975, **122**, 307–310.

71 C. A. Hudis and L. Gianni, *Oncologist*, 2011, **16(1)**, 1–11.

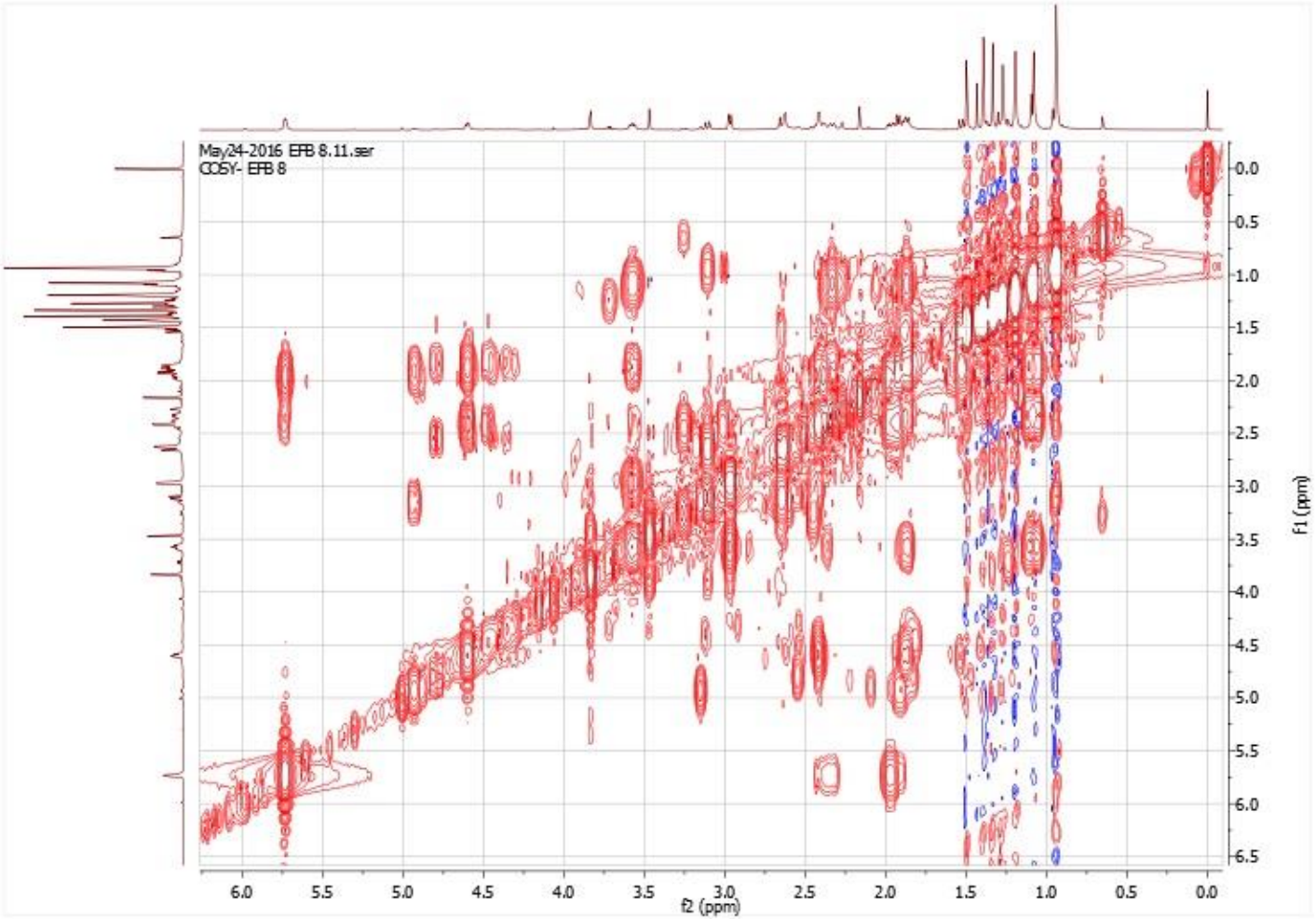
72 M. Orlando, C. Delporte, N. Backhouse, S. Erazo, R. Negrete, M. Sergio, J. L. López-pérez and A.

S. Feliciano, 2000, **56**, 0–4.

73 J. Song, H. Liu, Z. Li, C. Yang and C. Wan, *Oncol. Rep.*, 2015, **33**, 1867–1871.

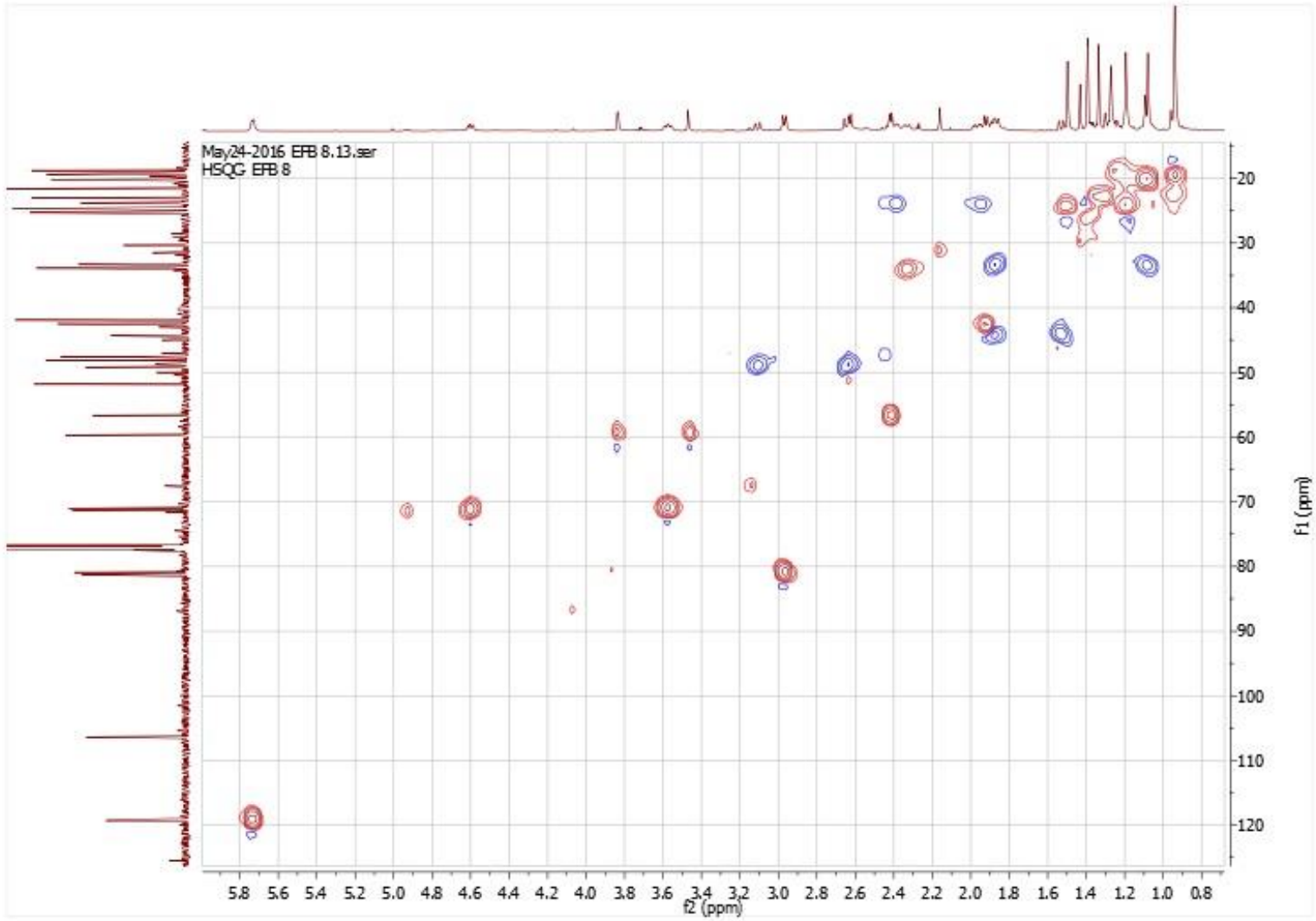
74 M. Soto-Hernández, J. C. Iñiguez, L. C. Arévalo-Galarza, E. Santiago-Osorio, I. Aguiñiga-Sánchez and L. del M. Ruíz-Posadas, in *Phytochemicals - Isolation, Characterisation and Role in Human Health*, InTech, 2015.

Appendices



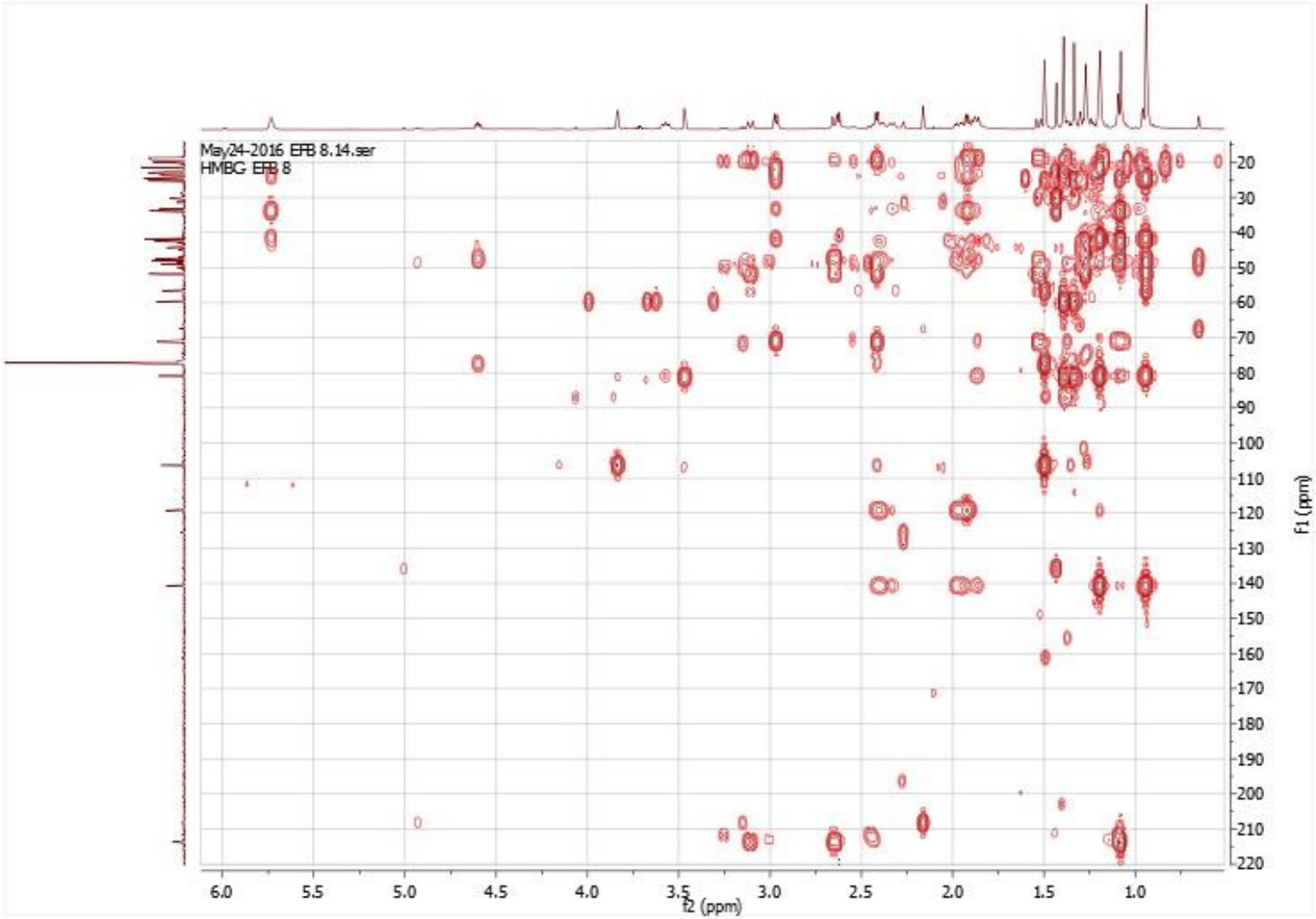
Appendix 1: COSY spectrum of compound **1**

a



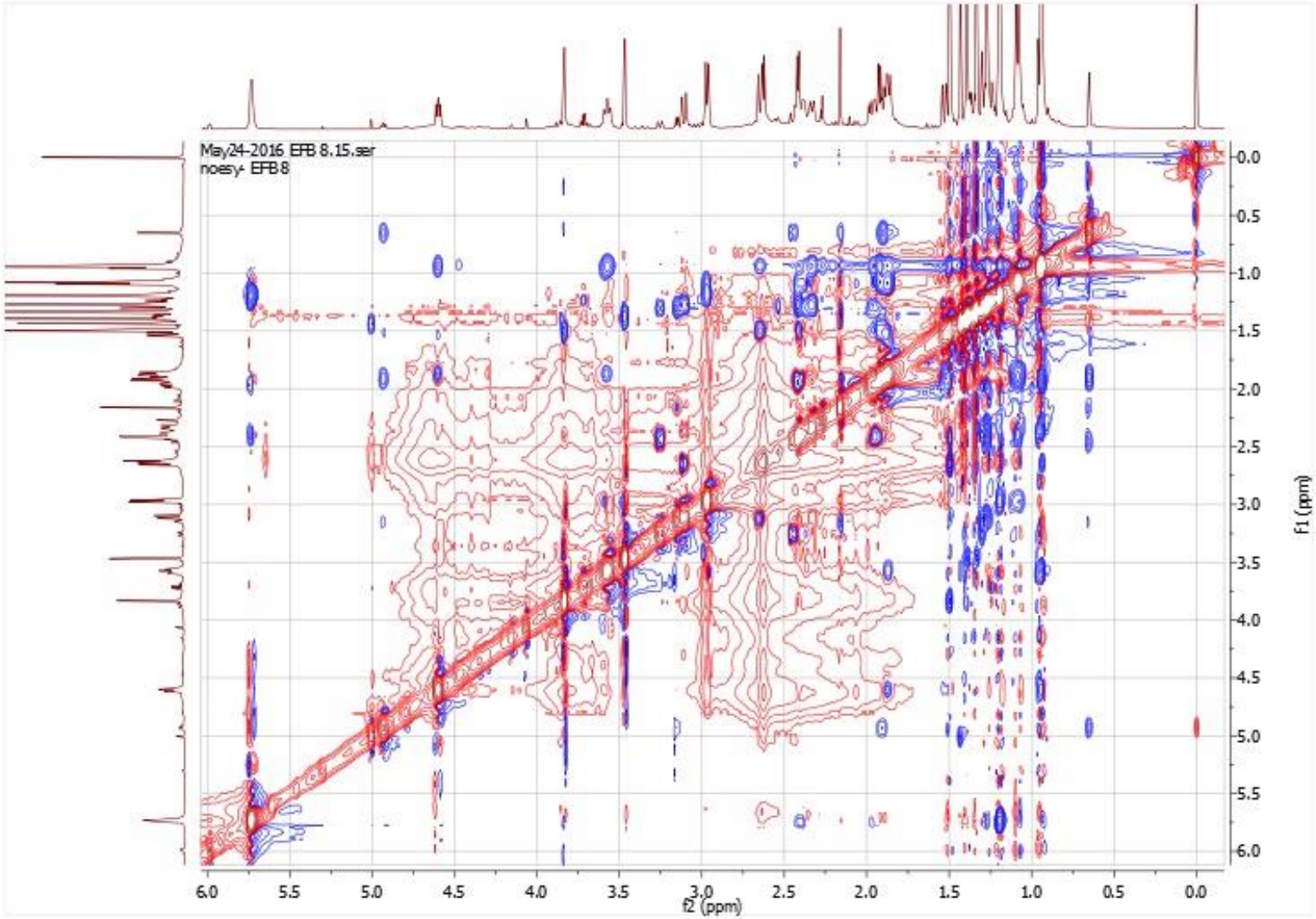
Appendix 2: HSQC spectrum of compound **1**

b



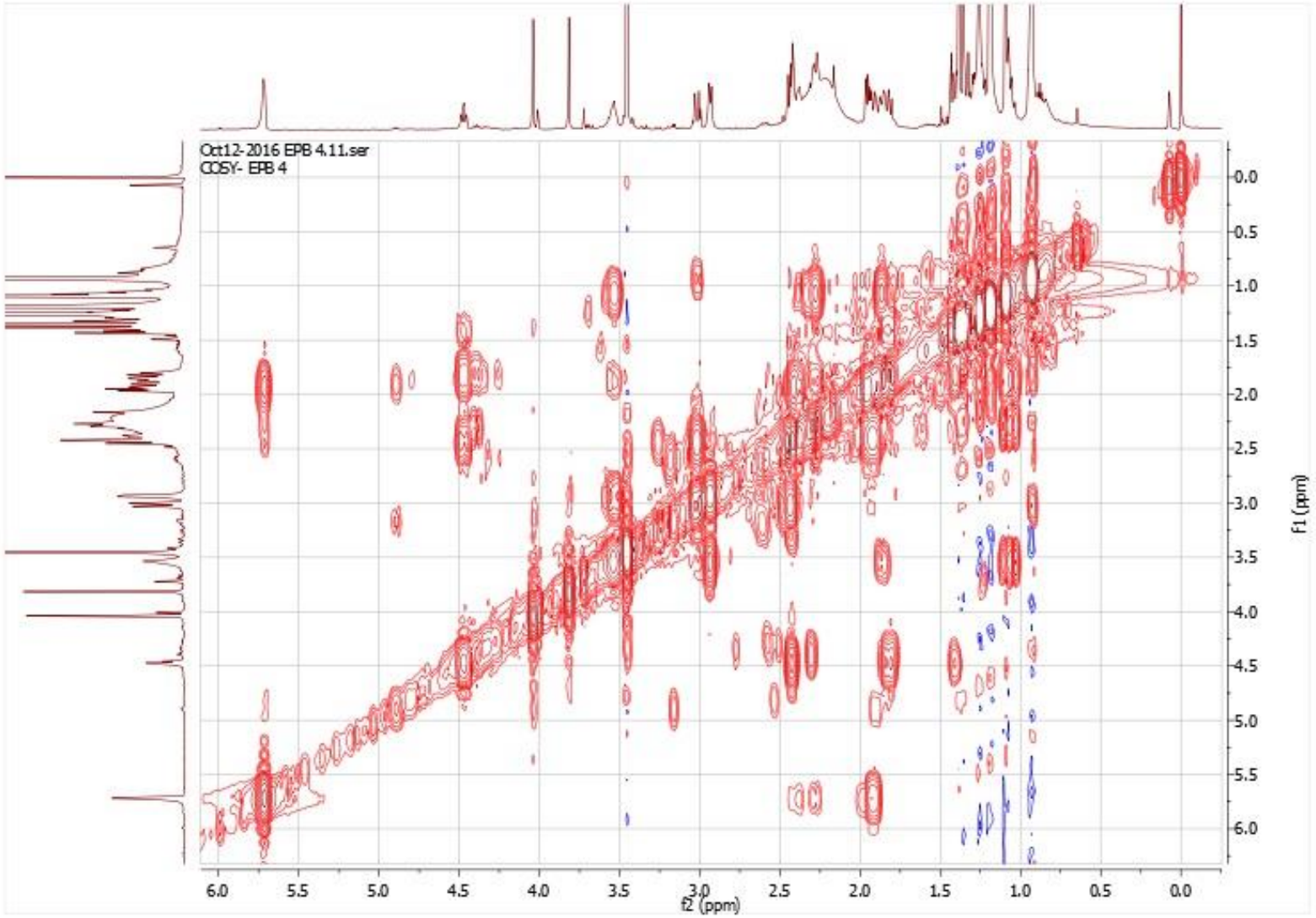
Appendix 3: HMBC spectrum of compound **1**

c



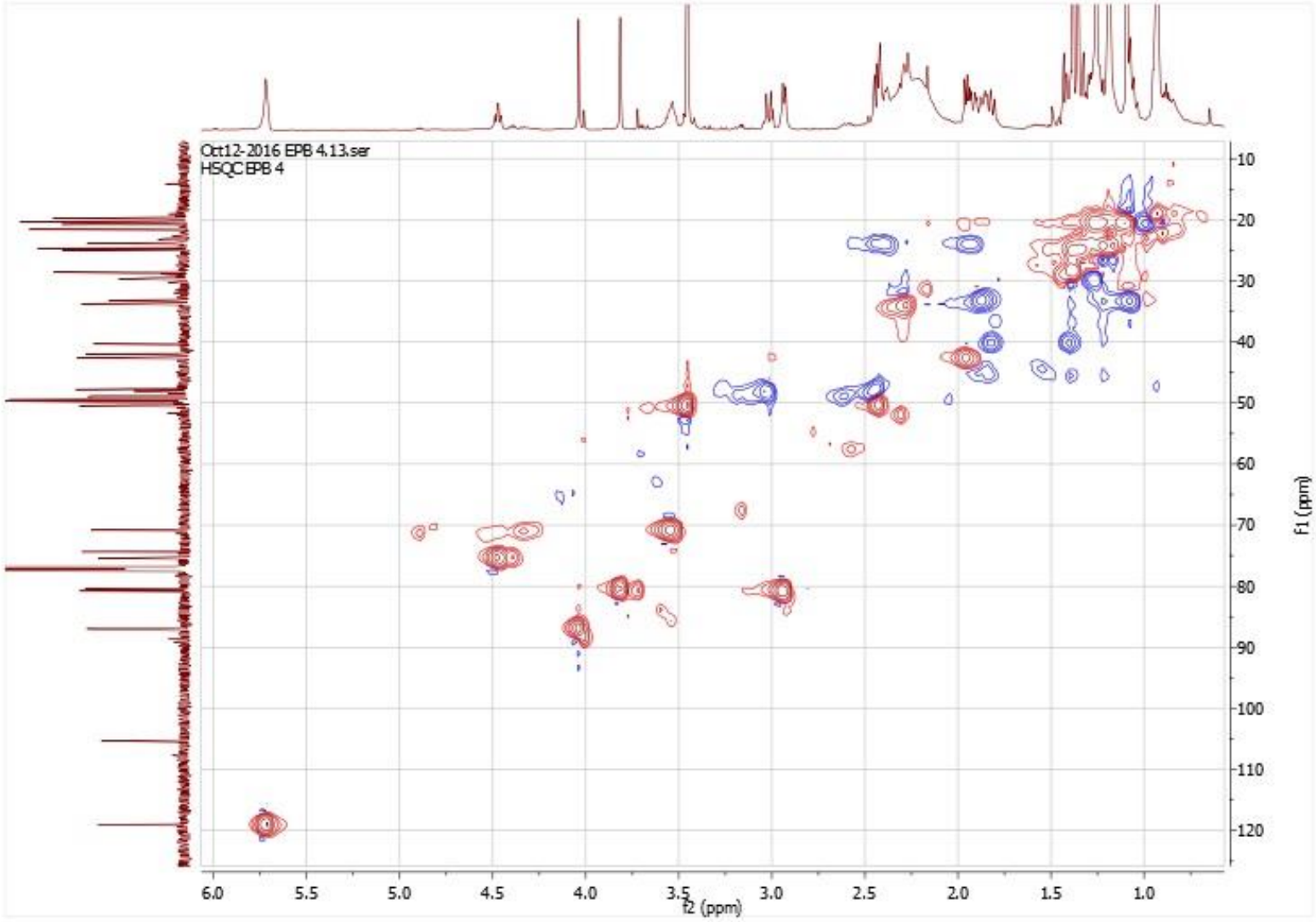
Appendix 4: NOESY spectrum of compound **1**

d



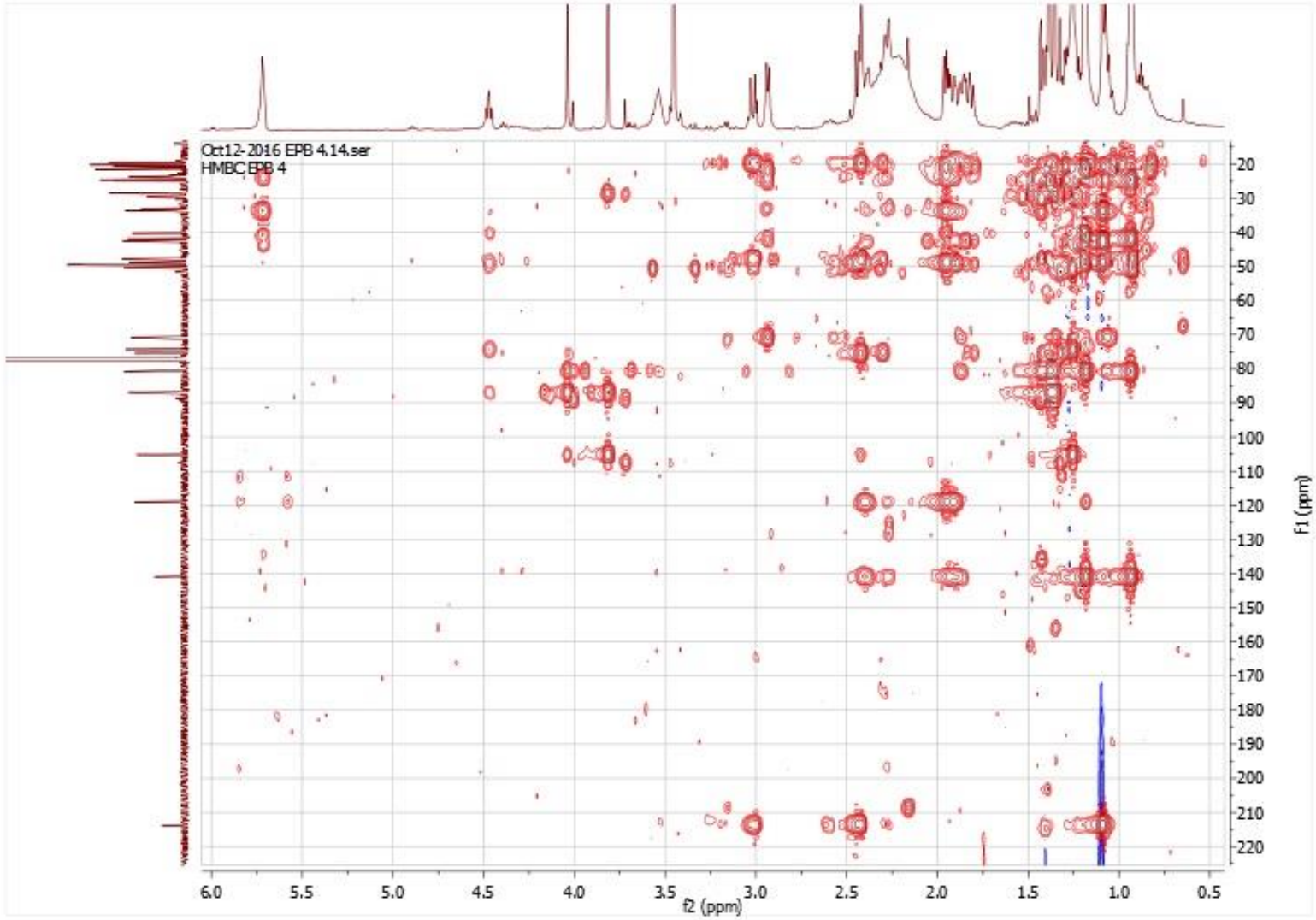
Appendix 5: COSY spectrum of compound **2**

e

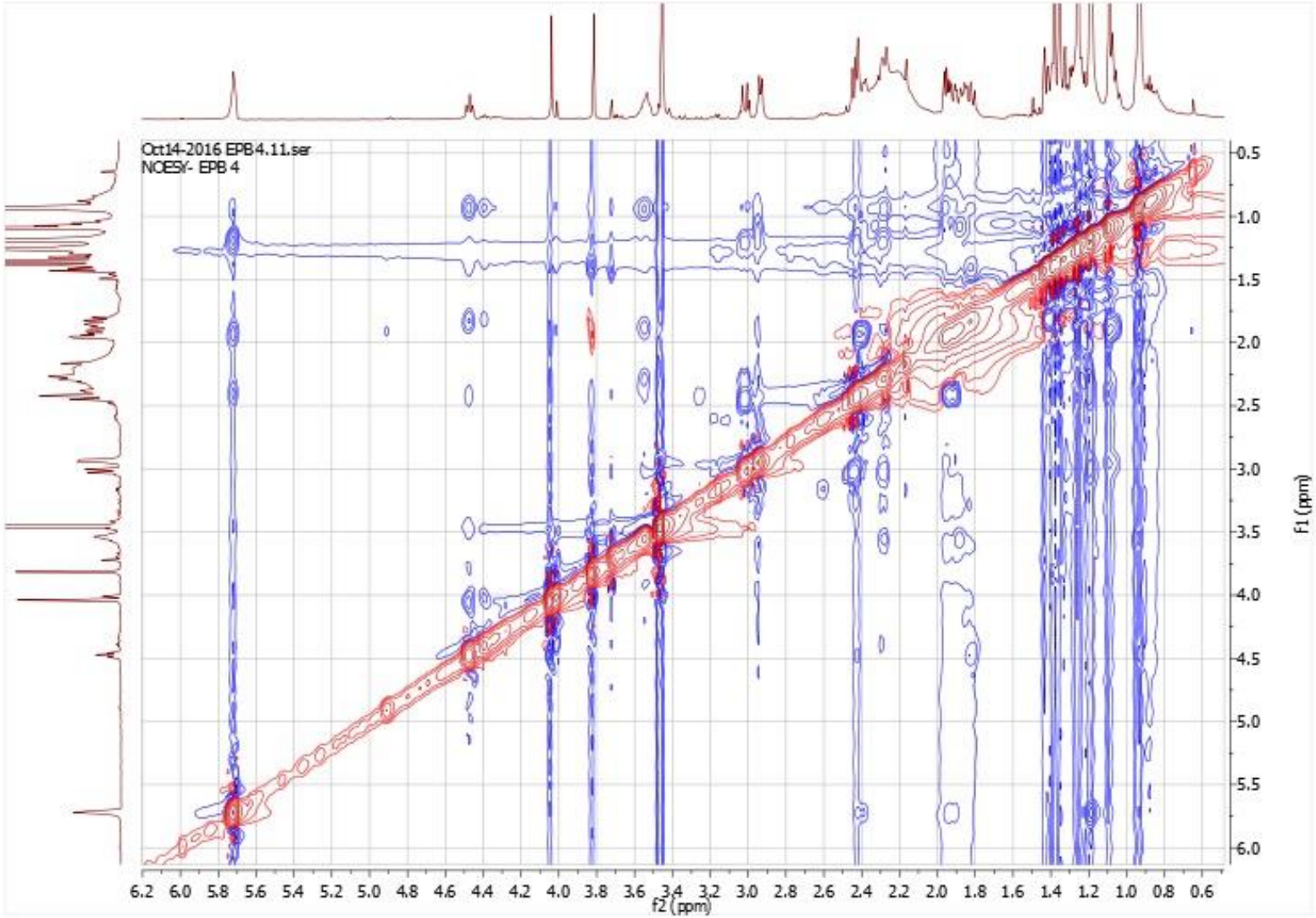


Appendix 6: HSQC spectrum of compound **2**

f

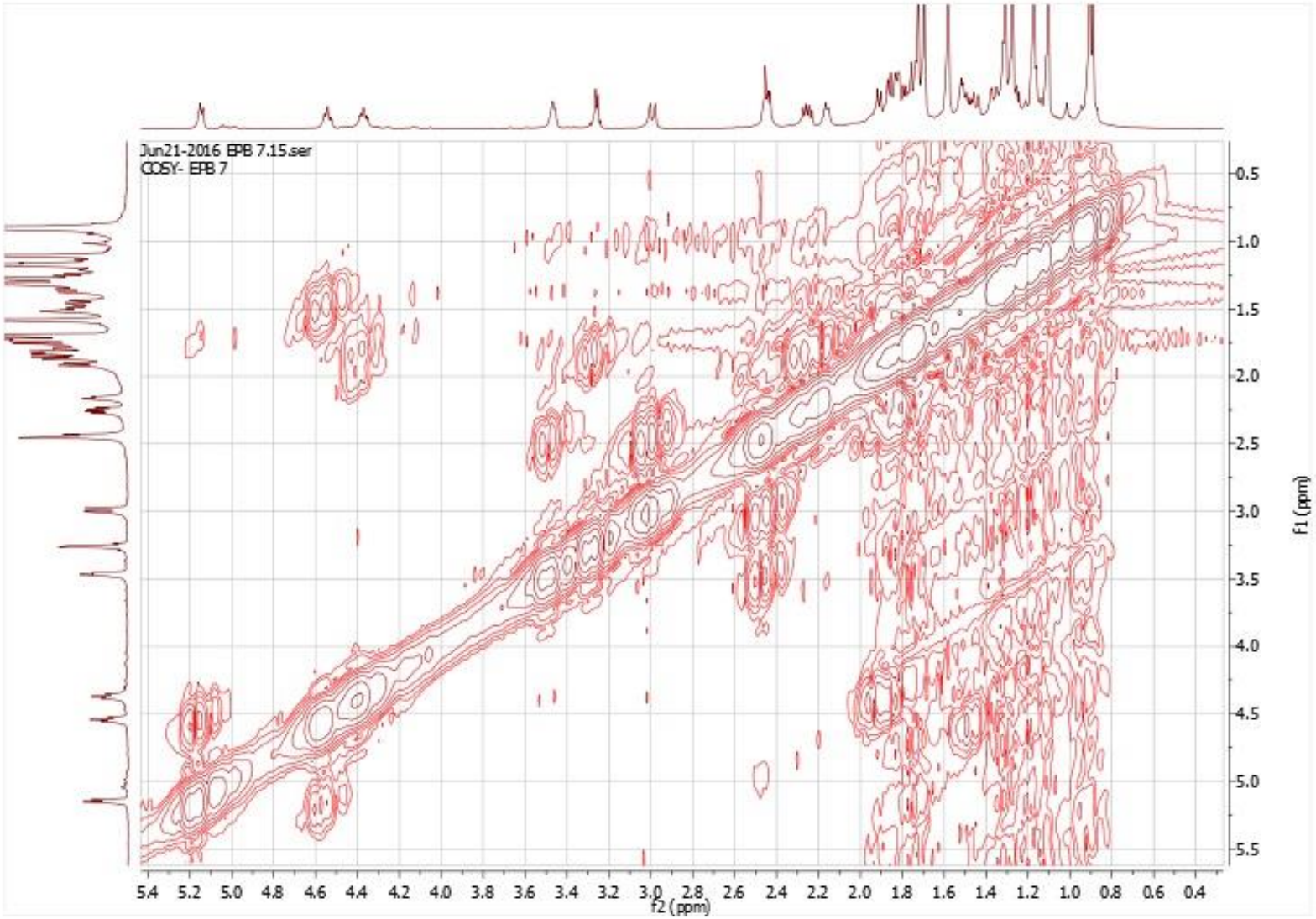


Appendix 7: HMBC spectrum of compound **2**

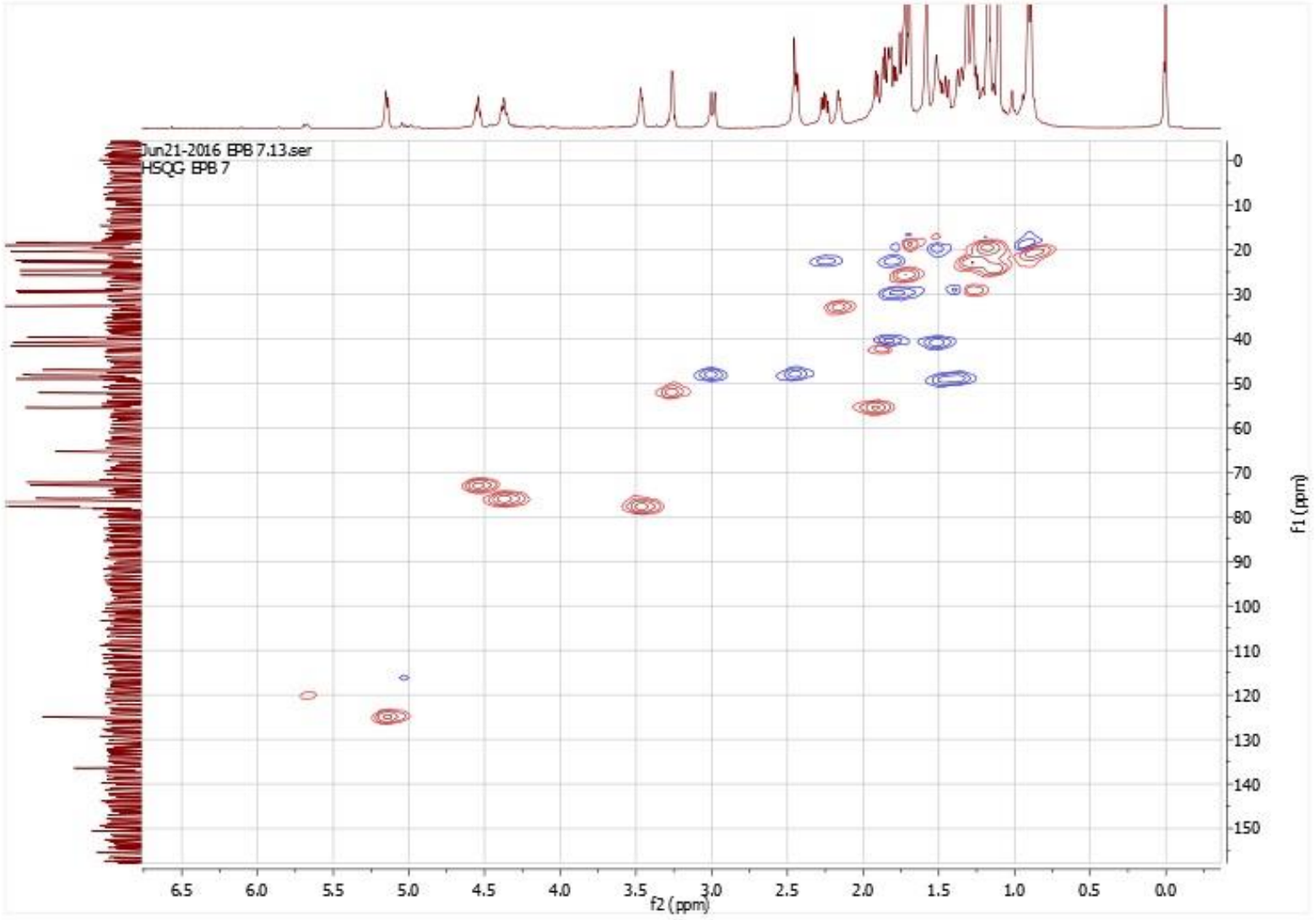


Appendix 8: NOESY spectrum of compound **2**

h

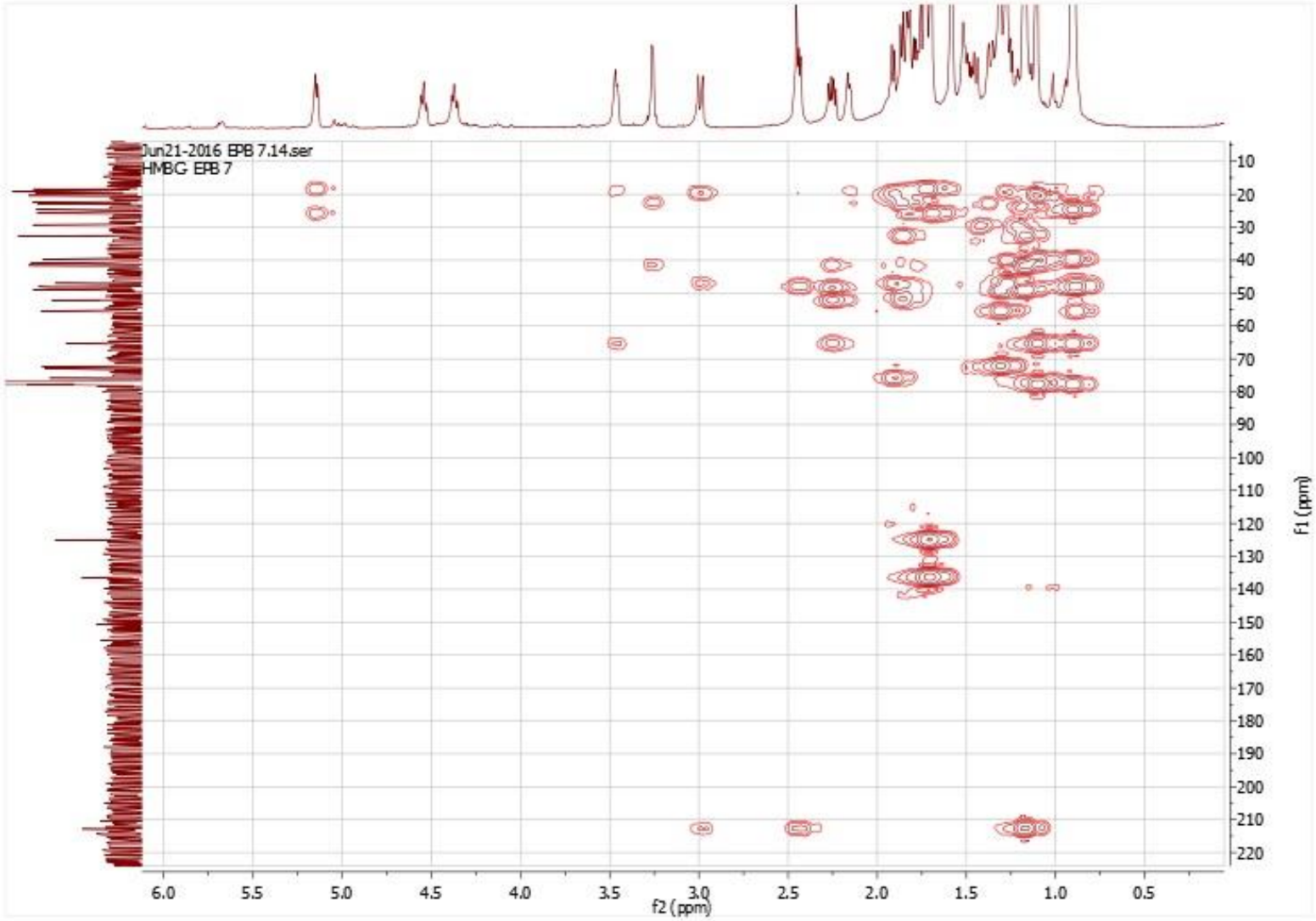


Appendix 9: COSY spectrum of compound **3**



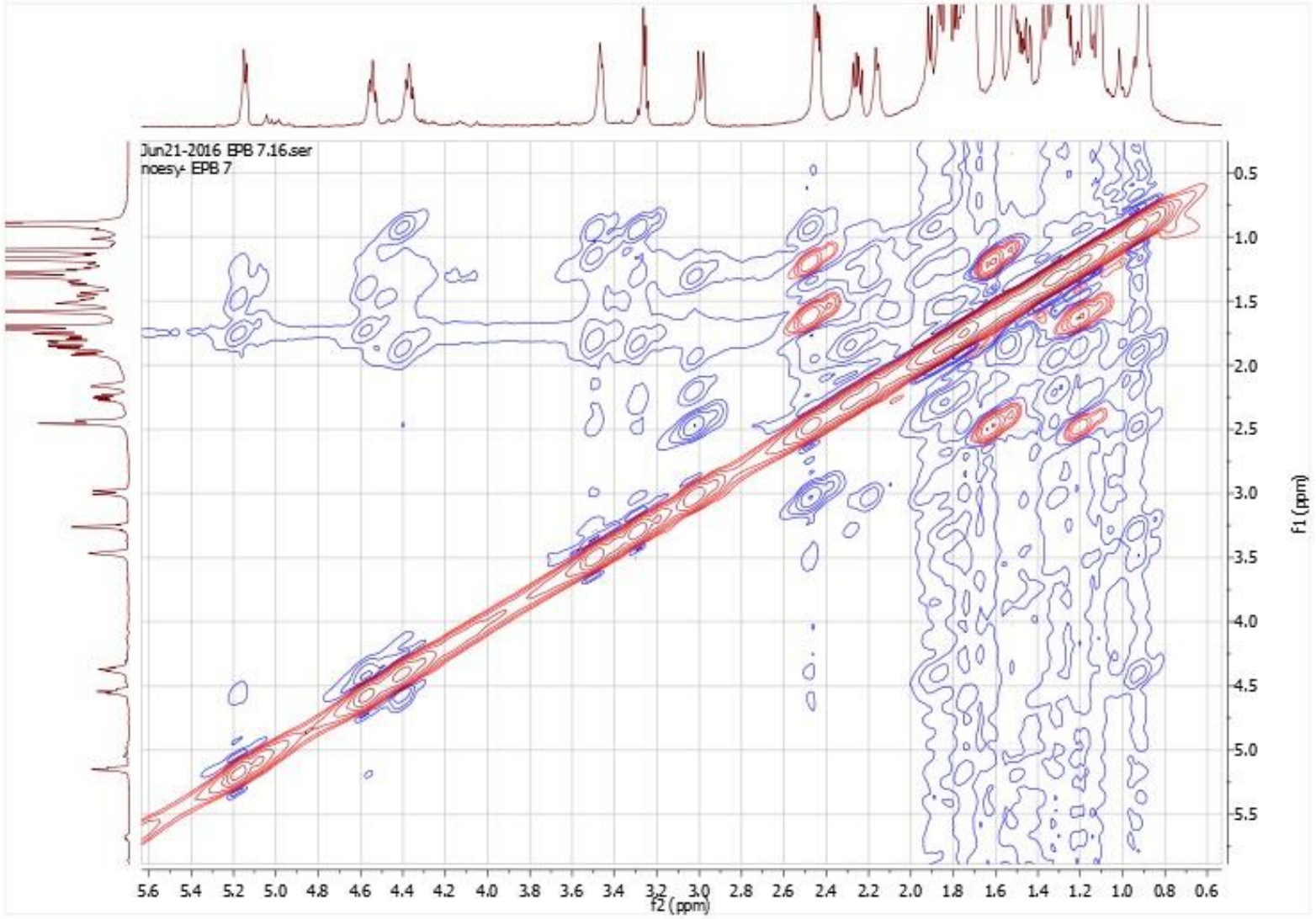
Appendix 10: HSQC spectrum of compound **3**

j

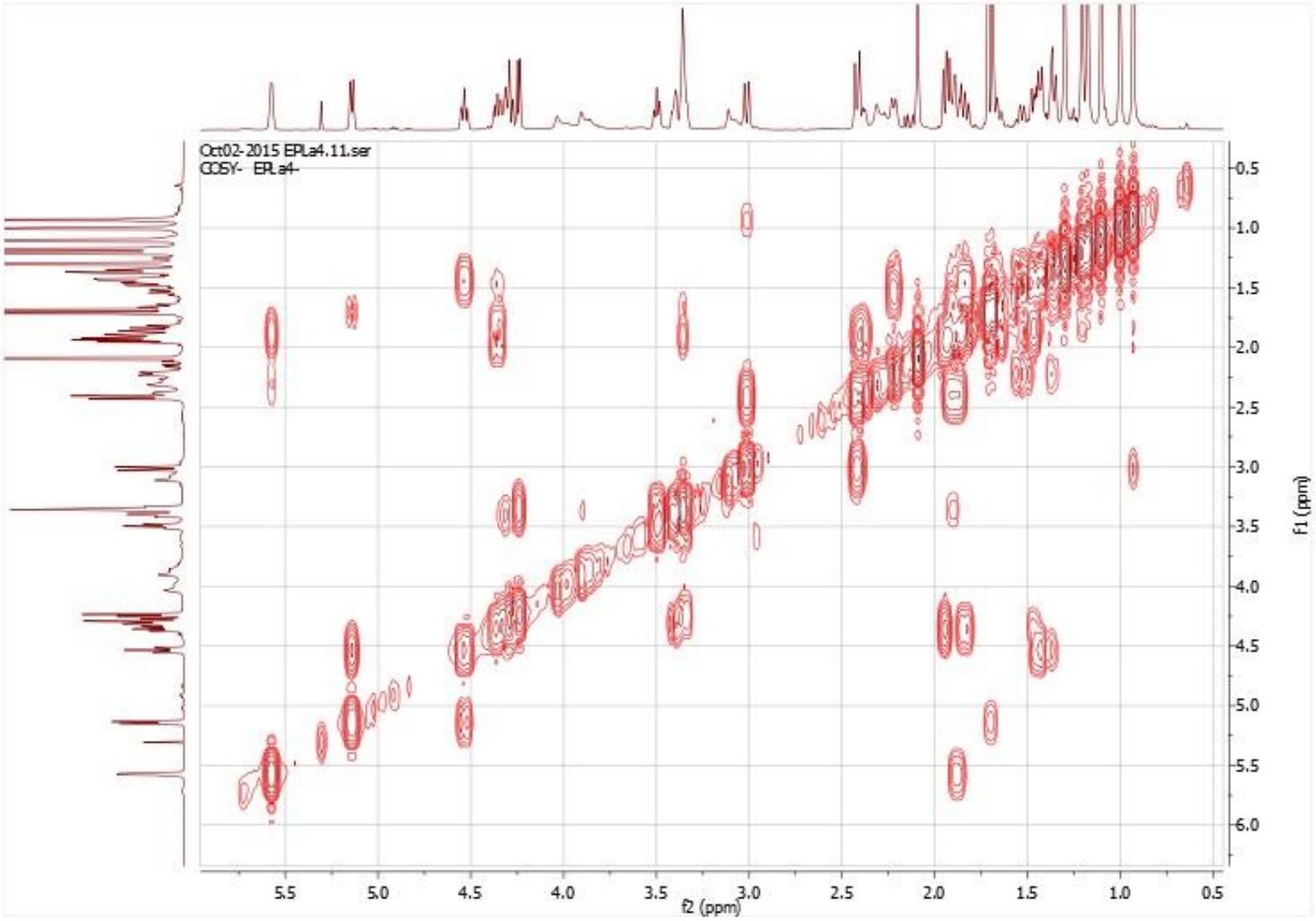


Appendix 11: HMBC spectrum of compound **3**

k

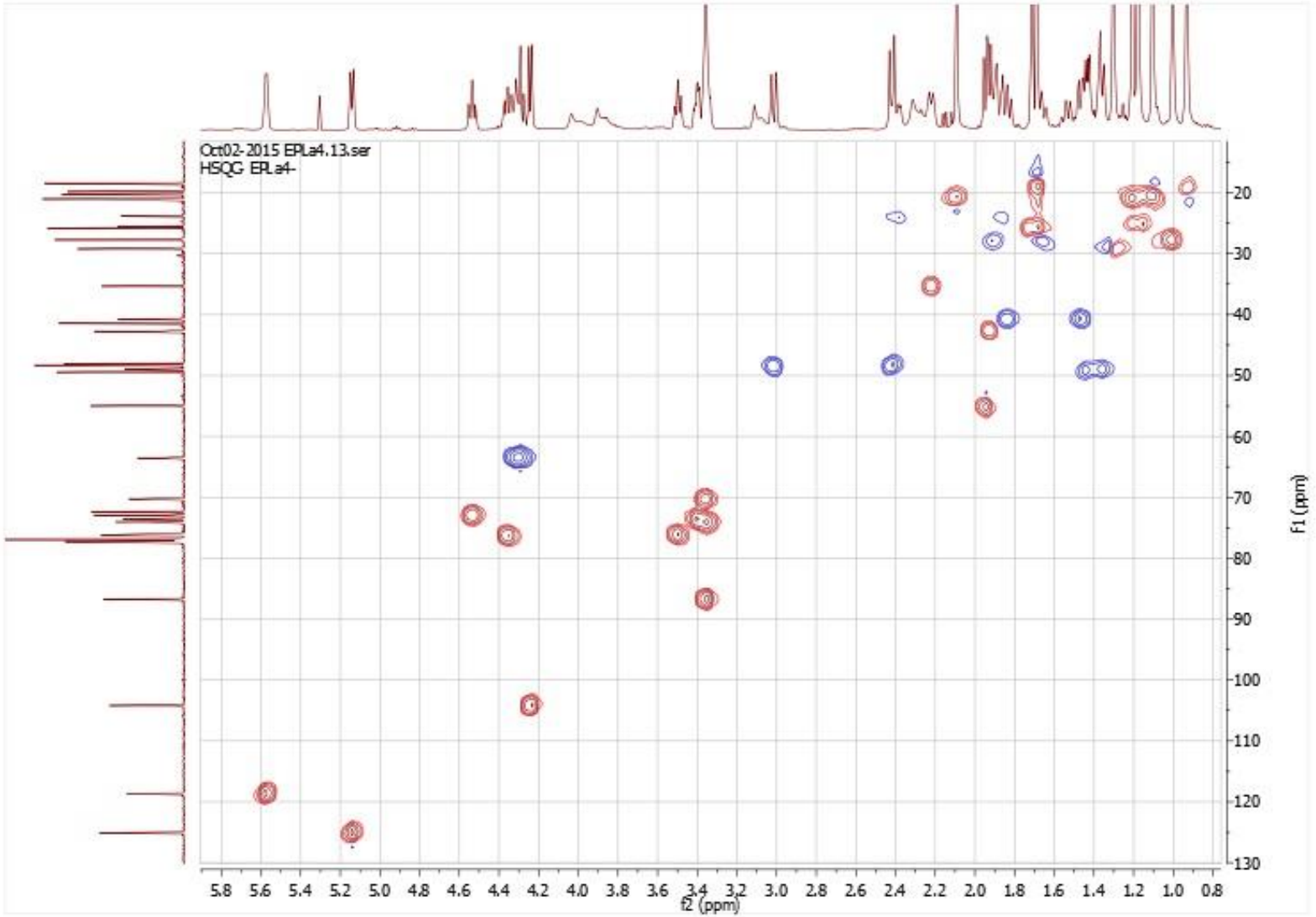


Appendix 12: NOESY spectrum of compound **3**



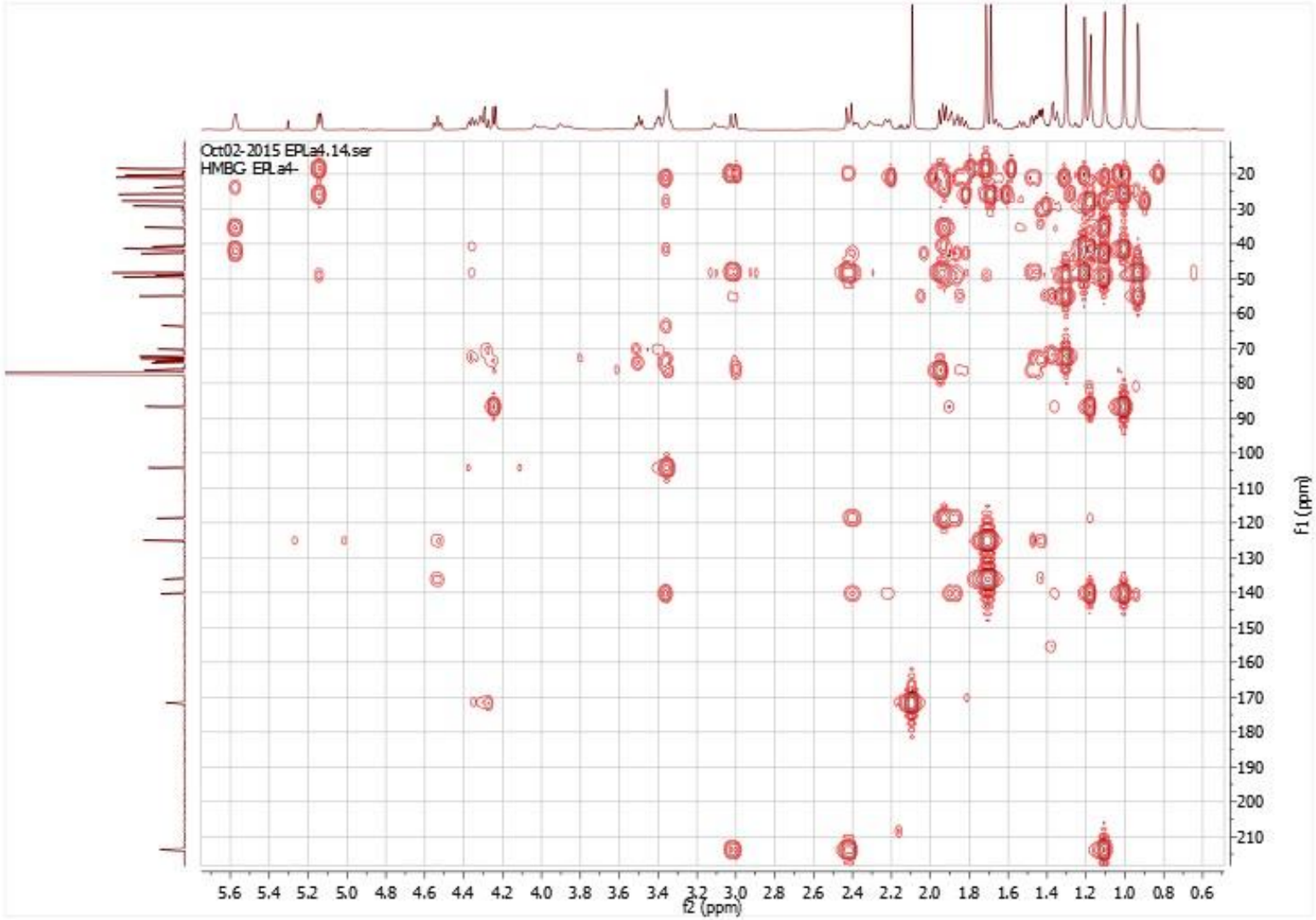
Appendix 13: COSY spectrum of compound **4**

m



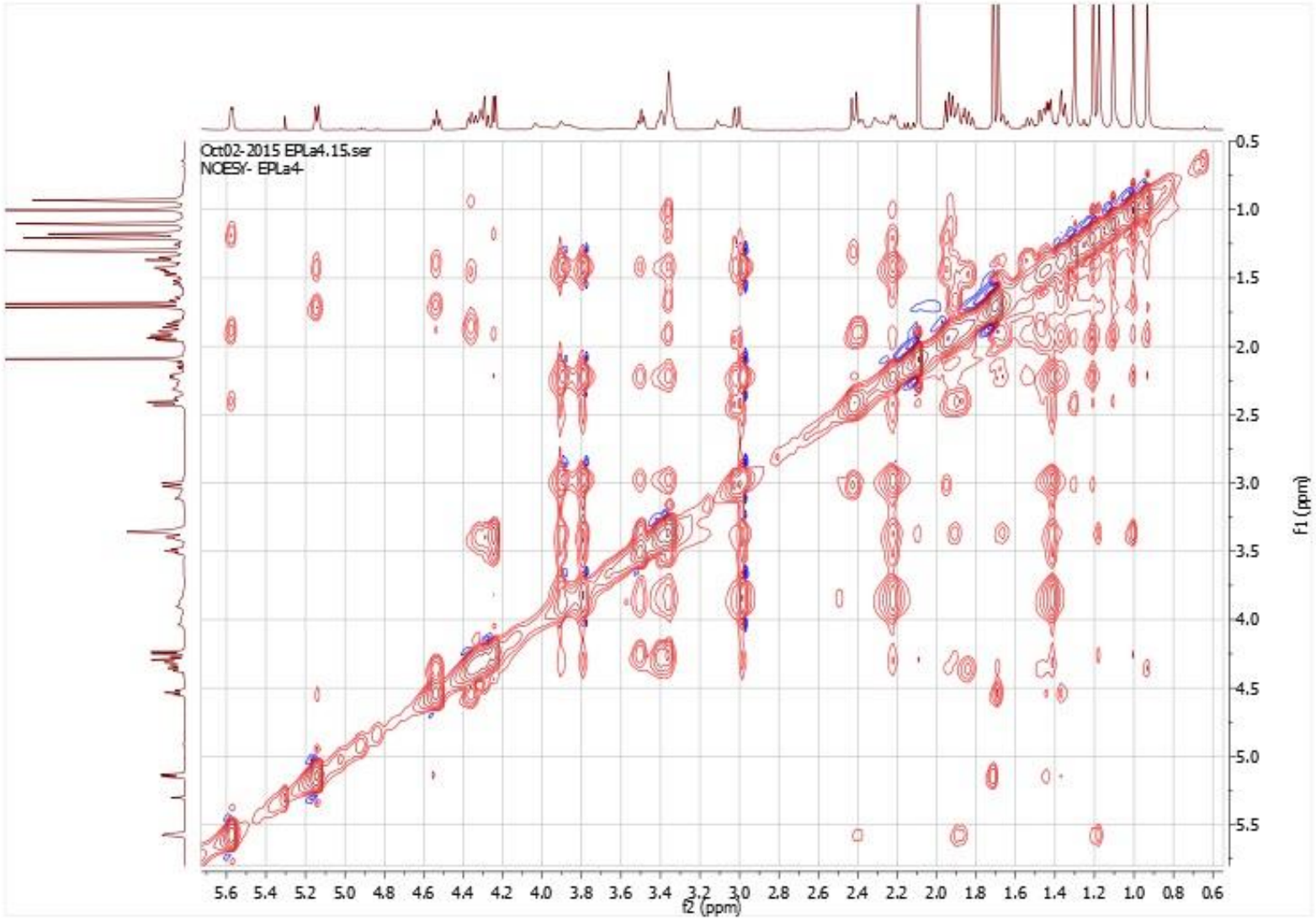
Appendix 14: HSQC spectrum of compound **4**

n



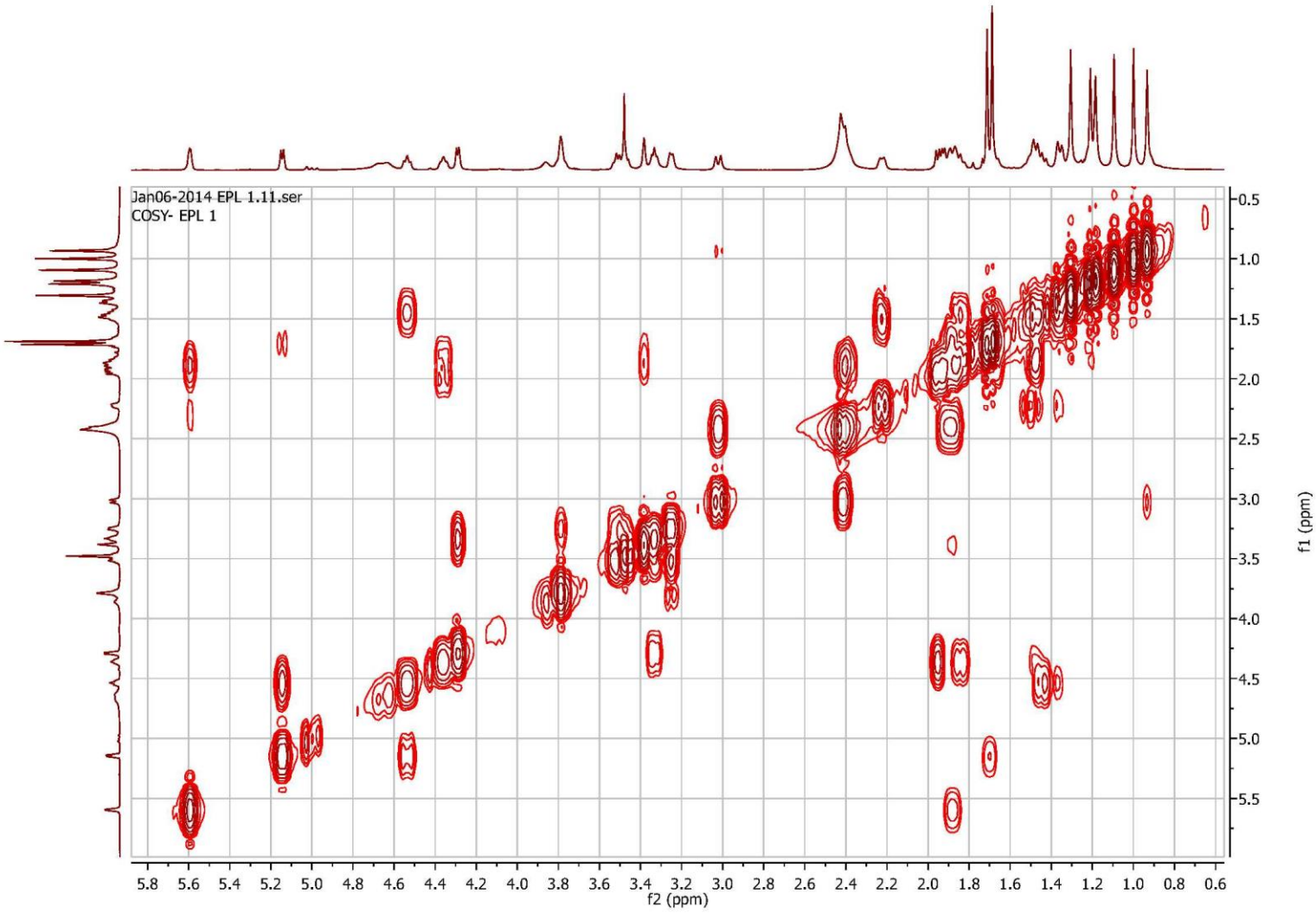
Appendix 15: HMBC spectrum of compound **4**

o



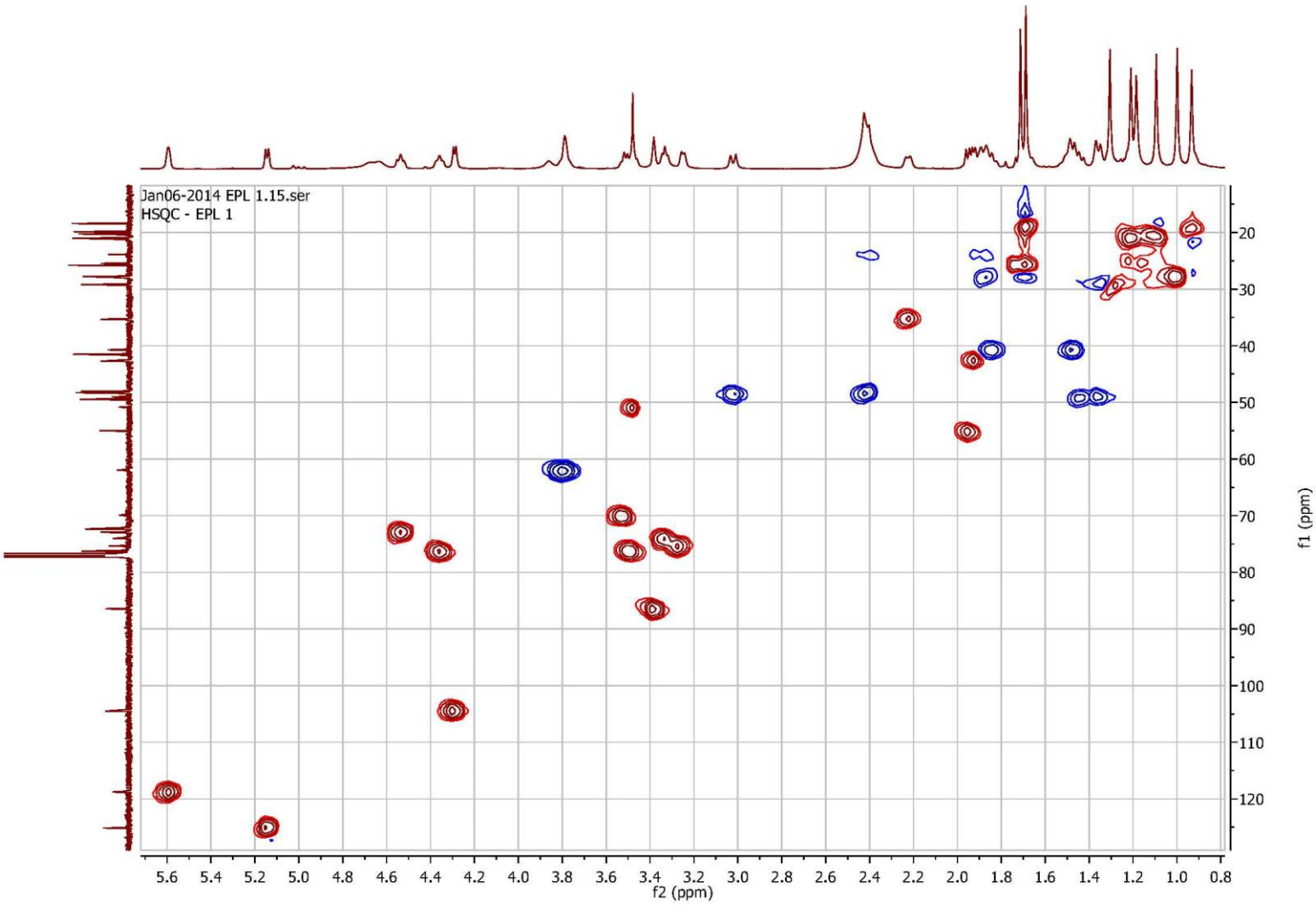
Appendix 16: NOESY spectrum of compound **4**

p



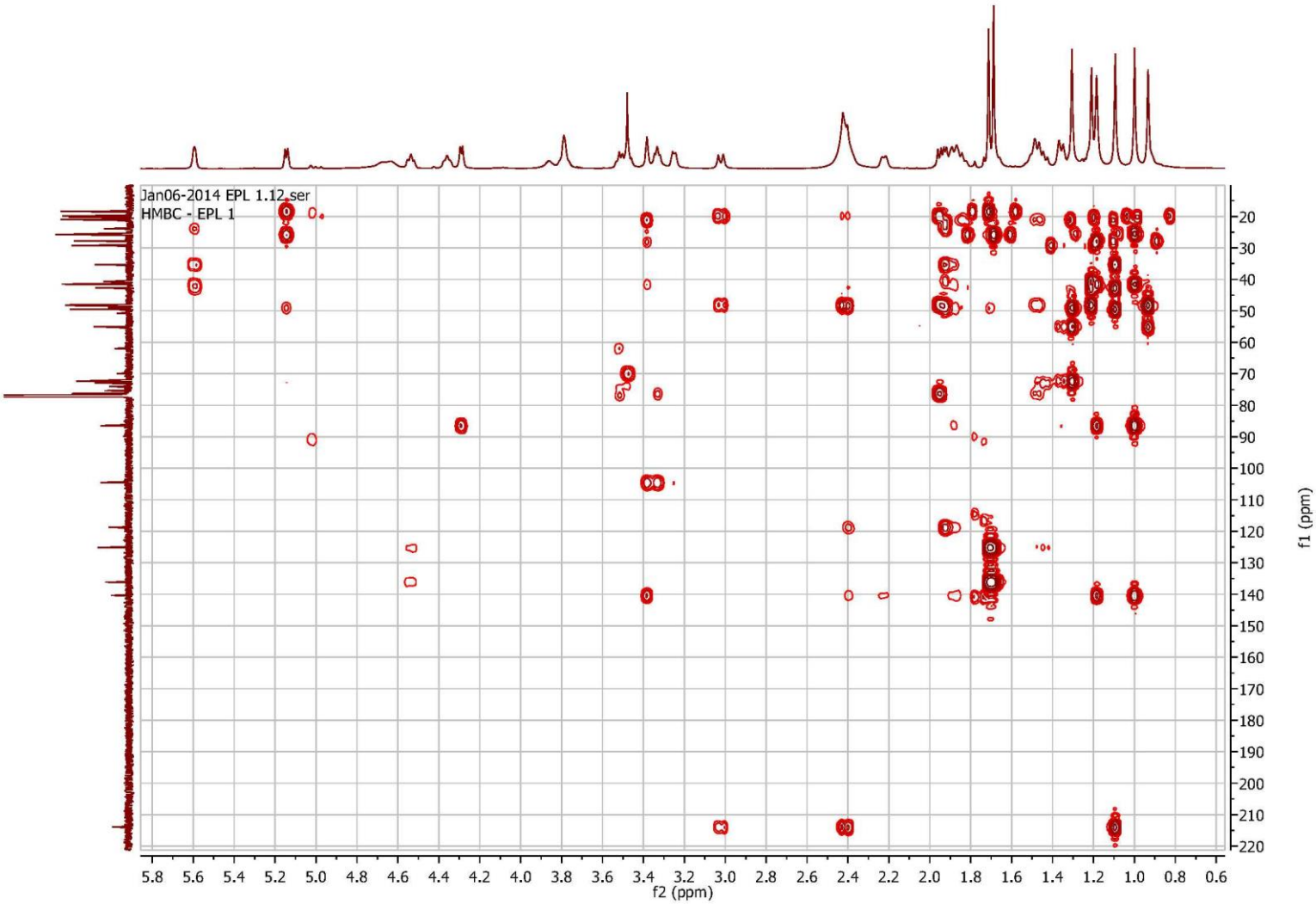
Appendix 17: COSY spectrum of compound **6**

q

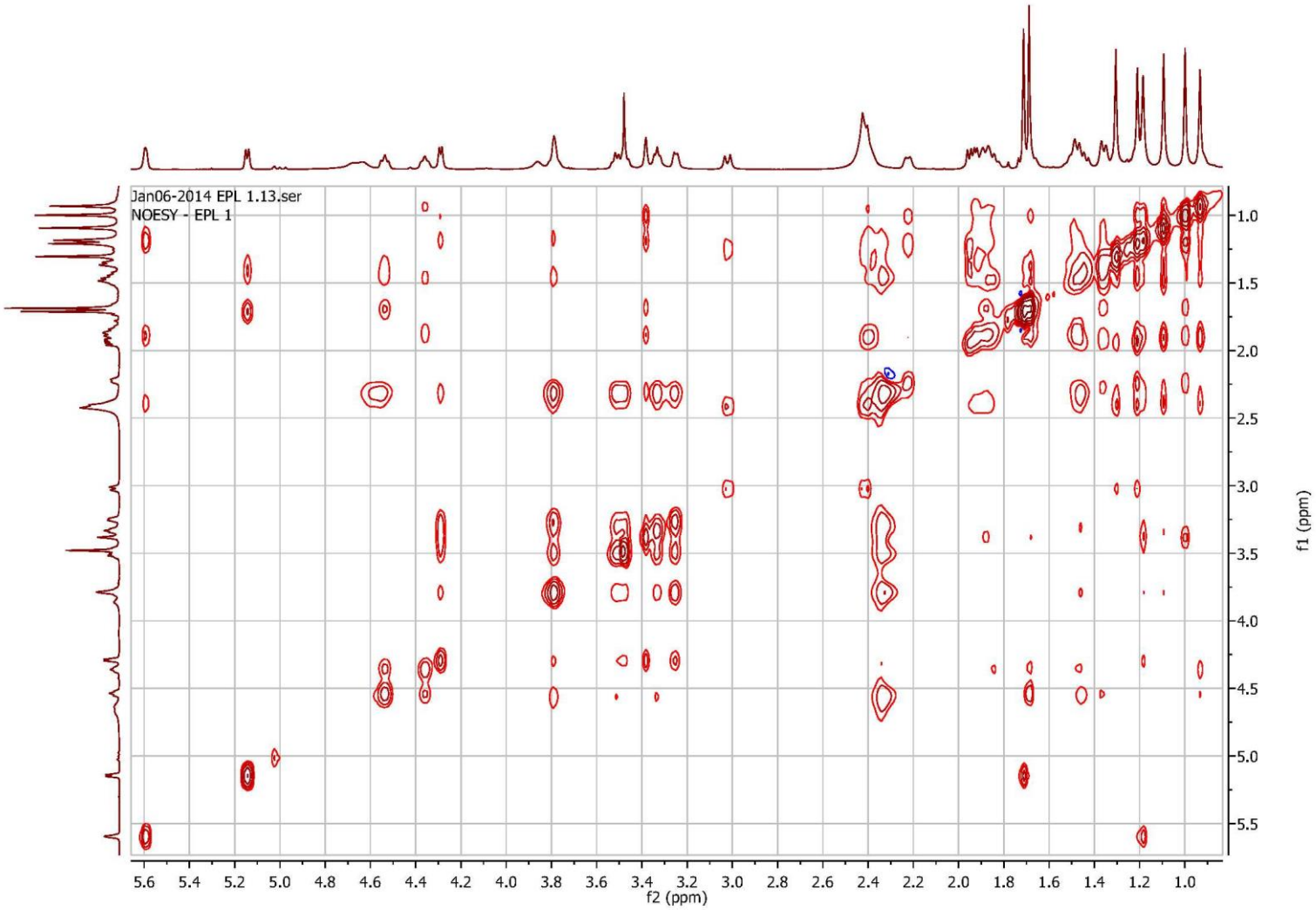


Appendix 18: HSQC spectrum of compound **6**

r



Appendix 19: HMBC spectrum of compound **6**



Appendix 20: NOESY spectrum of compound **6**

t

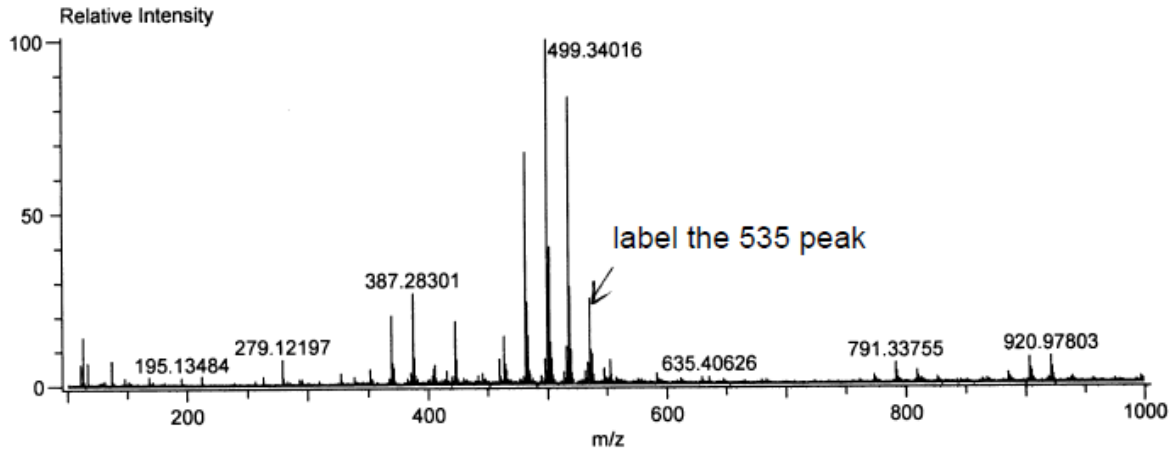
Data:EPB8
Sample Name:
Description:
Ionization Mode:ESI+
History:Determine m/z[Peak Detect[Centroid,30,Area];Correct Base[0.5%]];Correct Ba...

Acquired:7/15/2016 2:20:01 PM
Operator:AccuTOF
Mass Calibration data:Calibration1
Created:7/15/2016 2:30:01 PM
Created by:AccuTOF

Charge number:1
Element:^{12}C:0 .. 40, ^{1}H:0 .. 50, ^{16}O:0 .. 15

Tolerance:50.00(ppm), 5.00 .. 15.00(mmu)

Unsaturation Number:0.0 .. 25.0 (Fractio...



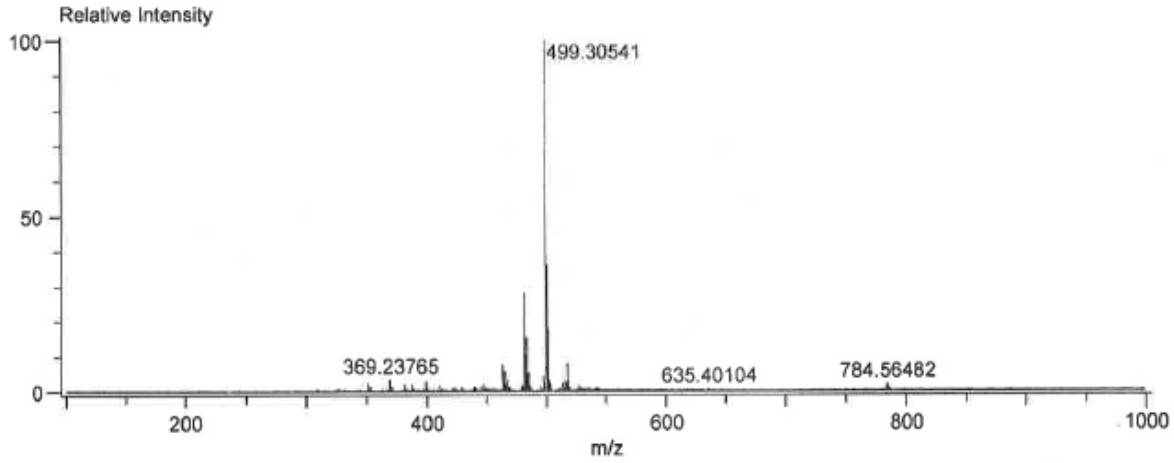
Mass	Intensity	Calc. Mass	Mass Difference (mmu)	Mass Difference (ppm)	Possible Formula
535.32516	21815.17	535.32709	-1.93	-3.61	$^{12}C_{30}{}^{1}H_{47}{}^{16}O_{8}$
		535.32122	3.94	7.36	$^{12}C_{37}{}^{1}H_{43}{}^{16}O_{3}$
		535.31184	13.32	24.89	$^{12}C_{26}{}^{1}H_{47}{}^{16}O_{11}$

Appendix 21: MS spectrum of compound **1**

Data:EPB4
Sample Name:
Description:
Ionization Mode:ESI+
History:Determine m/z[Peak Detect[Centroid,30,Area];Correct Base[0.5%]];Correct Ba...

Acquired:5/9/2016 12:33:30 PM
Operator:AccuTOF
Mass Calibration data:Calibration3
Created:5/9/2016 3:34:35 PM
Created by:AccuTOF

Charge number:1 Tolerance:30.00(ppm), 5.00 .. 15.00(mmu) Unsaturation Number:0.0 .. 25.0 (Fractio...
Element:^{12}C:0 .. 50, ^{1}H:0 .. 100, ^{14}N:0 .. 5, ^{16}O:0 .. 10



Mass	Intensity	Calc. Mass	Mass Difference (mmu)	Mass Difference (ppm)	Possible Formula
499.30541	237527.59	499.30596	-0.55	-1.11	$^{12}C_{30}{}^{1}H_{43}{}^{16}O_6$
		499.30462	0.79	1.58	$^{12}C_{28}{}^{1}H_{41}{}^{14}N_3{}^{16}O_5$
		499.30730	-1.89	-3.79	$^{12}C_{31}{}^{1}H_{39}{}^{14}N_4{}^{16}O_2$
		499.30864	-3.23	-6.47	$^{12}C_{33}{}^{1}H_{41}{}^{14}N_1{}^{16}O_3$
		499.30194	3.47	6.95	$^{12}C_{25}{}^{1}H_{43}{}^{14}N_2{}^{16}O_8$
		499.30060	4.81	9.64	$^{12}C_{23}{}^{1}H_{41}{}^{14}N_5{}^{16}O_7$
		499.31049	-5.08	-10.18	$^{12}C_{21}{}^{1}H_{45}{}^{14}N_3{}^{16}O_{10}$
		499.30009	5.32	10.66	$^{12}C_{37}{}^{1}H_{39}{}^{16}O_1$
		499.31132	-5.91	-11.84	$^{12}C_{36}{}^{1}H_{39}{}^{14}N_2$
		499.29875	6.66	13.34	$^{12}C_{35}{}^{1}H_{37}{}^{14}N_3$
		499.29792	7.49	15.01	$^{12}C_{20}{}^{1}H_{43}{}^{14}N_4{}^{18}O_{10}$
		499.31317	-7.76	-15.55	$^{12}C_{24}{}^{1}H_{43}{}^{14}N_4{}^{16}O_7$
		499.31452	-9.11	-18.24	$^{12}C_{26}{}^{1}H_{45}{}^{14}N_1{}^{16}O_8$
		499.29607	9.34	18.71	$^{12}C_{32}{}^{1}H_{39}{}^{14}N_2{}^{18}O_3$
		499.31585	-10.44	-20.92	$^{12}C_{27}{}^{1}H_{41}{}^{14}N_5{}^{18}O_4$
		499.29472	10.69	21.40	$^{12}C_{30}{}^{1}H_{37}{}^{14}N_5{}^{16}O_2$
		499.31720	-11.79	-23.60	$^{12}C_{29}{}^{1}H_{43}{}^{14}N_2{}^{18}O_5$
		499.29339	12.02	24.08	$^{12}C_{29}{}^{1}H_{41}{}^{14}N_1{}^{16}O_6$
		499.29204	13.37	26.77	$^{12}C_{27}{}^{1}H_{39}{}^{14}N_4{}^{16}O_5$
		499.31988	-14.47	-28.97	$^{12}C_{32}{}^{1}H_{41}{}^{14}N_3{}^{16}O_2$
		499.29071	14.70	29.45	$^{12}C_{26}{}^{1}H_{43}{}^{18}O_9$

$M+H^+ - 2H_2O$

Appendix 22: MS spectrum of compound **2**

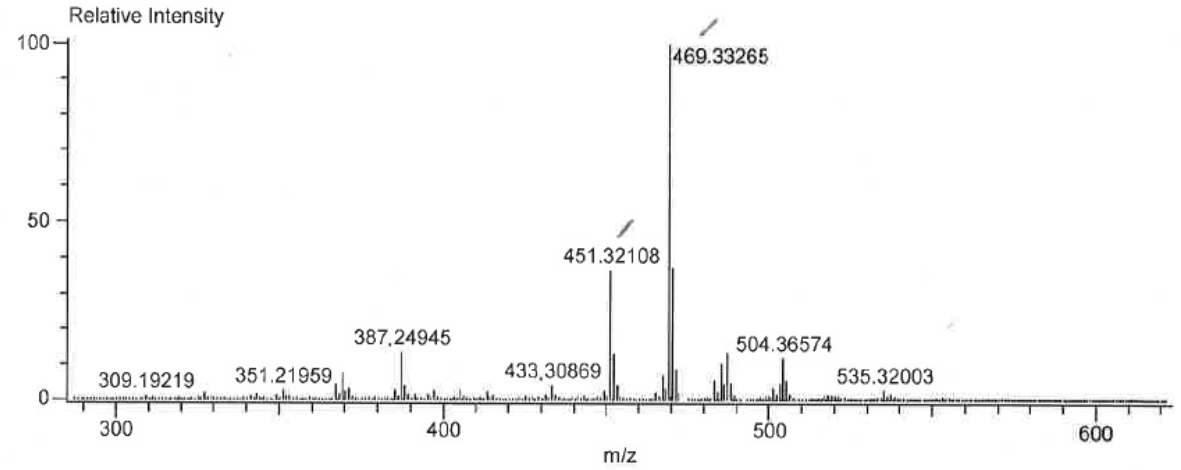
Data:EPB7
Sample Name:
Description:
Ionization Mode:ESI+
History:Determine m/z[Peak Detect[Centroid,30,Area];Correct Base[0,5%]];Correct Ba...

Acquired:7/29/2016 11:16:35 AM
Operator:AccuTOF
Mass Calibration data:Int Calib 240117
Created:1/26/2017 11:02:40 AM
Created by:AccuTOF

Charge number:1
Element:^{12}C:0 .. 40, ^{1}H:0 .. 50, ^{16}O:0 .. 10

Tolerance:30.00(ppm), 0.00 .. 30.00(mmu)

Unsaturation Number:0.0 .. 25.0 (Fractio...



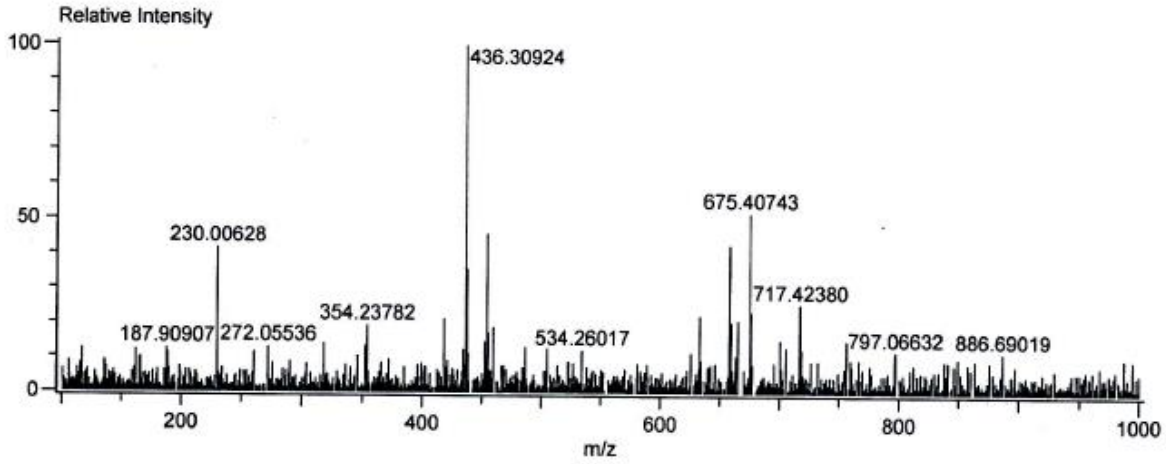
Mass	Intensity	Calc. Mass	Mass Difference (mmu)	Mass Difference (ppm)	Possible Formula
451.32108	80314.00	451.32122	-0.13	-0.30	$^{12}C_{30}{}^{1}H_{43}{}^{16}O_3$
		451.32709	-6.01	-13.31	$^{12}C_{23}{}^{1}H_{47}{}^{16}O_8$
469.33265	220208.50	469.33178	0.87	1.85	$^{12}C_{30}{}^{1}H_{45}{}^{16}O_4$
487.34113	29592.75	487.34235	-1.21	-2.49	$^{12}C_{30}{}^{1}H_{47}{}^{16}O_5$
		487.33648	4.66	9.56	$^{12}C_{37}{}^{1}H_{43}$
		487.32709	14.04	28.81	$^{12}C_{26}{}^{1}H_{47}{}^{16}O_8$

Appendix 23: MS spectrum of compound **3**

Data:EPLa4x3
Sample Name:
Description:
Ionization Mode:ESI+
History:Determine m/z[Peak Detect[Centroid,30,Area];Correct Base[0.5%]];Correct Ba...

Acquired:11/17/2015 9:36:24 AM
Operator:AccuTOF
Mass Calibration data:iCalibration
Created:11/17/2015 9:44:42 AM
Created by:AccuTOF

Charge number:1 Tolerance:20.00(ppm), 5.00 .. 15.00(mmu) Unsaturation Number:0.0 .. 25.0 (Fractio...
Element:^{12}C:0 .. 50, ^{1}H:0 .. 50, ^{14}N:0 .. 10, ^{16}O:0 .. 10



Mass	Intensity	Calc. Mass	Mass Difference (mmu)	Mass Difference (ppm)	Possible Formula
436.30924	6456.97	436.30898	0.26	0.60	$^{12}C_{28}{}^{1}H_{40}{}^{14}N_{2}{}^{16}O_{2}$
		436.30763	1.60	3.67	$^{12}C_{26}{}^{1}H_{38}{}^{14}N_{5}{}^{16}O_{1}$
		436.31217	-2.93	-6.71	$^{12}C_{17}{}^{1}H_{40}{}^{14}N_{8}{}^{16}O_{5}$
		436.30630	2.94	6.74	$^{12}C_{25}{}^{1}H_{42}{}^{14}N_{1}{}^{16}O_{5}$
		436.30629	2.94	6.75	$^{12}C_{24}{}^{1}H_{38}{}^{14}N_{8}$
		436.31300	-3.76	-8.62	$^{12}C_{33}{}^{1}H_{40}$
		436.31351	-4.27	-9.79	$^{12}C_{19}{}^{1}H_{42}{}^{14}N_{5}{}^{16}O_{6}$
		436.30495	4.28	9.82	$^{12}C_{23}{}^{1}H_{40}{}^{14}N_{4}{}^{16}O_{4}$
		436.31485	-5.61	-12.85	$^{12}C_{20}{}^{1}H_{38}{}^{14}N_{9}{}^{16}O_{2}$
		436.31485	-5.61	-12.87	$^{12}C_{21}{}^{1}H_{44}{}^{14}N_{2}{}^{16}O_{7}$
		436.30362	5.62	12.88	$^{12}C_{22}{}^{1}H_{44}{}^{16}O_{8}$
		436.30361	5.63	12.89	$^{12}C_{21}{}^{1}H_{38}{}^{14}N_{7}{}^{16}O_{3}$
		436.31619	-6.95	-15.93	$^{12}C_{22}{}^{1}H_{40}{}^{14}N_{6}{}^{16}O_{3}$
		436.30227	6.96	15.96	$^{12}C_{20}{}^{1}H_{42}{}^{14}N_{3}{}^{16}O_{7}$
		436.30227	6.97	15.97	$^{12}C_{19}{}^{1}H_{36}{}^{14}N_{10}{}^{16}O_{2}$
		436.31753	-8.29	-19.01	$^{12}C_{24}{}^{1}H_{42}{}^{14}N_{3}{}^{16}O_{4}$
		436.30093	8.31	19.04	$^{12}C_{18}{}^{1}H_{40}{}^{14}N_{6}{}^{16}O_{6}$
675.40743	3321.63	675.40494	2.48	3.68	$^{12}C_{44}{}^{1}H_{49}{}^{14}N_{7}$
		675.40092	6.51	9.63	$^{12}C_{39}{}^{1}H_{49}{}^{14}N_{9}{}^{16}O_{2}$

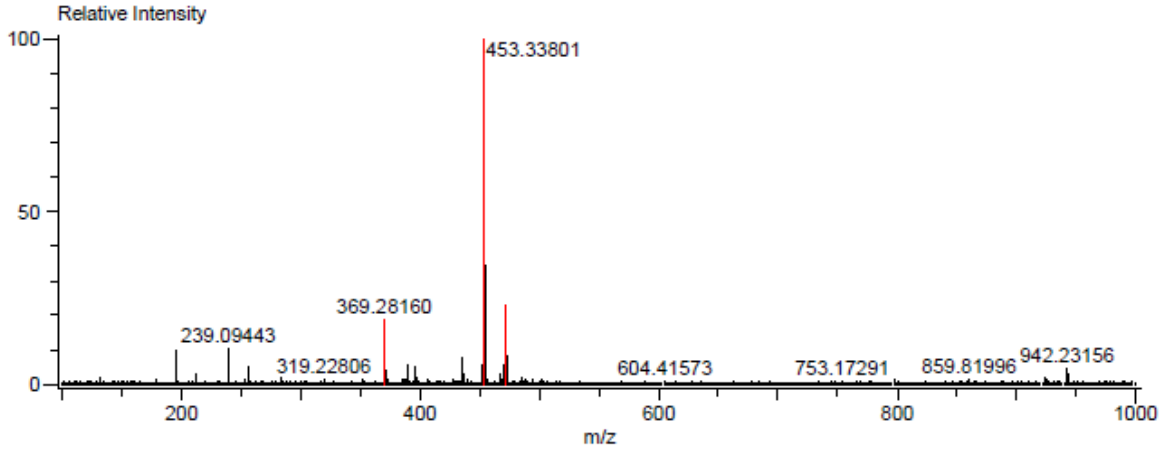
C38H59O10, Δ = 4.22 ppm

Appendix 24: MS spectrum of compound **4**

Data:EPL 11
Sample Name:
Description:
Ionization Mode:ESI+
History:Determine m/z[Peak Detect[Centroid,30,Area];Correct Base[0.5%]];Correct Bas...

Acquired:3/17/2015 2:13:00 PM
Operator:AccuTOF
Mass Calibration data:Calibration
Created:3/17/2015 2:19:59 PM
Created by:

Charge number:1
Tolerance:15.00(ppm), 5.00 .. 15.00(mmu)
Unsaturation Number:0.0 .. 25.0 (Fraction...
Element:^{12}C:0 .. 60, ^{1}H:10 .. 60, ^{14}N:0 .. 5, ^{16}O:0 .. 15



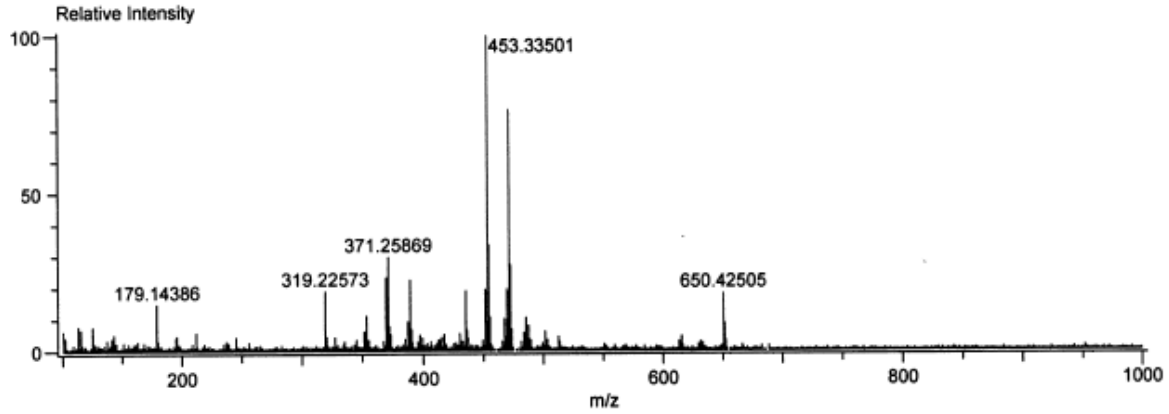
Mass	Intensity	Calc. Mass	Mass Difference (mmu)	Mass Difference (ppm)	Possible Formula	Unsaturation Number
369.28160	13340.75	369.27935	2.25	6.09	$^{12}C_{25}{}^{1}H_{37}{}^{16}O_2$	7.5
		369.27801	3.59	9.73	$^{12}C_{23}{}^{1}H_{35}{}^{14}N_3{}^{16}O_1$	8.0
		369.28656	-4.96	-13.43	$^{12}C_{19}{}^{1}H_{37}{}^{14}N_4{}^{16}O_3$	3.5
453.33801	70618.99	453.33687	1.14	2.53	$^{12}C_{30}{}^{1}H_{45}{}^{16}O_3$	8.5
		453.33955	-1.54	-3.39	$^{12}C_{33}{}^{1}H_{43}{}^{14}N_1$	13.0
		453.33553	2.49	5.49	$^{12}C_{28}{}^{1}H_{43}{}^{14}N_3{}^{16}O_2$	9.0
		453.34140	-3.39	-7.47	$^{12}C_{21}{}^{1}H_{47}{}^{14}N_3{}^{16}O_7$	0.0
		453.33285	5.17	11.40	$^{12}C_{25}{}^{1}H_{45}{}^{14}N_2{}^{16}O_5$	4.5
		453.34408	-6.07	-13.38	$^{12}C_{24}{}^{1}H_{45}{}^{14}N_4{}^{16}O_4$	4.5
		453.33150	6.51	14.36	$^{12}C_{23}{}^{1}H_{43}{}^{14}N_5{}^{16}O_4$	5.0
471.34766	16202.04	471.34743	0.22	0.47	$^{12}C_{30}{}^{1}H_{47}{}^{16}O_4$	7.5
		471.34877	-1.11	-2.36	$^{12}C_{31}{}^{1}H_{43}{}^{14}N_4$	12.5
		471.34609	1.57	3.32	$^{12}C_{28}{}^{1}H_{45}{}^{14}N_3{}^{16}O_3$	8.0
		471.35011	-2.46	-5.21	$^{12}C_{33}{}^{1}H_{45}{}^{14}N_1{}^{16}O_1$	12.0
		471.34341	4.25	9.01	$^{12}C_{25}{}^{1}H_{47}{}^{14}N_2{}^{16}O_6$	3.5
		471.34207	5.59	11.86	$^{12}C_{23}{}^{1}H_{45}{}^{14}N_5{}^{16}O_5$	4.0
		471.35464	-6.99	-14.82	$^{12}C_{24}{}^{1}H_{47}{}^{14}N_4{}^{16}O_5$	3.5

Appendix 25: MS spectrum of compound **5**

Data:EPL1
Sample Name:
Description:
Ionization Mode:ESI+
History:Determine m/z[Peak Detect[Centroid,30,Area];Correct Base[0.5%]];Correct Base[5.0%]...

Acquired:1/15/2014 4:53:53 PM
Operator:AccuTOF
Mass Calibration data:DART Calib 150114 P...
Created:1/15/2014 5:07:45 PM
Created by:AccuTOF

Charge number:1
Tolerance:15.00(ppm), 5.00 .. 15.00(mmu)
Unsaturation Number:0.0 .. 25.0 (Fraction:Bo...
Element:^{12}C:10 .. 60, ^{1}H:10 .. 60, ^{14}N:0 .. 10, ^{23}Na:0 .. 0, ^{16}O:0 .. 20



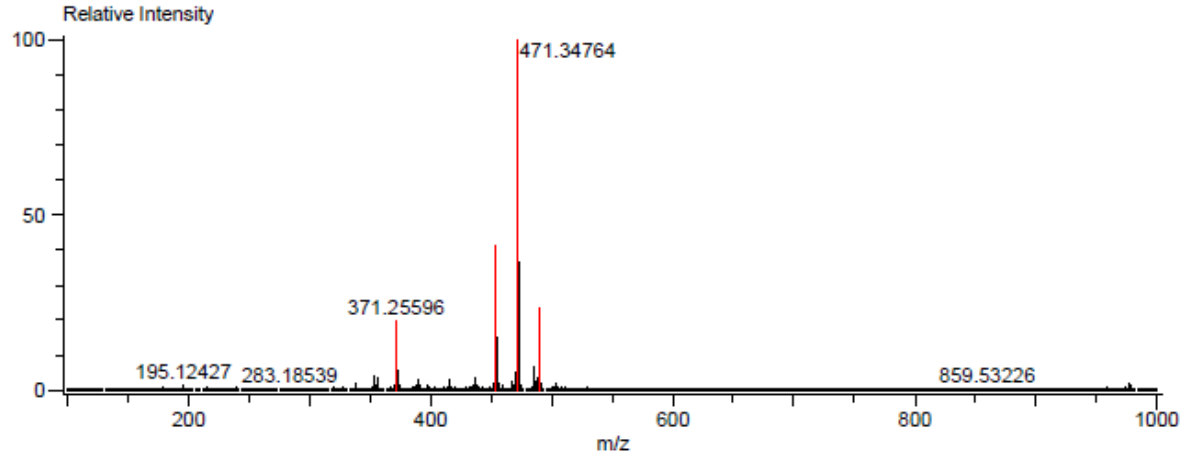
Mass	Intensity	Calc. Mass	Mass Difference (mmu)	Mass Difference (ppm)	Possible Formula	Unsaturation Number	
453.33501	54475.84	453.33553	-0.52	-1.15	$^{12}C_{28}{}^{1}H_{43}{}^{14}N_{3}{}^{16}O_{2}$	9.0	
		453.33418	0.82	1.82	$^{12}C_{26}{}^{1}H_{41}{}^{14}N_{6}{}^{16}O_{1}$	9.5	
		453.33687	-1.86	-4.11	$^{12}C_{30}{}^{1}H_{45}{}^{16}O_{3}$	8.5	
		453.33285	2.16	4.77	$^{12}C_{25}{}^{1}H_{45}{}^{14}N_{2}{}^{16}O_{5}$	4.5	
		453.33284	2.17	4.78	$^{12}C_{24}{}^{1}H_{39}{}^{14}N_{9}$	10.0	
		453.33150	3.50	7.73	$^{12}C_{23}{}^{1}H_{43}{}^{14}N_{5}{}^{16}O_{4}$	5.0	
		453.33871	-3.71	-8.18	$^{12}C_{17}{}^{1}H_{43}{}^{14}N_{9}{}^{16}O_{5}$	1.0	
		453.33955	-4.54	-10.02	$^{12}C_{33}{}^{1}H_{43}{}^{14}N_{1}$	13.0	
		453.33017	4.84	10.68	$^{12}C_{22}{}^{1}H_{47}{}^{14}N_{1}{}^{16}O_{8}$	0.0	
		453.33016	4.85	10.69	$^{12}C_{21}{}^{1}H_{41}{}^{14}N_{8}{}^{16}O_{3}$	5.5	
		453.34006	-5.05	-11.14	$^{12}C_{19}{}^{1}H_{45}{}^{14}N_{8}{}^{16}O_{6}$	0.5	
		453.32882	6.18	13.64	$^{12}C_{20}{}^{1}H_{45}{}^{14}N_{4}{}^{16}O_{7}$	0.5	
		453.34139	-6.39	-14.09	$^{12}C_{20}{}^{1}H_{41}{}^{14}N_{10}{}^{16}O_{2}$	5.5	
		453.34140	-6.39	-14.10	$^{12}C_{21}{}^{1}H_{47}{}^{14}N_{3}{}^{16}O_{7}$	0.0	
471.34618	41566.00	471.34609	0.08	0.18	$^{12}C_{26}{}^{1}H_{45}{}^{14}N_{3}{}^{16}O_{3}$	8.0	
		471.34743	-1.26	-2.67	$^{12}C_{30}{}^{1}H_{47}{}^{16}O_{4}$	7.5	
		471.34475	1.43	3.03	$^{12}C_{26}{}^{1}H_{43}{}^{14}N_{6}{}^{16}O_{2}$	8.5	
		471.34877	-2.60	-5.51	$^{12}C_{31}{}^{1}H_{43}{}^{14}N_{4}$	12.5	
		471.34341	2.76	5.87	$^{12}C_{25}{}^{1}H_{47}{}^{14}N_{2}{}^{16}O_{6}$	3.5	
		471.34341	2.77	5.88	$^{12}C_{24}{}^{1}H_{41}{}^{14}N_{9}{}^{16}O_{1}$	9.0	
		471.34928	-3.10	-6.58	$^{12}C_{17}{}^{1}H_{45}{}^{14}N_{9}{}^{16}O_{6}$	0.0	
		471.35011	-3.94	-8.36	$^{12}C_{33}{}^{1}H_{45}{}^{14}N_{1}{}^{16}O_{1}$	12.0	
		471.34207	4.11	8.71	$^{12}C_{23}{}^{1}H_{45}{}^{14}N_{5}{}^{16}O_{5}$	4.0	
		471.34073	5.45	11.56	$^{12}C_{21}{}^{1}H_{43}{}^{14}N_{8}{}^{16}O_{4}$	4.5	
		471.35196	-5.78	-12.27	$^{12}C_{20}{}^{1}H_{43}{}^{14}N_{10}{}^{16}O_{3}$	4.5	
650.42505	9807.81	650.42546	-0.41	-0.64	$^{12}C_{34}{}^{1}H_{58}{}^{14}N_{4}{}^{16}O_{8}$	8.0	
		650.42412	0.93	1.43	$^{12}C_{32}{}^{1}H_{56}{}^{14}N_{7}{}^{16}O_{7}$	8.5	
		650.42361	1.44	2.21	$^{12}C_{46}{}^{1}H_{54}{}^{14}N_{2}{}^{16}O_{1}$	21.0	
		650.42680	-1.75	-2.69	$^{12}C_{35}{}^{1}H_{54}{}^{14}N_{5}{}^{16}O_{4}$	13.0	
		650.42681	-1.76	-2.70	$^{12}C_{38}{}^{1}H_{60}{}^{14}N_{1}{}^{16}O_{9}$	7.5	$M+NH_4^+$
		650.42278	2.27	3.48	$^{12}C_{31}{}^{1}H_{60}{}^{14}N_{3}{}^{16}O_{11}$	3.5	
		650.42278	2.27	3.49	$^{12}C_{30}{}^{1}H_{54}{}^{14}N_{10}{}^{16}O_{6}$	9.0	
		650.42227	2.78	4.27	$^{12}C_{44}{}^{1}H_{52}{}^{14}N_{5}$	21.5	
		650.42814	-3.10	-4.76	$^{12}C_{37}{}^{1}H_{56}{}^{14}N_{9}{}^{16}O_{5}$	12.5	

Appendix 26: MS spectrum of compound **6**

Data:EPL 6
Sample Name:
Description:
Ionization Mode:ESI+
History:Determine m/z[Peak Detect[Centroid,30,Area];Correct Base[0.5%]];Correct Bas...

Acquired:3/17/2015 2:15:54 PM
Operator:AccuTOF
Mass Calibration data:Calibration
Created:3/17/2015 2:23:44 PM
Created by:

Charge number:1
Tolerance:15.00(ppm), 5.00 .. 15.00(mmu)
Unsaturation Number:0.0 .. 25.0 (Fraction...
Element:^{12}C:0 .. 60, ^{1}H:10 .. 60, ^{14}N:0 .. 5, ^{16}O:0 .. 15



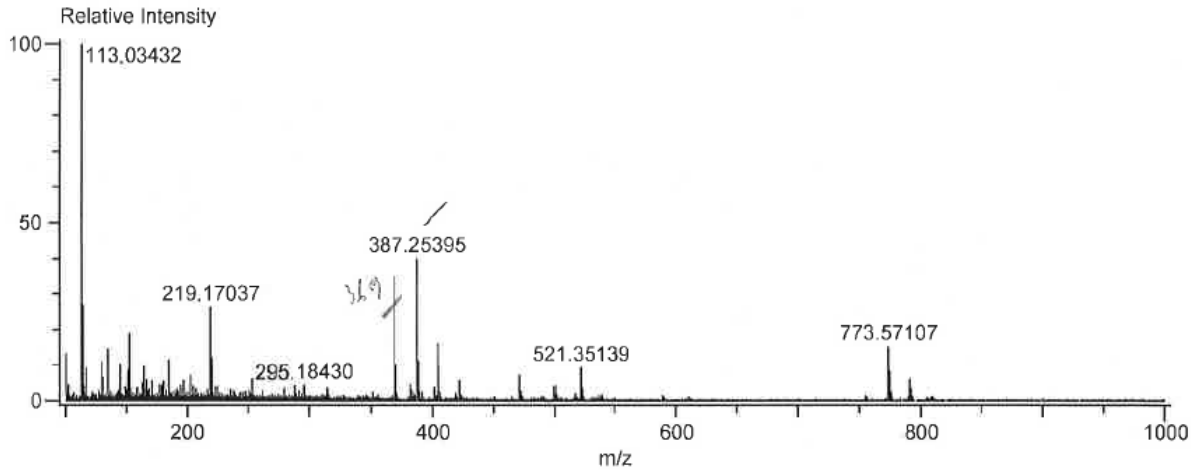
Mass	Intensity	Calc. Mass	Mass Difference (mmu)	Mass Difference (ppm)	Possible Formula	Unsaturation Number
371.25596	50337.66	371.25728	-1.32	-3.55	$^{12}C_{22}{}^{1}H_{33}{}^{14}N_{3}{}^{16}O_{2}$	8.0
		371.25460	1.36	3.67	$^{12}C_{19}{}^{1}H_{35}{}^{14}N_{2}{}^{16}O_{5}$	3.5
		371.25862	-2.66	-7.17	$^{12}C_{24}{}^{1}H_{35}{}^{16}O_{3}$	7.5
		371.25325	2.70	7.28	$^{12}C_{17}{}^{1}H_{33}{}^{14}N_{5}{}^{16}O_{4}$	4.0
		371.26130	-5.34	-14.39	$^{12}C_{27}{}^{1}H_{33}{}^{14}N_{1}$	12.0
453.33501	105089.25	453.33553	-0.52	-1.14	$^{12}C_{28}{}^{1}H_{43}{}^{14}N_{3}{}^{16}O_{2}$	9.0
		453.33687	-1.86	-4.10	$^{12}C_{30}{}^{1}H_{45}{}^{16}O_{3}$	8.5
		453.33285	2.16	4.77	$^{12}C_{25}{}^{1}H_{45}{}^{14}N_{2}{}^{16}O_{5}$	4.5
		453.33150	3.51	7.74	$^{12}C_{23}{}^{1}H_{43}{}^{14}N_{5}{}^{16}O_{4}$	5.0
		453.33955	-4.54	-10.01	$^{12}C_{33}{}^{1}H_{43}{}^{14}N_{1}$	13.0
		453.33017	4.84	10.69	$^{12}C_{22}{}^{1}H_{47}{}^{14}N_{1}{}^{16}O_{8}$	0.0
		453.32882	6.19	13.65	$^{12}C_{20}{}^{1}H_{45}{}^{14}N_{4}{}^{16}O_{7}$	0.5
		453.34140	-6.39	-14.09	$^{12}C_{21}{}^{1}H_{47}{}^{14}N_{3}{}^{16}O_{7}$	0.0
471.34764	255015.25	471.34743	0.21	0.44	$^{12}C_{30}{}^{1}H_{47}{}^{16}O_{4}$	7.5
		471.34877	-1.13	-2.39	$^{12}C_{31}{}^{1}H_{43}{}^{14}N_{4}$	12.5
		471.34609	1.55	3.29	$^{12}C_{28}{}^{1}H_{45}{}^{14}N_{3}{}^{16}O_{3}$	8.0
		471.35011	-2.47	-5.24	$^{12}C_{33}{}^{1}H_{45}{}^{14}N_{1}{}^{16}O_{1}$	12.0
		471.34341	4.23	8.98	$^{12}C_{25}{}^{1}H_{47}{}^{14}N_{2}{}^{16}O_{6}$	3.5
		471.34207	5.57	11.83	$^{12}C_{23}{}^{1}H_{45}{}^{14}N_{5}{}^{16}O_{5}$	4.0
		471.35464	-7.00	-14.85	$^{12}C_{24}{}^{1}H_{47}{}^{14}N_{4}{}^{16}O_{5}$	3.5
489.35550	59099.59	489.35666	-1.15	-2.35	$^{12}C_{28}{}^{1}H_{47}{}^{14}N_{3}{}^{16}O_{4}$	7.0
		489.35398	1.53	3.13	$^{12}C_{25}{}^{1}H_{49}{}^{14}N_{2}{}^{16}O_{7}$	2.5
		489.35800	-2.49	-5.10	$^{12}C_{30}{}^{1}H_{49}{}^{16}O_{5}$	6.5
		489.35263	2.87	5.87	$^{12}C_{23}{}^{1}H_{47}{}^{14}N_{5}{}^{16}O_{6}$	3.0
		489.35213	3.38	6.91	$^{12}C_{37}{}^{1}H_{45}$	15.5
		489.35934	-3.83	-7.83	$^{12}C_{31}{}^{1}H_{45}{}^{14}N_{4}{}^{16}O_{1}$	11.5
		489.36068	-5.17	-10.57	$^{12}C_{33}{}^{1}H_{47}{}^{14}N_{1}{}^{16}O_{2}$	11.0

Appendix 27: MS spectrum of compound **7**

Data:EPB5_291116
Sample Name:
Description:
Ionization Mode:ESI+
History:Determine m/z[Peak Detect[Centroid,30,Area];Correct Base[0.5%]];Correct Ba...

Acquired:11/29/2016 11:54:37 AM
Operator:AccuTOF
Mass Calibration data:Int Calib 240117
Created:1/26/2017 11:12:46 AM
Created by:AccuTOF

Charge number:1
Tolerance:30.00(ppm), 0.00 .. 30.00(mmu)
Unsaturation Number:0.0 .. 25.0 (Fractio...
Element:^{12}C:0 .. 40, ^{1}H:0 .. 50, ^{16}O:0 .. 10



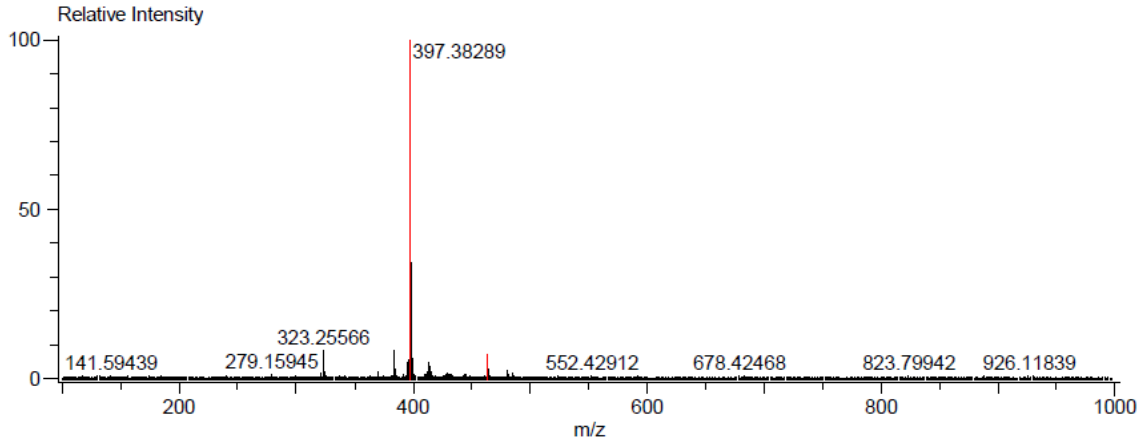
Mass	Intensity	Calc. Mass	Mass Difference (mmu)	Mass Difference (ppm)	Possible Formula
369.24347	66346.75	369.24297	0.50	1.35	$^{12}C_{24}{}^{1}H_{33}{}^{16}O_3$
387.25395	75910.60	387.25353	0.42	1.09	$^{12}C_{24}{}^{1}H_{35}{}^{16}O_4$
405.27179	17977.50	405.27935	-7.57	-18.67	$^{12}C_{28}{}^{1}H_{37}{}^{16}O_2$
		405.26410	7.69	18.98	$^{12}C_{24}{}^{1}H_{37}{}^{16}O_5$

Appendix 28: MS spectrum of compound **8**

Data:EPL 7
Sample Name:
Description:
Ionization Mode:ESI+
History:Determine m/z[Peak Detect[Centroid,30,Area];Correct Base[0.5%]];Correct Bas...

Acquired:3/17/2015 2:57:49 PM
Operator:AccuTOF
Mass Calibration data:Calibration
Created:3/17/2015 3:01:28 PM
Created by:

Charge number:1 Tolerance:15.00(ppm), 5.00 .. 15.00(mmu) Unsaturation Number:0.0 .. 25.0 (Fraction...
Element:^{12}C:0 .. 60, ^{1}H:10 .. 60, ^{14}N:0 .. 5, ^{16}O:0 .. 15



Mass	Intensity	Calc. Mass	Mass Difference (mmu)	Mass Difference (ppm)	Possible Formula	Unsaturation Number
397.38289	111644.25	397.38343	-0.54	-1.35	$^{12}C_{29}{}^{1}H_{49}$	5.5
		397.37940	3.49	8.77	$^{12}C_{24}{}^{1}H_{49}{}^{14}N_{2}{}^{16}O_{2}$	1.5
		397.37806	4.83	12.15	$^{12}C_{22}{}^{1}H_{47}{}^{14}N_{5}{}^{16}O_{1}$	2.0
463.37611	7677.50	463.37739	-1.29	-2.77	$^{12}C_{27}{}^{1}H_{49}{}^{14}N_{3}{}^{16}O_{3}$	5.0
		463.37471	1.39	3.01	$^{12}C_{24}{}^{1}H_{51}{}^{14}N_{2}{}^{16}O_{6}$	0.5
		463.37873	-2.63	-5.67	$^{12}C_{29}{}^{1}H_{51}{}^{16}O_{4}$	4.5
		463.37337	2.74	5.91	$^{12}C_{22}{}^{1}H_{49}{}^{14}N_{5}{}^{16}O_{5}$	1.0
		463.38007	-3.97	-8.56	$^{12}C_{30}{}^{1}H_{47}{}^{14}N_{4}$	9.5
		463.38141	-5.31	-11.46	$^{12}C_{32}{}^{1}H_{49}{}^{14}N_{1}{}^{16}O_{1}$	9.0

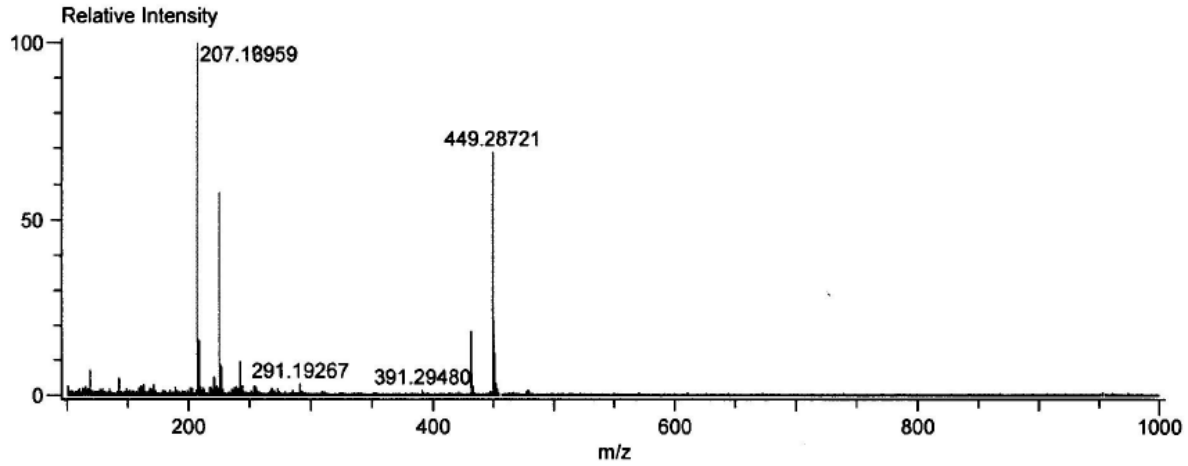
$[M-H2O]^+$ m/z 397.3829

Appendix 29: MS spectrum of compound **9**

Data: ``
Sample Name:
Description:
Ionization Mode:ESI+
History:Determine m/z[Peak Detect[Centroid,30,Area];Correct Base[0.5%]];Correct Ba...

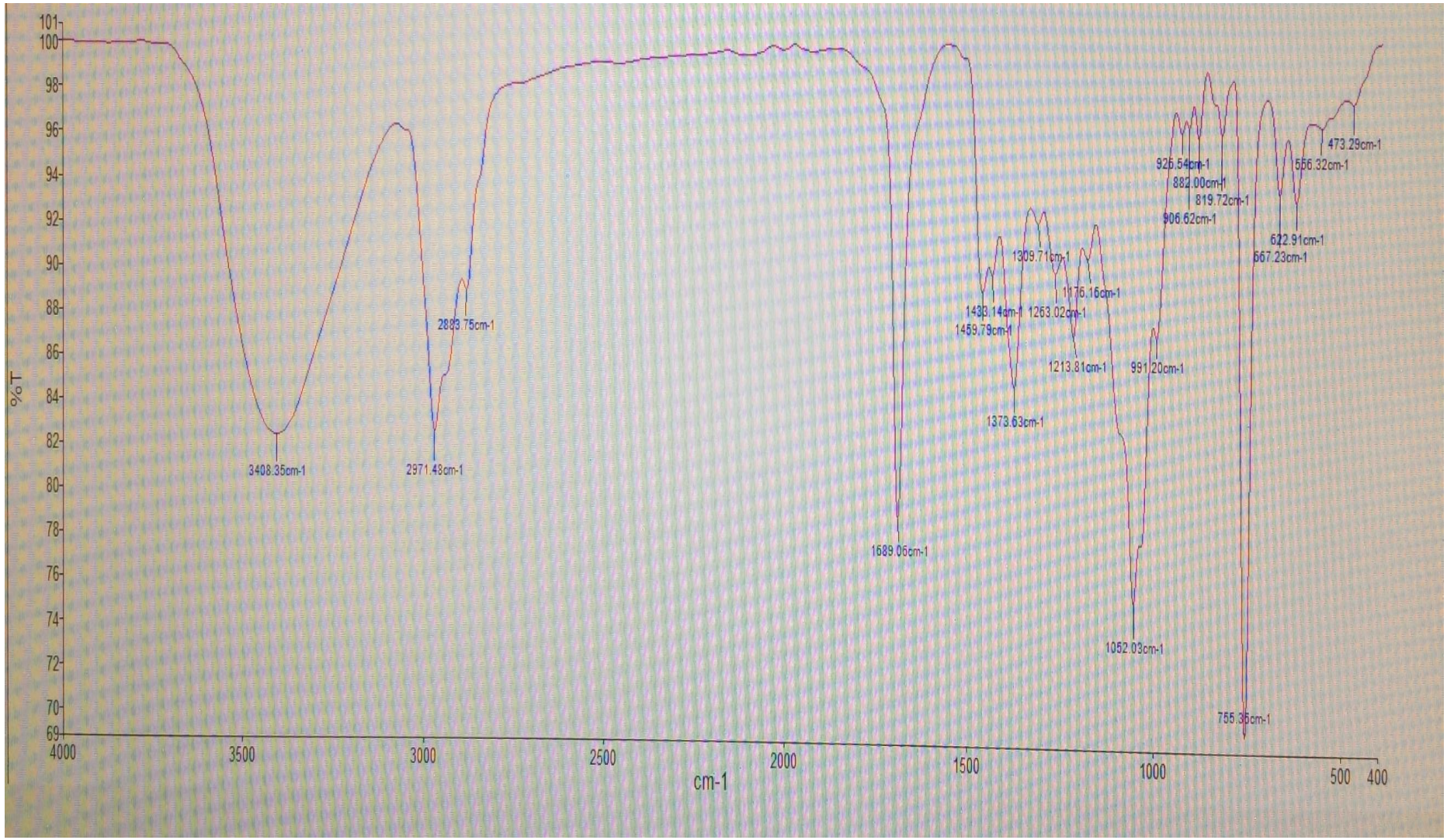
Acquired:! ``
Operator:AccuTOF
Mass Calibration data:DART Calib 06091...
Created:9/6/2013 4:22:23 PM
Created by:AccuTOF

Charge number:1 Tolerance:15.00(ppm), 5.00 .. 15.00(mmu) Unsaturation Number:0.0 .. 25.0 (Fractio...
Element:^{12}C:0 .. 40, ^{1}H:0 .. 60, ^{14}N:0 .. 5, ^{23}Na:0 .. 0, ^{16}O:0 .. 10

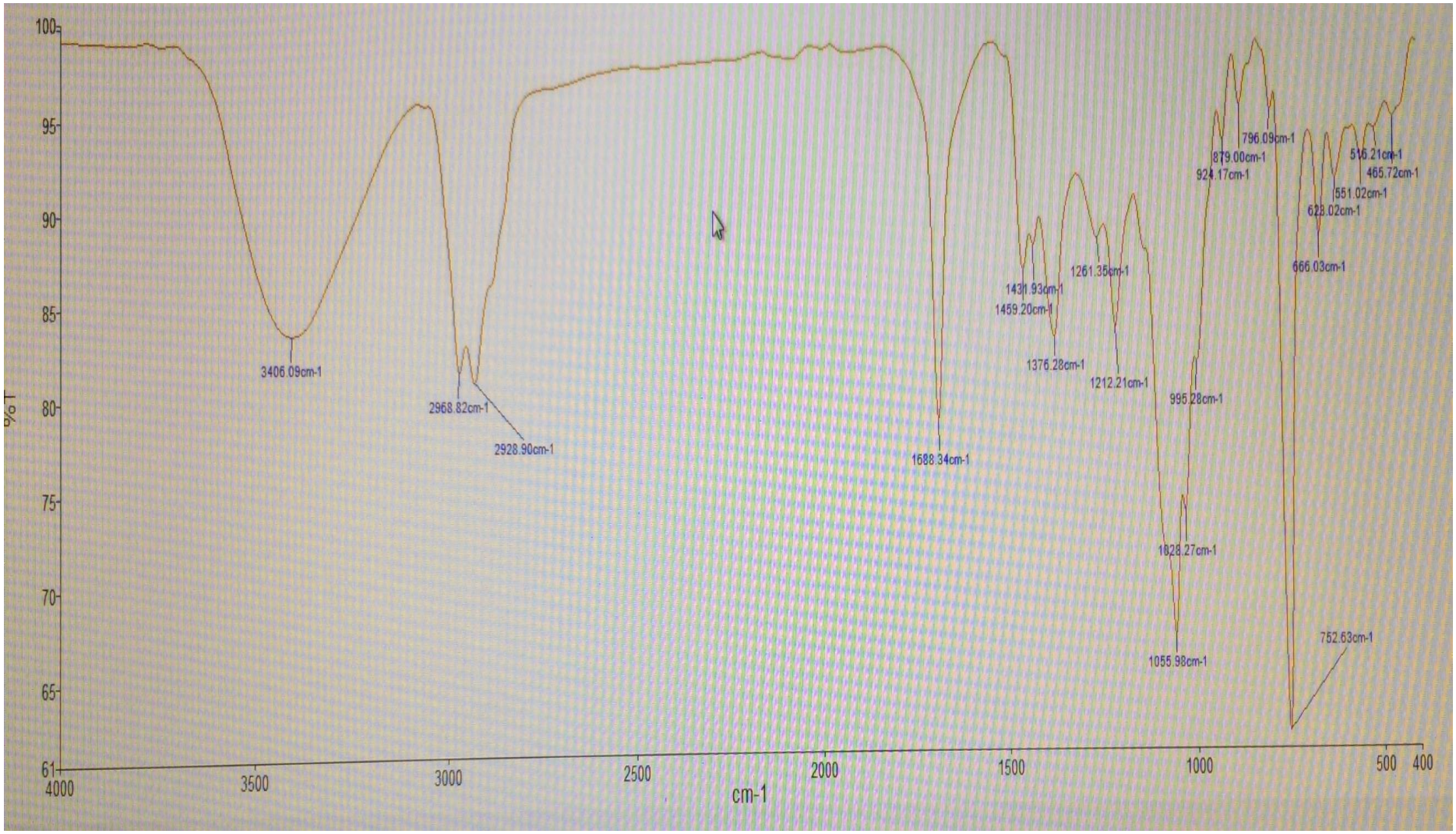


Mass	Intensity	Calc. Mass	Mass Difference (mmu)	Mass Difference (ppm)	Possible Formula	Unsaturation Number
207.13959	81535.62	207.13850	1.09	5.26	$^{12}C_{13}{}^{1}H_{19}{}^{16}O_2$	4.5
		207.13716	2.43	11.74	$^{12}C_{11}{}^{1}H_{17}{}^{14}N_3{}^{16}O_1$	5.0
225.15047	46904.25	225.15175	-1.28	-5.68	$^{12}C_{16}{}^{1}H_{19}{}^{14}N_1$	8.0
		225.14907	1.40	6.23	$^{12}C_{13}{}^{1}H_{21}{}^{16}O_3$	3.5
		225.14773	2.74	12.19	$^{12}C_{11}{}^{1}H_{19}{}^{14}N_3{}^{16}O_2$	4.0
449.28721	55967.65	449.28629	0.92	2.05	$^{12}C_{21}{}^{1}H_{41}{}^{14}N_2{}^{16}O_8$	2.5
		449.28897	-1.76	-3.92	$^{12}C_{24}{}^{1}H_{39}{}^{14}N_3{}^{16}O_5$	7.0
		449.28495	2.26	5.03	$^{12}C_{19}{}^{1}H_{39}{}^{14}N_5{}^{16}O_7$	3.0
		449.28444	2.77	6.16	$^{12}C_{33}{}^{1}H_{37}{}^{16}O_1$	15.5
		449.29031	-3.10	-6.91	$^{12}C_{26}{}^{1}H_{41}{}^{16}O_6$	6.5
		449.28310	4.11	9.15	$^{12}C_{31}{}^{1}H_{35}{}^{14}N_3$	16.0
		449.29165	-4.44	-9.89	$^{12}C_{27}{}^{1}H_{37}{}^{14}N_4{}^{16}O_2$	11.5
		449.29299	-5.78	-12.87	$^{12}C_{29}{}^{1}H_{39}{}^{14}N_1{}^{16}O_3$	11.0

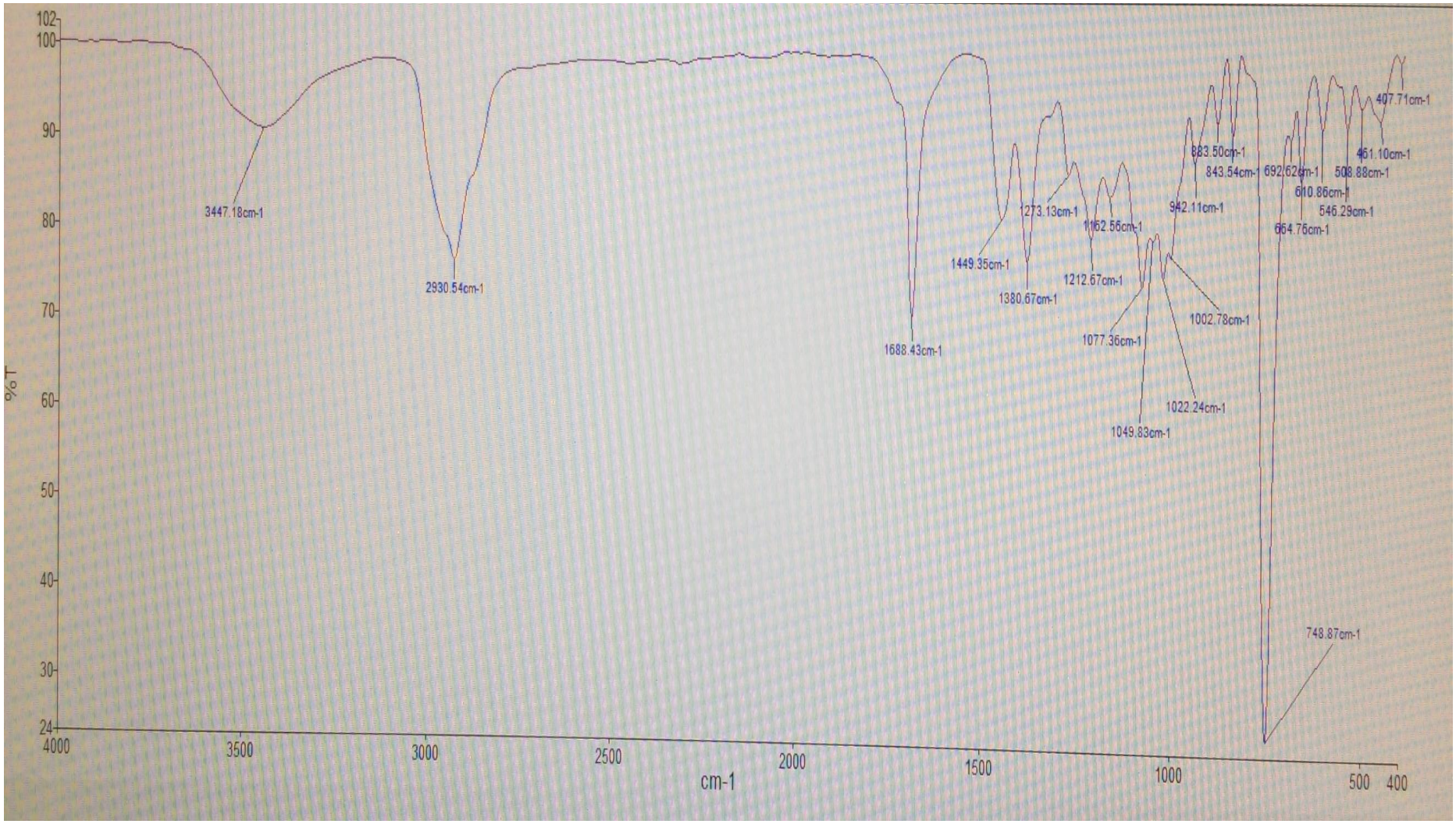
Appendix 30: MS spectrum of compound **10**



Appendix 31: IR spectrum of compound **1**



Appendix 32: IR spectrum of compound **2**



Appendix 33: IR spectrum of compound **3**

b